HADRON SPECTROSCOPY AND STRONG QCD

Eberhard Klempt

Helmholtz-Institut für Strahlen– und Kernphysik
Universität Bonn
Nußallee 14-16, D-53115 Bonn, GERMANY
e-mail: klempt@hiskp.uni-bonn.de

June 2003

Why hadron spectroscopy ?

- **Spectroscopy is a powerful tool to study internal dynamics**
  1. **Balmer formula** $\longrightarrow$ **Hydrogen atom**
  2. **Magic numbers** $\longrightarrow$ **Tensor forces in nuclear physics**
  3. **Existance of Ω** $\longrightarrow$ **Triumph of SU(3)**
  4. **No 'ionized' protons** $\longrightarrow$ **Confinement**
  5. $c\bar{c}$ **and** $b\bar{b}$ **families** $\longrightarrow$ **One-gluon exchange plus linear confinement**
- **Baryons have** $\mathrm{N_F = N_C}$
  1. **True non-abelian system** $\longrightarrow$ **test of QCD related ideas**
  2. **Rich dynamics of three-body system** $\longrightarrow$ **Insights beyond meson physics**
  3. **Truely complicated** $\longrightarrow$ **Intellectually and experimentally demanding**

- **Getting started**
- **Particles and interactions**
- **Particle decays and partial wave analysis**
- **The E/ι saga and the first glueball**
- **The quest for the scalar glueball**
- **Baryons**
- **Summary and conclusions**

Literature:

1. **S. Godfrey and J. Napolitano,**
   "Light meson spectroscopy,"
   Rev. Mod. Phys. 71, 1411 (1999)
   arXiv:hep-ph/9811410.

2. **K. Hagiwara** *et al.* **[Particle Data Group Collaboration],**
   "Review Of Particle Physics,"
   Phys. Rev. D 66 (2002) 010001.

3. **Franz Gross,**
   "Relativistic Quantum Mechanics and Field Theory,"
   Publisher: Wiley, John and Sons.

4. **F.E.C. Close,**

5. **A.D. Martin, T. Spearman,**
   "Elementary Particle Theory,"
   North Holland, Amsterdam, 1970

Getting started

- **Historical remarks**
- **Mesons and their quantum numbers**
- **Resonances in strong interactions**
- **Heavy quarks**
- **D and B mesons**

1 Getting started

1.1 Historical remarks

Nuclear interactions

- Hideki Yukawa, 1935, "On the Interaction of Elementary Particles. I." (Proc. Phys.-Math. Soc. Japan, 17, p. 48)
- Proposed a new field theory of nuclear forces
- Predicted the existence of a meson, now called π-meson or pion.

Coulomb potential **Strong Interaction**

$$eV_{QED} = \frac{e^2}{r} \quad \Longrightarrow \quad V_{strong} = \frac{g^2}{r} \cdot e^{-m_\pi r}$$

- Discovery of pion by C. Powell, 1947
- Nobel prize to Yukawa, 1949 $\hbar = c = 1$

Examples

The fine structure constant is defined as

$$\alpha = \frac{e^2}{4\pi\epsilon_0 \hbar c}, \alpha = 1/137.036$$

A second important number to remember is

$$\hbar c = 197.327 (\sim 200) \text{ MeV fm}$$

- What is the clasical electron radius ?

$$r_e = \frac{\alpha}{m_e} = \frac{197.327}{137.036 \; 0.511} \frac{\text{MeV fm}}{\text{MeV}} = 2.8 \text{ fm}$$

- Bohr formula

$$E_{mn} = E_R \left(\frac{1}{m^2} - \frac{1}{n^2} \right) \quad E_R = hcR_H = \tfrac{1}{2}\alpha^2 c^2 m_{red}$$

Strangeness

In 1947, Rochester and Butler found reactions of the type

$\pi^- p \to \Lambda K_s^0$

where both particles had long lifetimes.

$$\Lambda \to p\pi^- \qquad \tau = 2.6\ 10^{-10}\,\mathrm{s}$$

$$K_s^0 \to \pi^+\pi^- \qquad \tau = 0.9\ 10^{-10}\,\mathrm{s}$$

- **Particles are produced by strong interactions,**
- **and in pairs (associated prod., Pais, 1952)**
- **They decay by weak interaction**
- **Gell-Mann (1953) and Nishijima (1955) introduced additive quantum number, called strangeness.**
- **Proton, Neutron, Λ: building blocks ?**
- **Gell-Mann (1964): quark model with up, down, strange quarks.**

The particle zoo

A large number of strongly interacting particles were discovered,

- **3 pions at 135 MeV**

  π^+, π^- **with** $\tau = \mathbf{2.6\ 10^{-8}\,s}$ $\quad \pi^+ \rightarrow \mu^+\nu_\mu;\ \mu^+ \rightarrow \mathbf{e}^+\bar{\nu}_\mu\nu_\mathbf{e}$

  $\pi^\mathbf{0}$ **with** $\tau = \mathbf{8.4\ 10^{-17}\,s}$ $\quad \pi^\mathbf{0} \rightarrow \gamma\gamma$

- $\eta(\mathbf{547})$ **with** $\mathbf{\Gamma = 1.2\,keV}$ $\quad \eta(\mathbf{547}) \rightarrow \mathbf{2}\gamma,\ \mathbf{3}\pi^\mathbf{0},\ \pi^+\pi^-\pi^\mathbf{0},\ \pi^+\pi^-\gamma$

- $\eta'(\mathbf{958})$ **with** $\mathbf{\Gamma = 200\,keV}$ $\quad \rightarrow 2\gamma, 2\pi^0\eta, \pi^+\pi^-\eta, \pi^+\pi^-\gamma$

- $\mathbf{K}^+$, $\mathbf{K}^-$, $\mathbf{K}^0_s$, $\mathbf{K}^0_l$

- **3** $\rho^{+-\mathbf{0}}(\mathbf{770})$ **;** $\rho \rightarrow \mathbf{2}\pi; \mathbf{\Gamma = 150\,MeV}$

- **1** $\omega(\mathbf{782})$ **;** $\omega \rightarrow \pi^+\pi^-\pi^\mathbf{0}; \mathbf{\Gamma = 8.4\,MeV}$

- **4** $\mathbf{K}^*(\mathbf{892})$ **;** $\mathbf{K}^*(\mathbf{892}) \rightarrow \mathbf{K}\pi$

- **3** $\mathrm{a}_2(1320)$**; 1** $\mathrm{f}_2(1270)$**; 4** $\mathrm{K}_2(1430)$ **and** $\mathbf{\Gamma = 50\,MeV}$

- **... and many more.**

The quark model:

- **Mesons consist of a quark and an antiquark, $\mathbf{q\bar{q}}$**
  with the quarks u, d, s we expect families (with identical spin and parities) of 9 mesons.
  Example:

$$\pi^+, \pi^\mathbf{0}, \pi^-, \eta(\mathbf{548}), \eta'(\mathbf{958}), \mathbf{K}^+, \mathbf{K}^\mathbf{0}, \overline{\mathbf{K}}^\mathbf{0}, \mathbf{K}^-$$

$$\mathbf{K}^\mathbf{0} \pm \overline{\mathbf{K}}^\mathbf{0} \to \mathbf{K}^\mathbf{0}_\mathbf{s}, \mathbf{K}^\mathbf{0}_\mathbf{l}$$

- **Baryons consist of 3 quarks, qqq**
  We might expect (wrong !) families of 27 baryons
  but the Pauli principle reduces greatly the number of states.

1.2 Mesons and their quantum numbers

Quarks have Spin 1/2 and baryon number 1/3
Antiquarks have Spin 1/2 and baryon number -1/3
They couple to B=0 and Spin $S = 1$ **or** $S = 0$
Mesons (conventional) are $q\bar{q}$ **and thus may have the following properties:**

- **Parity** $P = (-1)^{L+1}$
  Parity of angular momentum $P = (-1)^L$
  Quarks have intrinsic parity $P = 1$
  Antiquarks have intrinsic parity $P = -1$
- **Charge conjugation** $C = (-1)^{L+S}$
  defined for neutral mesons only
- **Isospin** I
- G**-parity** $G = (-1)^{L+1+I}$
  G**-parity is conserved in strong interactions**
  (Not conserved when chiral symmetry is broken !)

Note:

- $\mathbf{J^{PC}}$ **are measured quantities.**
- $\mathbf{^{2s+1}L_J}$ **are internal quantum numbers in a non-relativistic quark model**

		J^{PC}	$^{2s+1}L_J$	I=1	I=0 ($n\bar{n}$)	I=0 $s\bar{s}$	Strange
L=0	S=0	0^{-+}	$^1S_0$	π	η	η'	K
	S=1	1^{--}	$^3S_1$	ρ	ω	ϕ	K^*
L=1	S=0	1^{+-}	$^1P_1$	b_1	h_1	h'_1	K_1
	S=1	0^{++}	$^3P_0$	a_0	f_0	f'_0	K^*_0
		1^{++}	$^3P_1$	a_1	f_1	f'_1	K_1
		2^{++}	$^3P_2$	a_2	f_2	f'_2	K^*_2

L=2	**S=0**	$\mathbf{2^{-+}}$	$\mathbf{^1D_2}$	$\pi_\mathbf{2}$	$\eta_\mathbf{2}$	$\eta'_\mathbf{2}$	$\mathbf{K_2}$
	S=1	$\mathbf{1^{--}}$	$\mathbf{^3D_1}$	ρ	ω	ϕ	$\mathbf{K_1^*}$
		$\mathbf{2^{--}}$	$\mathbf{^3D_2}$	$\rho_\mathbf{2}$	$\omega_\mathbf{2}$	$\phi_\mathbf{2}$	$\mathbf{K_2}$
		$\mathbf{3^{--}}$	$\mathbf{^3D_3}$	$\rho_\mathbf{3}$	$\omega_\mathbf{3}$	$\phi_\mathbf{3}$	$\mathbf{K_3^*}$
L=3	**S=0**	$\mathbf{3^{+-}}$	$\mathbf{^1F_3}$	$\mathbf{b_3}$	$\mathbf{h}$	$\mathbf{h'_3}$	$\mathbf{K_3}$
	S=1	$\mathbf{2^{++}}$	$\mathbf{^3F_2}$	$\mathbf{a_2}$	$\mathbf{f_2}$	$\mathbf{f'_2}$	$\mathbf{K_2^*}$
		$\mathbf{3^{++}}$	$\mathbf{^3F_3}$	$\mathbf{a_3}$	$\mathbf{f_3}$	$\mathbf{f'_3}$	$\mathbf{K_3}$
		$\mathbf{4^{++}}$	$\mathbf{^3F_4}$	$\mathbf{a_4}$	$\mathbf{f_4}$	$\mathbf{f'_4}$	$\mathbf{K_4^*}$
L=4	**S=0**	$\mathbf{4^{-+}}$	$\mathbf{^1G_2}$	$\pi_\mathbf{4}$	$\eta_\mathbf{4}$	$\eta'_\mathbf{4}$	$\mathbf{K_4}$
	S=1	$\mathbf{3^{--}}$	$\mathbf{^3G_1}$	$\rho_\mathbf{3}$	$\omega_\mathbf{3}$	$\phi_\mathbf{3}$	$\mathbf{K_3^*}$
		$\mathbf{4^{--}}$	$\mathbf{^3G_2}$	$\rho_\mathbf{4}$	$\omega_\mathbf{4}$	$\phi_\mathbf{4}$	$\mathbf{K_4}$
		$\mathbf{5^{--}}$	$\mathbf{^3G_3}$	$\rho_\mathbf{5}$	$\omega_\mathbf{5}$	$\phi_\mathbf{5}$	$\mathbf{K_5^*}$

The nonet of pseudoscalar mesons $\mathbf{J^{PC} = 0^{-+}}$

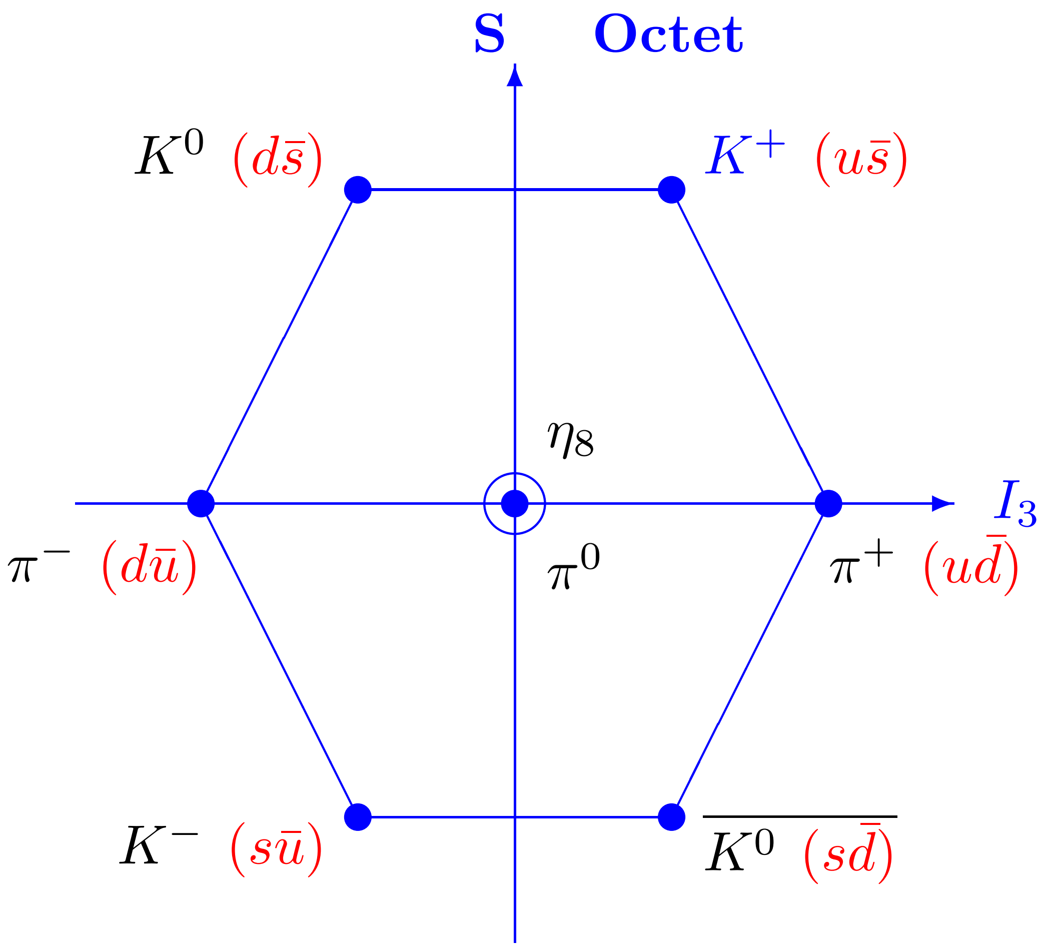

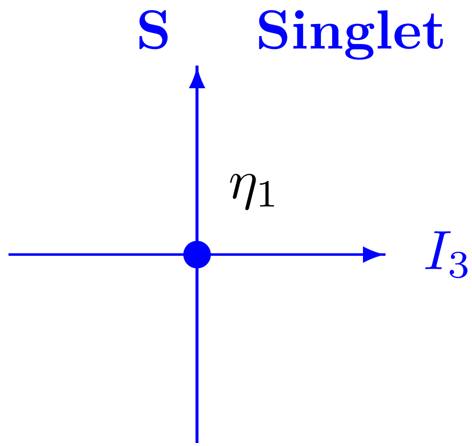

$$|\pi^0> = \frac{1}{\sqrt{2}}(\mathbf{u\bar{u} + d\bar{d}});$$

$$|\eta_8> = \frac{1}{\sqrt{6}}\left(\mathbf{u\bar{u} + d\bar{d} - 2s\bar{s}}\right) \quad ; \qquad |\eta_1> = \frac{1}{\sqrt{3}}\left(\mathbf{u\bar{u} + d\bar{d} + s\bar{s}}\right)$$

Mixing angles and GMO formulae

$$|\eta> = \quad \cos\Theta_{ps}|\eta_8> - \quad \sin\Theta_{ps}|\eta_1>$$
$$|\eta'> = \quad \sin\Theta_{ps}|\eta_8> + \quad \cos\Theta_{ps}|\eta_1>$$

Extension to include a possible glueball content:

$$|\eta> = \quad X_\eta \cdot \frac{1}{\sqrt{2}}\left(u\bar{u} + d\bar{d}\right) + \quad Y_\eta \cdot (s\bar{s}) + \quad Z_\eta \cdot (\text{glue})$$
$$|\eta'> = \quad X_{\eta'} \cdot \frac{1}{\sqrt{2}}\left(u\bar{u} + d\bar{d}\right) + \quad Y_{\eta'} \cdot (s\bar{s}) + \quad Z_{\eta'} \cdot (\text{glue})$$

light quark **strange quark** **inert**

$$Z_\eta = Z_{\eta'} \sim 0$$

See: T. Feldmann,
"Quark structure of pseudoscalar mesons,"
Int. J. Mod. Phys. A15 (2000) 159

Mixing angles, examples

$$\boldsymbol{\Theta_{PS} = 0} \qquad \begin{aligned} |\eta> &= \frac{1}{\sqrt{6}}\left(u\bar{u} + d\bar{d} - 2s\bar{s}\right) \\ |\eta'> &= \frac{1}{\sqrt{3}}\left(u\bar{u} + d\bar{d} + s\bar{s}\right) \end{aligned}$$

$$\boldsymbol{\Theta_{PS} = -11.1^\circ} \qquad \begin{aligned} |\eta> &= \frac{1}{\sqrt{2}}\left(\frac{1}{\sqrt{2}}(u\bar{u} + d\bar{d}) - s\bar{s}\right) \\ |\eta'> &= \frac{1}{\sqrt{2}}\left(\frac{1}{\sqrt{2}}(u\bar{u} + d\bar{d}) + s\bar{s}\right) \end{aligned}$$

$$\boldsymbol{\Theta_{PS} = -19.3^\circ} \qquad \begin{aligned} |\eta> &= \frac{1}{\sqrt{3}}\left(u\bar{u} + d\bar{d} - s\bar{s}\right) \\ |\eta'> &= \frac{1}{\sqrt{6}}\left(u\bar{u} + d\bar{d} + 2s\bar{s}\right) \end{aligned}$$

$$\boldsymbol{\Theta_{PS} = 35.3^\circ} \qquad \begin{aligned} |\eta> &= s\bar{s} \\ |\eta'> &= \frac{1}{\sqrt{2}}\left(u\bar{u} + d\bar{d}\right) \end{aligned}$$

The nonet of vector mesons $\mathbf{J^{PC} = 1^{--}}$

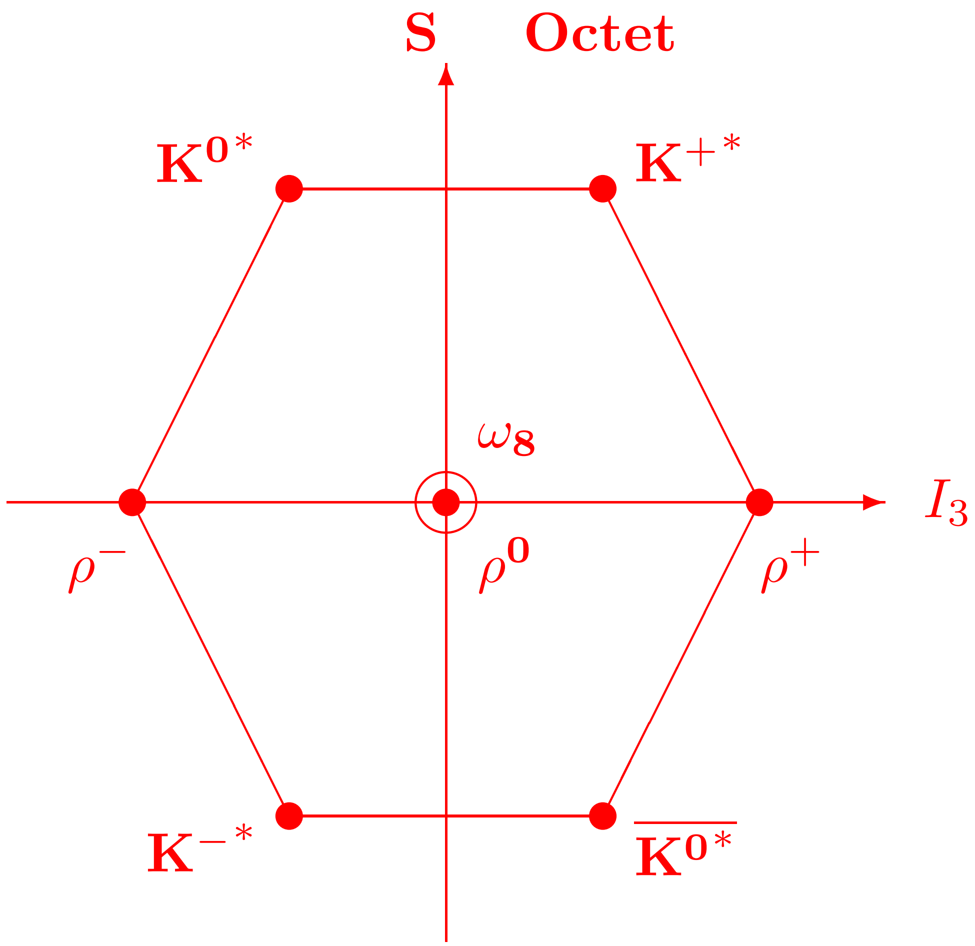

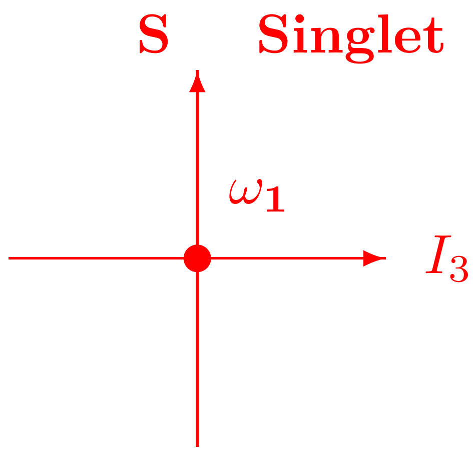

The nonet of tensor mesons $J^{PC} = 2^{++}$

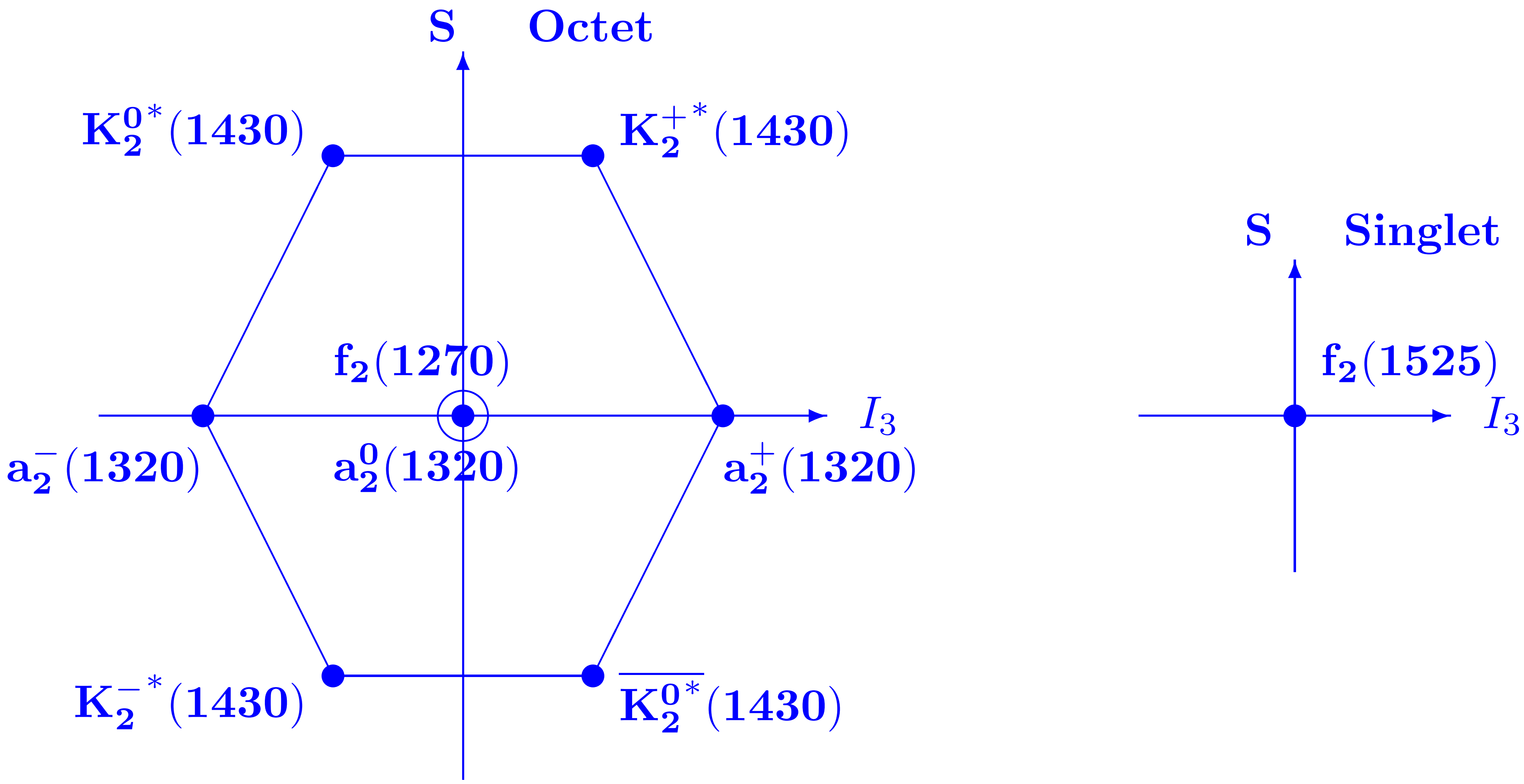

$\Theta_V = 35.3^\circ$	$\vert\omega>$	$=$	$\frac{1}{\sqrt{2}}\left(u\bar{u} + d\bar{d}\right)$	$=$	$f_2(1270)$	$\Theta_T = 35.3^\circ$
	$\vert\Phi>$	$=$	$s\bar{s}$	$=$	$f_2(1525)$	

The Gell-Mann-Okubo mass formula

$$\mathbf{M_\pi = M_0 + 2M_q}$$

$$\mathbf{M_K = M_0 + M_q + M_s}$$

$$\mathbf{M_\eta = M_8 \cos^2 \Theta + M_1 \sin^2 \Theta}$$

$$\mathbf{M_{\eta'} = M_8 \sin^2 \Theta + M_1 \cos^2 \Theta}$$

$$\mathbf{M_1 = M_0 + 4/3M_q + 2/3M_s}$$

$$\mathbf{M_8 = M_0 + 2/3M_q + 4/3M_s}$$

Quadratic mass formula:

$$\cos^2 \Theta = \frac{3M_\eta^2 + M_\pi^2 - 4M_K^2}{4M_K^2 - 3M_{\eta'}^2 - M_\pi^2}$$

Linear mass formula:

$$\cos^2 \Theta = \frac{3M_\eta + M_\pi - 4M_K}{4M_K - 3M_{\eta'} - M_\pi}$$

Nonet members	Θ_{linear}	Θ_{quad}
$\pi, \mathbf{K}, \eta', \eta$	-23°	-10°
$\rho, \mathbf{K}^*, \mathbf{\Phi}\ , \omega$	36°	39°
$\mathbf{a_2(1320), K_2^*(1430), f_2(1525), f_2(1270)}$	26°	29°

1.3 Resonances in strong interactions

- **In 1952, E. Fermi and collaborators measured the cross section for $\pi^+ p \to \pi^+ p$ and found it steeply raising.**

H. L. Anderson, E. Fermi, E. A. Long and D. E. Nagle, "Total cross-sections of positive pions in hydrogen," Phys. Rev. 85 (1952) 936.

$\Delta^{++}(1232)$: **width 150 MeV**

$\hbar/\Gamma \sim 0.45\ 10^{-23}$ s

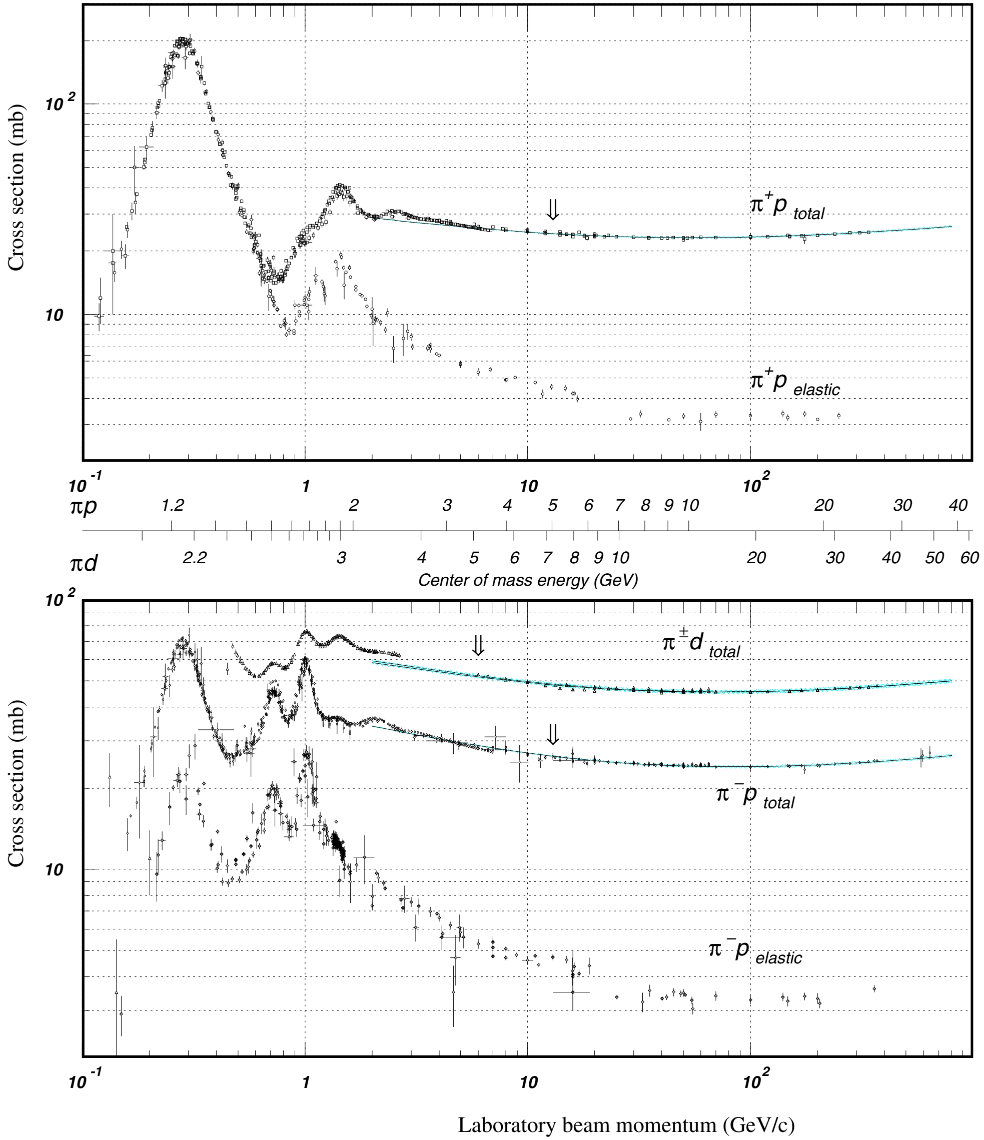

Clebsch Gordon coefficients

Maximum cross section:

- $\sigma_{\mathbf{tot},\pi^+\mathbf{p}} = \mathbf{210\,mb}$
- $\sigma_{\mathbf{el},\pi^+\mathbf{p}} = \mathbf{210\,mb}$
- $\sigma_{\mathbf{tot},\pi^-\mathbf{p}} = \mathbf{70\,mb}$
- $\sigma_{\mathbf{el},\pi^-\mathbf{p}} = \mathbf{23\,mb}$

WHY ?

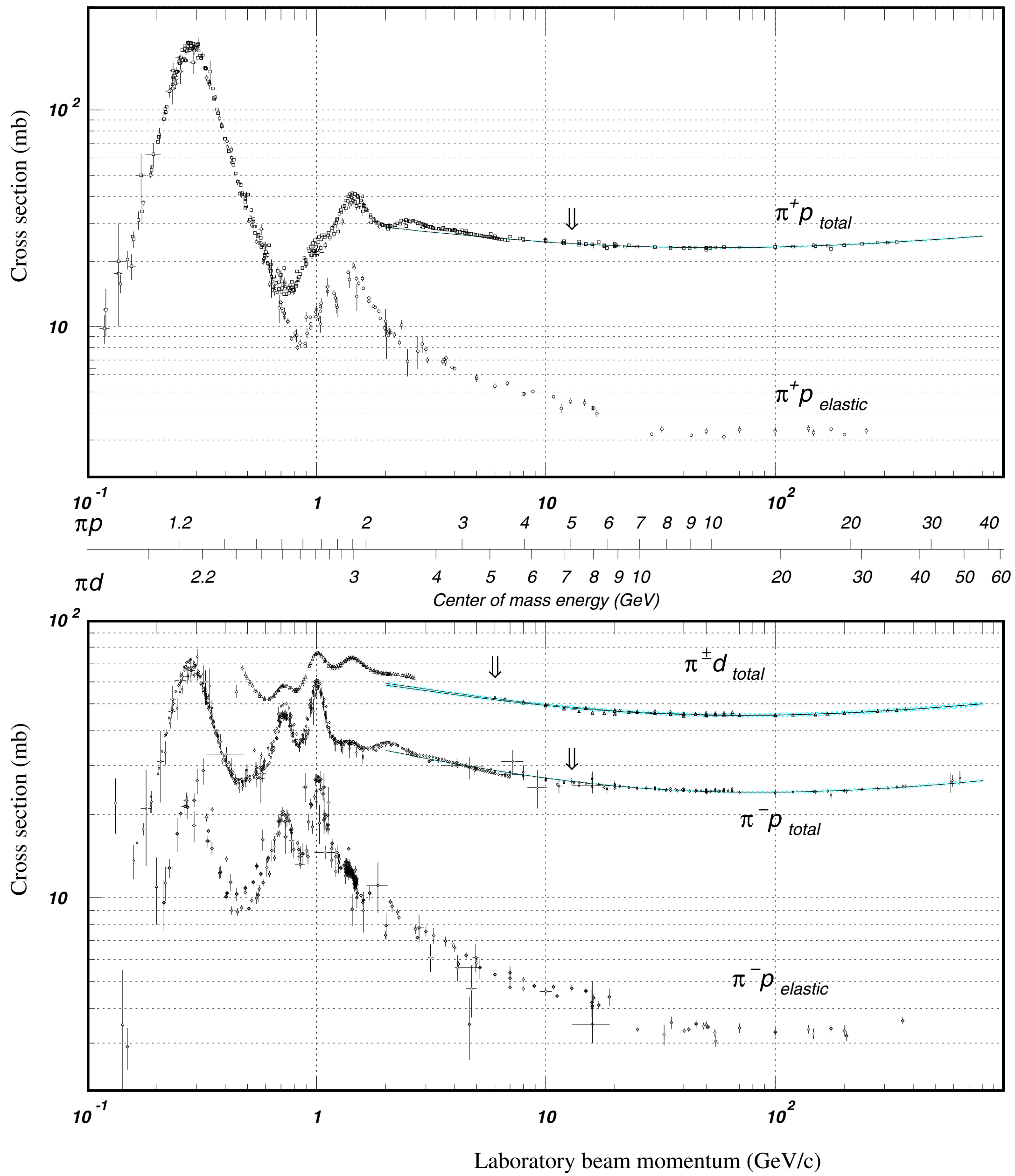

Notation:

		J	J	...
		M	M	...
m_1	m_2	Coefficients		
m_1	m_2			
.	.			

1/2×1/2

		1
		+1
+1/2	+1/2	1

		1	0
		0	0
+1/2	−1/2	1/2	1/2
−1/2	+1/2	1/2	−1/2

		1
		−1
−1/2	−1/2	1

1×1/2

		3/2
		+3/2
+1	+1/2	1

		3/2	1/2
		+1/2	+1/2
+1	−1/2	1/3	2/3
0	+1/2	2/3	−1/3

		3/2	1/2
		−1/2	−1/2
0	−1/2	2/3	1/3
−1	+1/2	1/3	−2/3

		3/2
		−3/2
−1	−1/2	1

2×1

		3
		+3
+2	+1	1

		3	2
		+2	+2
+2	0	1/3	2/3
+1	+1	2/3	−1/3

		3	2	1
		+1	+1	+1
+2	−1	1/15	1/3	3/5
+1	0	8/15	1/6	−3/10
0	+1	6/15	−1/2	1/10

		3	2	1
		0	0	0
+1	−1	1/5	1/2	3/10
0	0	3/5	0	−2/5
−1	+1	1/5	−1/2	3/10

		3	2	1
		−1	−1	−1
0	−1	6/15	1/2	1/10
−1	0	8/15	−1/6	−3/10
−2	+1	1/15	−1/3	3/5

		3	2
		−2	−2
−1	−1	2/3	1/3
−2	0	1/3	−2/3

		3
		−3
−2	−1	1

1×1

		2
		+2
+1	+1	1

		2	1
		+1	+1
+1	0	1/2	1/2
0	+1	1/2	−1/2

		2	1	0
		0	0	0
+1	−1	1/6	1/2	1/3
0	0	2/3	0	−1/3
−1	+1	1/6	−1/2	1/3

		2	1
		−1	−1
0	−1	1/2	1/2
−1	0	1/2	−1/2

		2
		−2
−1	−1	1

3/2×1

		5/2
		+5/2
+3/2	+1	1

		5/2	3/2
		+3/2	+3/2
+3/2	0	2/5	3/5
+1/2	+1	3/5	−2/5

		5/2	3/2	1/2
		+1/2	+1/2	+1/2
+3/2	−1	1/10	2/5	1/2
+1/2	0	3/5	1/15	−1/3
−1/2	+1	3/10	−8/15	1/6

		5/2	3/2	1/2
		−1/2	−1/2	−1/2
+1/2	−1	3/10	8/15	1/6
−1/2	0	3/5	−1/15	−1/3
−3/2	+1	1/10	−2/5	1/2

		5/2	3/2
		−3/2	−3/2
−1/2	−1	3/5	2/5
−3/2	0	2/5	−3/5

		5/2
		−5/2
−3/2	−1	1

2×1/2

		5/2
		+5/2
+2	1/2	1

		5/2	3/2
		3/2	+3/2
+2	−1/2	1/5	4/5
+1	+1/2	4/5	−1/5

		5/2	3/2
		+1/2	+1/2
+1	−1/2	2/5	3/5
0	+1/2	3/5	−2/5

		5/2	3/2
		−1/2	−1/2
0	−1/2	3/5	2/5
−1	+1/2	2/5	−3/5

		5/2	3/2
		−3/2	−3/2
−1	−1/2	4/5	1/5
−2	+1/2	1/5	−4/5

		5/2
		−5/2
−2	−1/2	1

3/2×1/2

		2
		+2
+3/2	+1/2	1

		2	1
		+1	+1
+3/2	−1/2	1/4	3/4
+1/2	+1/2	3/4	−1/4

		2	1
		0	0
+1/2	−1/2	1/2	1/2
−1/2	+1/2	1/2	−1/2

		2	1
		−1	−1
−1/2	−1/2	3/4	1/4
−3/2	+1/2	1/4	−3/4

		2
		−2
−3/2	−1/2	1

- $\sigma_{\mathbf{tot},\pi^+\mathbf{p}} = \sigma_{\pi^+\mathbf{p}\to\pi^+\mathbf{p}} = \mathbf{CG}_{(\mathbf{I=1/2,I_3=1/2})+(\mathbf{I=1,I_3=1})\to\ (\mathbf{I=3/2,I_3=3/2})} \times \mathbf{CG}_{(\mathbf{I=3/2,I_3=3/2})\to\ (\mathbf{I=1/2,I_3=1/2})+(\mathbf{I=1,I_3=1})} = \mathbf{1} \times \mathbf{1} \propto \mathbf{210\,mb}$

- $\sigma_{\mathbf{el},\pi^+\mathbf{p}} = \sigma_{\pi^+\mathbf{p}\to\pi^+\mathbf{p}} = \mathbf{CG}_{(\mathbf{I=1/2,I_3=1/2})+(\mathbf{I=1,I_3=1})\to\ (\mathbf{I=3/2,I_3=3/2})} \times \mathbf{CG}_{(\mathbf{I=3/2,I_3=3/2})\to\ (\mathbf{I=1/2,I_3=1/2})+(\mathbf{I=1,I_3=1})} = \mathbf{1} \times \mathbf{1} \propto \mathbf{210\,mb}$

- $\sigma_{\mathbf{tot},\pi^-\mathbf{p}} = \sigma_{\pi^-\mathbf{p}\to\pi^-\mathbf{p}} + \sigma_{\pi^-\mathbf{p}\to\pi^0\mathbf{n}} = \mathbf{CG}_{(\mathbf{I=1/2,I_3=1/2})+(\mathbf{I=1,I_3=-1})\to\ (\mathbf{I=3/2,I_3=-1/2})} + \mathbf{CG}_{(\mathbf{I=1/2,I_3=-1/2})+(\mathbf{I=1,I_3=0})+(\mathbf{I=3/2,I_3=-1/2})} = \mathbf{1/3 \times 2/3 + 1/3 \times 1/3} \propto \mathbf{70\,mb}$

- $\sigma_{\mathbf{el},\pi^-\mathbf{p}} = \sigma_{\pi^-\mathbf{p}\to\pi^-\mathbf{p}} = \mathbf{CG}_{(\mathbf{I=1/2,I_3=1/2})+(\mathbf{I=1,I_3=-1})\to\ (\mathbf{I=3/2,I_3=-1/2})} \times \mathbf{CG}_{(\mathbf{I=3/2,I_3=-1/2})\to\ (\mathbf{I=1/2,I_3=1/2})+(\mathbf{I=1,I_3=-1})} = \mathbf{1/3 \times 1/3} \propto \mathbf{23\,mb}$

1.4 Heavy Quarks

Discovery of the J/ψ

A narrow resonance was discovered in the 1974 "November revolution of particle physics" in two reactions:

- **Proton + Be $\rightarrow$ e^+e^- + anything**
  at the BNL (Long Island, New York)
  J. J. Aubert *et al.*, "Experimental observation of a heavy particle J," Phys. Rev. Lett. 33, 1404 (1974).

- **e^+e^- annihilation to hadrons $\mu^+\mu^-, e^+e^-$**
  in the SPEAR storage ring at Stanford
  J. E. Augustin *et al.*, "Discovery of a narrow resonance in e^+e^- annihilation," Phys. Rev. Lett. 33, 1406 (1974).

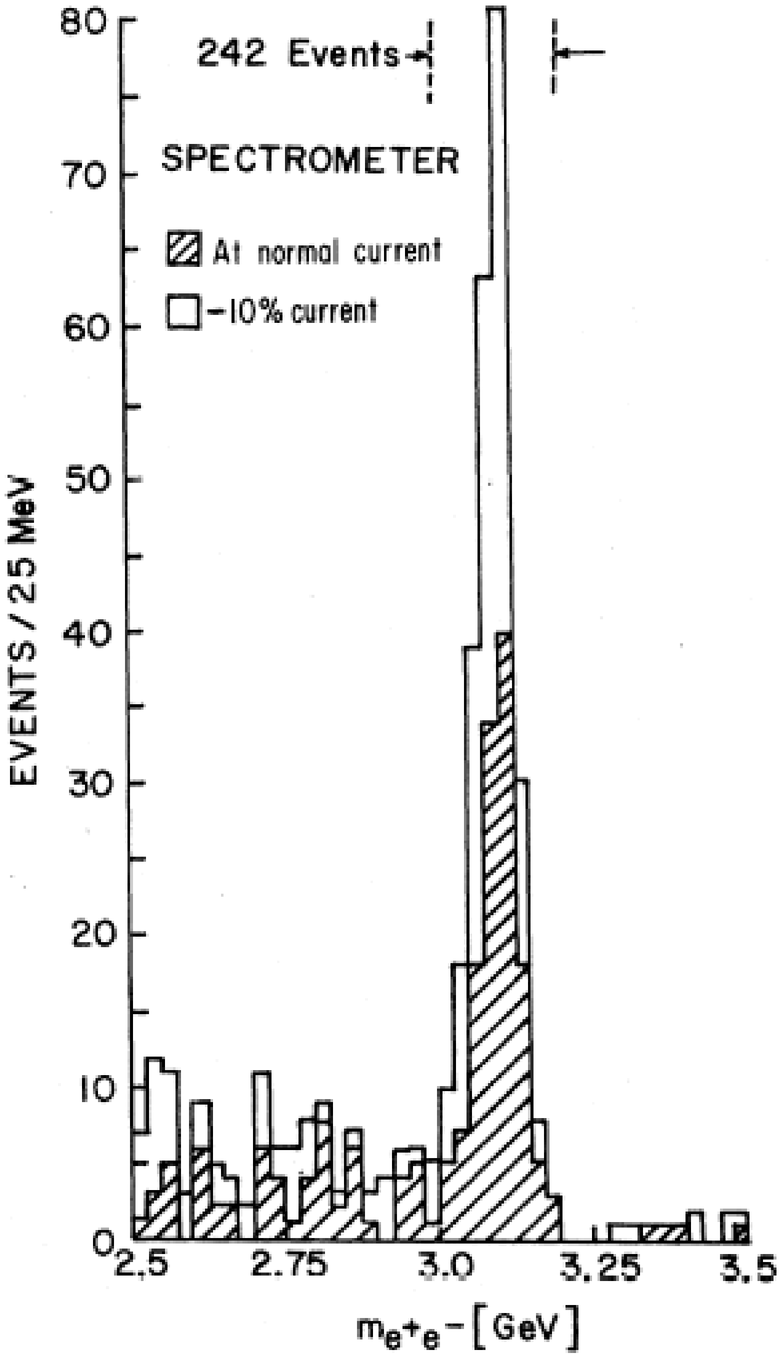

Observation of a heavy particle J
J. J. Aubert et al.

Electrons and positrons are identified by Cerenkov radiation and time and flight, their momenta are measured in two spectrometers.

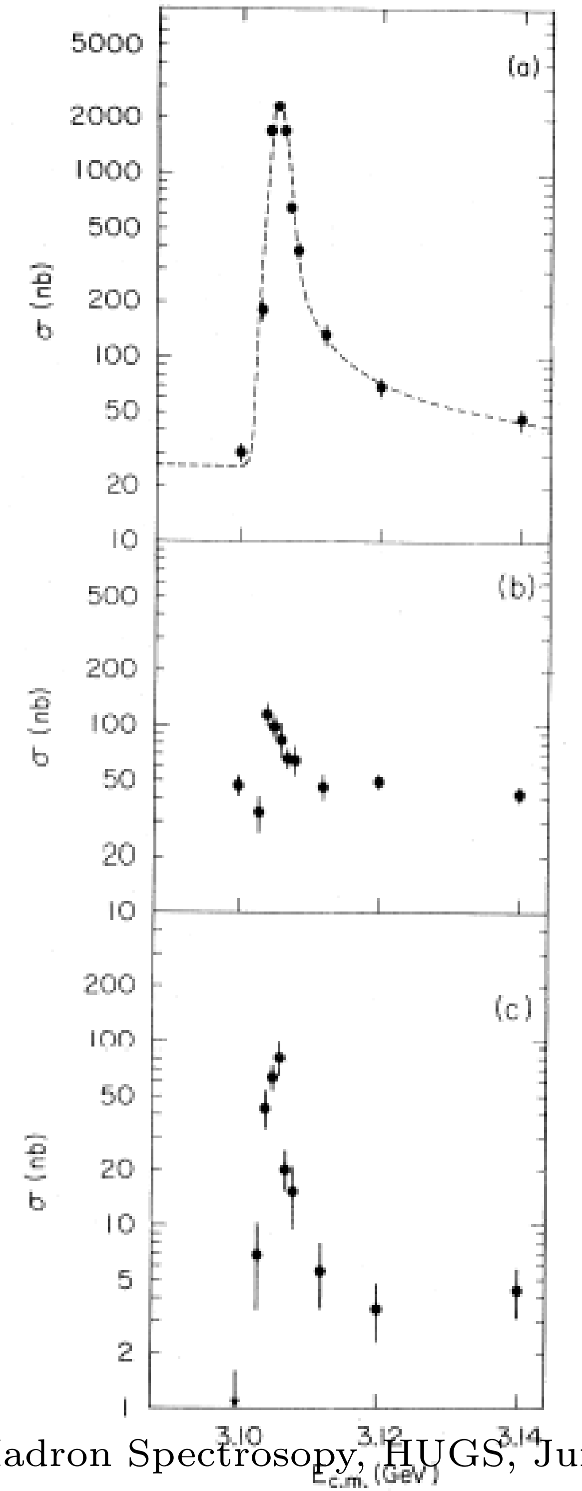

Discovery of a Narrow Resonance (ψ) in e^+e^- Annihilation

J.E. Augustin et al.

Results from the SPEAR e^+e^- storage ring. Width of the resonance is less than 1.3 MeV. Due to production mode spin, parity and charge conjugation are likely $J^{PC} = 1^{--}$ (as the ρ-meson).

Narrow resonance: $\rightarrow$ OZI rule $\rightarrow$ new quantum number charm:

$$\mathbf{J/\psi = c\bar{c}}$$

The curve is asymmetric due to photon radiation. Interference is seen between intermediate photon and J/ψ production.

Width of the J/ψ

The J/ψ mass is (3096.87 ± 0.04) MeV, the width 87 ± 5 keV.
Comparison: ρ mass is 770 MeV, its width 150 MeV.
The J/ψ is extremely narrow. How narrow? See PDG

Total cross section:

$$\sigma(E) = (4\pi)(\lambda^2/4\pi^2)\frac{\Gamma^2/4}{[(E-E_R)+\Gamma^2/4)]}\frac{2J+1}{(2s_1+1)(2s_2+1)}$$

with $\lambda/2\pi = 1/p = 2/E$ de Broglie wave length of e^+ and e^- in cms
E cms energy, Γ total width.

In case of specific reactions, like $e^+e^- \to \psi \to e^+e^-$, replace

$$\Gamma^2 \to \Gamma_{\text{initial}}\Gamma_{\text{final}} = \Gamma^2_{e^+e^-}.$$

$\Gamma_{e^+e^-}$ partial width
$s_1 = s_2 = 1/2$ electron (positron) spin; J=1 spin of J/ψ

Then:

$$\sigma(\mathbf{E_{e^+e^-\to\psi\to e^+e^-}}) = (\mathbf{3}\pi)(\lambda^{\mathbf{2}}/\mathbf{4}\pi^{\mathbf{2}})\frac{\mathbf{\Gamma^2_{e^+e^-}/4}}{\mathbf{(E-E_R)+\Gamma^2/4}}$$

Substituting $\tan\theta = \mathbf{2(E-E_R)/\Gamma}$**:**

$$\int_{\mathbf{0}}^{\infty}\sigma(\mathbf{E})\mathbf{dE} = \frac{\mathbf{3}\pi^{\mathbf{2}}}{\mathbf{2}}\frac{\lambda^{\mathbf{2}}}{\mathbf{4}\pi^{\mathbf{2}}}\frac{\mathbf{\Gamma^2_{e^+e^-}}}{\mathbf{\Gamma^2}}\mathbf{\Gamma}.$$

This results in

$$\mathbf{\Gamma^2_{e^+e^-}} = \frac{\mathbf{6}\pi^{\mathbf{2}}}{\mathbf{E^2\Gamma}}$$

$$\mathbf{\Gamma} = \mathbf{\Gamma_{e^+e^-}} + \mathbf{\Gamma}_{\mu^+\mu^-} + \mathbf{\Gamma_{hadrons}}$$

Imposing $\mathbf{\Gamma_{e^+e^-}} = \mathbf{\Gamma}_{\mu^+\mu^-}$ **yields 3 equations and thus 3 unknown widths.**

The OZI rule and flavor tagging

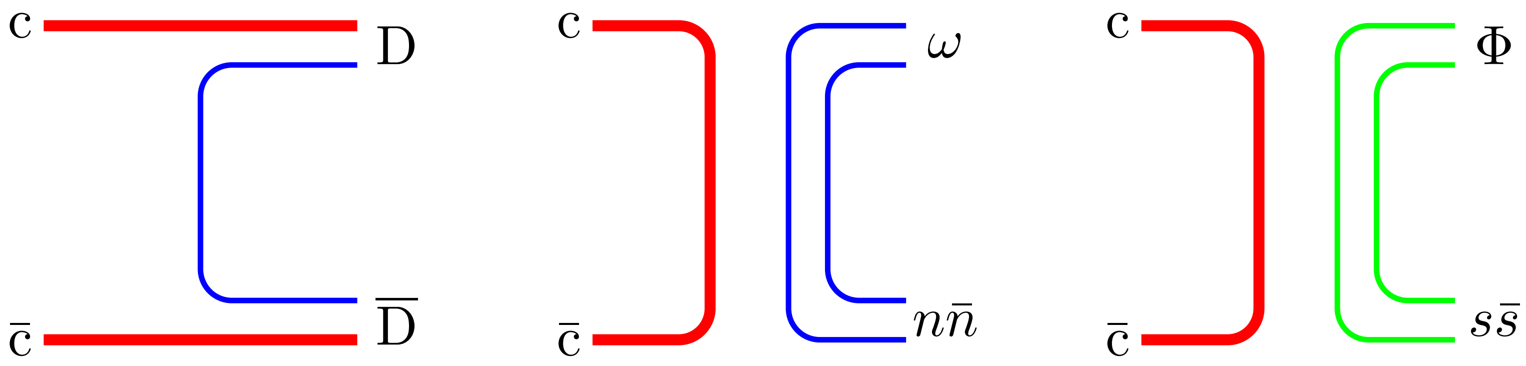

The decay J/ψ into mesons with open charm (left) is forbidden due to energy conservation. The two right diagrams require annihilation of c$\bar{c}$ into gluons. This is suppressed.

Recoiling against an ω, mesons with n$\bar{n}$ quark structure are expected. If a Φ is observed we expect mesons with hidden strangeness s$\bar{s}$.

Example: The ratio $\Phi\eta'/\omega\eta'$ is proportional to the ratio of s$\bar{s}$/n$\bar{n}$ in the η' wave function.

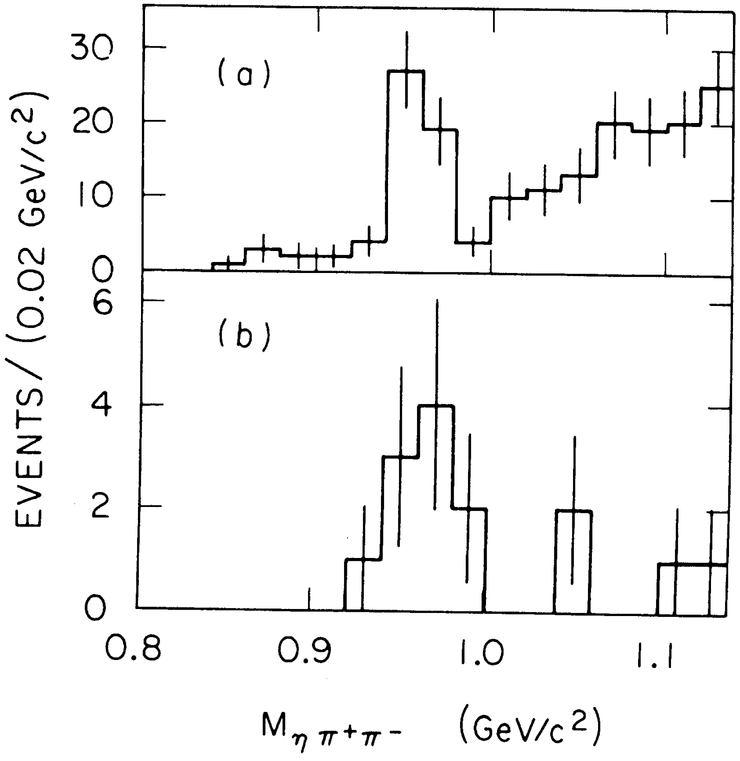

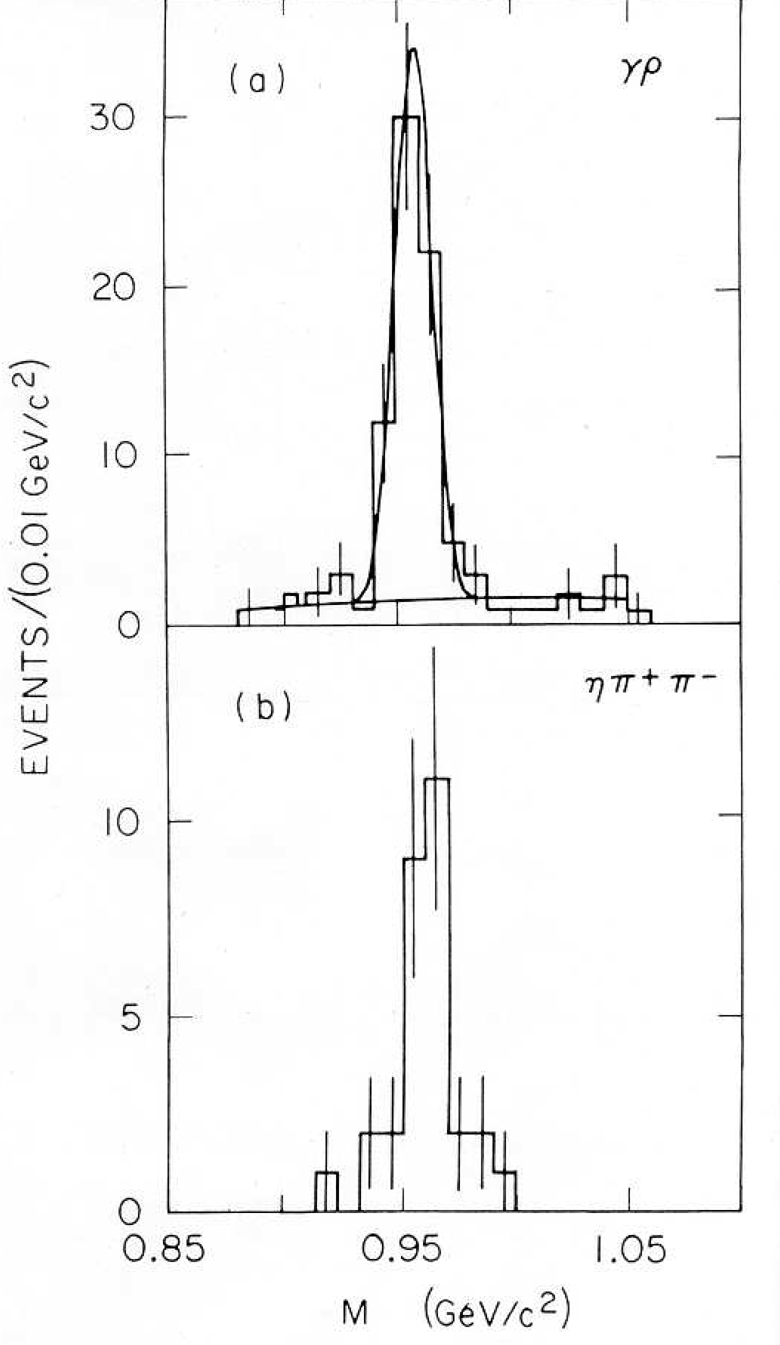

J/ψ $\rightarrow$ $\omega\eta'$ (top)

$\Phi\eta'$ (right)

D. Coffman *et al.* [MARK-III Collaboration], "Measurements of J/ψ decays into a vector and a pseudoscalar meson," Phys. Rev. D 38, 2695 (1988) [Erratum-ibid. D 40, 3788 (1989)].

$\Rightarrow$ $\mathbf{\Theta}_{\text{pseudoscalar}}$

Cross section $e^+e^- \to$ hadrons.

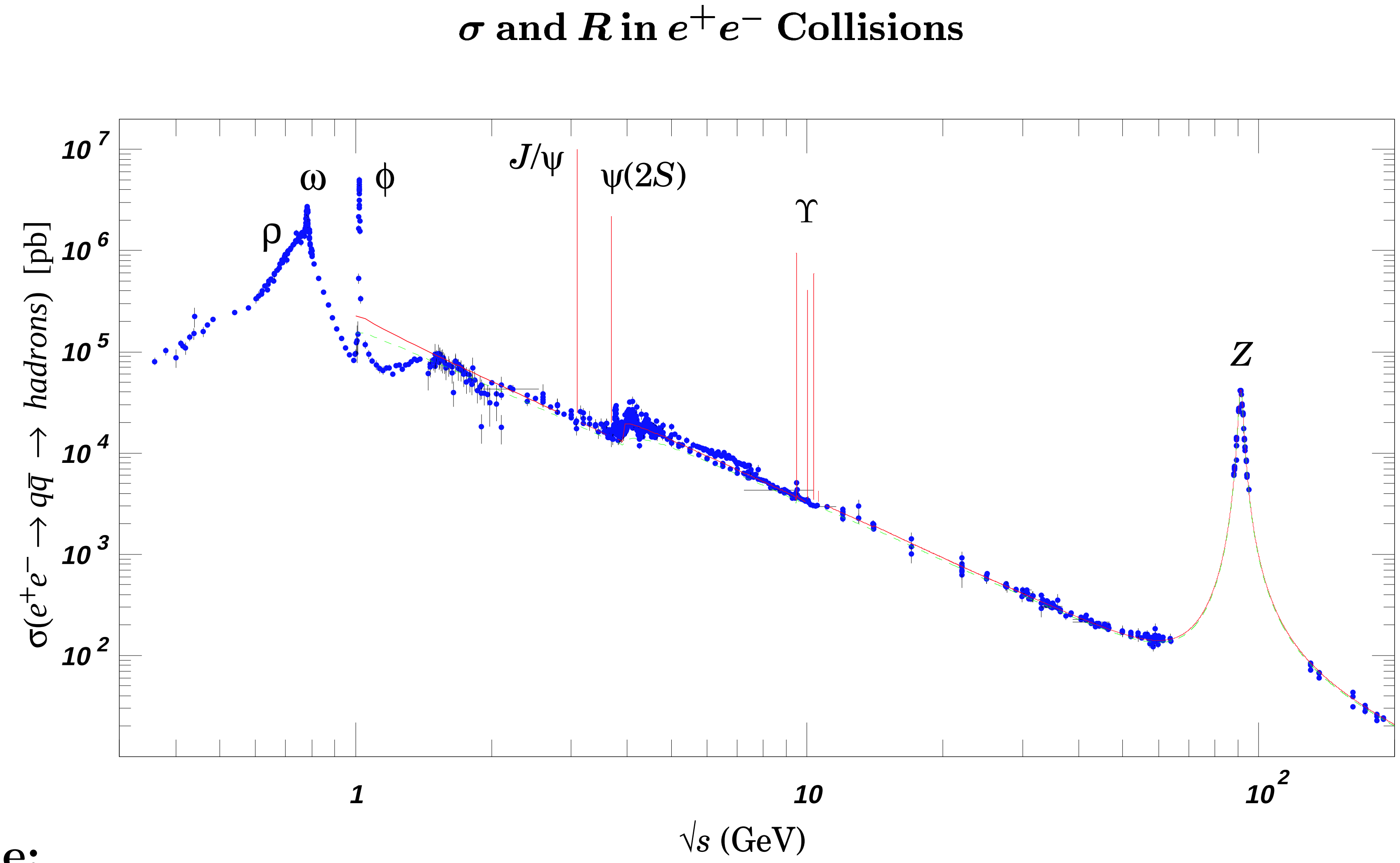

Note:

- **At low energies dominated by ρ, ω, Φ**
- **Cross section is given by $4\pi\alpha^2/3\,s\sum Q_i^2$**

- There are two narrow $c\bar{c}$ and three narrow $b\bar{b}$ states.
- Above a new flavor threshold, the cross section increases by $3e_q^2$
- The ratio R of cross section for $e^+e^- \rightarrow$ hadrons over that to $\mu^+\mu^-$ is given by $R = 3 \times \sum e_q^2$ and increases above quark-antiquark thresholds.

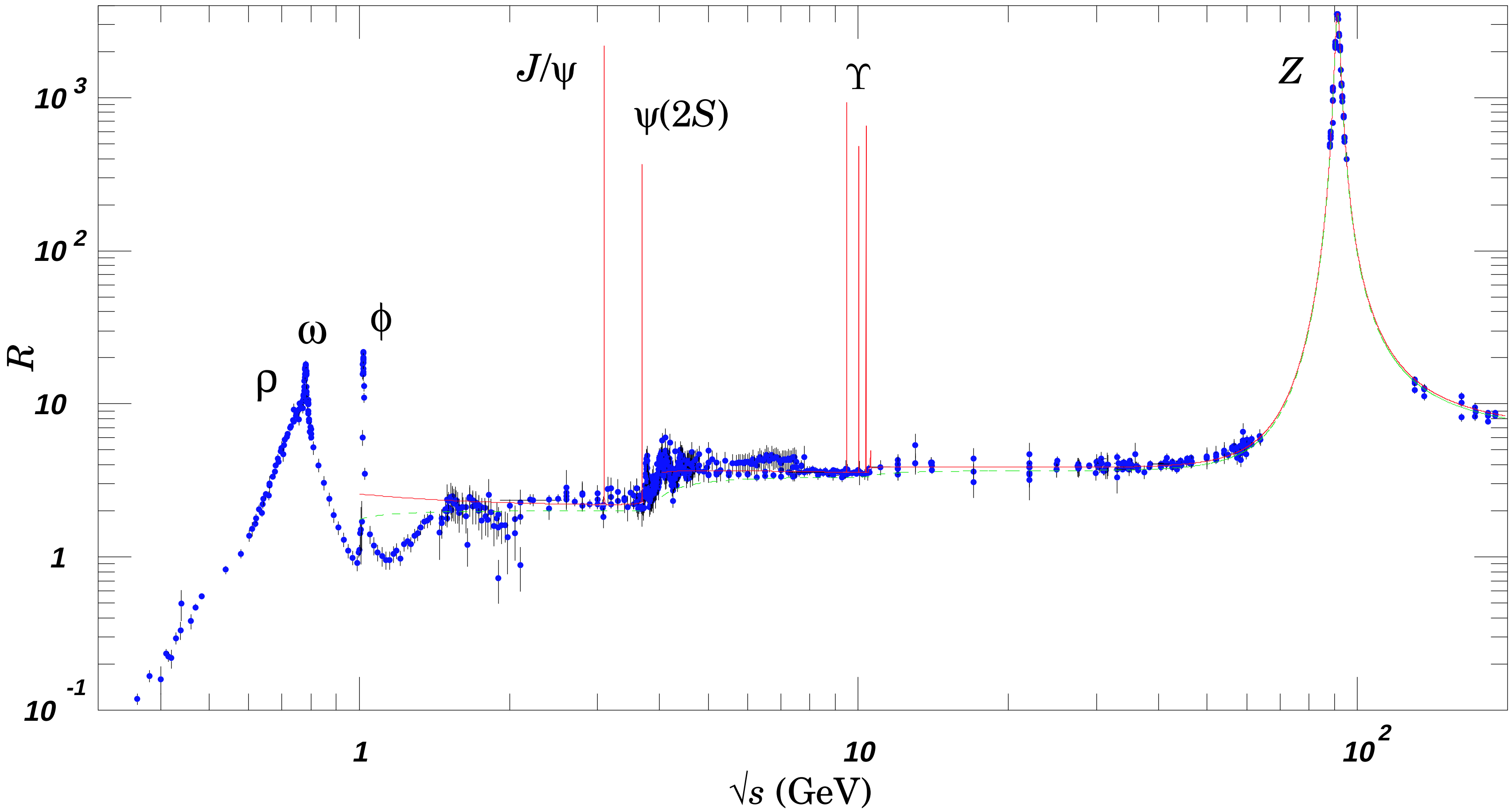

- A closer look reveals additional peaks in the cross sections, decaying into mesons with open charm like D^+D^- or $D^0\overline{D^0}$.
- Mass $D^\pm = 1870\,\mathrm{MeV}$ $D^0 = 1865\,\mathrm{MeV}$
- Quark content: $c\bar{d}$ and $d\bar{c}$ $c\bar{u}$ and $u\bar{c}$

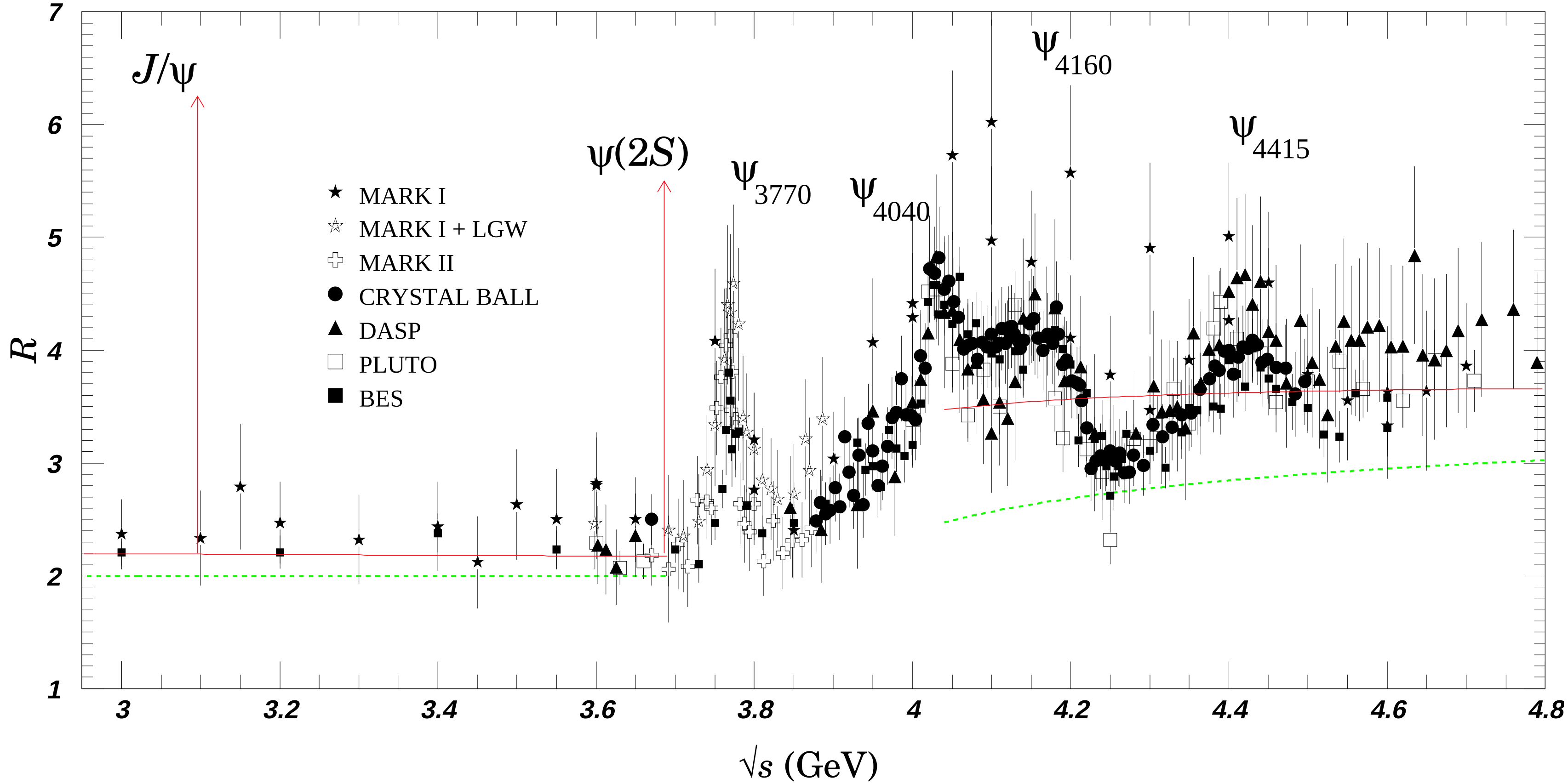

$e^+e^- \rightarrow$ hadrons versus $\mu^+\mu^-$ in the $c\bar{c}$ region.

All resonances have $J^{PC} = 1^{--}$

$\mathbf{J/\psi \to e^+e^-}$

Van Royen Weisskopf equation (from ortho-positronium decay):

$$\Gamma(J/\psi \to e^+e^-) = \frac{16\pi\alpha^2 Q^2}{M_V^2}|\psi(0)|^2$$

Here, Q^2 is the squared sum of contributing quark charges:

Meson	wave function	Q^2	
ρ^0:	$\frac{1}{\sqrt{2}}\left(u\bar{u} - d\bar{d}\right)$	$\left[\frac{1}{\sqrt{2}}\left(2/3 - (-1/3)\right)\right]^2$	$1/2$
ω:	$\frac{1}{\sqrt{2}}\left(u\bar{u} + d\bar{d}\right)$	$\left[\frac{1}{\sqrt{2}}\left(2/3 + (-1/3)\right)\right]^2$	$1/18$
Φ:	$(s\bar{s})$	$(1/3)^2$	$1/9$
J/ψ:	$(c\bar{c})$	$(2/3)^2$	$4/9$

Important: Photon couples to ρ in amplitude 3 times stronger than to ω.

Charmonium states in radiative decays

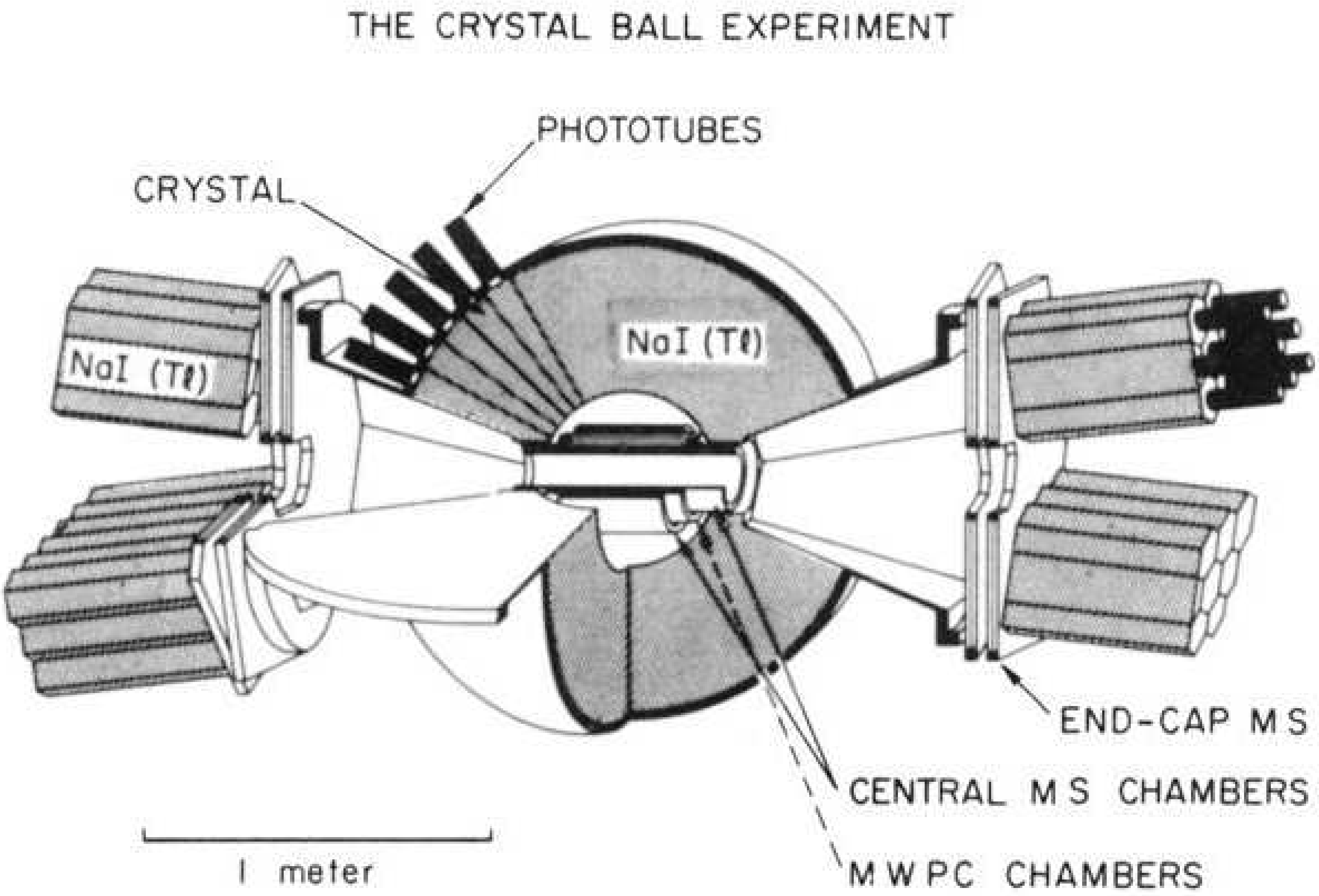

The Crystal Ball detector.

The Crystal Ball: γ from $\psi(2S)$, background subtracted.

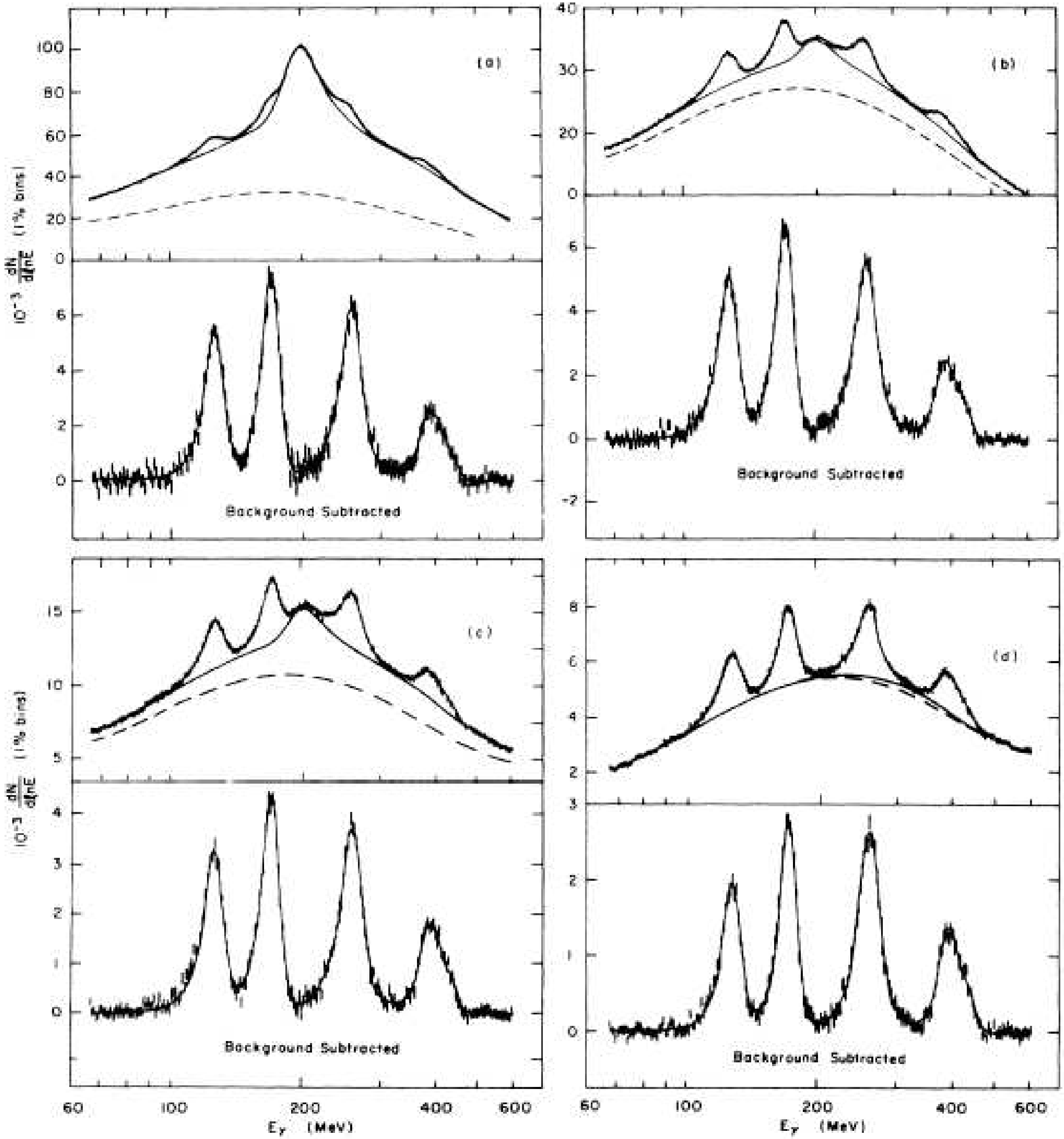

Crystal Ball:
γ transition
from $\psi(2S)$ (left)
and J/ψ (right)
to the η_c.

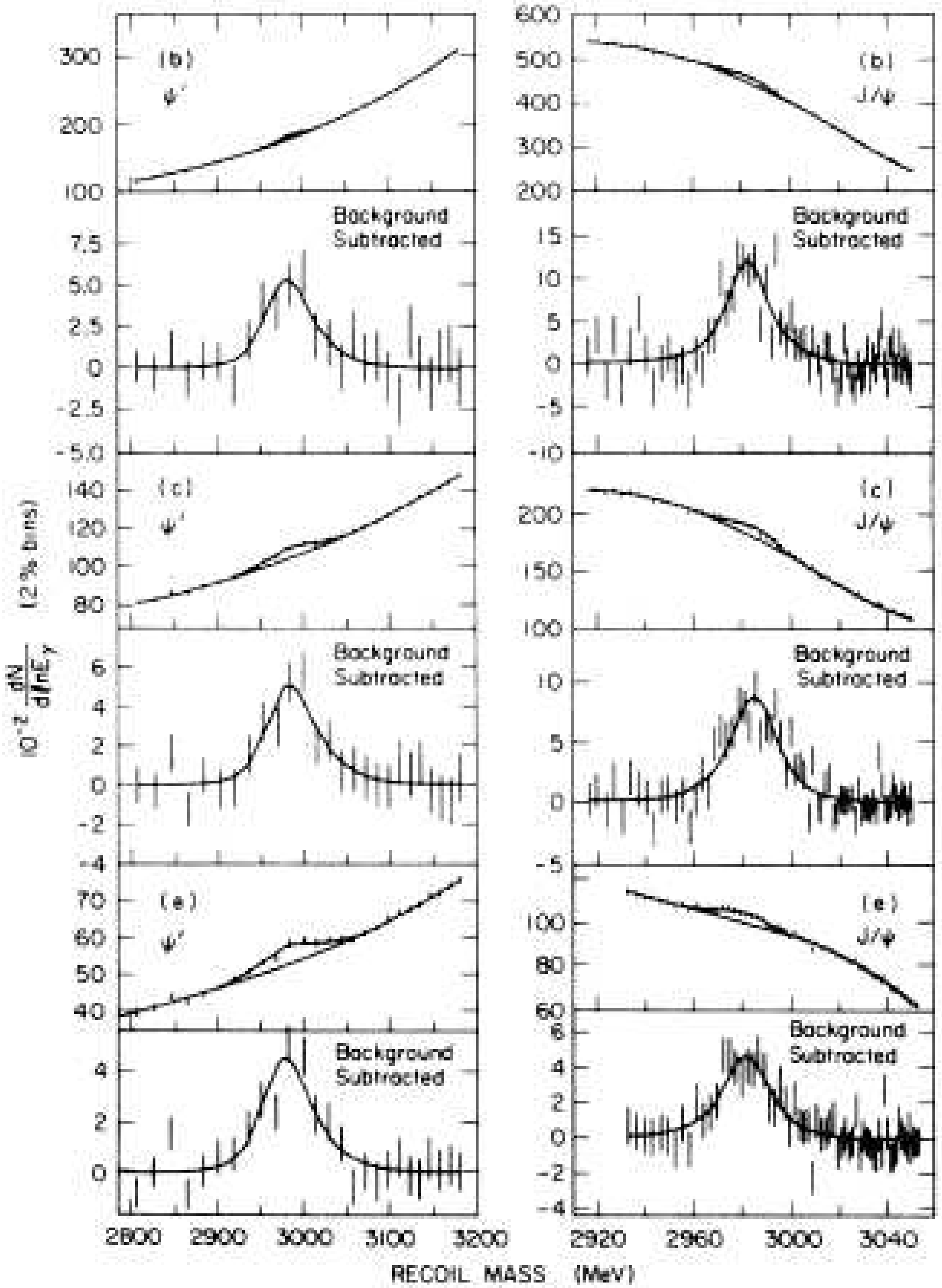

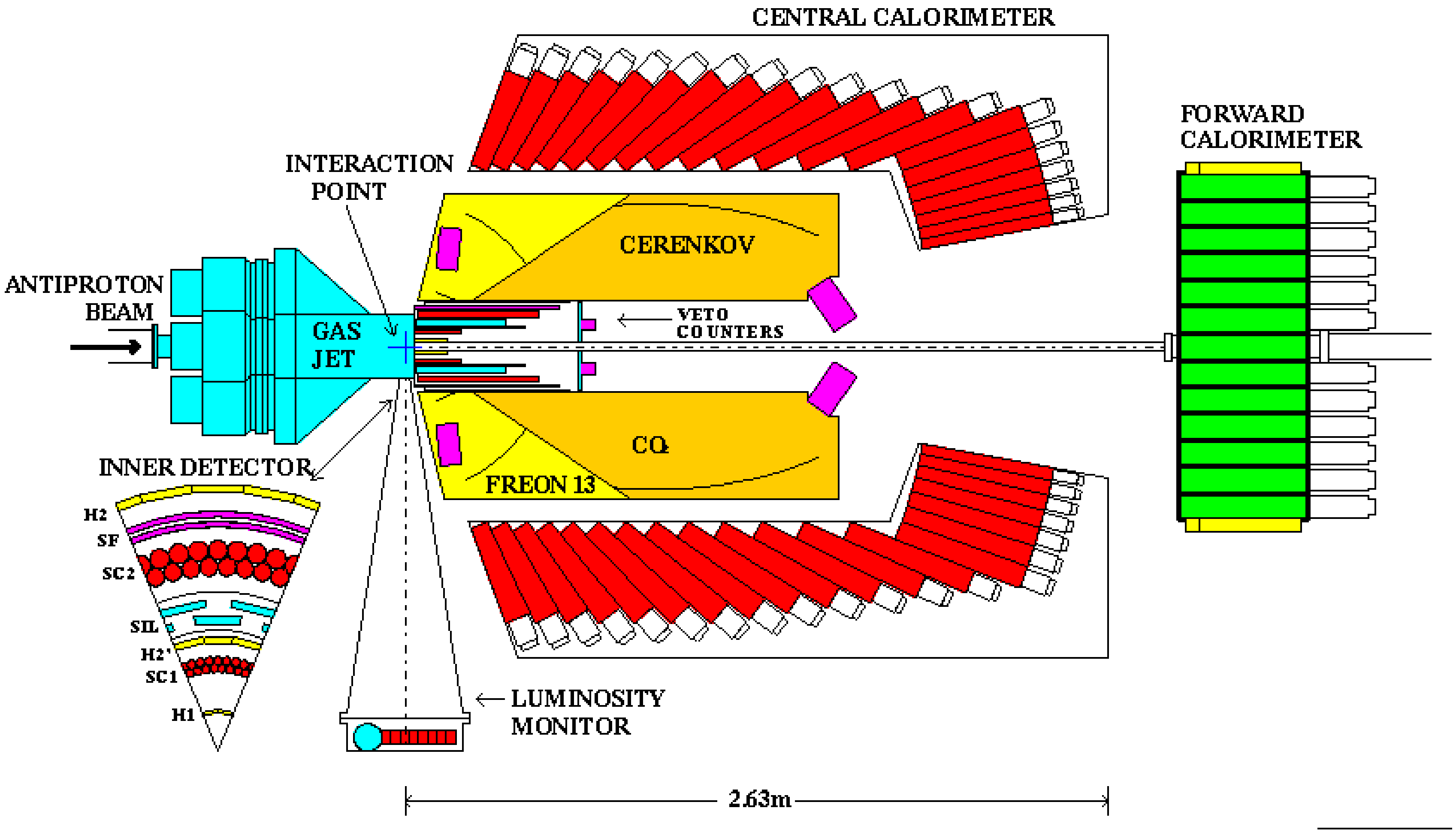

Experiment E760/E835 at FNAL $\sqrt{s} = m_p \cdot \sqrt{2(1 + m_p E_{\bar{p}})}$

- **Hydrogen gas jet target with** $\rho_{jet} = 3 \cdot 10^{14} H_2/cc$
- $\sigma_{hadronic} = 100mb$ **Very good P.I. required!** $\sigma_{c\bar{c}} = 1\mu b$
- **Small decay fractions, e.g. for** $\eta_c \to \gamma\gamma$

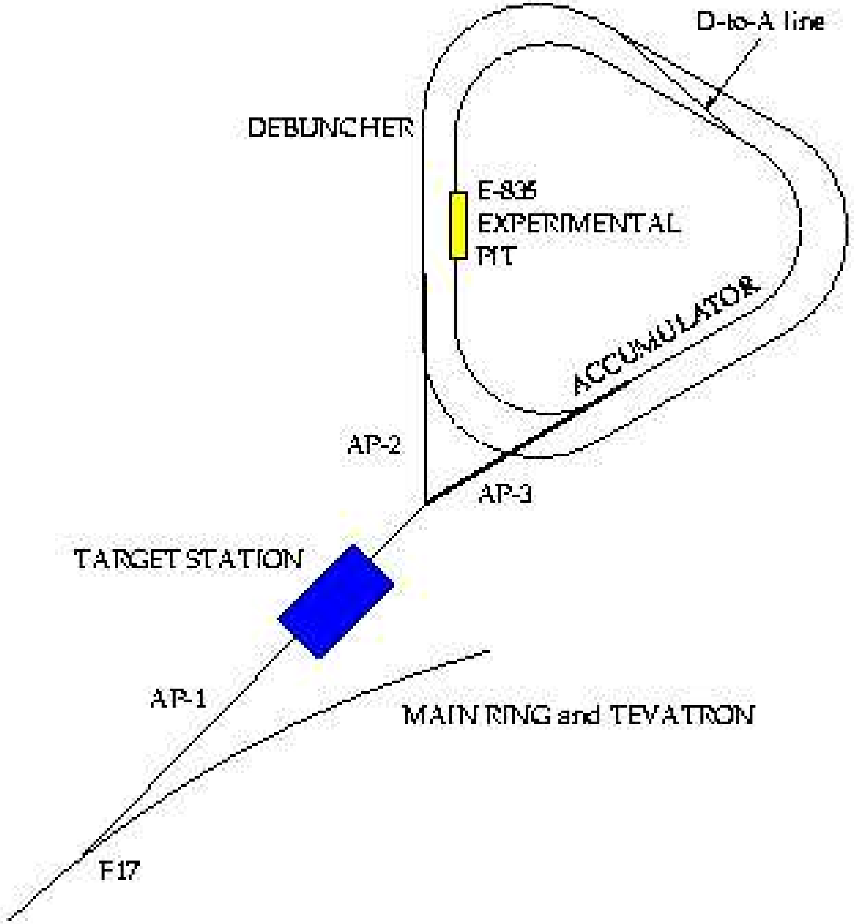

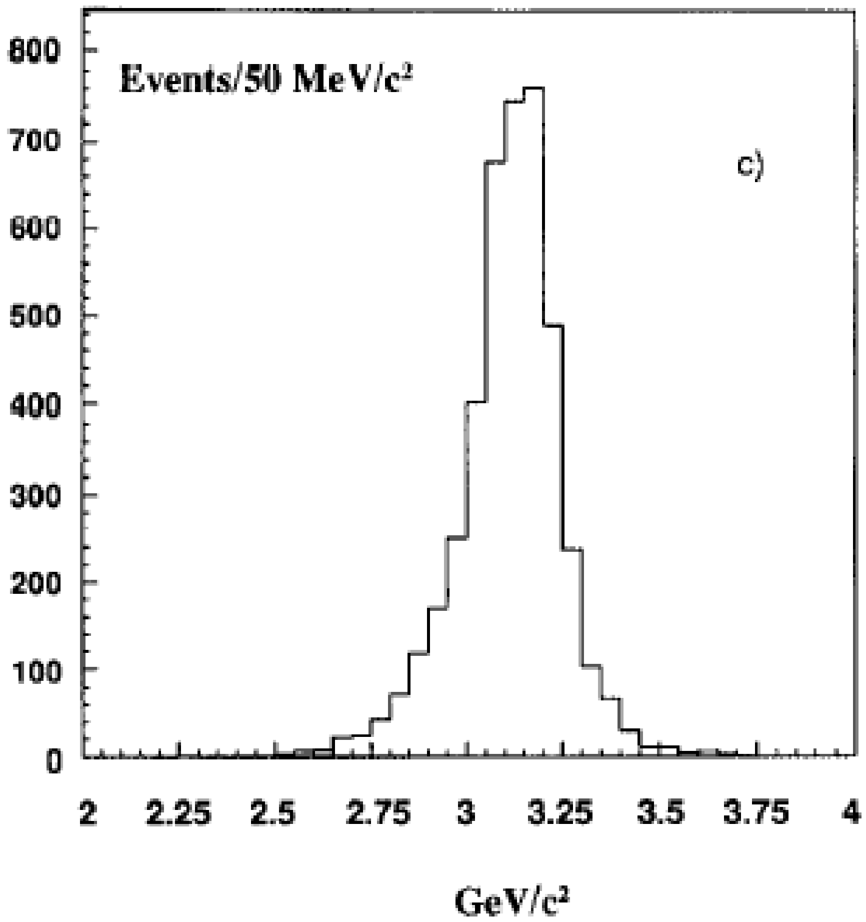

- $8 \cdot 10^{11}$ **antiprotons circulating in Fermilab accumulator ring with** $f_{rev} = 0.63$**MHz**

The e^+e^- invariant mass as reconstructed in E760 for events with a χ_2.

- **Luminosity** $L = N_{\bar{p}} f_{rev} \rho_{jet} \quad = \quad 2 \cdot 10^{31}/cm^2 sec$
- $R = L\sigma$ $\qquad R = 3 \cdot 10^6/sec$

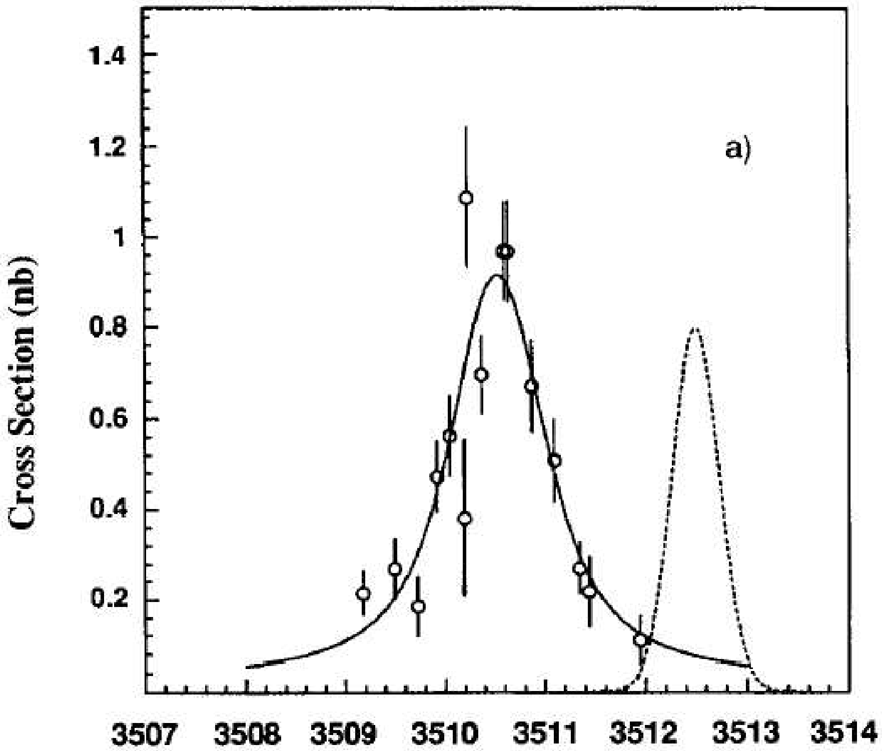

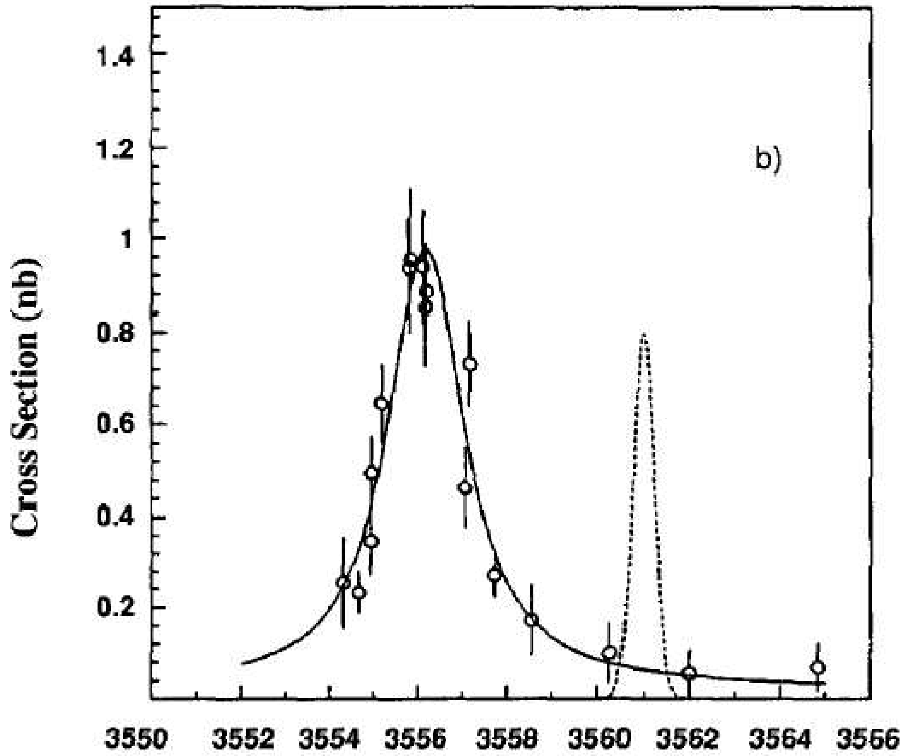

The number of J/ψ per $\bar{\text{p}}$ momentum bin in the χ_1 and χ_2 mass regions.

Peak cross section is 1nb compared to 100mb total hadronic: 10^{-5}

Mass and width can be determined!

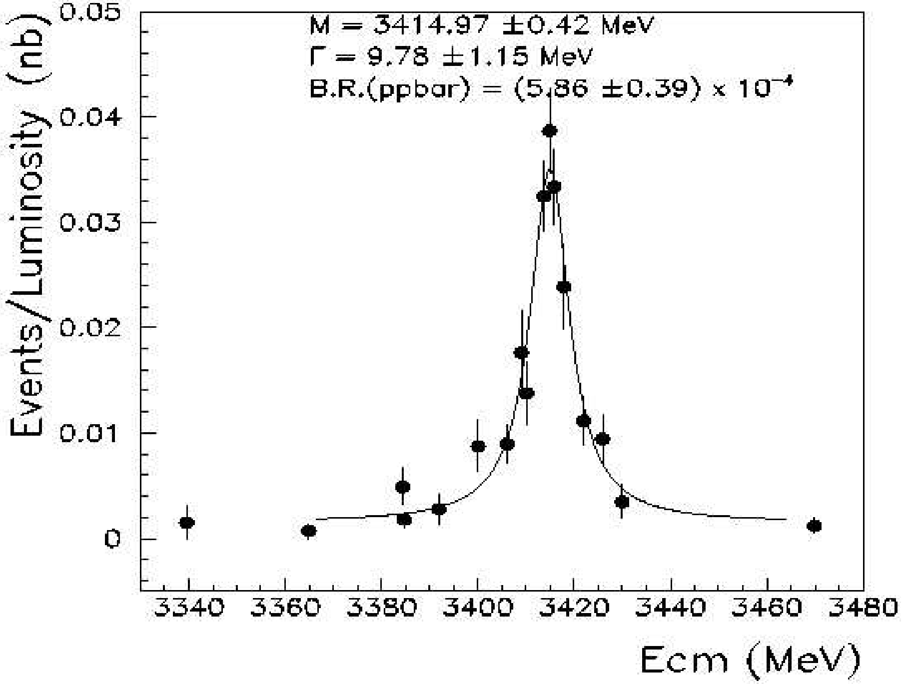

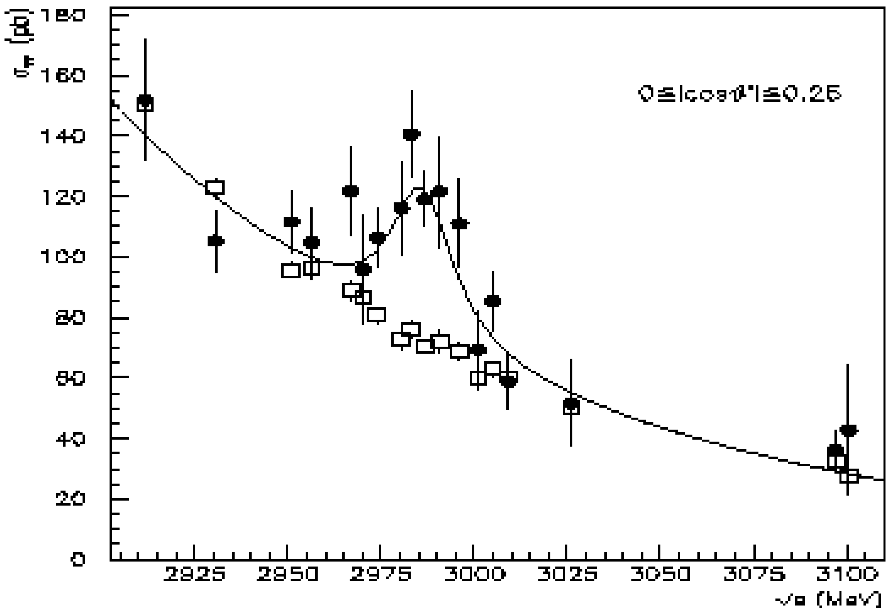

The number of J/ψ per $\bar{\text{p}}$ momentum bin in the χ_0 mass region.

The $\eta_c \to 2\gamma$.

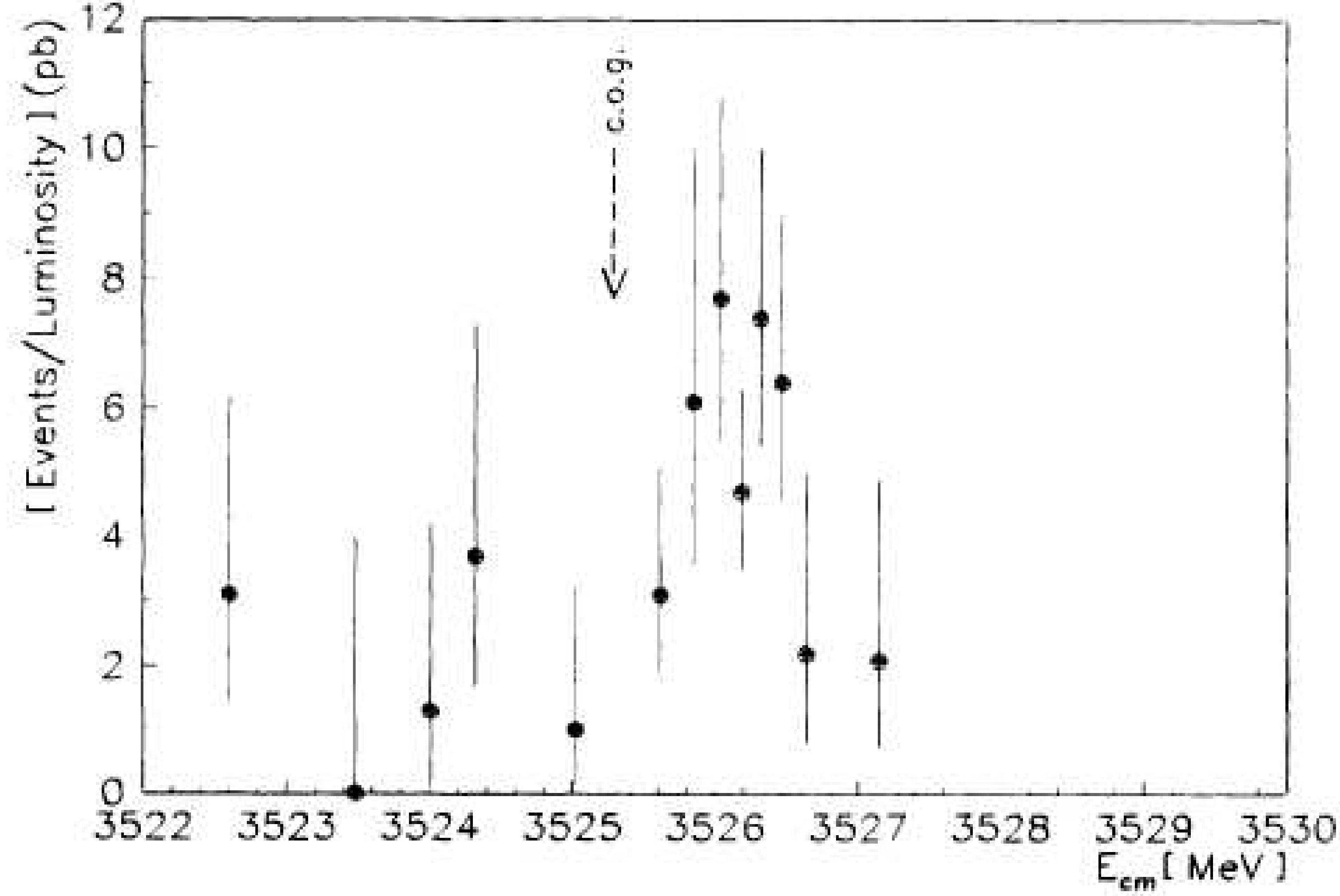

Evidence for the $h_1(c)$.

Not confirmed in later runs!

A new player: BES at Bejing

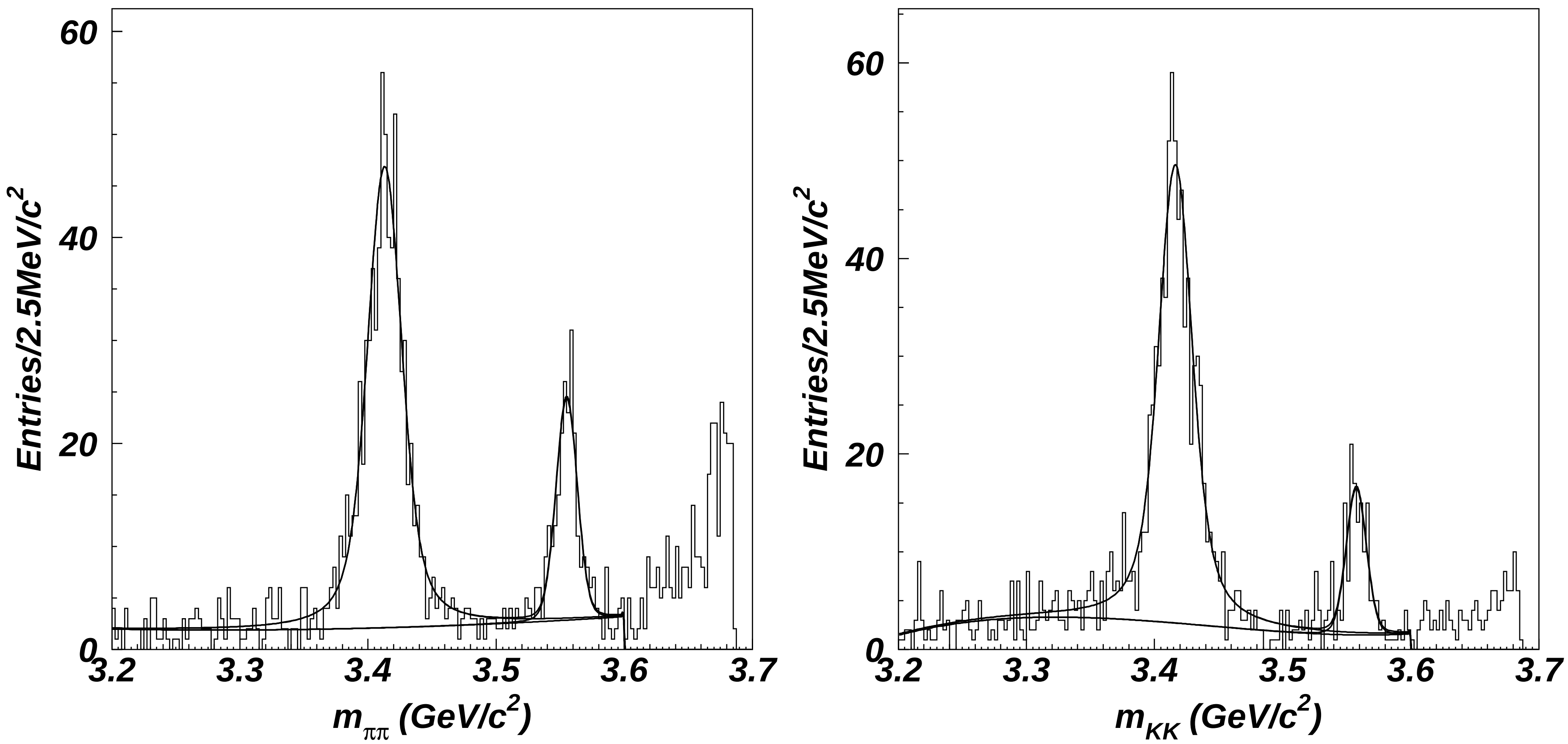

- **So far:** $\mathbf{3.79 \times 10^6}$ ψ**(2S) annihilations.**
- **Studied:** $\psi(\mathbf{2S}) \to \gamma\pi^+\pi^-$, $\gamma\mathbf{K}^+\mathbf{K}^-$ **and** $\gamma\mathbf{p\bar{p}}$
- **The (near) future: Cornell and CLEO-C**

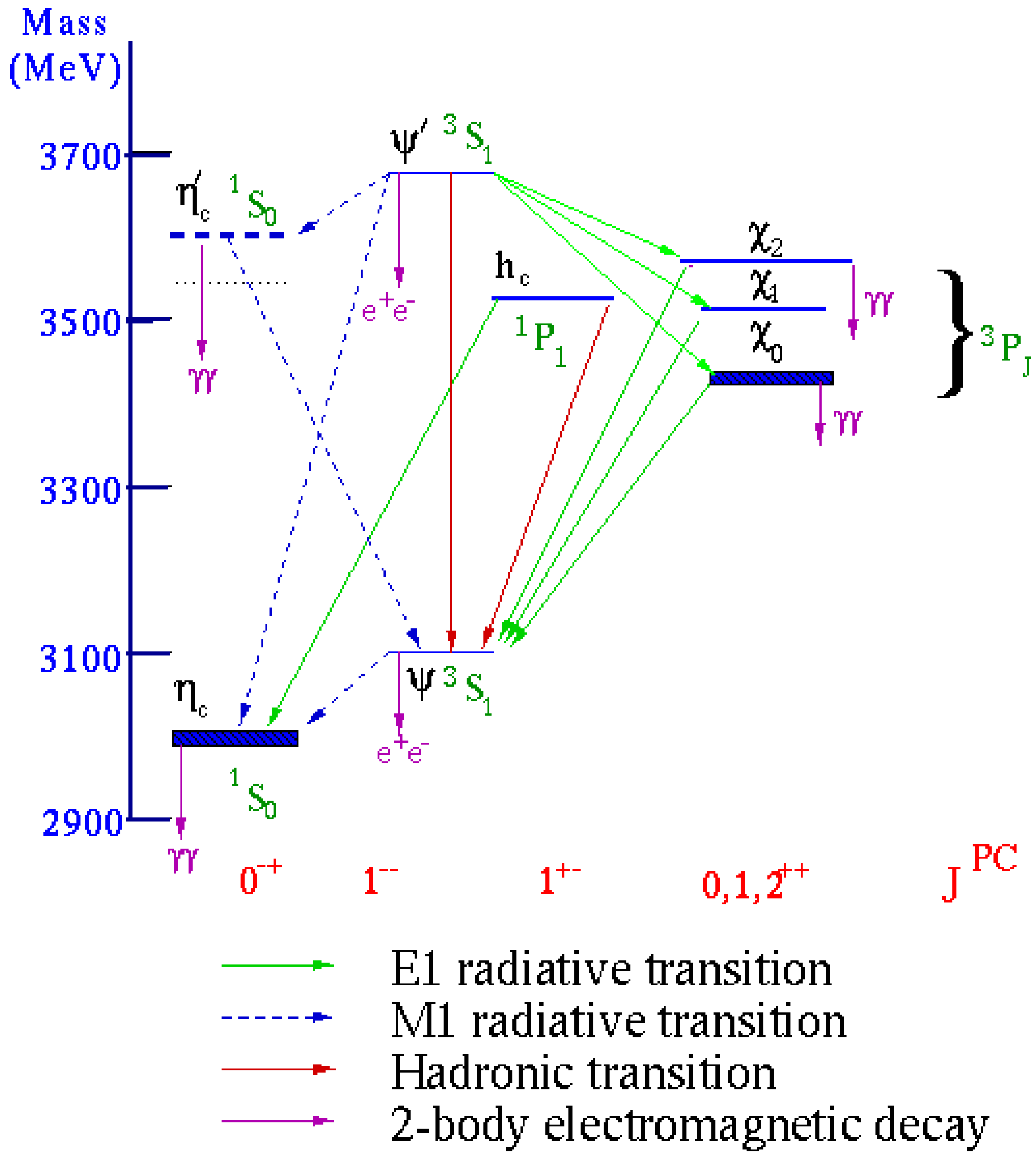

Charmonium energy levels ressamble positronium

1.5 D and B mesons

- **Mesons with one charmed quark are called D-mesons,**
- **with one charmed and one strange quark D_s;**
- **mesons with one bottom quark B-mesons,**
- **with one bottom and one charmed quark B_s**
- **Baryons with one charmed (bottom) quark Λ_c or Λ_b, Σ_c or Σ_b, and so on.**
- **But the forces are the same!**

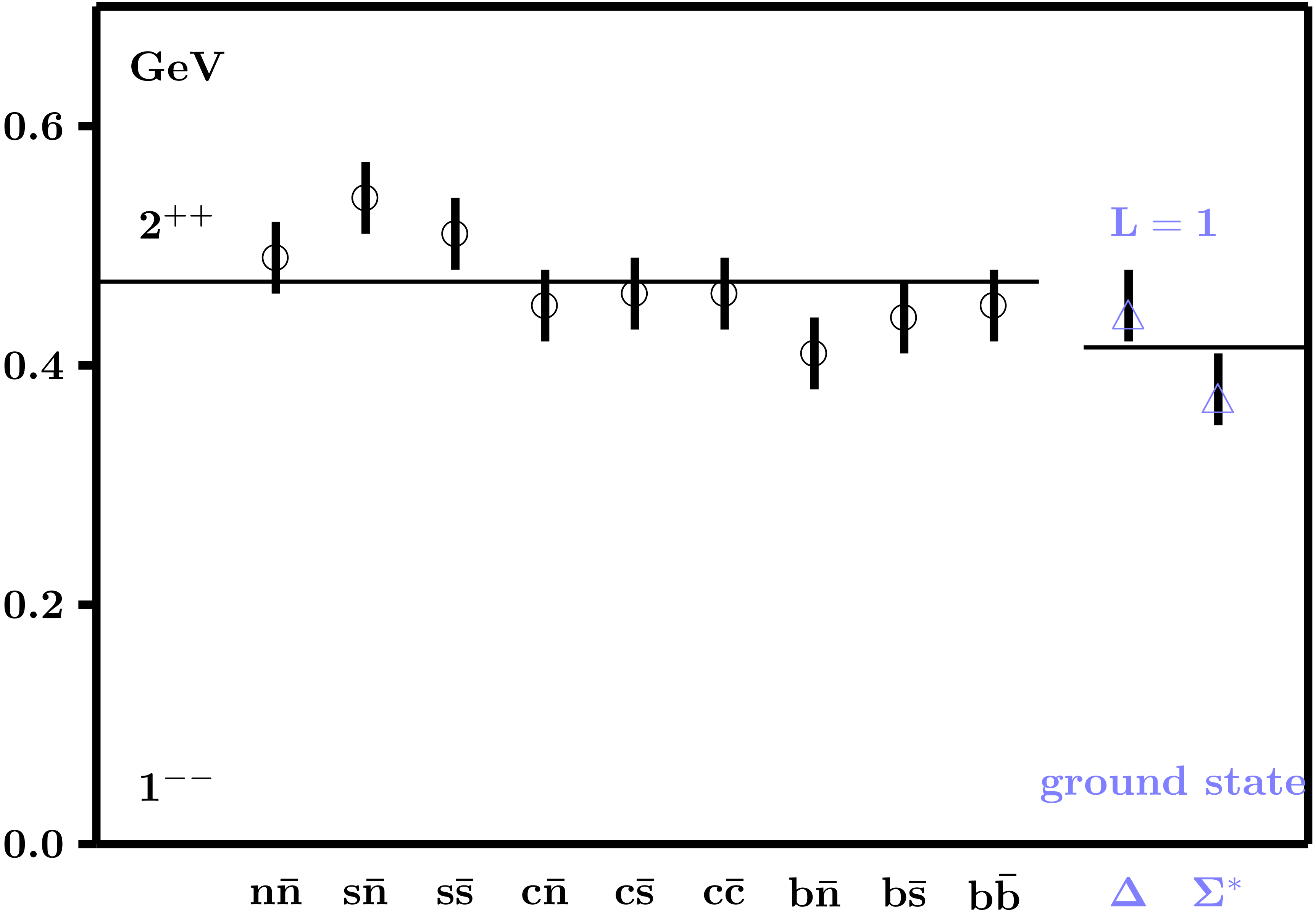

Mass differences between ground states and L=1 states

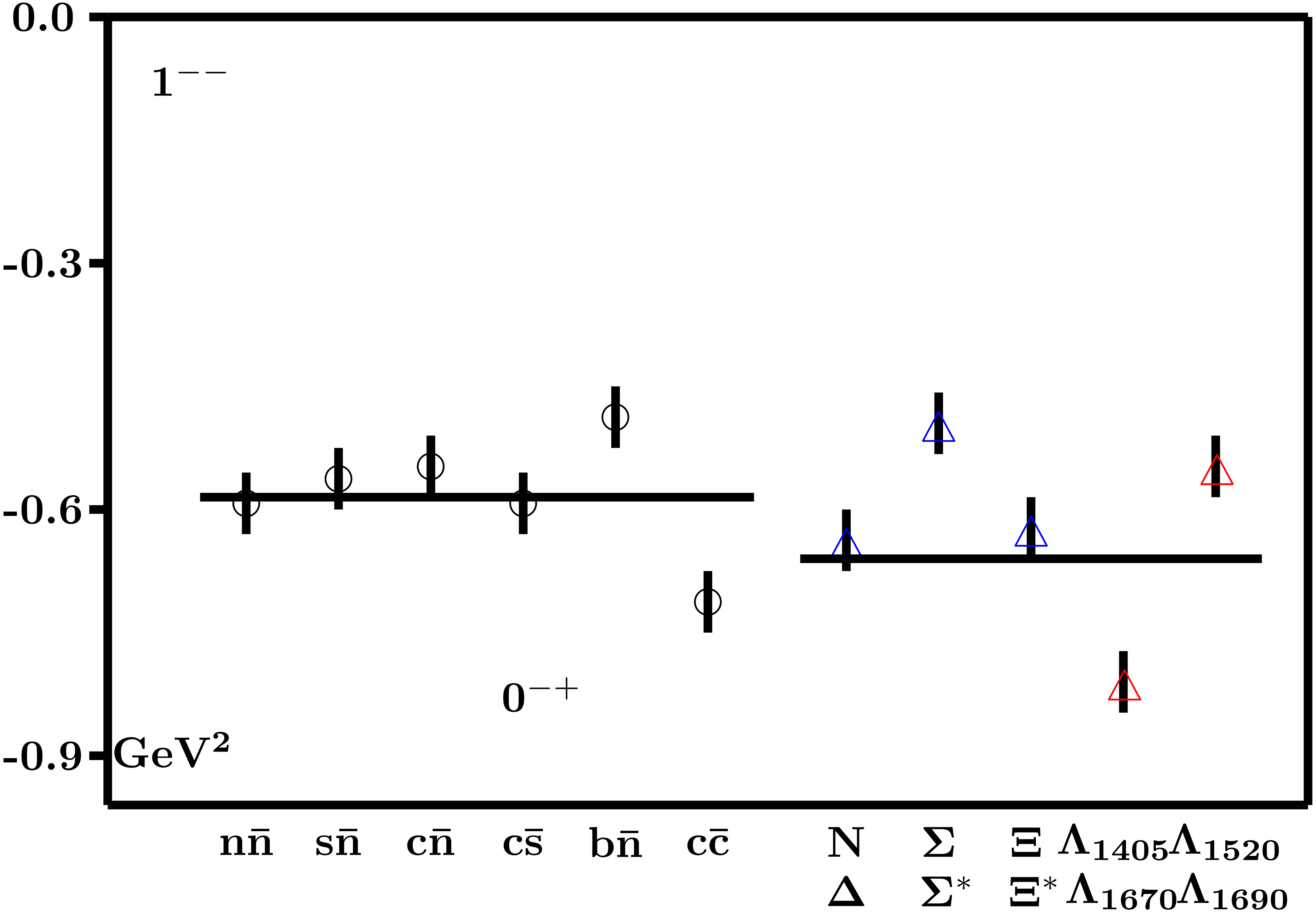

Mass square differences between PS and V mesons (circles), for L=0 octet-decuplet and L=1 singlet-octet baryons.

Spectrum of excited D_s mesons from the BABAR experiment (SLAC).

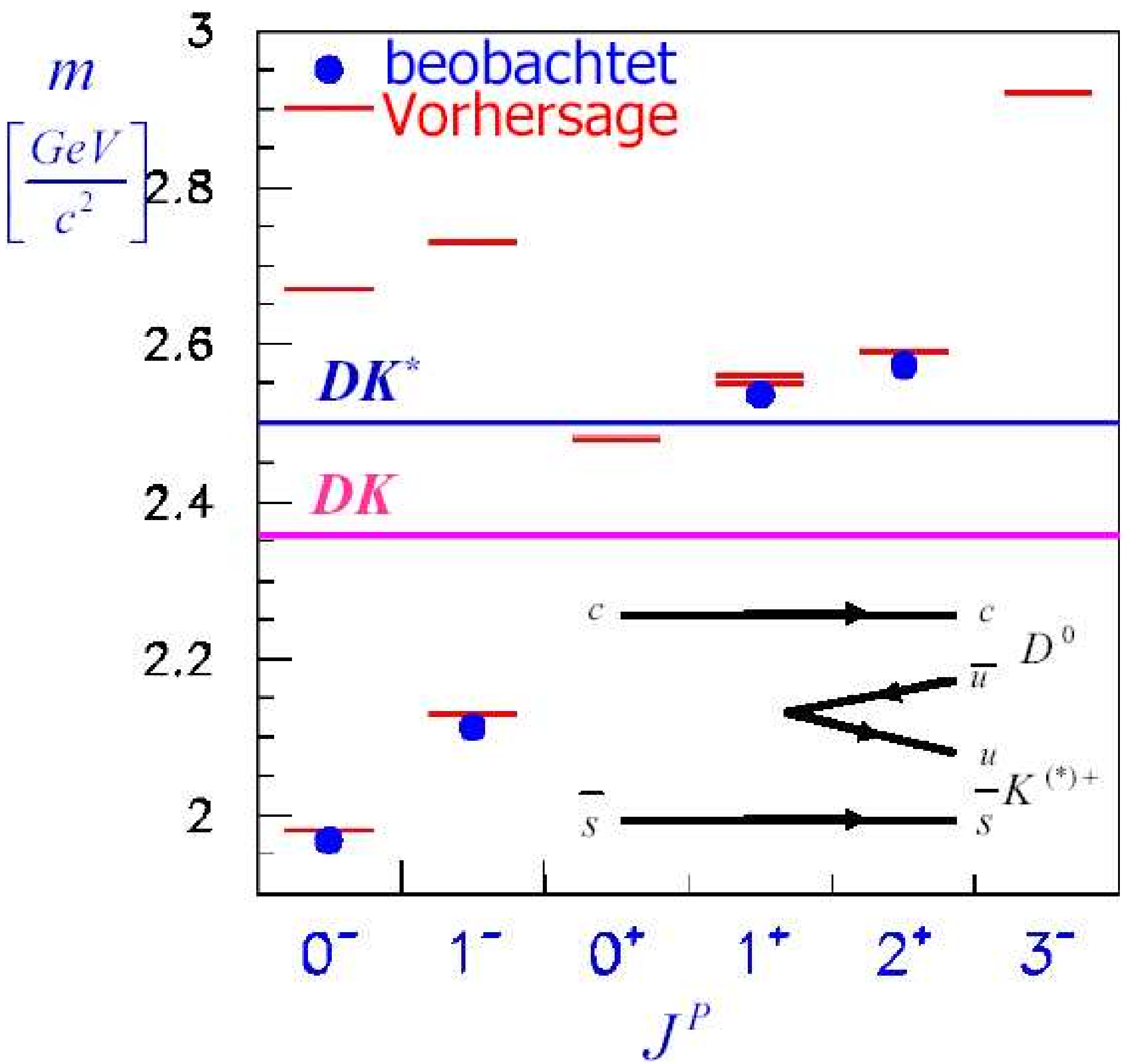

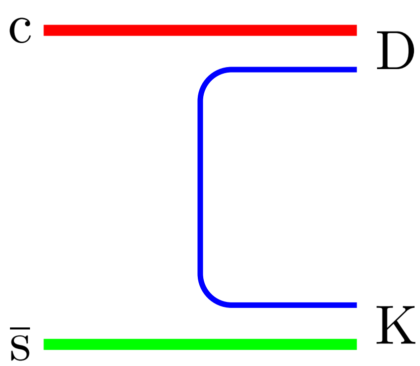

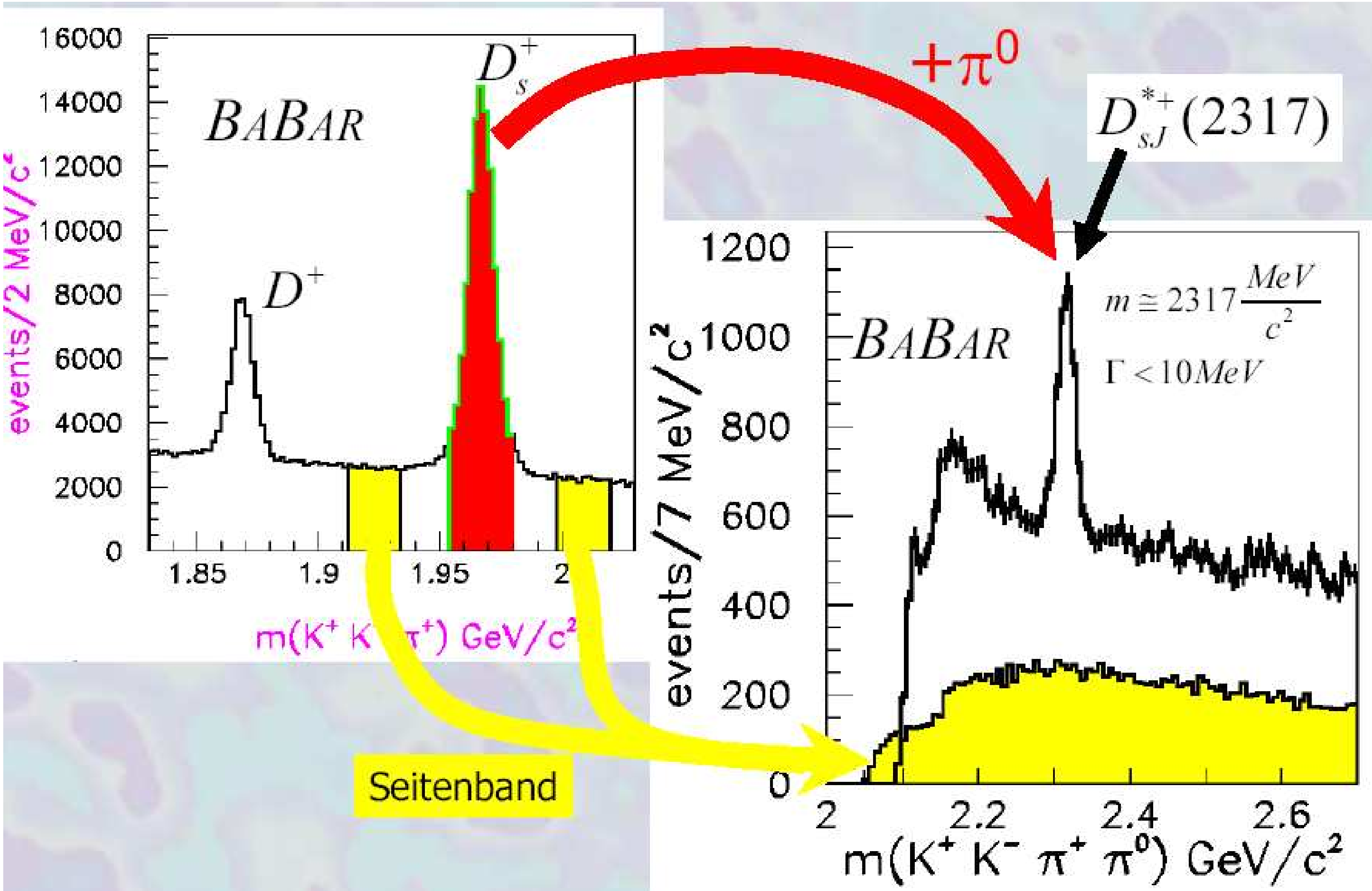

BABAR
D_s^+
D^+
$+\pi^0$
$D_{sJ}^{*+}(2317)$
$m \cong 2317 \frac{MeV}{c^2}$
$\Gamma < 10 MeV$
events/2 MeV/c²
m(K⁺ K⁻ π⁺) GeV/c²
events/7 MeV/c²
m(K⁺ K⁻ π⁺ π⁰) GeV/c²
Seitenband

The new state does not correspond to expections. Is it:

- four-quark states
- D K molecule ?
- indication for wrong models ?

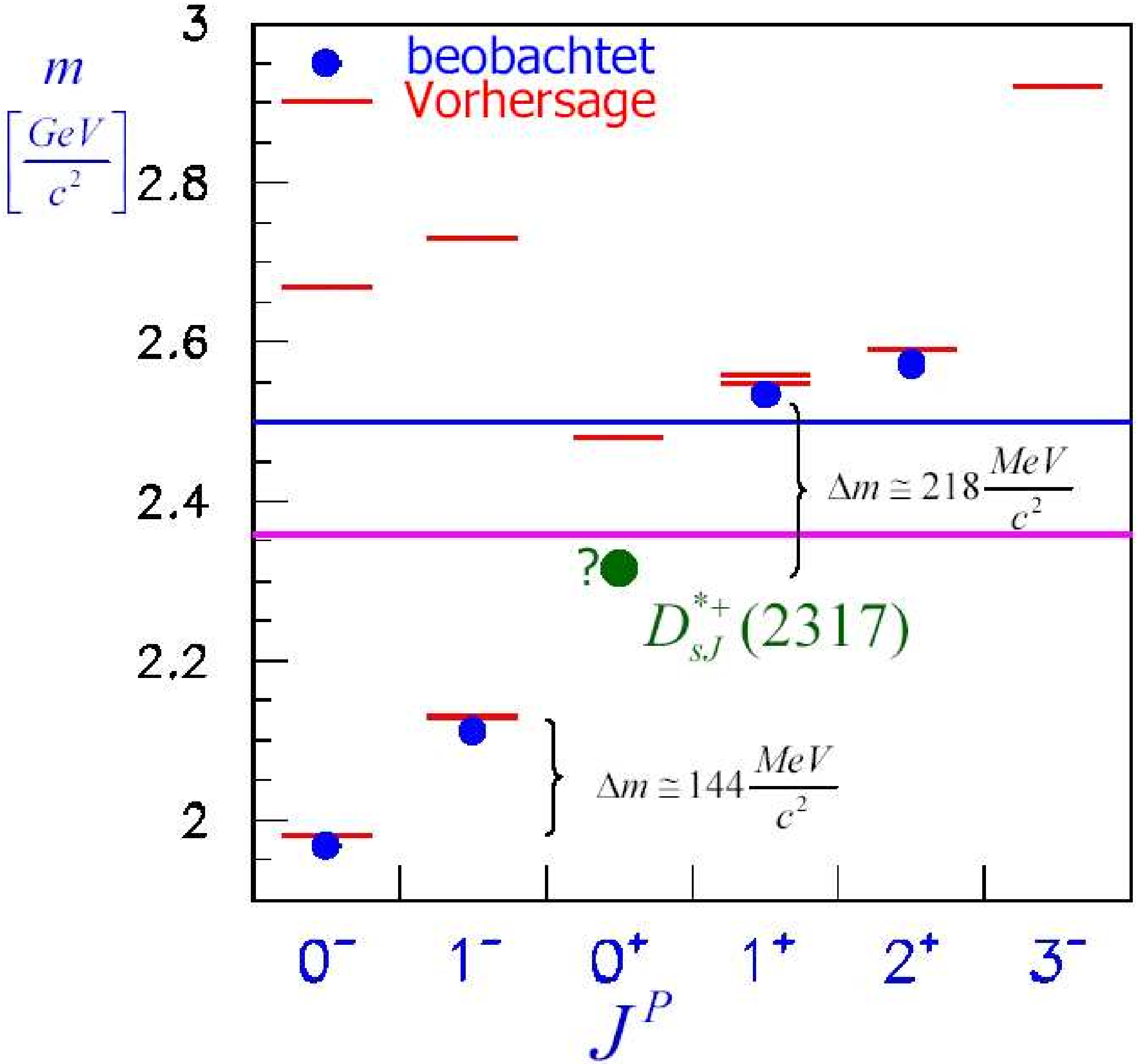

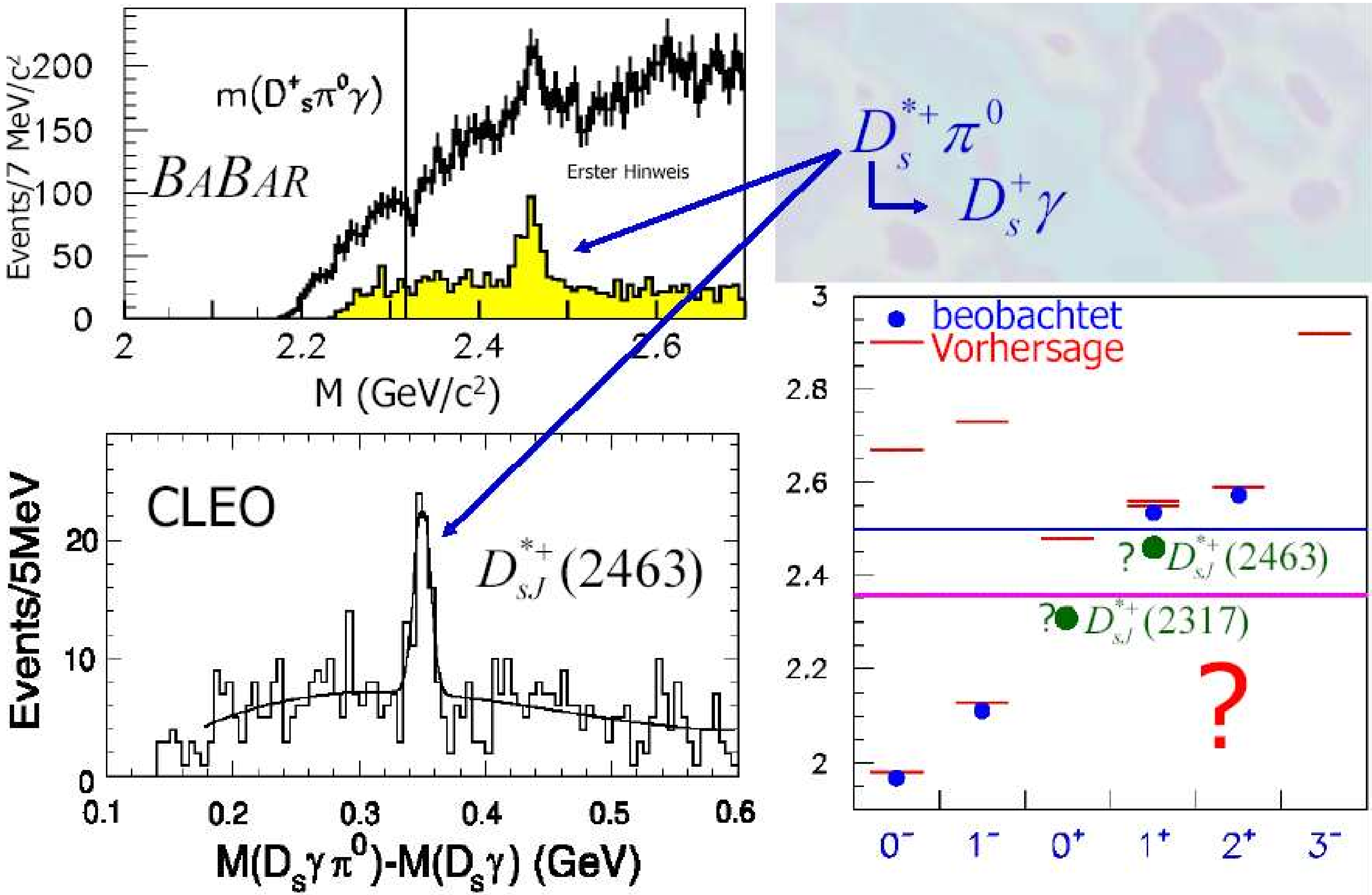
Events/7 MeV/c²
m(D⁺ₛπ⁰γ)
BABAR
Erster Hinweis
M (GeV/c²)
$D_s^{*+}\pi^0$
$\hookrightarrow D_s^+\gamma$
CLEO
Events/5MeV
$D_{sJ}^{*+}(2463)$
M(D$_s\gamma\pi^0$)-M(D$_s\gamma$) (GeV)
beobachtet
Vorhersage
?$D_{sJ}^{*+}(2463)$
?$D_{sJ}^{*+}(2317)$
?
0⁻
1⁻
0⁺
1⁺
2⁺
3⁻

Particles and interactions

- **The particles: quarks and leptons**
- **The interactions**
- **Quark models for mesons**

2 Particles and their interaction

2.1 The particles: quark and leptons

Fundamental particles: fermions with spin 1/2

Interactions: through exchange of bosons with spin 0,1,2

Leptons and their quantum numbers

Classification	e^-/v_e	μ^-/v_μ	τ^-/v_τ
e-lepton number	**1**	**0**	**0**
μ**-lepton number**	**0**	**1**	**0**
τ**-lepton number**	**0**	**0**	**1**

No $\tau^- \rightarrow$ e$^-\gamma$ decays

Quarks and their quantum numbers

Classification	d	u	s	c	b	t
Charge	**-1/3**	**2/3**	**-1/3**	**2/3**	**-1/3**	**2/3**
Isospin I	**1/2**	**1/2**	**0**	**0**	**0**	**0**
I_3	**-1/2**	**1/2**	**0**	**0**	**0**	**0**
Strangeness s	**0**	**0**	**-1**	**0**	**0**	**0**
Charm c	**0**	**0**	**0**	**1**	**0**	**0**
Beauty (bottom) b	**0**	**0**	**0**	**0**	**-1**	**0**
Truth (top) t	**0**	**0**	**0**	**0**	**0**	**1**

The charge of mesons is given by the sign of the flavor.

Examples:

$$\text{Charge}(\text{K}^+) = \text{Charge}(u\bar{s}) = +1$$
$$\text{Charge}(\text{D}^+) = \text{Charge}(c\bar{d}) = +1$$
$$\text{Charge}(\text{B}^-) = \text{Charge}(b\bar{u}) = -1$$

Quark masses:

Classification	d	u	s	c	b	t
Current mass	10	5.6	120 MeV	1.5	5	175 GeV
Constituent mass	330	330	450 MeV	1.5	5	175 GeV

Quark colors: **red** **blue** **green**

Color is confined: no free color ever observed

Mesons: $q\bar{q}$ $q\bar{q}$ $q\bar{q}$

Baryons **qqq**

Quarks and leptons and their interactions

$$\begin{pmatrix} u_{red} \\ d_{red} \end{pmatrix} \quad \begin{pmatrix} c_{red} \\ s_{red} \end{pmatrix} \quad \begin{pmatrix} t_{red} \\ b_{red} \end{pmatrix}$$

$$\begin{pmatrix} u_{green} \\ d_{green} \end{pmatrix} \quad \begin{pmatrix} c_{green} \\ s_{green} \end{pmatrix} \quad \begin{pmatrix} t_{green} \\ b_{green} \end{pmatrix}$$

$$\begin{pmatrix} u_{blue} \\ d_{blue} \end{pmatrix} \quad \begin{pmatrix} c_{blue} \\ s_{blue} \end{pmatrix} \quad \begin{pmatrix} t_{blue} \\ b_{blue} \end{pmatrix}$$

$$\begin{pmatrix} \nu_e \\ e \end{pmatrix} \quad \begin{pmatrix} \nu_\mu \\ \mu \end{pmatrix} \quad \begin{pmatrix} \nu_\tau \\ \tau \end{pmatrix}$$

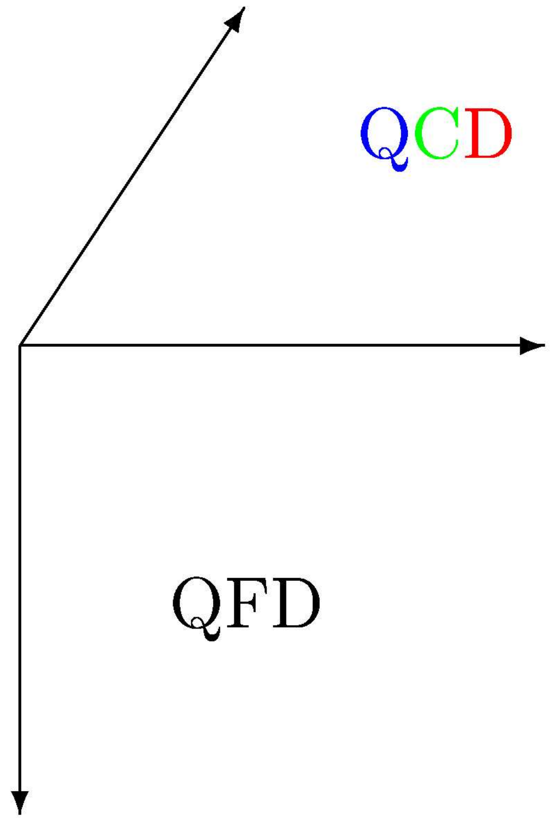

The Standard Model and QCD

$$SU(3) \otimes SU(2) \otimes U(1)$$

$$\Downarrow \qquad\qquad \Downarrow \qquad\qquad \Downarrow$$

8 gluons $\qquad W^{\pm}, Z^0 \qquad$ **photon**

strong interactions **electro-weak interactions**

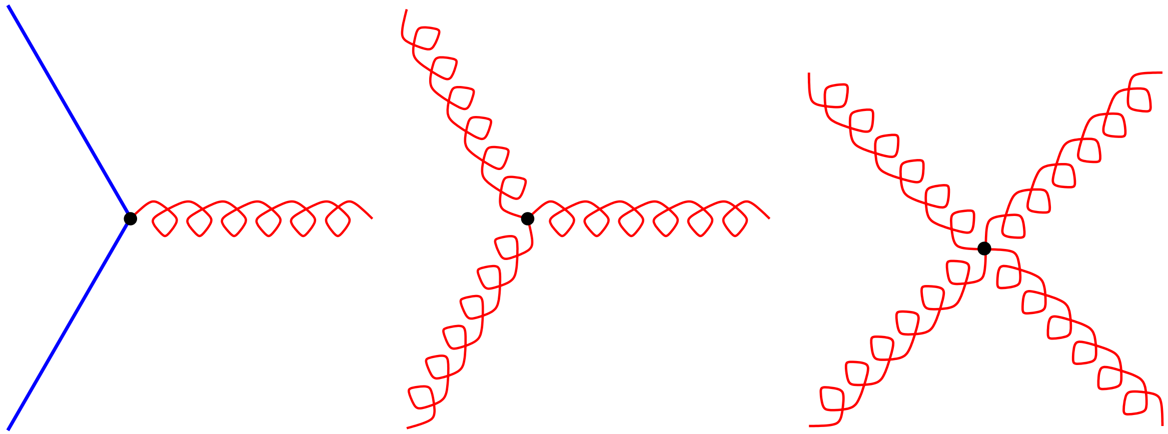

Coupling vertices

QCD with color-electromagnetic fields

$$F_{\mu\nu}{}^{a} = \delta_{\mu} A_{\nu}{}^{a} - \delta_{\nu} A_{\mu}{}^{a} + g_s f_{abc} A_{\mu}{}^{b} A_{\nu}^{c}$$

yields renormalizable gauge theory.

The static $Q\bar{Q}$ potential as a function of separation !

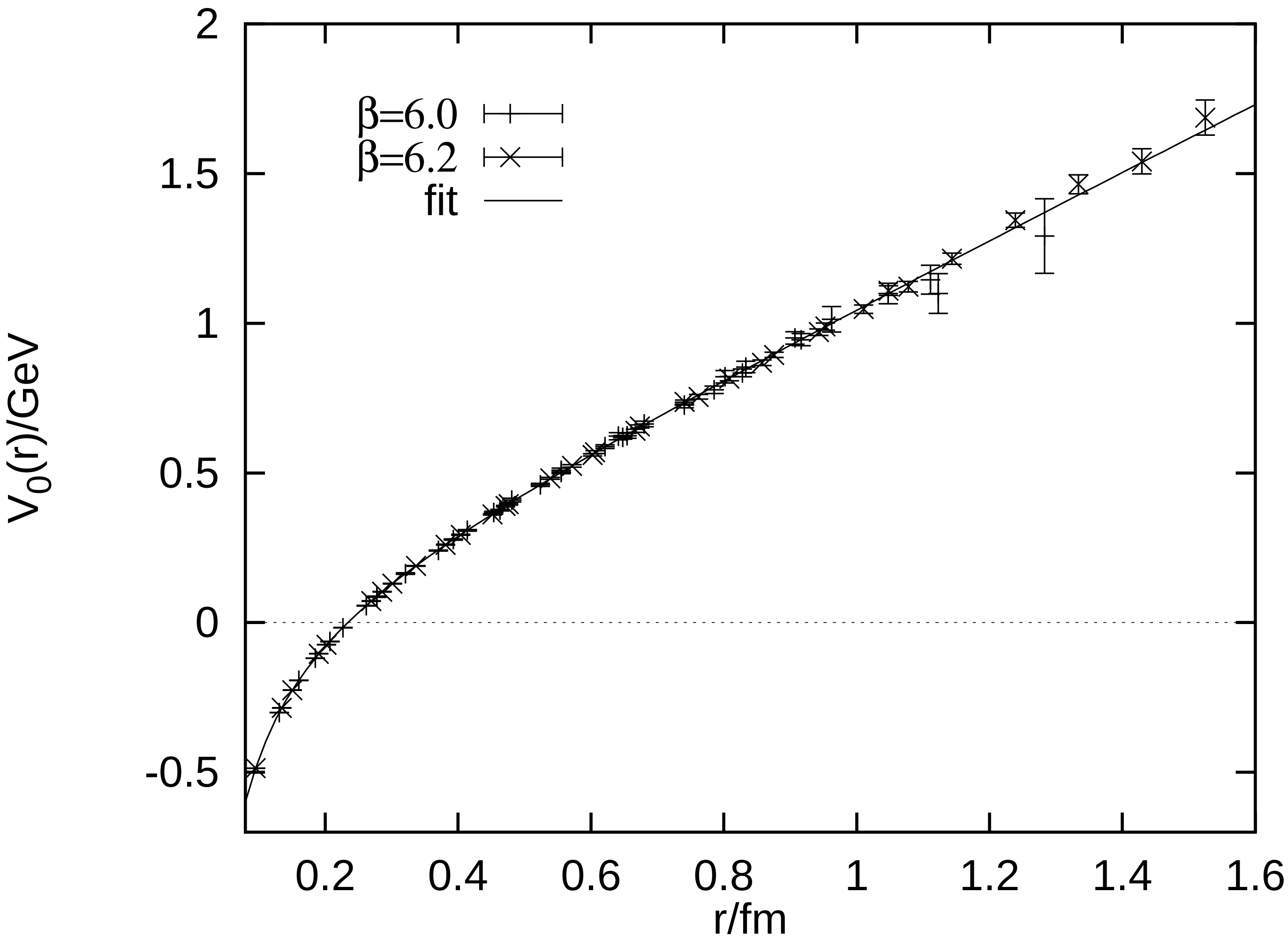

G. S. Bali, K. Schilling and A. Wachter, "Complete O(v2) corrections to the static interquark potential from SU(3) gauge theory," Phys. Rev. D 56 (1997) 2566.**

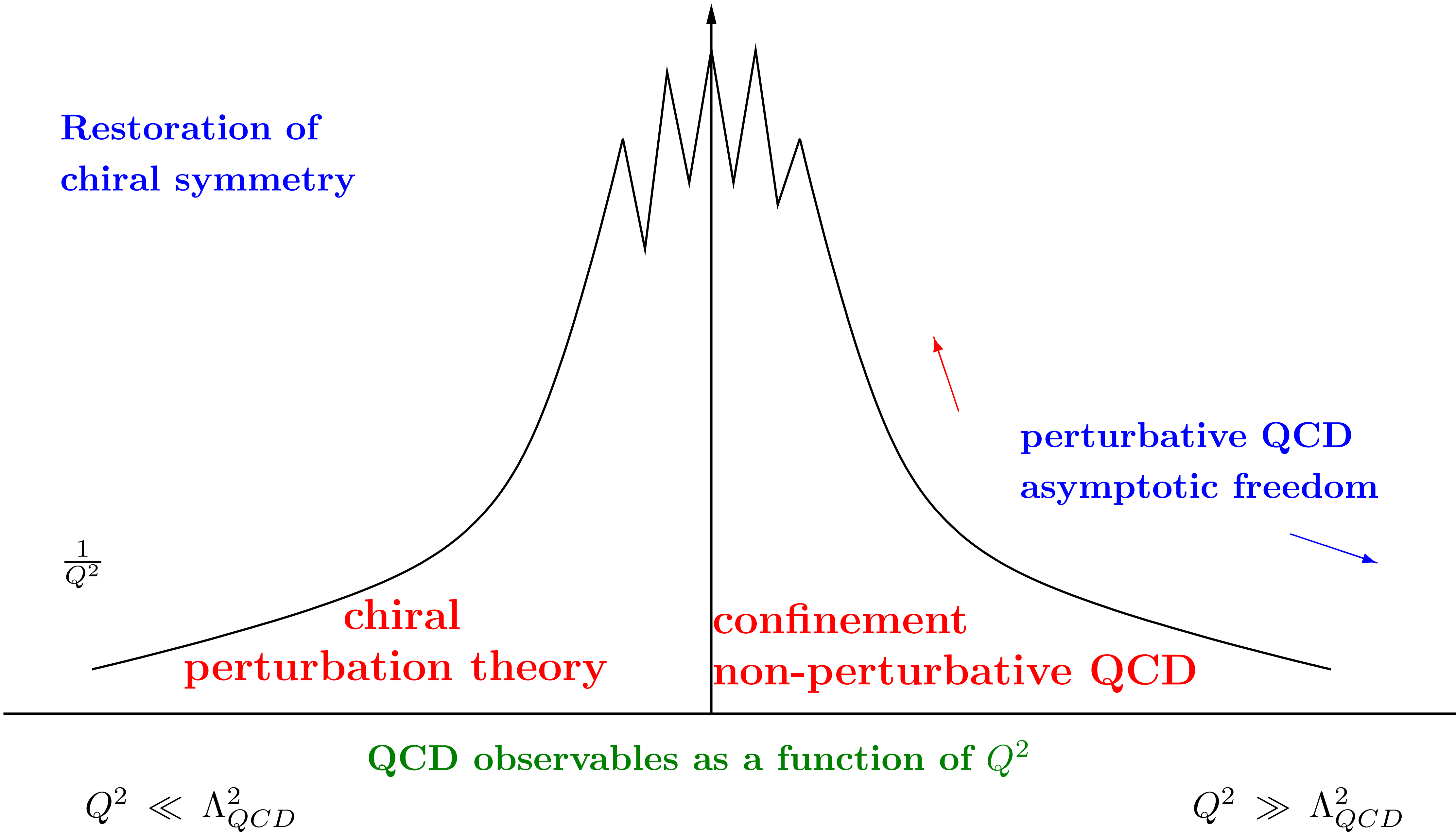
Restoration of
chiral symmetry
perturbative QCD
asymptotic freedom
$\frac{1}{Q^2}$
chiral
perturbation theory
confinement
non-perturbative QCD
QCD observables as a function of Q^2
$Q^2 \ll \Lambda^2_{QCD}$
$Q^2 \gg \Lambda^2_{QCD}$

From large energies to large distances

Can we understand bound systems within the QCD frame?

NO!

Concepts: QCD inspired models

- **Bag models**
- **Effective one-gluon exchange**
- **Flux tube models**
- **Instanton interactions**
- **QCD sum rules**
- **Lattice QCD**

In the Standard Model of particle physics, strong interactions are described by Quantum Chromodynamics (QCD), a local gauge theory with quarks and gluons as elementary degrees of freedom. The interaction is governed by the strong fine-structure constant α_s which depends on the four-momentum transfer Q of a given strong process. As α_s decreases with increasing Q, perturbation theory can be applied in high-energy reactions. At momentum scales given by typical hadron masses, perturbative QCD breaks down due to a rapid increase of α_s. This is the realm of 'strong QCD'. Not only α_s changes but also the relevant degrees of freedom change from current quarks and gluons to constituent quarks, instantons and vacuum condensates. To understand this transition is one of the most challenging intellectual problem. A clarification of the following central issues in strong interactions is needed:

- **What are relevant degrees of freedom that govern hadronic phenomena ?**
- **What is the relation between parton degrees of freedom in the infinite momentum frame and the structure of hadrons in the rest frame ?**
- **What are the mechanisms for confinement and for chiral symmetry breaking ?**
- **Are deconfinement and chiral symmetry restoration linked, and can precursor phenomena be seen in nuclear physics ?**

The answers to these questions will not be the direct result of some experiments. Models need to link observables to these fundamental questions. Significant observables are the nucleon excitation spectrum and their electromagnetic couplings including their off-shell behaviour, and the response of hadronic properties to the exposure by a nuclear enviroment.

2.2 Quark models for mesons

- **Quarks are confined**
  Phenomenological potential $\mathbf{V = V_0 + a\,r}$; a string constant;
  $\mathbf{a = 1\,GeV/fm}$.
- **At small distances:**
  $V = -\frac{4}{3}\frac{\alpha_s}{r}$**; one-gluon exchange.**
- **At large distances: quarks develop effective masses.**
  What is the effective interaction bet constituent quarks ?
  Effective one-gluon exchange ? Exchange of pseudoscalar mesons ? Instanton-induced interactions ?

2.2.1 The Godfrey-Isgur model

First unified constituent quark model for all $q\bar{q}$-mesons was developed by Godfrey and Isgur: (see: Stephan Godfrey and Nathan Isgur, *Mesons in a relativized quark model with chromodynamics*, Phys. Rev. D 32 (1985) 189)
Basic ingredients:

$$\mathbf{H\Psi = (H_0 + V)\Psi = E\Psi}, \qquad \mathbf{H_0} = \sqrt{\mathbf{m_q}^{\mathbf{2}} + |\boldsymbol{p}|^{\mathbf{2}}} + \sqrt{\mathbf{m_{\bar{q}}}^{\mathbf{2}} + |\boldsymbol{p}|^{\mathbf{2}}}\,,$$

with $\boldsymbol{p}$ the relative momentum in the CM-frame, and

$$\mathbf{V = H^c + H^{hf} + H^{LS} + H^A}$$

which contains the central potential (linear confinement and Coulomb-potential), the spin-spin and tensor interaction and an annihilation contribution for flavor-neutral mesons.

The potential is generated by an (instantaneous) short-range $\gamma^\mu \cdot \gamma_\mu$, vector-like (gluon) exchange, where

$$\mathbf{G}(\mathbf{Q^2}) = -\frac{\mathbf{4}}{\mathbf{3}}\,\alpha_\mathbf{s}(\mathbf{Q^2})\frac{\mathbf{4}\pi}{\mathbf{Q^2}}$$

where $\alpha_\mathbf{s}(\mathbf{Q^2}) = \sum_\mathbf{k} \alpha_\mathbf{k}\, \mathrm{e}^{-\frac{\mathbf{Q^2}}{4\gamma_\mathbf{k}^2}}$ is the running coupling, with $\alpha_\mathbf{s}(\mathbf{0})$ finite, and a long-range confining potential $\mathbf{S}(\mathbf{Q^2})$, $\mathbf{S}(\mathbf{r}) = \mathbf{br} + \mathbf{c}$. Here, $\boldsymbol{Q} = \boldsymbol{p}' - \boldsymbol{p}$ and $\boldsymbol{P} = \frac{\mathbf{1}}{\mathbf{2}}(\boldsymbol{p}' + \boldsymbol{p})$:

$$\chi^\dagger_{s'}\chi^\dagger_{\bar{s}'}\, V^{eff}(\boldsymbol{P}, \boldsymbol{r})\chi_s\chi_{\bar{s}} =$$
$$\int \frac{\mathrm{d}^3 Q}{(2\pi)^3}\, \mathrm{e}^{i\boldsymbol{Q}\cdot\boldsymbol{r}}\bar{u}(\boldsymbol{p}', s')\bar{v}(-\boldsymbol{p}, \bar{s})\, \left[G(Q^2)\gamma^\mu \cdot \gamma_\mu - S(Q^2)\mathbf{I}\cdot\mathbf{I}\right] u(\boldsymbol{p}, s')v(-\boldsymbol{p}', \bar{s}')\,.$$

This is further modified by "smearing the potentials":

$$\tilde{\mathbf{f}}_\mathbf{ij}(\mathbf{r}) = \int \mathbf{d^3 r'}\, \frac{\sigma^\mathbf{3}_\mathbf{ij}}{\pi^{\frac{\mathbf{3}}{\mathbf{2}}}}\, \mathrm{e}^{-\sigma^\mathbf{2}_\mathbf{ij}|\boldsymbol{r}-\boldsymbol{r}'|^\mathbf{2}}\mathbf{f}_\mathbf{ij}(\mathbf{r}')\,,$$

and thus avoiding the singularities at the origin, where

$$\sigma_{ij}^2 = \sigma_0^2 \left[\frac{1}{2} + \frac{1}{2} \left(\frac{4m_i m_j}{(m_i + m_j)^2} \right)^4 \right] + s^2 \left[\frac{2m_i m_j}{m_i + m_j} \right]^2$$

and relativistic effects are parametrized by the modifications

$$\tilde{G}^C(r) \rightarrow \sqrt{1 + \frac{p^2}{E\bar{E}}} \qquad \frac{\tilde{V}^i(r)}{m_1 m_2} \rightarrow \left(\frac{m_1 m_2}{E_1 E_2} \right)^{\frac{1}{2} + \epsilon_i}$$

There are no spin-orbit forces in the Hamiltonian

Excuse: Absent in data, compensated by Thomas precession ?
Referred to as "Spin-Orbit-Problem" in the literature.

Annihilation

Annihilation is taken into account by parameterizing the annihilation amplitude as

$$\mathcal{A}(^{2S+1}L_J)_{ij} = 4\pi(2L+1)\left\{ A(^{2S+1}L_J)\left[\frac{\alpha_s(M_i^2)\alpha_s(M_j^2)}{\pi^2}\right]^{\frac{n}{2}}\right\}\frac{S_L(\Psi_i)S_L(\Psi_j)}{m_i m_j},$$

with $S_L(\Psi) = \frac{1}{(2\pi)^{\frac{3}{2}}}\int d^3p\, \frac{1}{\sqrt{4\pi}}\Phi(p)\left(\frac{p}{E}\right)^L \frac{m}{E}$

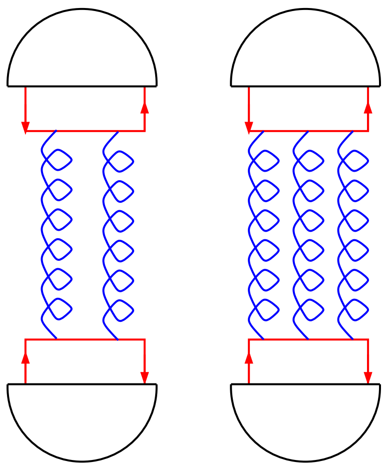

$n = 2$ **or** $n = 3$ **for** $C = +$**;**$C = -$**, respectively,**

for non-pseudoscalar flavour-neutral mesons:

$$\{\ldots\} \quad \rightarrow \quad \left\{ A_0 \, \mathrm{e}^{\frac{m_i^2 + m_j^2}{{M_0}^2}} + \frac{2\pi}{3} \left(\ln(2) - 1\right) \frac{\alpha_s(M_i^2)\alpha_s(M_j^2)}{\pi^2} \right\} \quad \textbf{or, alternatively,}$$

$$\{\ldots\} \quad \rightarrow \quad \left\{ A_0 \left[1 - \left(\frac{M}{M_0} \right)^4 \right] \mathrm{e}^{\frac{m_i^2 + m_j^2}{{M_0}^2} - \frac{M^4}{4{M_0}^4}} + \frac{2\pi}{3} \left(\ln(2) - 1\right) \frac{\alpha_s^2({M_0}^2)}{\pi^2} \right\}$$

for pseudoscalar, isoscalar mesons. Here M_i are the annihilation-unperturbed mesons masses .

Parameters of the Godfrey-Isgur model

masses	m_n	**220**	**MeV**	m_s	**419**	**MeV**
confinement	**b**	**910**	**MeV/fm**	**c**	**-253**	**MeV**
OGE	$\alpha_s(0)$	**0.60**		Λ	**200**	**MeV**
	ϵ_{SS}	**-0.168**		ϵ_T	**0.025**	
	ϵ_{LS}^C	**-0.035**		ϵ_{LS}^S	**0.055**	
"smearing"	σ_0	**0.11**	**fm**	s	**1.55**	
annihilation	$A(^3S_1)$	**2.5**		$A(^3P_2)$	**-0.8**	
	A_0	**0.5 (0.55)**		M_0	**550(1170)**	**MeV**

Godfrey-Isgur Mass spectra

All mesons are assumed to be "ideally mixed", except

Meson	ΔM**(calc)[MeV]**	ΔM**(exp)[MeV]**
η	**370 (340)**	**410**
η'	**810(780)**	**820**
η''	$\pm$**100 (-30)**	**-20 / 140**
η''''	– **(250)**	–
ω	**10**	**15** $\pm$ **10**
ϕ	**250**	**250** $\pm$ **10**
f_2	**-40**	**-45** $\pm$ **15**
${f'}_2$	**315**	**200** $\pm$ **20**

where $\Delta M = M_{I=0} - M_{I=1}$ **is the mass shift due to the annihilation-contribution. In all other channels it seems to be ignored.**

Isoscalar Mesons

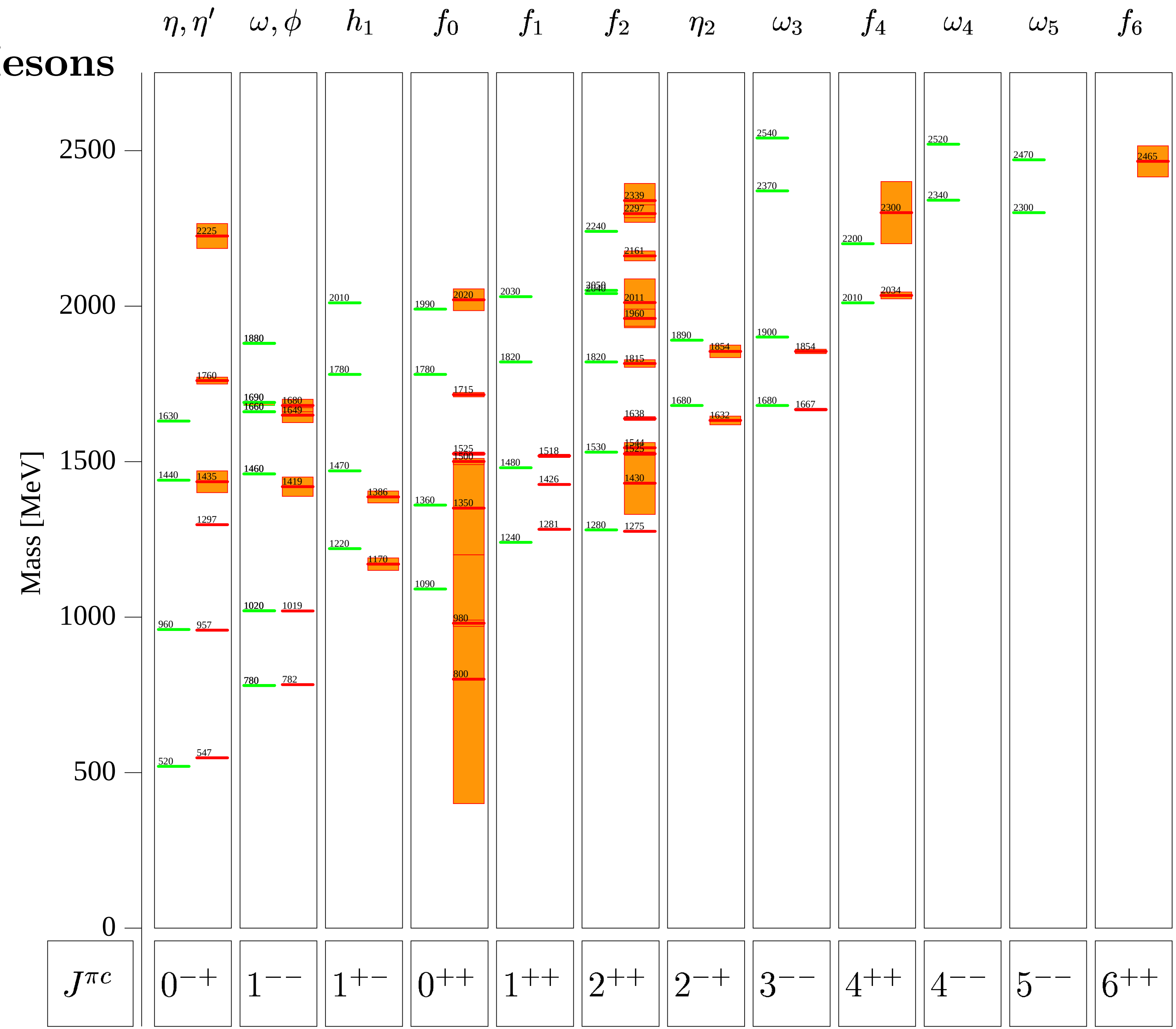

Light Mesons, isospin dependence

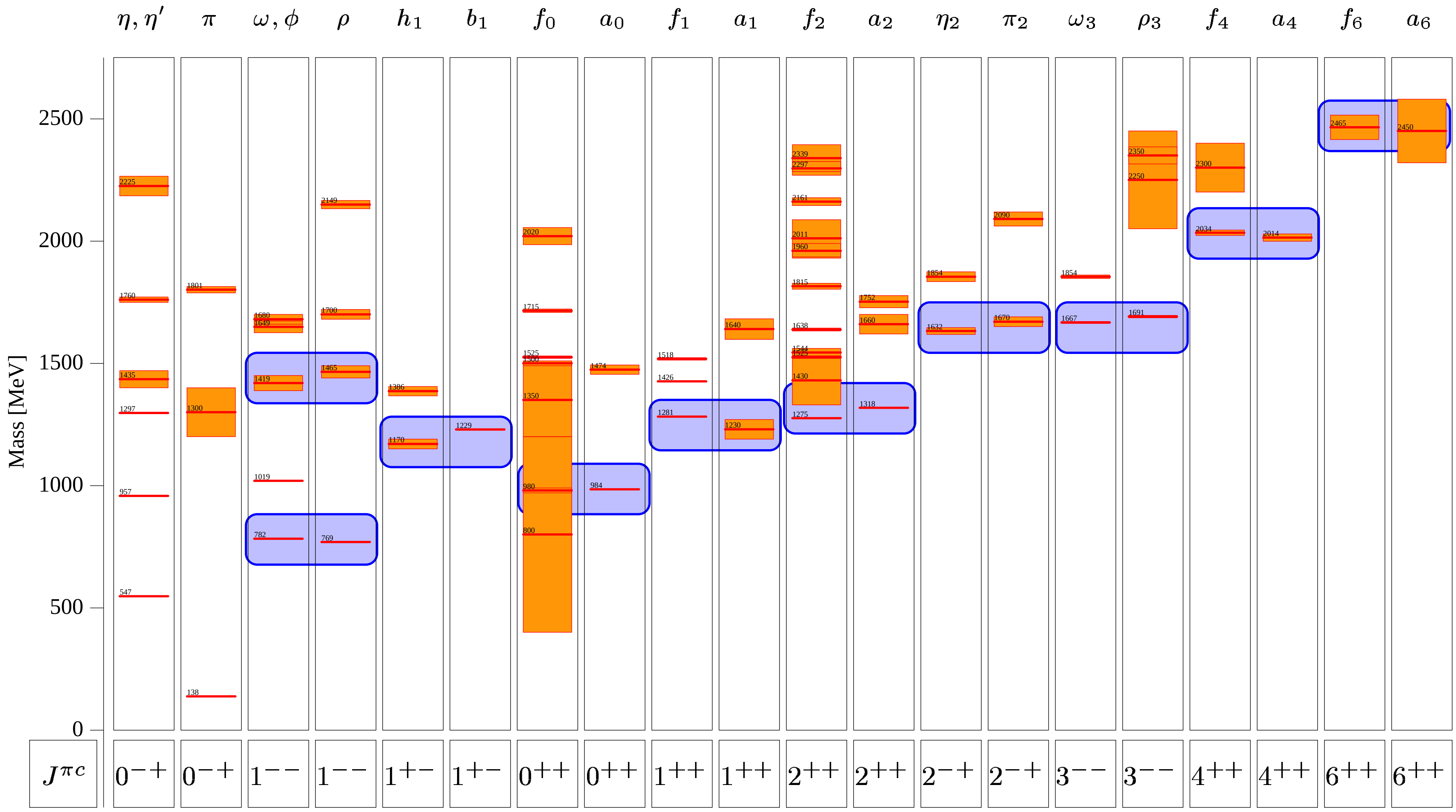

Strange mesons

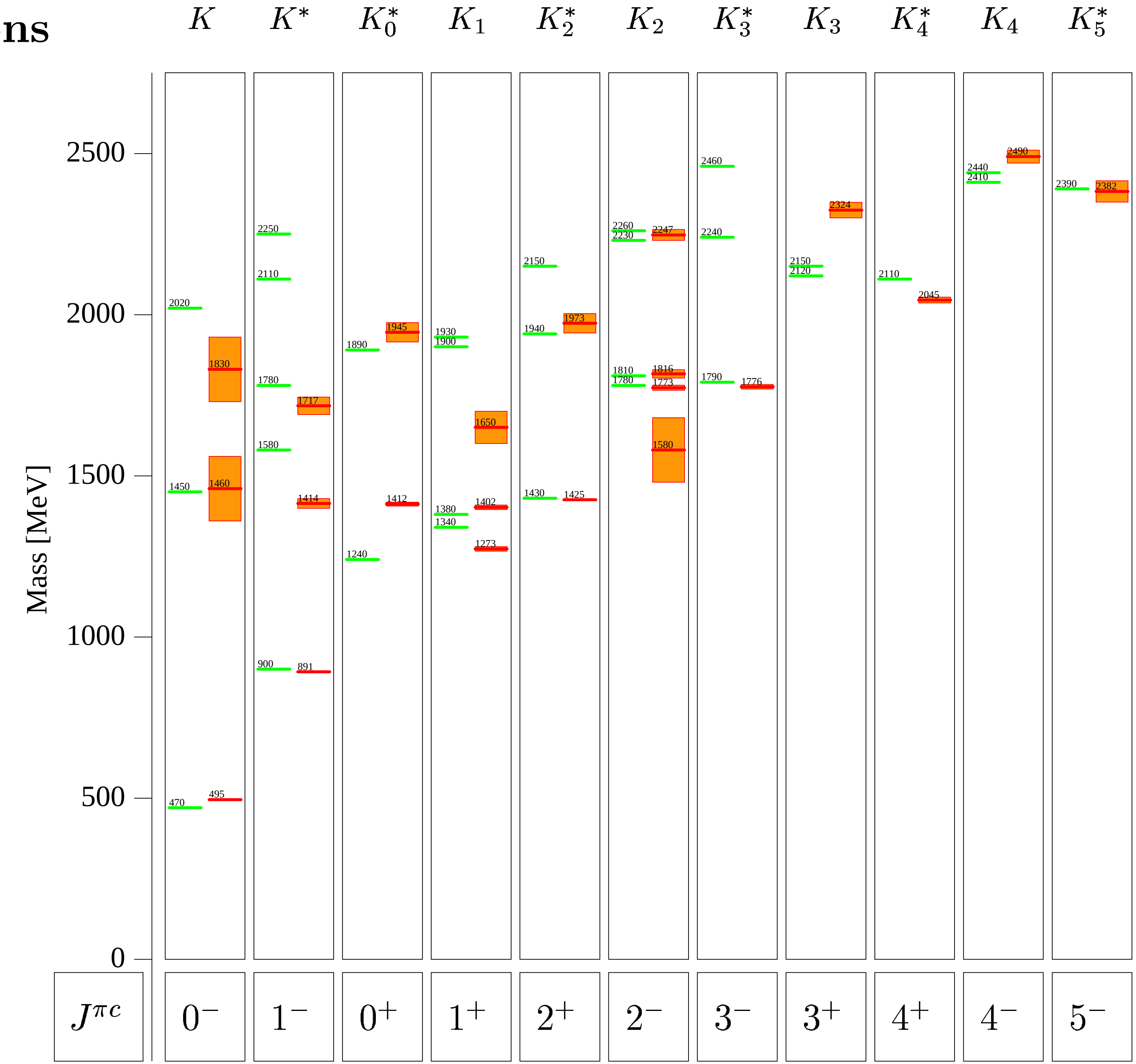

Isovector Mesons

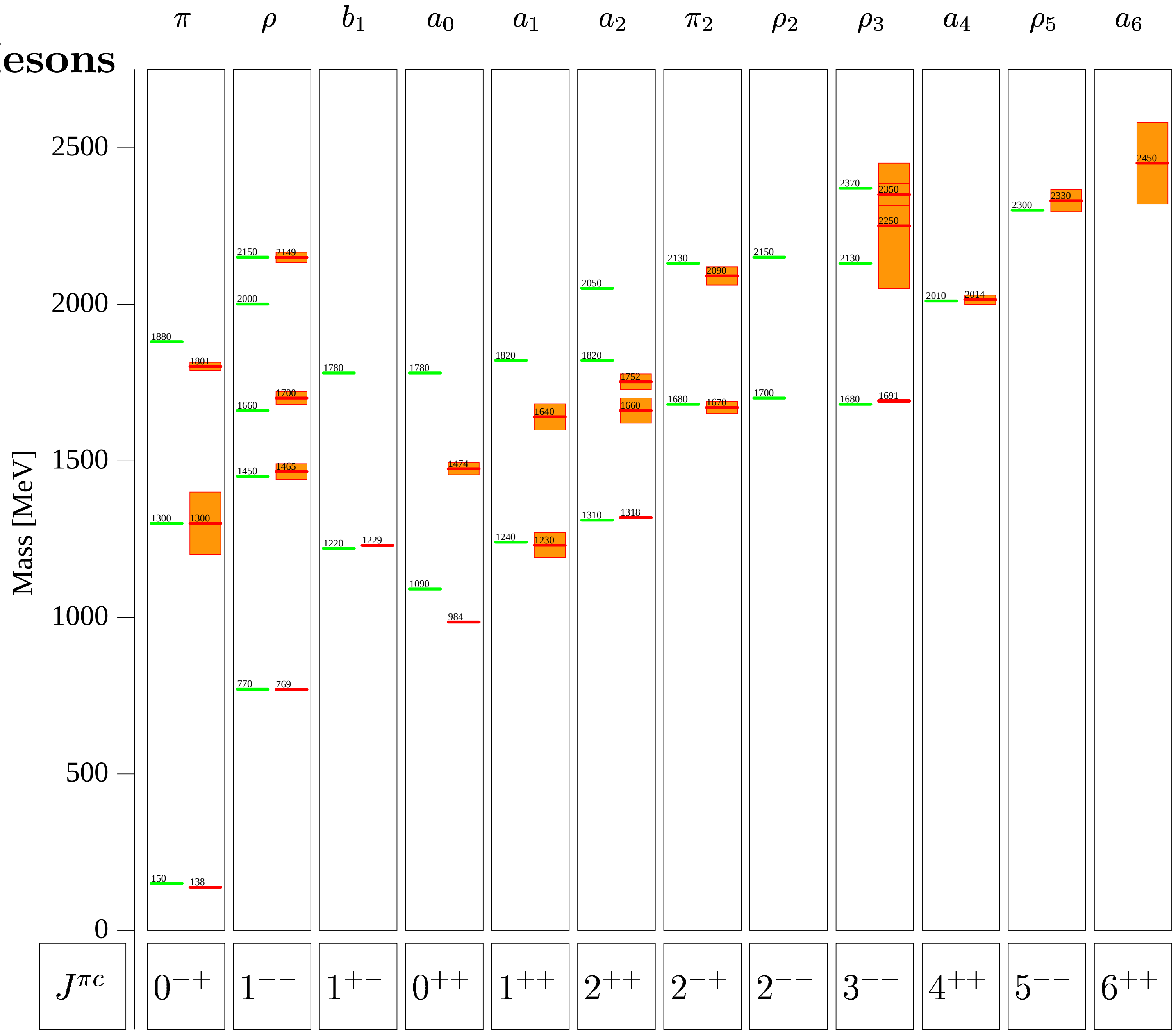

The Bonn model

- **Starting from field theory**
- **Nonrelativistic reduction of Salpater equation**
- **Confinement potential with Dirac structure**
  two variants, called $\mathcal{A}$ and $\mathcal{B}$
- **Instanton-induced interactions**
  for pseudoscalar and scalar mesons

U. Loring, B. C. Metsch and H. R. Petry, "The light baryon spectrum in a relativistic quark model with instanton-induced quark forces: The non-strange baryon spectrum and ground-states," "The light baryon spectrum in a relativistic quark model with instanton-induced quark forces: The strange baryon spectrum," Eur. Phys. J. A 10, (2001) 395, 447

Salpeter-model parameters

		Model $\mathcal{A}$		Model $\mathcal{B}$	
masses	m_n	**306**	**MeV**	**419**	**MeV**
	m_s	**503**	**MeV**	**550**	**MeV**
confinement	a_C	**-1751**	**MeV**	**-1135**	**MeV**
	b_C	**2076**	**MeV/fm**	**1300**	**MeV/fm**
	$\Gamma \cdot \Gamma$	$\frac{1}{2}(\mathbf{1} \cdot \mathbf{1} - \gamma_0 \cdot \gamma_0)$		$\frac{1}{2}(\mathbf{1} \cdot \mathbf{1} - \gamma_5 \cdot \gamma_5 - \gamma^\mu \cdot \gamma_\mu)$	
instanton	g	**1.73**	**GeV^{-2}**	**1.63**	**GeV^{-2}**
induced	g'	**1.54**	**GeV^{-2}**	**1.35**	**GeV^{-2}**
interaction	λ	**0.30**	**fm**	**0.42**	**fm**

Isovector Mesons

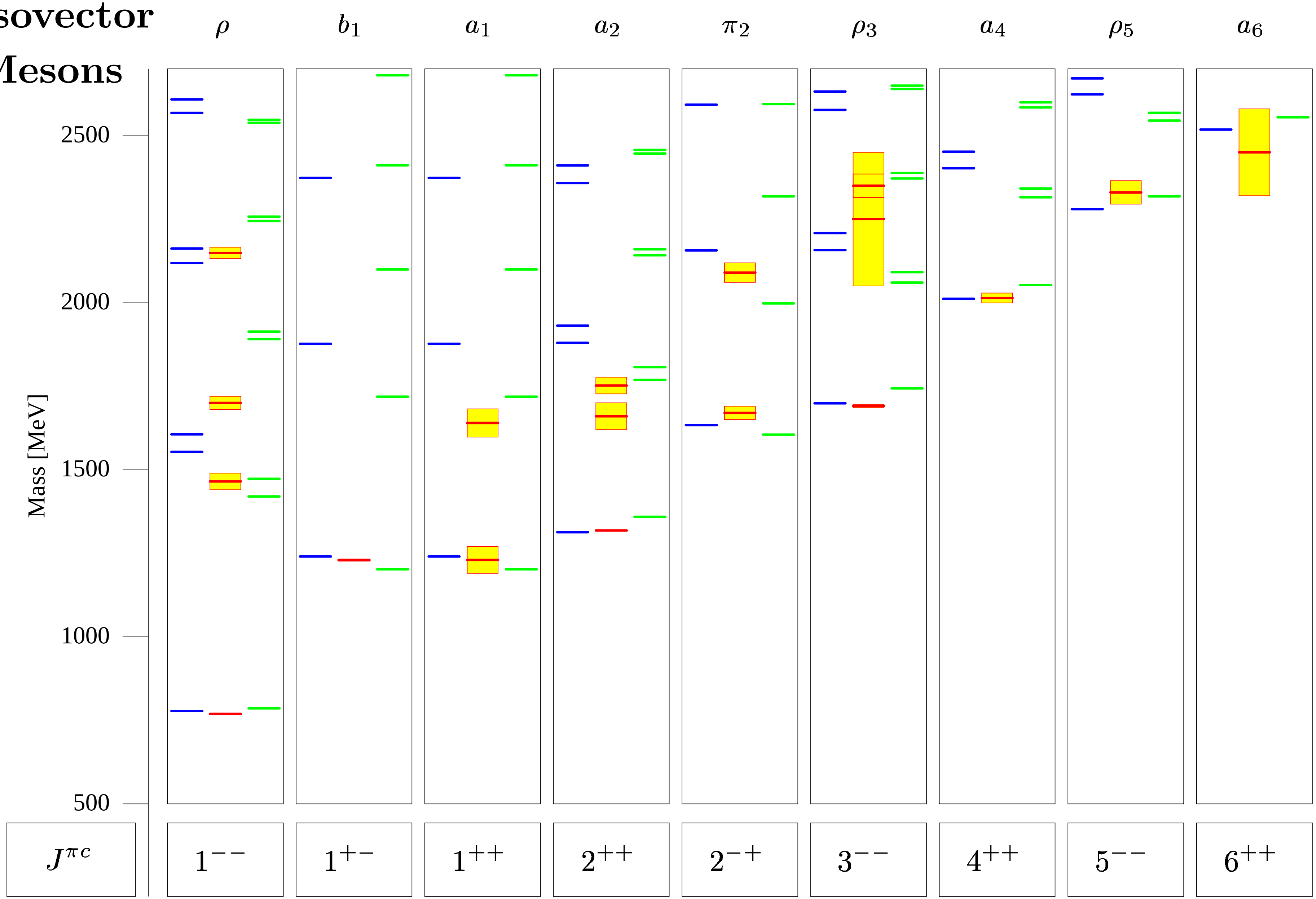

Strange Mesons

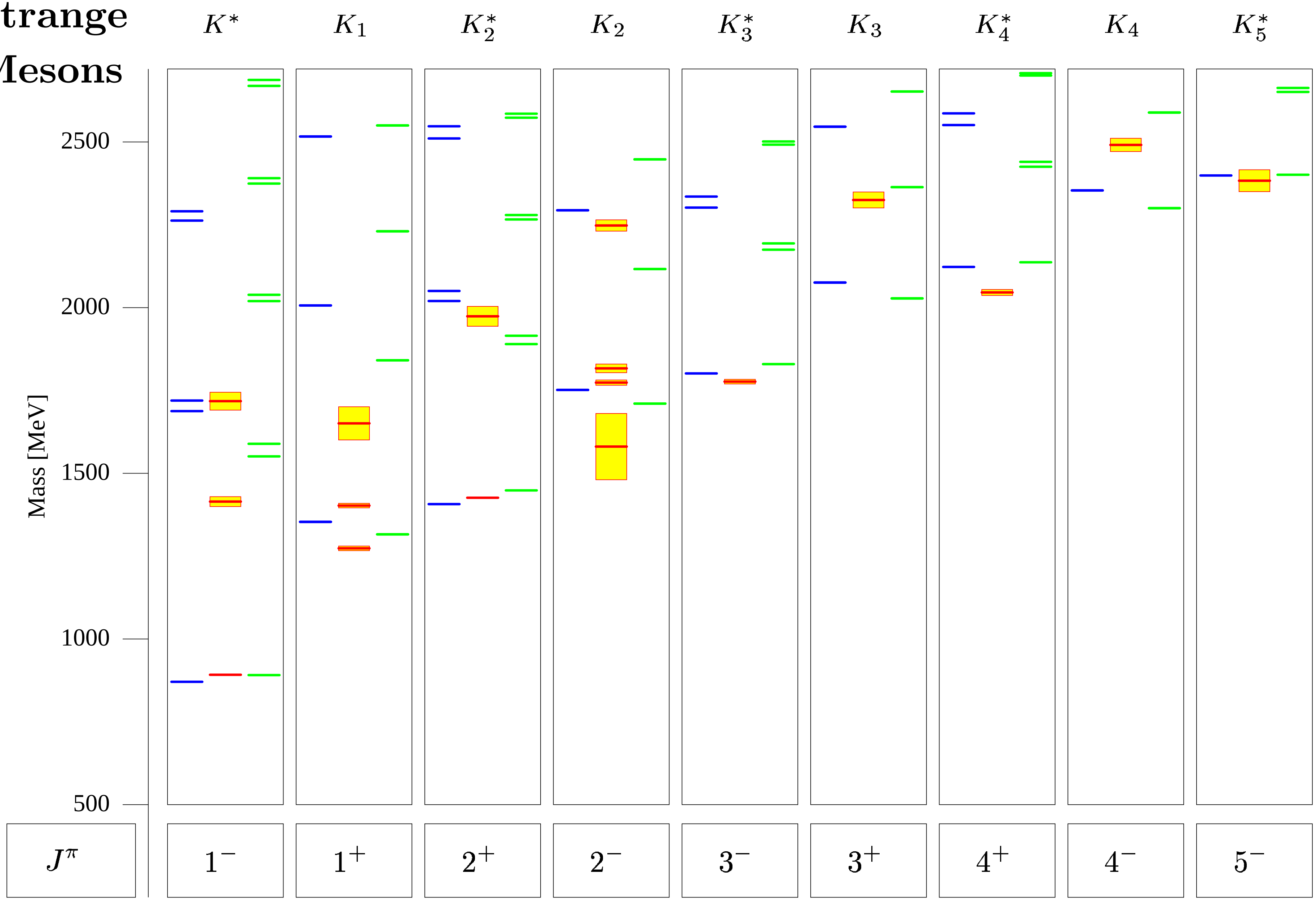

Isoscalar Mesons

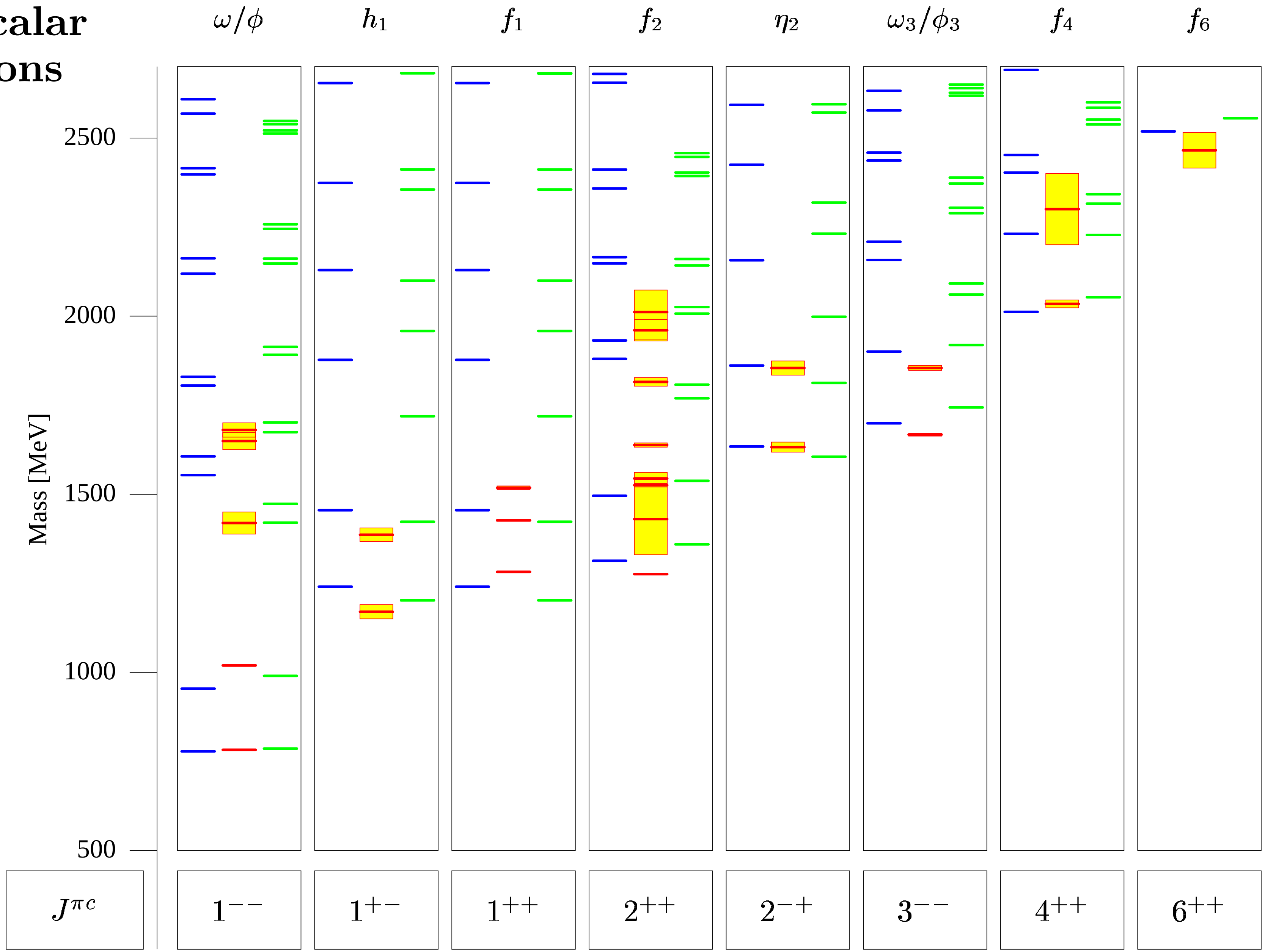

What are instantons?

Strong interactions of massless quarks: **Chiral symmetry**

However, symmetry is broken

- **Strong fluctuations of gluon fields**
- **QCD allows solutions with vortices (topological charge, winding number)**
- **Quarks can be bound to these vortices (zero modes)**
- **Quarks can flip spin under change of topological charge**
- **Chirality of quarks is not conserved**
- **Chiral symmetry is spontaneously broken**
- **Glodstone boson acquire mass**

Symmetry breaking :

	Magnetism	QCD
spontaneous	Weiss-districts	Constituent quarks $m_u \sim 120$ MeV
induced	magnetic field	Higgs field $m_u \sim 4$ MeV $m_d \sim 7$ MeV

Instantons on the lattice

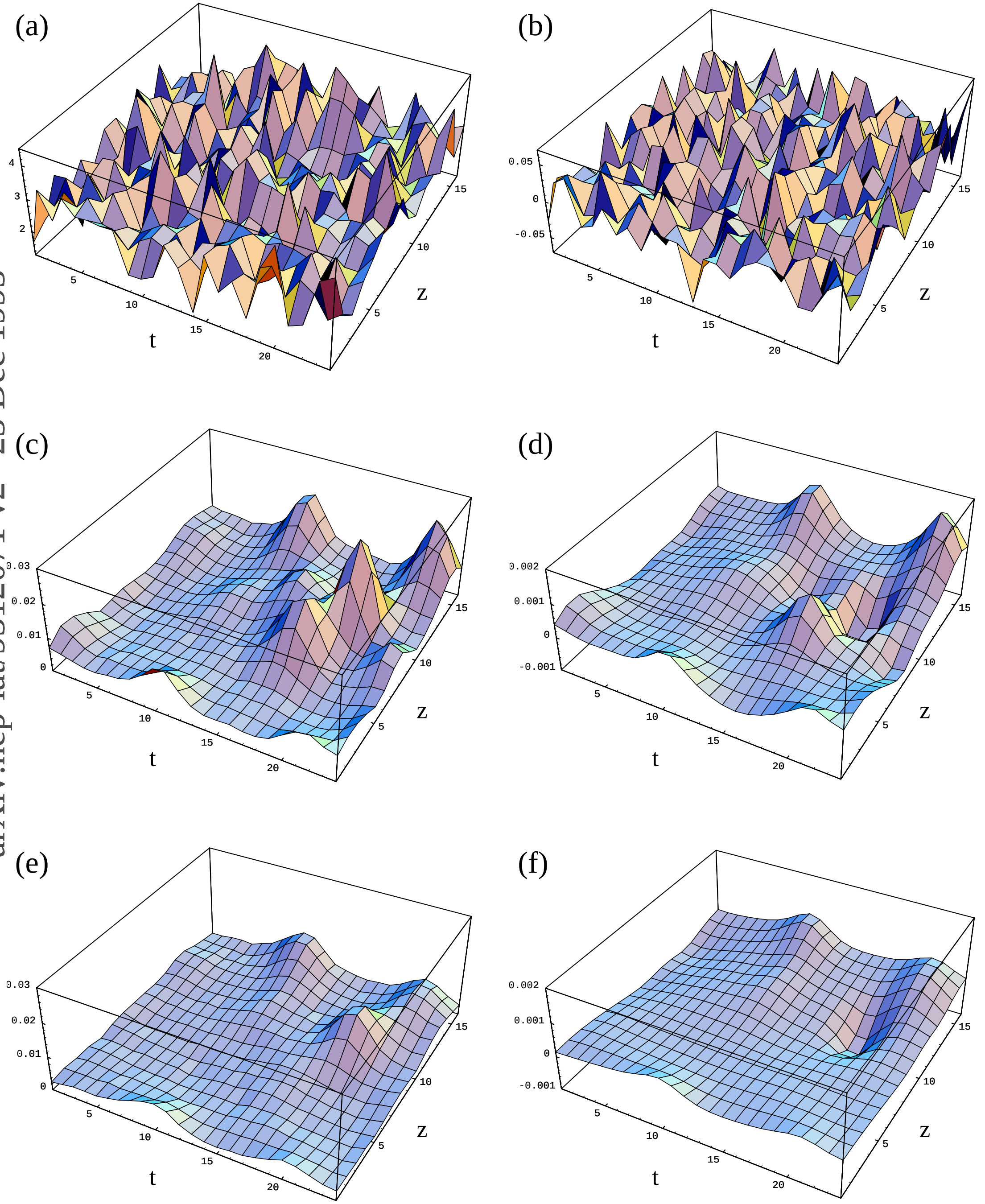

Action density (left) and topological charge (right) as functions of space and time before cooling (a,b) and after cooling (c-f).

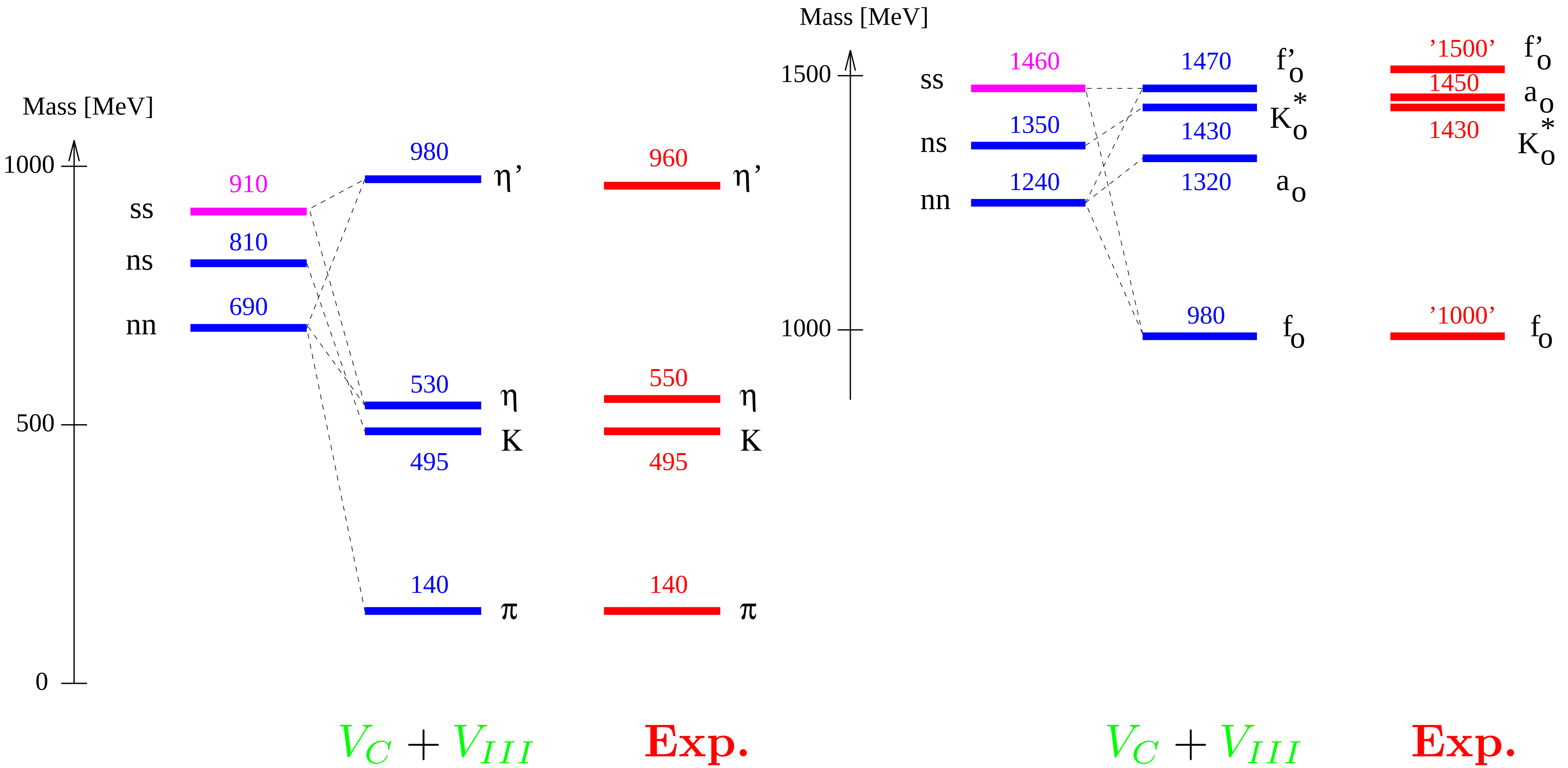

Mass [MeV]
1000
500
0
ss
ns
nn
910
810
690
980
530
495
140
η'
η
K
π
960
550
495
140
η'
η
K
π
$V_C + V_{III}$
Exp.
Mass [MeV]
1500
1000
ss
ns
nn
1460
1350
1240
1470
1430
1320
980
f'_o
K^*_o
a_o
f_o
'1500'
1450
1430
'1000'
f'_o
a_o
K^*_o
f_o
$V_C + V_{III}$
Exp.

Particle decays and partial wave analysis

- **Introduction**
- **Three-body decays**
- **Elements of scattering theory**
- **Angular distribution**
- **Flavor structure of mesons**

3 Particle decays and partial wave analysis

3.1 Introduction

The aim of an analysis is

- to determine masses and widths of resonances
  Breit-Wigner amplitude; Flatte formula, K-Matrix
- to determine their spins and parities
  Decay angular distributions, Zemach, Rarita-Schwinger or helicity formalism
- and their partial decay widths to different final states
  multichannel analyses
- and their flavor structure
  SU(2) and SU(3)

Particle decays

The transition rate for particle decays are given by Fermi's golden rule:

$$T_{if} = 2\pi |\mathcal{M}|^2 \rho(E_f)$$

$\mathbf{T_{if}}$ is the transition probability per unit time. With N particles the number of decays in the time interval dt is $\mathbf{NT_{if}dt}$ or

$$dN = -NT_{if}dt$$

and

$$N = N_0 e^{-T_{if}t} = N_0 e^{-(t/\tau)} = N_0 e^{-\Gamma t}$$

$$\Gamma\tau = \hbar = 1$$

(uncertainty priniple).

How to describe a short-lived state in QM ?

Consider a state with energy $E_0 = \hbar\omega$; it is characterised by a wave function

$$\psi(t) = \psi_0(t)e^{-iE_0 t}$$

Now we allow it to decay:

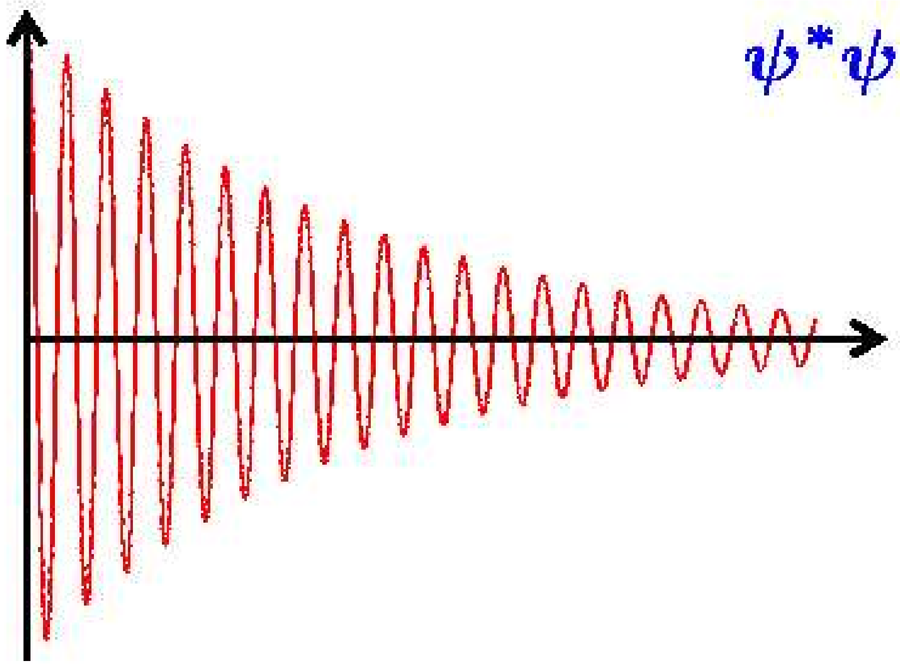

$$\psi^*\psi = \psi_0^*(t)\psi_0(t) = \psi_0^*(t=0)\psi_0(t=0)\mathbf{e^{-t/\tau}}.$$

Probabilty density must decay exponentially. $\longrightarrow$

$$\psi(t) = \psi(t=0)e^{-iE_0 t}\mathbf{e^{-t/2\tau}}$$

A damped oscillation contains not only one frequency. The frequency distribution can be calculated by the Fourier transformation:

$$f(\omega) = f(E) = \int_0^\infty \psi(t=0) e^{-iE_0 t - t/2\tau} e^{iEt} dt$$
$$= \int_0^\infty \psi(t=0) e^{-i((E_0 - E)t - 1/2\tau)t} dt$$

$$= \frac{\boldsymbol{\psi(t=0)}}{\mathbf{(E_0 - E) - i/(2\tau)}}$$

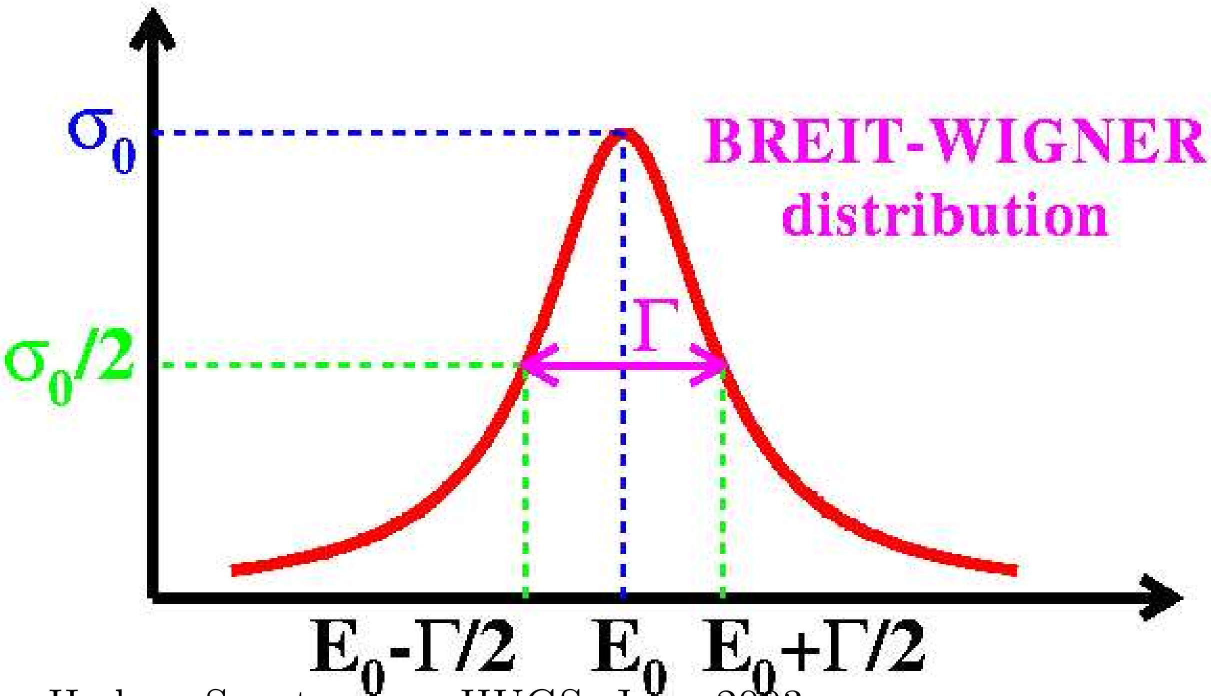

Probability to find the energy E:

$$f^*(E) f(E) = \frac{\mathbf{|\psi(t=0)|^2}}{\mathbf{(E_0 - E)^2 + 1/(2\tau)^2}}$$

$$(\tau = 1/\Gamma) \rightarrow \frac{\mathbf{(\Gamma/2)^2}}{\mathbf{(E_0 - E)^2 + (\Gamma/2)^2}}$$

Resonances are described by amplitudes !

$$BW(E) = \frac{\mathbf{\Gamma/2}}{\mathbf{(E_0 - E) - i\Gamma/2}} = \frac{\mathbf{1/2}}{\mathbf{(E_0 - E)/\Gamma - i/2}}$$

With

$$\mathbf{2\,(E_0 - E)/\Gamma} = \cot\delta : \qquad \mathbf{f(E)} = \frac{\mathbf{1}}{\cot\delta - \mathbf{i}} = \mathbf{e^{i\delta}}\sin\delta = \frac{\mathbf{i}}{\mathbf{2}}\left(\mathbf{1 - e^{-2i\delta}}\right)$$

This formula is derived from S matrix. δ is called phase shift. The amplitude is zero for $\Gamma/(E - E_0) << 0$ and starts to be real and positive with an small positive imaginary part. For $\Gamma/(E - E_0) >> 0$ the amplititude is small, real and positive with an small negative imaginary part. The amplitude is purely imaginary (i) for $E = E_0$. The phase δ goes from 0 to $\pi/2$ at resonance and to π at high energies.

Argand circle

Scattering amplitude T in case of inelastic scattering. Definition of phase δ and inelasticity η.

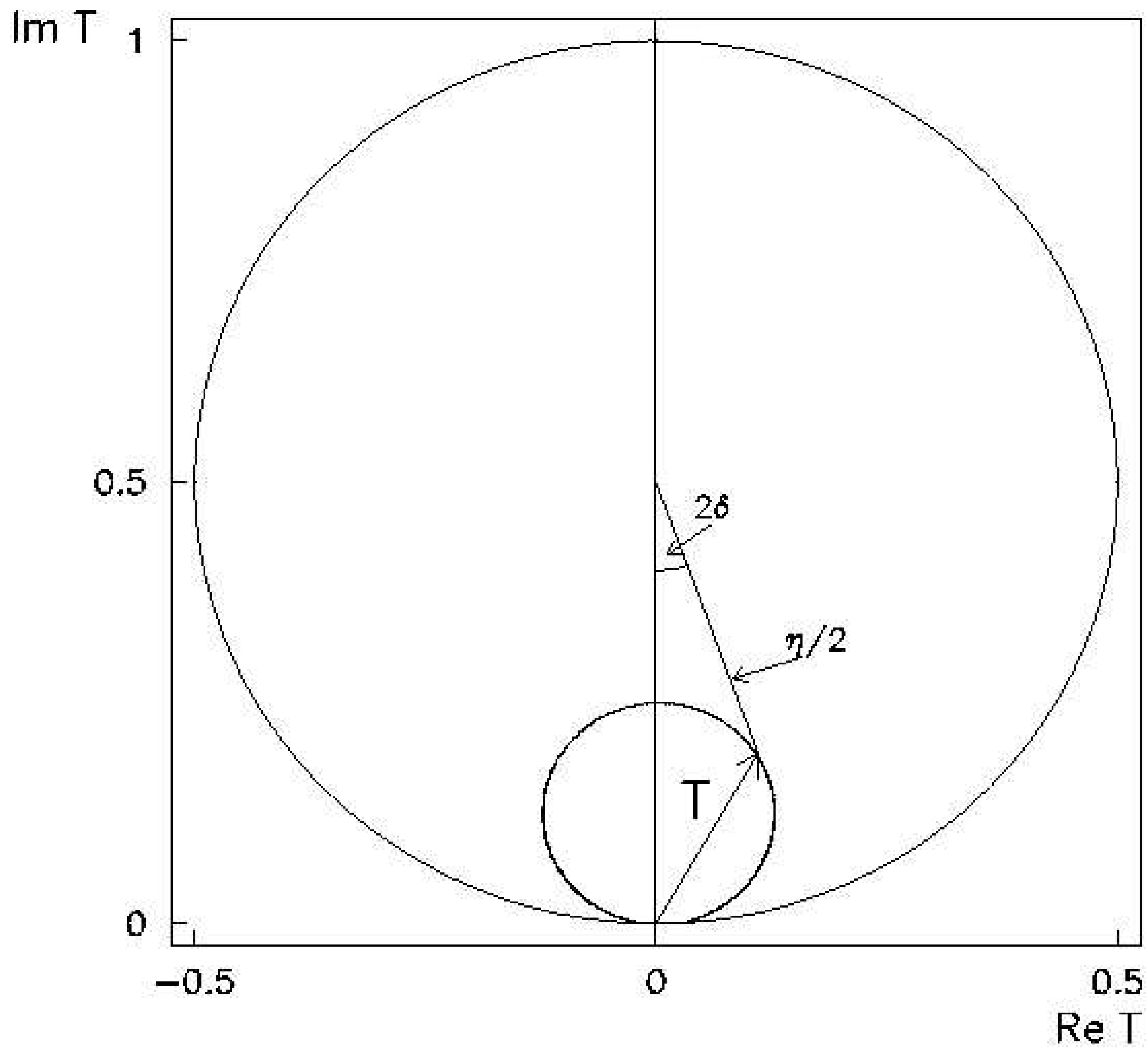

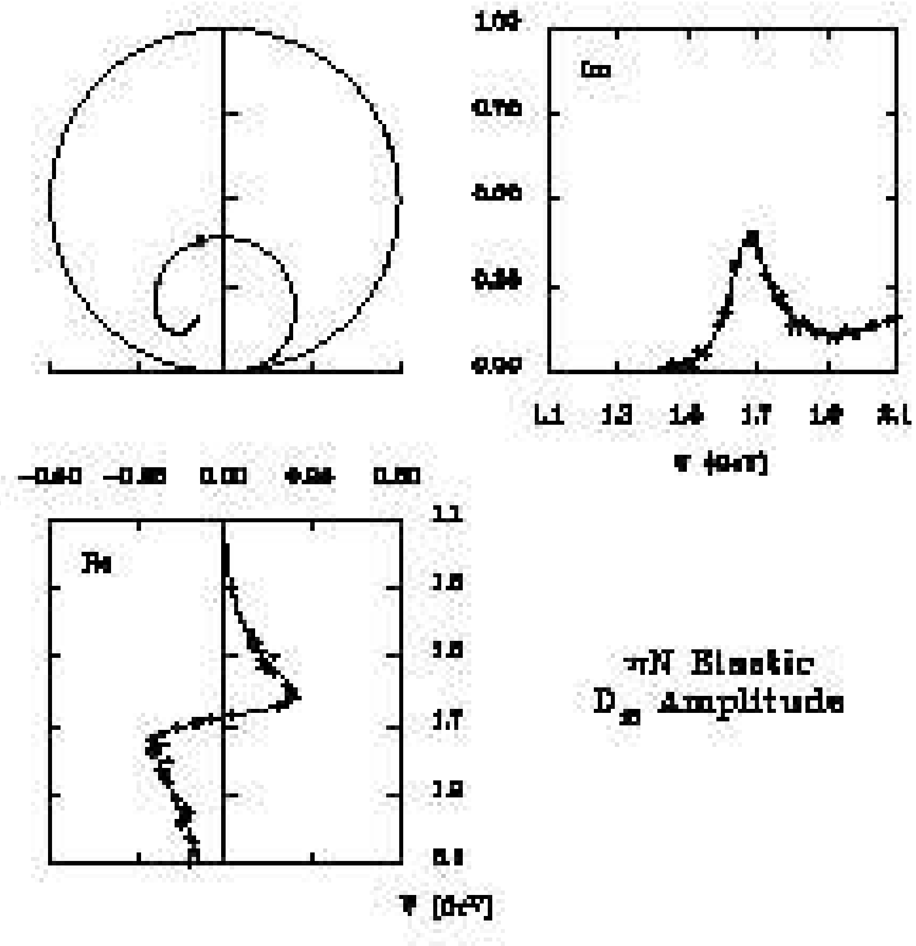

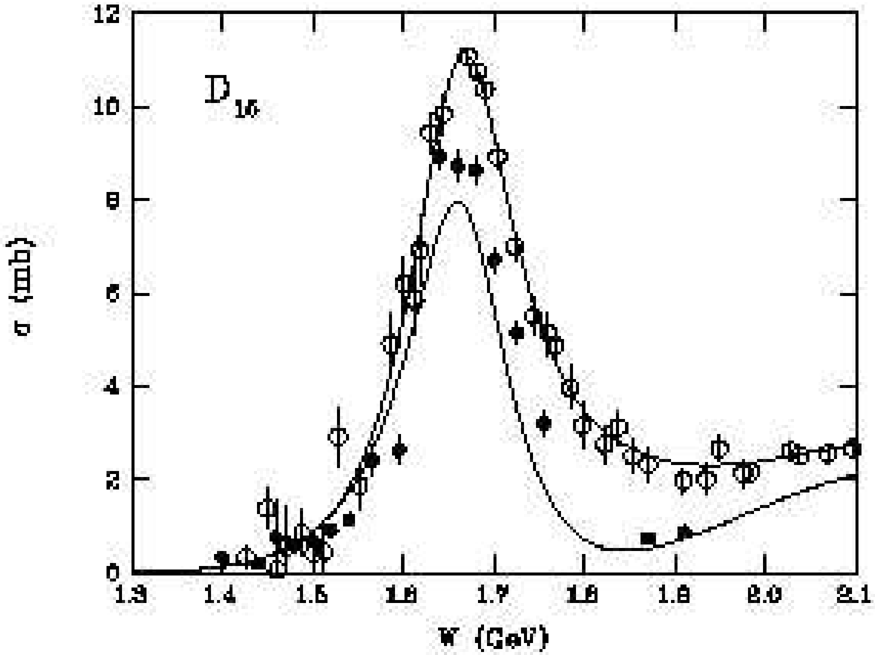

Elastic channel (upper curve), $\pi p \rightarrow \pi\pi p$ (lower curve), difference $\pi p \rightarrow \eta p$ or $\pi p \rightarrow \Lambda K$

Argand diagram and cross section for $\pi^- p \rightarrow \pi^- p$ via formation of the N(1650)$D_{1,5}$ resonance (L=2). From:

D. M. Manley, "Multichannel analyses of anti-K N scattering," PiN Newslett. 16 (2002) 74.

3.2 Three-body decays

A particularly important case is that of annihilation into three final-state particles, $\mathbf{M \rightarrow (m_1, m_2, m_3)}$.

- **There are 12 dynamical variables (3 four-vectors).**
- **These are constrained by energy and momentum conservation.**
- **Three masses can be identified.**
- **There are three arbitrary Euler angles defining the orientation the three-body system in space.**

Two variables need (and suffice) to be identify the full dynamics. The two variables are customly chosen as squared invariant masses $\mathbf{{m_{12}}^2}$ and $\mathbf{{m_{13}}^2}$. Then the partial width can be expressed as

$$d\Gamma = \frac{1}{(2\pi)^3}\frac{1}{32M} \cdot \overline{|\mathcal{M}|^2} \cdot dm_{12}^2 dm_{13}^2$$

Events are uniformly distributed in the $\mathbf{(m_{12}^2, m_{13}^2)}$ plane if the reaction leading to the three particle final state has no internal dynamics. This is the Dalitz plot.

Warnings:

1. If the decaying particle has a spin $J \neq 0$, summation over the spin components is required.
2. If a spinning particle is produced in flight, the spin may be aligned, the components m_j can have a non-statistical distribution.

The Dalitz plot

Events are represented in a Dalitz plot by one point in a plane defined by m^2_{12} in x and m^2_{23} in y direction. Since the Dalitz plot represents the phase space, the distribution is flat in case of absence of any dynamical effects. An example is the Dalitz plot for

$$K^0_L \rightarrow \pi^+\pi^-\pi^0$$

Resonances in m^2_{12} are given by a vertical line, in m^2_{23} as horizontal lines. Since

$$m^2_{13} = (M^2_p + m^2_1 + m^2_2 + m^2_3) - (m^2_{12} - m^2_{23})$$

particles with defined m^2_{13} mass are found on the second diagonal.

From the invariant mass of particles 2 and 3

$$m_{23}^2 = (E_2 + E_3)^2 - (\boldsymbol{p}_2 + \boldsymbol{p}_3)^2$$

we derive

$$m_{23}^2 = (m_2^2 + m_3^2 + 2 \cdot E_2 \cdot E_3) - (2 \cdot |\boldsymbol{q}_2| \cdot |\boldsymbol{q}_3|) \cdot \cos\theta$$

with θ being the angle between $\boldsymbol{q_2}$ and $\boldsymbol{q_3}$. This can be rewritten as

$$m_{23}^2 = \left[\left(m_{23}^2\right)_{max} + \left(m_{23}^2\right)_{min}\right] + \left[\left(m_{23}^2\right)_{max} - \left(m_{23}^2\right)_{min}\right] \cdot \cos\theta$$

For a fixed value of $\mathbf{m_{1,2}}$ the momentum vector $\boldsymbol{p_3}$ has a $\cos\theta$ direction w.r.t. the recoil $\boldsymbol{p_1}$ which is proportional to $\mathbf{m_{23}^2}$.

Example:

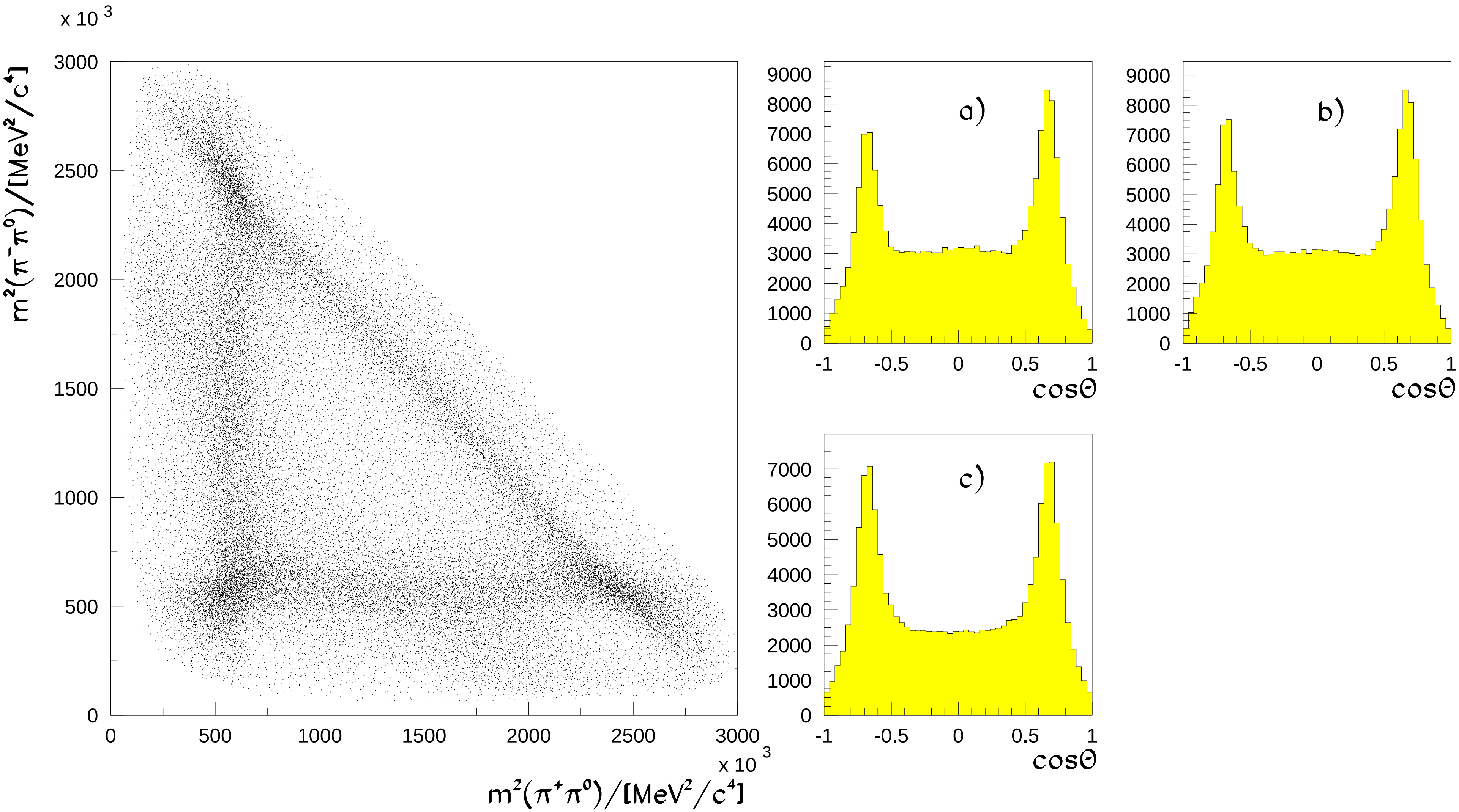

The $\pi^+\pi^-\pi^0$ Dalitz plot in $\mathrm{p\bar{p}}$ annihilation at rest, and ρ^+ (a), ρ^- (b) and ρ^0 (c) decay angular distributions.

The Dalitz plot shows striking evidence for internal dynamics. High-density bands are visible at fixed values of $\mathbf{m^2_{12}}, \mathbf{m^2_{13}}$, and $\mathbf{m^2_{23}}$. The three bands correspond to the sequential annihilation modes $\mathbf{p\bar{p}} \rightarrow |\rho^+ >|\pi^- >$, $|\rho^- >|\pi^+ >$, and $|\rho^0 >|\pi^0 >$, respectively. The enhancements due to ρ production as intermediate states is described by dynamical functions $\mathcal{F}$.

The Figures on the right shows the density distribution choosing a slice $\mathbf{m^2_{12}} = \mathbf{m^2_{|\rho^+>}} \pm \mathbf{\Delta m^2_{|\rho^+>}}$ and plotting the number of events as a function of $\mathbf{m^2_{13}}$. All three ρ decay angular distributions exhibit two peaks. Their significance is immediately evident from the Dalitz plot. The three bands due to the three ρ charged states cross; at the crossing two amplitudes interfere and the observed intensity increases by a factor of four as one should expect from quantum mechanics. Apart from the peaks the decay angular distribution is approximately given by $\sin^2\theta$, hence $\mathcal{A} \sim \sin\theta$. The three ρ production amplitudes have obviously the same strength indicating that the $\mathbf{p\bar{p}}$ initial state(s) from which ρ production occur(s) must have isospin zero.

3.3 Elements of scattering theory

Consider two-body scattering from the initial state i to the final state f, $ab \to cd$. Then

$$\frac{d\sigma_{fi}}{d\Omega} = \frac{1}{(8\pi)^2 s}\frac{q_f}{q_i}|\mathcal{M}_{fi}|^2 = |f_{fi}(\Omega)|^2$$

where $s = m^2$ = squared CMS energy; q break-up momenta. In case of spins, one has to average over initial spin components and sum over final spin components. The scattering amplitude can be expanded into partial-wave amplitudes:

$$f_{fi}(\Omega) = \frac{1}{q_i}\sum(2J+1)T^J_{fi}D^{J*}_{\lambda\mu}(\Phi,\Theta,0)$$

One may remove the probability that the particles do not interact by $S = I + iT$. Probability conservation yields $SS^\dagger = I$ from which one may define

$$K^{-1} = T^{-1} + iI$$

From time reversal: K is real and symmetric.

Below the lowest inelasticity threshold

$$\mathbf{S} = \mathbf{e}^{\mathbf{2i}\delta} \qquad \mathbf{T} = \mathbf{e}^{\mathbf{i}\delta}\mathbf{sin}\delta$$

For a two-channel problem, the S-matrix is 2×2.

$$\mathbf{S_{ik}S^*_{jk}} = \delta_{\mathbf{ij}}$$

and

$$\mathbf{S_{11}} = \eta\mathbf{e}^{\mathbf{2i}\delta_1}$$

$$S_{22} = \eta e^{2i\delta_2}$$

$$S_{12} = ie^{i\delta_1+\delta_2}\sqrt{1-\eta^2}$$

The T matrix is so far not relativistically invariant. This can be achieved by introducing $\hat{T}$:

$$\mathbf{T_{ij}} = \left(\rho_{\mathbf{i}}^{\frac{1}{2}}\right)\hat{\mathbf{T}}_{\mathbf{ij}}\left((\rho_{\mathbf{i}})^{\frac{1}{2}}\right)$$

where $\rho_{\mathbf{n}} = \mathbf{2q_n}/\mathbf{m}$ are phase space factors.

The amplitude now reads

$$\mathbf{\hat{T}^J_{fi}(\Omega) = \frac{1}{q_i}\sum(2J+1)\hat{T}^J_{fi}D^{J*}_{\lambda\mu}(\Phi,\Theta,0)}$$

with

$$\rho_\mathbf{n} = \mathbf{2q_n/m} = \sqrt{\left[\mathbf{1} - \left(\frac{\mathbf{m_a+m_b}}{\mathbf{m}}\right)^\mathbf{2}\right]\left[\mathbf{1} - \left(\frac{\mathbf{m_a-m_b}}{\mathbf{m}}\right)^\mathbf{2}\right]}$$

Now the following relations hold:

$$\hat{\mathbf{T}} = \frac{\mathbf{1}}{\rho}\mathbf{e}^{\mathbf{i}\delta}\mathbf{sin}\delta; \qquad \hat{\mathbf{K}}^{-\mathbf{1}} = \hat{\mathbf{T}}^{-\mathbf{1}} + \mathbf{i}\rho$$

$$\hat{\mathbf{T}} = \frac{\mathbf{1}}{\mathbf{1} - \rho_\mathbf{1}\rho_\mathbf{2}\hat{\mathbf{D}} - \mathbf{i}\left(\rho_\mathbf{1}\hat{\mathbf{K}}_\mathbf{11} + \rho_\mathbf{2}\hat{\mathbf{K}}_\mathbf{22}\right)}\begin{pmatrix} \hat{\mathbf{K}}_\mathbf{11} - \mathbf{i}\rho_\mathbf{2}\hat{\mathbf{D}} & \hat{\mathbf{K}}_\mathbf{12} \\ \hat{\mathbf{K}}_\mathbf{21} & \hat{\mathbf{K}}_\mathbf{22} - \mathbf{i}\rho_\mathbf{1}\hat{\mathbf{D}} \end{pmatrix}$$

and $\hat{\mathbf{D}} = \hat{\mathbf{K}}_\mathbf{11}\hat{\mathbf{K}}_\mathbf{22} - \hat{\mathbf{K}}^\mathbf{2}_\mathbf{12}$

In case of resonances, we have to introduce poles into the K-matrix:

$$\mathbf{K_{ij}} = \sum_{\alpha} \frac{\mathbf{g_{\alpha i}(m) g_{\alpha j}(m)}}{\mathbf{m_\alpha^2 - m^2}} + \mathbf{c_{ij}}$$

$$\hat{\mathbf{K}}_{\mathbf{ij}} = \sum_{\alpha} \frac{\mathbf{g_{\alpha i}(m) g_{\alpha j}(m)}}{\mathbf{(m_\alpha^2 - m^2)}\sqrt{\rho_{\mathbf{i}}\rho_{\mathbf{j}}}} + \hat{\mathbf{c}}_{\mathbf{ij}}$$

The coupling constants g are related to the partial decay widths

$$\mathbf{g_{\alpha i}^2 = m_\alpha \Gamma_{\alpha i}(m)} \qquad \mathbf{\Gamma_\alpha(m) = \sum_i \Gamma_{\alpha i}(m)}$$

The partial decay widths and couplings depend on the available phase space

$$\mathbf{g_{\alpha i}(m) = g_{\alpha i}(m_\alpha) B^l_{\alpha i}(q, q_\alpha}\sqrt{\rho_{\mathbf{i}}}$$

These formule can be used in the case of several resonances (sum over α) decaying into different final states (i). The K-matrix preserves unitarity and analyticity. It is a multi-channel approach.

Adding two resonances using a K-matrix

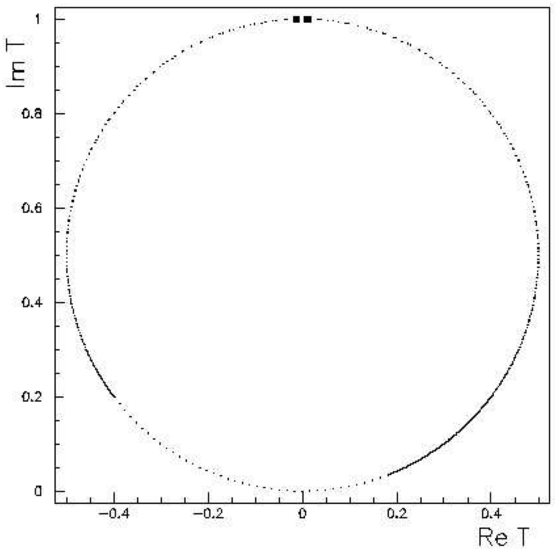

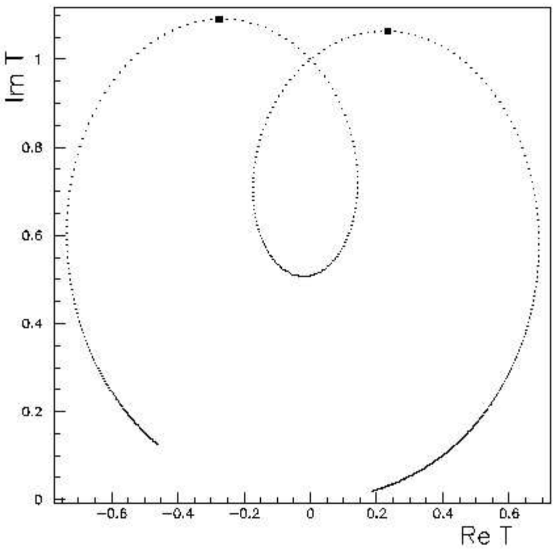

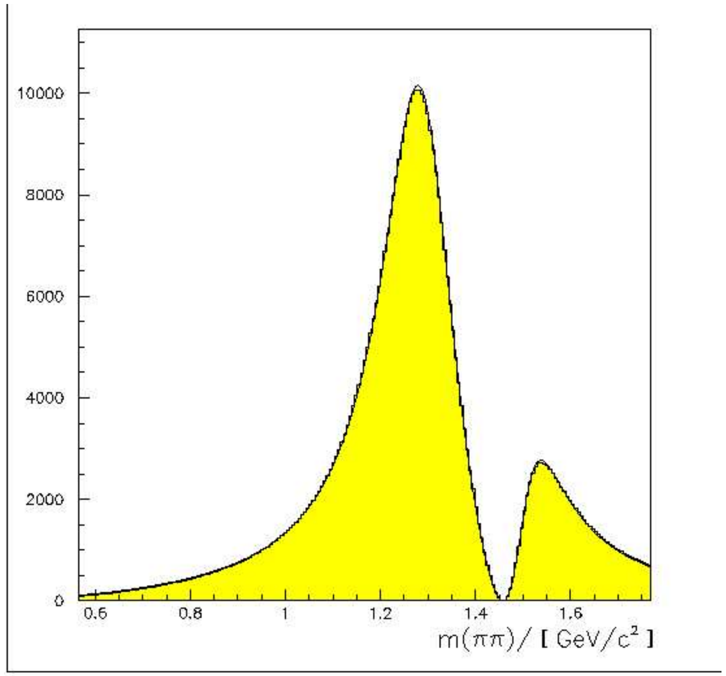

3.4 Angular distributions

Zemach formalism: **Back to our Dalitz plot: on the right are decay angular distributions. The ρ is emitted with a momentum p_ρ and then decays in a direction characterized, in the ρ rest frame, by one angle Θ and the momentum vector p_π.**

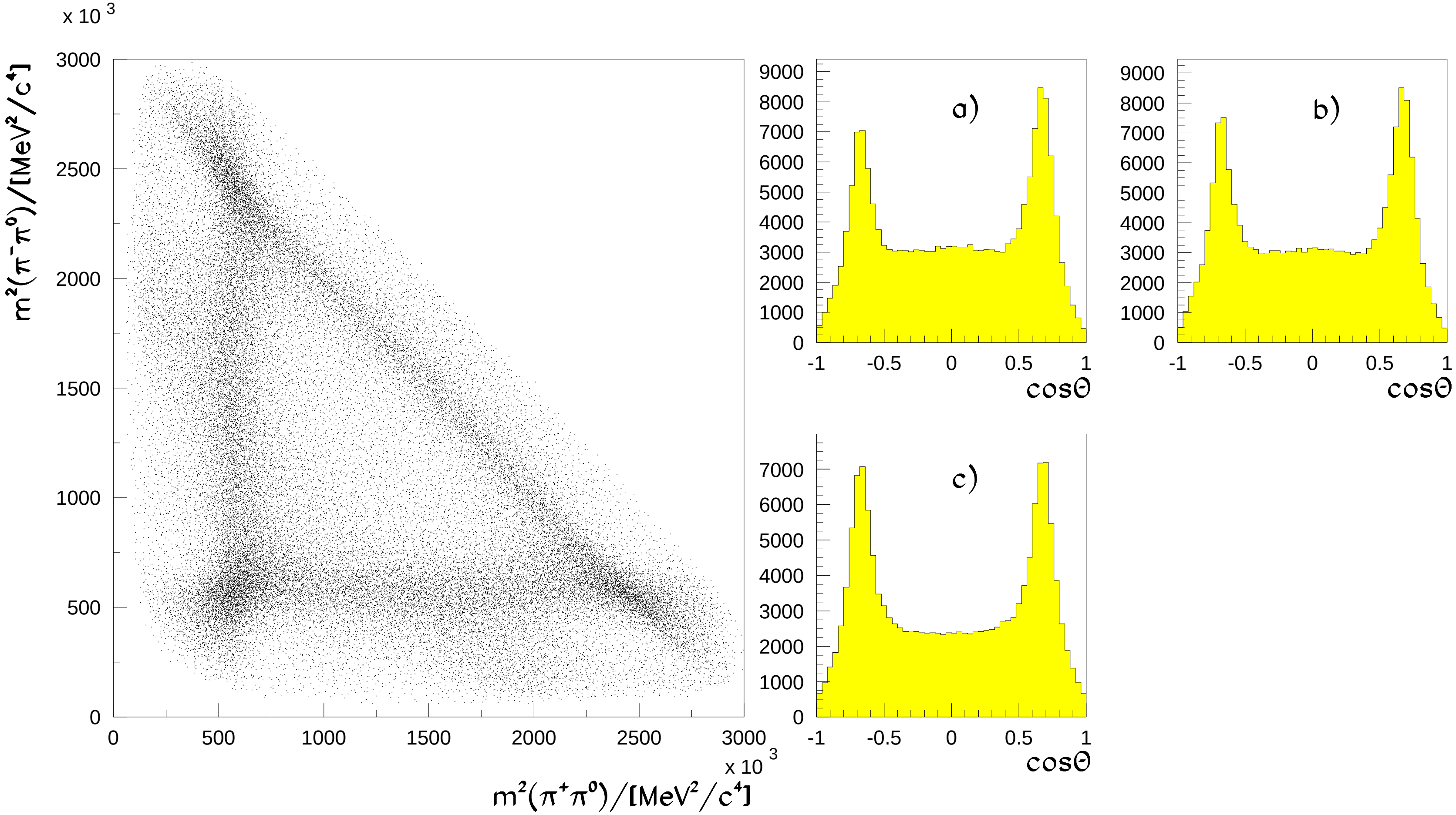

The $\mathrm{p\bar{p}}$ initial state has $\mathbf{L=0}$: The parity of the initial state is -1 (in both cases), the parities of π and ρ are -1; hence there must be an angular momentum $red\mathbf{l}_\rho = \mathbf{1}$ between π and ρ. This decay is described by the vector $\boldsymbol{p}_\rho$. The ρ decays also with one unit of angular momentum, with $\mathbf{l}_\pi = \mathbf{1}$. From the two rank-one tensors (=vectors) we have to construct the initial state:

$$J = S = \begin{cases} \mathbf{J} & \mathbf{^{2s+1}L_J} & \mathbf{J^{PC}} & \textbf{Zemach} & \textbf{angle} \\ \mathbf{0} & \mathbf{^1S_0} & \mathbf{0^{-+}} & \boldsymbol{p}_\rho \cdot \boldsymbol{p}_\pi & \mathbf{sin\Theta} \\ \mathbf{1} & \mathbf{^3S_1} & \mathbf{1^{--}} & \boldsymbol{p}_\rho \times \boldsymbol{p}_\pi & \mathbf{cos\Theta} \end{cases}$$

Higher spins:

- **Traceless, trace $\mathbf{t=0}$**

$$\sum \mathbf{t^i} = \mathbf{0}; \qquad \sum \mathbf{t^{ii}} = \mathbf{0}; \qquad \sum \mathbf{t^{iii}} = \mathbf{0}; \cdots$$

- **Symmetry**

$$\mathbf{t^{ij}} = \mathbf{t^{ji}}; \qquad \mathbf{t^{ijk}} = \mathbf{t^{jik}} = \mathbf{t^{ij}} = \mathbf{t^{ikj}}$$

- **Tensors are construct as products of lower-rank tensors**

$$\mathbf{t^i t^j} \Longrightarrow \tfrac{1}{2}(\mathbf{t^i t^j} + \mathbf{t^i t^j}) - \tfrac{1}{3}\mathbf{t^2}\delta^{\mathbf{ij}}$$

- **To reduce rank, multiply with $\delta^{\mathbf{ij}}\delta^{\mathbf{kl}}$ or ϵ^{ijk}**

3.4.1 Helicity formalism

M. Jacob and G. C. Wick, "On The General Theory Of Collisions For Particles With Spin," Annals Phys. 7 (1959) 404 [Annals Phys. 281 (2000) 774].

Thanks to Dr. Ulrike Thoma.

The helicity of a particle is defined as the projection of its total angular momentum $\boldsymbol{J} = \boldsymbol{l} + \boldsymbol{s}$ onto its direction of flight.

$$\lambda = \boldsymbol{J} \cdot \frac{\boldsymbol{p}}{|\boldsymbol{p}|} = l \cdot \frac{\boldsymbol{p}}{|\boldsymbol{p}|} + m_s = m_s \ ,$$

Consider a particle A decaying into particles B and C with spins s_1, s_2. The particles move along the z-axis (quantisation axis). The final state is described by $(2s_1+1)\cdot(2s_2+1)$ helicity states $|p\lambda_1\lambda_2\rangle$; λ_i are the helicities of the particles and p is their center of mass momentum.

A particle B which is emitted in a arbitrary direction can be described in spherical coordinates by the angles θ, ϕ.

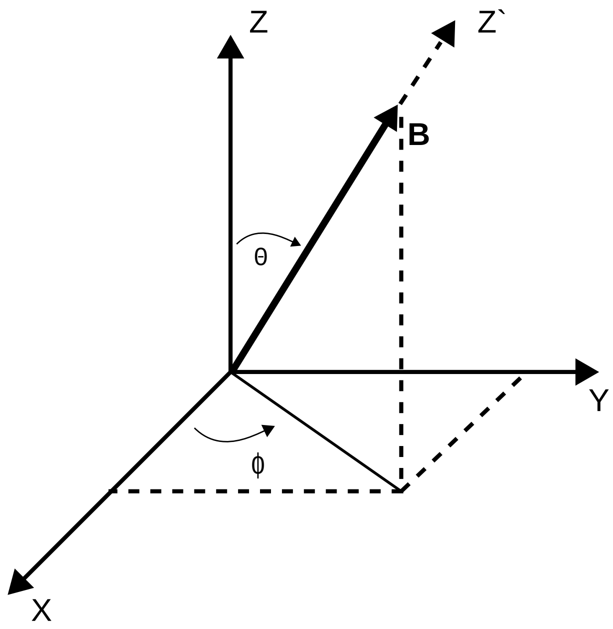

Coordinate system for $A \to BC$ decays.

In this case the helicity states are defined in the coordinate system Σ_3 which is produced by a rotation of Σ_1 into the new system.

$$R(\theta, \phi) = \mathrm{R}_{\mathrm{y2}}(\theta)\mathrm{R}_{\mathrm{z1}}(\phi)$$

Using d-functions the rotation can be written as

$$D^J_{mm'}(\theta, \phi) = e^{im'\phi} d^J_{mm'}(\theta)$$

The final states in system Σ_1 can be expressed as

$$|p\theta\phi\lambda_1\lambda_2 M\rangle_1 = D^J_{M\lambda}(-\theta,-\phi)\cdot|p\lambda_1\lambda_2\rangle_3$$

with $\lambda = \lambda_1 - \lambda_2$. The transition matrix for the decay is given by

$$\begin{aligned} f_{\lambda_1\lambda_2,M}(\theta,\phi) &= \langle p\theta\phi\lambda_1\lambda_2 M|\,T\,|M'\rangle = D^{J\,*}_{M\lambda}(-\theta,-\phi)\,\langle\lambda_1\lambda_2|\,T\,|M'\rangle \\ f_{\lambda_1\lambda_2,M}(\theta,\phi) &= D^J_{\lambda M}(\theta,\phi)T_{\lambda_1\lambda_2} \end{aligned}$$

The interaction is rotation invariant. The transition amplitude is a matrix with $(2s_1+1)(2s_2+1)$ rows and $(2J+1)$ columns. $D^J_{\lambda M}(\theta,\phi)$ describes the geometry (the rotation of the system Σ_3 where the helicity states are defined back into the CMS system of the resonance) $T_{\lambda_1\lambda_2}$ describes the dependences from the spins and the orbital angular momenta of the different particles in the decay process. The general form of $T_{\lambda_1\lambda_2}$ is given by

$$T_{\lambda_1\lambda_2} = \sum_{ls}\alpha_{ls}\,\langle J\lambda|ls0\lambda\rangle\,\langle s\lambda|s_1 s_2\lambda_1,-\lambda_2\rangle$$

where α_{ls} are unknown fit parameters.

The parameters define the decay spin and orbital angular momentum configuration. The brackets are Clebsch-Gordan couplings for $\boldsymbol{J} = \boldsymbol{l} + \boldsymbol{s}$ und $\boldsymbol{s} = \boldsymbol{s}_1 + \boldsymbol{s}_2$. The sum extends over all allowed l and s. Thus:

$$w_D(\theta, \phi) = Tr(\rho_f) = Tr(f \rho_i f^+)$$

ρ_f is the final state density matrix of the dimension (2s_1+1)(2s_2+1) and ρ_i is the initial density matrix of dimension (2J+1).

- **Multiple decay chains**

Assume that not only A decays into B and C but also B and C decay further into $B_1 B_2$ and $C_1 C_2$. The total helicity amplitude for a reaction $A \to BC$, $B \to B_1 B_2$, $C \to C_1 C_2$, has the form:

$$\begin{aligned} f_{tot} &= [f(B) \otimes f(C)]\, f(A) \\ &= \sum_{\lambda(B)\lambda(C)} \left[f_{\lambda(B1)\lambda(B2),\lambda(B)} \otimes f_{\lambda(C1)\lambda(C2),\lambda(C)} \right] f_{\lambda(B)\lambda(C),\lambda(A)} \end{aligned}$$

$\otimes$ represents the tensor product of two matrices.

The Figure shows in which cases this combination is done by a scalar or by a tensor product. The transition amplitude for the different single decays $f_{\lambda(x1)\lambda(x2),\lambda(x)}$ of $X \to X_1 X_2$ are calculated, and are then combined.

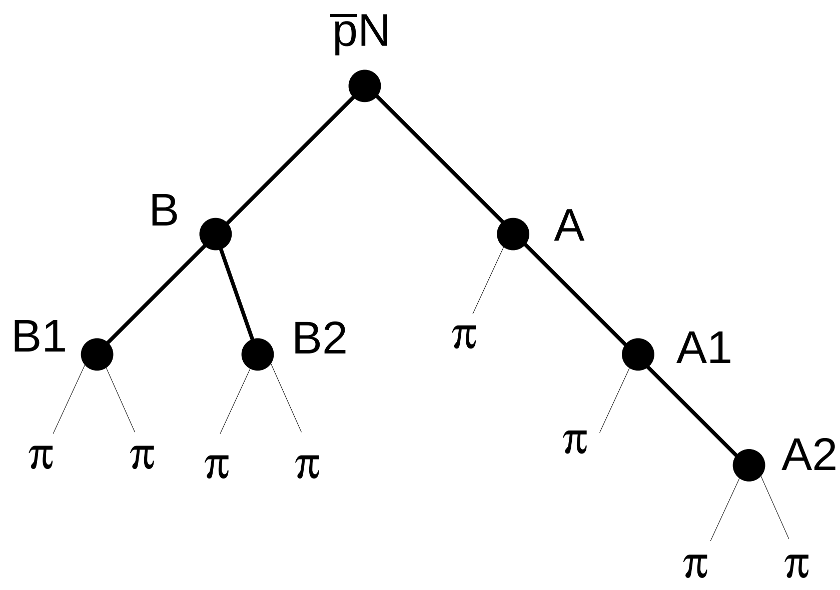

All decays in the figure are combined as tensor product (all $(J, m_J)_A$ with all $(J, m_J)_B$); all decays of a line are combined by a scalar product. Here the $(J, m_J)_{A1}$, depends directly on $(J, m_J)_A$. Thus the amplitude is determined to

$$f_{tot} = [\ (\ f(A2)f(A1)f(A)\ ) \otimes (\ [\ f(B2) \otimes f(B1)\ ]\ f(B)\ )\ ]\ f(\bar{p}N)$$

The decay angular distribution of a specific resonance depends on the whole process the state is produced in. Its spin density matrix is changed depending on the process it is produced in. This can be easily seen in the following example ($A \to B\pi, B \to B_1B_2$). The first decay changes the spin-density matrix of the decaying resonance B.

$$w_D(\theta,\phi) = Tr(f\rho_i f^+) =$$

$$= \Big(B \to B_1B_2\Big)\Big(A \to B\pi\Big) \left(\quad \rho_i \quad\right) \Big(A \to B\pi\Big)^T \Big(B \to B_1B_2\Big)^T$$

$$= \Big(B \to B_1B_2\Big) \left(\quad \rho_B \quad\right) \Big(B \to B_1B_2\Big)^T$$

3.4.2 The helicity formalism in photoproduction processes

In photoproduction a resonance is produced in the process and then decays. We first consider a nucleon resonance is produced and decays only into two particles, e.g.:

$$\gamma p \to N^* \to p\eta$$

The γp-system defines the z-axis $(\theta, \phi = 0)$ and determines the spin density matrix of the N^*-resonance.
The reaction $\gamma p \to N^*$ is related to $N^* \to \gamma p$ (which can be calculated using the formalism discussed above) by time reversal invariance.
Using

$$f_{\lambda_c\lambda_d,\lambda_a\lambda_b}(\theta) = (-1)^{\lambda'-\lambda} f_{\lambda_a\lambda_b,\lambda_c\lambda_d}(\theta) \qquad ([martin_spearman]\ p.232)$$

valid for $ab \to cd$ with $\lambda' = \lambda_c - \lambda_d$ and $\lambda = \lambda_a - \lambda_d$ we can write

$$f(\gamma p \to N^* \to p\eta) = f(N^* \to p\eta) \cdot f^T(N^* \to \gamma p)$$

Note that $\lambda' = \lambda_{N^*} = \lambda_p - \lambda_\gamma$ always holds.

The photoproduction amplitude needs to describe the decay of a resonance R $f(R \to N\,X)$ into the channel N X and its production $\gamma p \to R$ calculated using the transposed decay amplitude $f^T(R \to p\gamma)$. For photoproduction of spin 0 mesons this matrix has the form

$$f^{tot} = \begin{pmatrix} [\frac{1}{2}\,,\mathbf{-1};\,\frac{1}{2}] & [\text{-}\frac{1}{2}\,\text{-}1;\,\frac{1}{2}] & [\frac{1}{2}\,,\mathbf{+1};\,\frac{1}{2}] & [\text{-}\frac{1}{2}\,+1;\,\frac{1}{2}] \\ [\frac{1}{2}\,,\mathbf{-1};\text{-}\frac{1}{2}] & [\text{-}\frac{1}{2}\,\text{-}1;\text{-}\frac{1}{2}] & [\frac{1}{2}\,,\mathbf{+1};\text{-}\frac{1}{2}] & [\text{-}\frac{1}{2}\,+1;\text{-}\frac{1}{2}] \end{pmatrix} \tag{1}$$

where the numbers in the brackets represent $[\lambda_p, \lambda_\gamma; \lambda_{p^f}]$ with p, p^f being the initial and final state proton. The angular part of the differential cross section is then given by

$$\frac{\mathrm{d}\sigma}{\mathrm{d}\Omega} = \quad \sim \frac{\mathbf{1}}{\mathbf{4}} \cdot \sum_{\lambda_{\mathbf{p}}\lambda_\gamma\lambda'} |\mathbf{T}(\lambda_{\mathbf{p}}\lambda_\gamma\lambda_{\mathbf{p^f}})|^{\mathbf{2}}$$

Example

We now discuss the photoproduction of the S_{11} and P_{11} resonances and their decay into pη decay of a photoproduced resonance will be discussed first having a resonance second having a multipole picture in mind. The photons are assumed to be unpolarised.

$\gamma\mathrm{p} \to \mathrm{S}_{11} \to \mathrm{p}\eta$ **:** $\quad \mathbf{\frac{1}{2}}^- \to \mathbf{\frac{1}{2}}^+\mathbf{0}^-, \quad \ell = \mathbf{0}$

To determine the angular distribution of the decay process the helicity matrix $\mathrm{T}_{\lambda_1\lambda_2}$ has to be calculated,

$$T_{\pm\frac{1}{2},0} \quad = \quad \alpha_{0\,\frac{1}{2}} \left\langle \frac{1}{2} \pm \frac{1}{2} | 0\,\frac{1}{2}\,0 \pm \frac{1}{2} \right\rangle \left\langle \frac{1}{2} \pm \frac{1}{2} | \frac{1}{2}\,0 \pm \frac{1}{2}\,0 \right\rangle = \alpha_{0\,\frac{1}{2}} = const.$$

The transition matrix is then given by (the constant is arbitrarily set to 1):

$$f_{\pm\frac{1}{2}\,0,\,M}(\theta,\phi) = \begin{pmatrix} D^{\frac{1}{2}}_{\frac{1}{2}\,\frac{1}{2}} & D^{\frac{1}{2}}_{\frac{1}{2}\,-\frac{1}{2}} \\ D^{\frac{1}{2}}_{-\frac{1}{2}\,\frac{1}{2}} & D^{\frac{1}{2}}_{-\frac{1}{2}\,-\frac{1}{2}} \end{pmatrix} \tag{2}$$

(columns: $M_{S_{11}} = \frac{1}{2},\ -\frac{1}{2}$, rows $\lambda'_p = \frac{1}{2},\ -\frac{1}{2}$)

with $\phi = 0$ (process is symmetric over ϕ, z-axis corresponds to direction of flight) follows:

$$f_{S_{11}\to p\eta} = \begin{pmatrix} \cos(\frac{\theta}{2}) & -\sin(\frac{\theta}{2}) \\ \sin(\frac{\theta}{2}) & \cos(\frac{\theta}{2}) \end{pmatrix} \tag{3}$$

$\gamma p \to S_{11}$:

First, we calculate $S_{11} \to p\gamma$, for $\frac{1}{2}^- \to \frac{1}{2}^+ 1^-, \quad \ell = 0$. Two proton helicities occur: $\lambda_1 = \pm\frac{1}{2}$, and two photon helicities: $s_2 = 1$, $\lambda_2 = \pm 1$; $\lambda_2 = 0$ is excluded for real photons. One finds: $\mathrm{T}_{\frac{1}{2}\,-1} = \mathrm{T}_{-\frac{1}{2}\,+1} = 0$, $T_{-\frac{1}{2}\,-1} = -\sqrt{\frac{2}{3}}$, $T_{\frac{1}{2}\,1} = +\sqrt{\frac{2}{3}}$. Setting θ and ϕ to 0 (the γp is parallel to the z-axis), only $D^J_{\lambda\,M}(0,0)$ is not equal to zero only if $\lambda = M$.

$$f_{S_{11}\to p\gamma} = \begin{pmatrix} 0 & 0 \\ -\sqrt{\frac{2}{3}} & 0 \\ 0 & \sqrt{\frac{2}{3}} \\ 0 & 0 \end{pmatrix} \tag{4}$$

The rows correspond to different λ-values. Thus:

$$f(\gamma p \to S_{11}) = f^T(S_{11} \to p\gamma) = \begin{pmatrix} 0 & -\sqrt{\frac{2}{3}} & 0 & 0 \\ 0 & 0 & \sqrt{\frac{2}{3}} & 0 \end{pmatrix}$$

And for the whole reaction:

$\gamma p \to S_{11} \to p\eta$**:**

$$f_{\gamma p \to S_{11} \to p\eta} =$$

$$\begin{pmatrix} \cos(\frac{\theta}{2}) & -\sin(\frac{\theta}{2}) \\ \sin(\frac{\theta}{2}) & \cos(\frac{\theta}{2}) \end{pmatrix} \cdot \begin{pmatrix} 0 & -\sqrt{\frac{2}{3}} & 0 & 0 \\ 0 & 0 & \sqrt{\frac{2}{3}} & 0 \end{pmatrix} = \begin{pmatrix} 0 & -\sqrt{\frac{2}{3}}\cos(\frac{\theta}{2}) & -\sqrt{\frac{2}{3}}\sin(\frac{\theta}{2}) & 0 \\ 0 & -\sqrt{\frac{2}{3}}\sin(\frac{\theta}{2}) & \sqrt{\frac{2}{3}}\cos(\frac{\theta}{2}) & 0 \end{pmatrix}$$

$$\text{With} \qquad \frac{\mathrm{d}\sigma}{\mathrm{d}\Omega} = \; \sim \frac{1}{4} \cdot \sum_{\lambda_p \lambda_\gamma \lambda'} |T(\lambda_p \lambda_\gamma \lambda')|^2$$

one finds a flat angular distribution.

$$\frac{\mathrm{d}\sigma}{\mathrm{d}\Omega} \sim |A_{S_{11}}|^2$$

$\gamma \mathrm{p} \rightarrow \mathrm{P}_{11} \rightarrow \mathrm{p}\eta$

The helicity matrix for $P_{11} \rightarrow p\eta$ involves the quantum numbers: $\frac{1}{2}^+ \rightarrow \frac{1}{2}^+ 0^-, \quad \ell = 1$ and the matrix elements $T_{\pm\frac{1}{2},0} = \pm\frac{1}{\sqrt{3}}\alpha_{1\,\frac{1}{2}}$. The scattering amplitude is now given by

$$f_{P_{11}\rightarrow p\eta} = \begin{pmatrix} -\frac{1}{\sqrt{3}}\cos(\frac{\theta}{2}) & -\frac{1}{\sqrt{3}}(-\sin(\frac{\theta}{2})) \\ \frac{1}{\sqrt{3}}\sin(\frac{\theta}{2}) & \frac{1}{\sqrt{3}}\cos(\frac{\theta}{2}) \end{pmatrix}$$

In the next step $P_{11} \rightarrow p\gamma$ is calculated ($\frac{1}{2}^+ \rightarrow \frac{1}{2}^+ 1^-, \quad \ell = 1$). Two values for the spin s are possible: $s = \frac{1}{2}$, $s = \frac{3}{2}$. The Clebsch Gordan coefficients depend on s leading to a different $T_{\lambda_1\lambda_2}$ for the two spins. The D-matrices depend only on J, λ and M, so that they are the same for both cases. One finds:

$T_{+\frac{1}{2}\,-1} = T_{-\frac{1}{2}\,+1} = 0$ **and**

$T_{-\frac{1}{2}\,-1} = T_{+\frac{1}{2}\,+1} = \alpha_{1\,\frac{3}{2}}(-\frac{1}{3}) + \alpha_{1\,\frac{1}{2}}(+\frac{\sqrt{2}}{3}) = -a$

$$f_{\gamma p \to P_{11}} = f^T_{P_{11} \to p\gamma} = \begin{pmatrix} 0 & -a & 0 & 0 \\ 0 & 0 & -a & 0 \end{pmatrix}$$

And for the whole process:

$\gamma p \to P_{11} \to p\eta$**:**

$$f_{\gamma p \to P_{11} \to p\eta} = \begin{pmatrix} 0 & +\frac{1}{\sqrt{3}}a\ \cos(\frac{\theta}{2}) & -\frac{1}{\sqrt{3}}a\ \sin(\frac{\theta}{2}) & 0 \\ 0 & -\frac{1}{\sqrt{3}}a\ \sin(\frac{\theta}{2}) & -\frac{1}{\sqrt{3}}a\ \cos(\frac{\theta}{2}) & 0 \end{pmatrix}$$

which leads again to a flat angular distribution; the differential cross section does not depend on θ**.**

Finally we assume that both resonances are produced; their interference leads to a non-flat angular distribution:

$$f_{\gamma p \to (S_{11}+P_{11}) \to p\eta} = \begin{pmatrix} 0 & (-\frac{2}{\sqrt{3}}S_{11} + \frac{a}{\sqrt{3}}P_{11})\cos(\frac{\theta}{2}) & (-\frac{2}{\sqrt{3}}S_{11} - \frac{a}{\sqrt{3}}P_{11})\sin(\frac{\theta}{2}) & 0 \\ 0 & (-\frac{2}{\sqrt{3}}S_{11} - \frac{a}{\sqrt{3}}P_{11})\sin(\frac{\theta}{2}) & (\frac{2}{\sqrt{3}}S_{11} - \frac{a}{\sqrt{3}}P_{11})\cos(\frac{\theta}{2}) & 0 \end{pmatrix}$$

with $s = \frac{2}{\sqrt{3}}S_{11}$ **and** $p = \frac{a}{\sqrt{3}}P_{11}$ **we get:**

$$\begin{aligned} \frac{\mathrm{d}\sigma}{\mathrm{d}\Omega} &\sim \frac{1}{4} \cdot 2 \left[\sin^2(\frac{\theta}{2}) \cdot |s+p|^2 + \cos^2(\frac{\theta}{2}) \cdot |s-p|^2\right] \\ &\sim |s|^2 + |p|^2 - 2Re(s^*p) \cdot \cos(\theta) \end{aligned}$$

The interference term $2Re(s^*p) \cdot \cos(\theta)$ **produces a non-flat angular distribution.**

3.5 Flavor structure of mesons

Isoscalar coefficients for meson decays

$\mathbf{1 \rightarrow 8 \otimes 8}$

$$(\Lambda) \rightarrow (N\overline{K} \;\; \Sigma\pi \;\; \Lambda\eta \;\; \Xi K) = \frac{1}{\sqrt{8}}(2 \quad 3 \quad -1 \quad -2)^{1/2}$$

- $\mathbf{a_2(1320) \rightarrow |\eta>_1 \pi = g_1}$
- $\mathbf{a_2(1320) \rightarrow |\eta>_8 \pi = \sqrt{\frac{1}{5}} g_8}$
- $\mathbf{a_2(1320) \rightarrow |\eta>_{s\bar{s}} \pi = 0 \rightarrow}$ $\mathbf{g_1 = -\sqrt{\frac{4}{5}} g_8}$

$\mathbf{8_1 \rightarrow 8 \otimes 8}$

$$\begin{pmatrix} N \\ \Sigma \\ \Lambda \\ \Xi \end{pmatrix} \rightarrow \begin{pmatrix} N\pi & N\eta & \Sigma K & \Lambda K & \\ N\overline{K} & \Sigma\pi & \Lambda\pi & \Sigma\eta & \Xi K \\ N\overline{K} & \Sigma\pi & \Lambda\eta & \Xi K & \\ \Sigma\overline{K} & \Lambda\overline{K} & \Xi\pi & \Xi\eta & \end{pmatrix} = \frac{1}{\sqrt{20}} \begin{pmatrix} 9 & -1 & -9 & -1 & \\ -6 & 0 & 4 & 4 & -6 \\ 2 & -12 & -4 & -2 & \\ 9 & -1 & -9 & -1 & \end{pmatrix}^{1/2}$$

$$\frac{R(a_2(1320) \rightarrow \eta_8 \pi)}{R(a_2(1320) \rightarrow \eta_1 \pi)} = 1/2.$$

$\mathbf{8_2 \rightarrow 8 \otimes 8}$

$$\begin{pmatrix} N \\ \Sigma \\ \Lambda \\ \Xi \end{pmatrix} \rightarrow \begin{pmatrix} N\pi & N\eta & \Sigma K & \Lambda K & \\ N\overline{K} & \Sigma\pi & \Lambda\pi & \Sigma\eta & \Xi K \\ N\overline{K} & \Sigma\pi & \Lambda\eta & \Xi K & \\ \Sigma\overline{K} & \Lambda\overline{K} & \Xi\pi & \Xi\eta & \end{pmatrix} = \frac{1}{\sqrt{12}} \begin{pmatrix} 3 & 3 & 3 & -3 & \\ 2 & 8 & 0 & 0 & -2 \\ 6 & 0 & 0 & 6 & \\ 3 & 3 & 3 & -3 & \end{pmatrix}^{1/2}$$

3 couplings:

- **1:** **C'=1 ($\mathbf{d_{ijk}}$)** $\mathbf{f_2(1270), f2(1525) \rightarrow \pi\pi, \eta\eta, \eta\eta', K\bar{K}}$
- **$\mathbf{8_1}$:** **C'=1 ($\mathbf{d_{ijk}}$)** $\mathbf{f_2(1270), f2(1525) \rightarrow \pi\pi, \eta\eta, \eta\eta', K\bar{K}}$
  and $\mathbf{a_2(1320) \rightarrow \eta\pi, K\bar{K};\;\; K_2^*(1430) \rightarrow K\pi, K\eta, K\eta'}$
- **$\mathbf{8_2}$:** **C'=-1 ($\mathbf{f_{ijk}}$)** $\mathbf{a_2(1320) \rightarrow \rho\pi}$

SU(3) couplings for π and ρ like mesons.

decay	symmetric	antisymmetric
$\pi \rightarrow \pi\pi$	$\mathbf{0}$	$\frac{\sqrt{2}}{\sqrt{3}}$
$\pi \rightarrow \mathbf{K\bar{K}}$	$\frac{1}{\sqrt{6}}$	$\frac{\sqrt{3}}{\sqrt{10}}$
$\pi \rightarrow \pi\eta, \pi\phi$	$\mathbf{0}$	$\frac{\cos\theta_\eta - \sqrt{2}\sin\theta_\eta}{\sqrt{5}}$
$\pi \rightarrow \pi\eta', \pi\omega$	$\mathbf{0}$	$\frac{\sin\theta_\eta + \sqrt{2}\cos\theta_\eta}{\sqrt{5}}$

SU(3) couplings for K like mesons without nonet mixing.

decay	symmetric	antisymmetric
$\mathbf{K} \rightarrow \mathbf{K}\pi$	$\frac{3}{\sqrt{20}}$	$\frac{\mathbf{1}}{\mathbf{2}}$
$\mathbf{K} \rightarrow \mathbf{K}\eta, \mathbf{K}\phi$	$\frac{\cos\theta_\eta + 2\sqrt{2}\sin\theta_\eta}{\sqrt{20}}$	$\frac{\cos\theta_\eta}{\mathbf{2}}$
$\mathbf{K} \rightarrow \mathbf{K}\eta', \mathbf{K}\omega$	$\frac{2\sqrt{2}\cos\theta_\eta - \sin\theta_\eta}{\sqrt{20}}$	$\frac{\sin\theta_\eta}{\mathbf{2}}$

SU(3) couplings for η', $f_2(1270)$ and ω (dominant $u\bar{u}$ and $d\bar{d}$) like mesons with nonet mixing. i and f denote the initial and final state nonet mixing angle respectively.

decay	symmetric	antisymmetric
$\mathbf{f} \to \pi\pi$	$\sqrt{\mathbf{3}}\frac{\sqrt{2}\cos\theta_f+\sin\theta_f}{\sqrt{10}}$	$\mathbf{0}$
$\mathbf{f} \to \mathbf{K\bar{K}}$	$\frac{\sin\theta_f-2\sqrt{2}\cos\theta_f}{\sqrt{10}}$	$\frac{\sin\theta_\mathbf{f}}{\mathbf{2}}$
$\mathbf{f} \to \eta\eta, \phi\phi$	$\frac{-\cos\theta_\eta^2\sin\theta_f-\sqrt{2}(2\sin\theta_f\cos\theta_\eta\sin\theta_\eta-\cos\theta_f)}{\sqrt{5}}$	$\mathbf{0}$
$\mathbf{f} \to \eta'\eta', \omega\omega$	$\frac{\sin\theta_\eta^2\sin\theta_f+\sqrt{2}(2\sin\theta_f\cos\theta_\eta\sin\theta_\eta+\cos\theta_f)}{\sqrt{5}}$	$\mathbf{0}$
$\mathbf{f} \to \eta\eta', \phi\omega$	$\frac{\sin\theta_f(\sqrt{2}(\cos\theta_\eta^2-\sin\theta_\eta^2)-\cos\theta_\eta\sin\theta_\eta}{\sqrt{5}}$	$\mathbf{0}$

SU(3) couplings for η, $f_2'(1525)$ and ϕ (dominant $s\bar{s}$) like mesons with nonet mixing. i and f denote the initial and final state nonet mixing angle respectively.

decay	symmetric	antisymmetric
$f' \to \pi\pi$	$\sqrt{3}\frac{\sqrt{2}\sin\theta_f - \cos\theta_f}{\sqrt{10}}$	0
$f' \to K\bar{K}$	$\frac{\cos\theta_f + 2\sqrt{2}\sin\theta_f}{\sqrt{10}}$	$\frac{\cos\theta_f}{2}$
$f' \to \eta\eta, \phi\phi$	$\frac{-\cos\theta_\eta^2 \cos\theta_f - \sqrt{2}(2\cos\theta_f \cos\theta_\eta \sin\theta_\eta + \sin\theta_f)}{\sqrt{5}}$	0
$f' \to \eta'\eta', \omega\omega$	$\frac{\sin\theta_\eta^2 \sin\theta_f + \sqrt{2}(2\sin\theta_f \cos\theta_\eta \sin\theta_\eta + \cos\theta_f)}{\sqrt{5}}$	0
$f' \to \eta\eta', \phi\omega$	$\frac{\cos\theta_f(\sqrt{2}(\cos\theta_\eta^2 - \sin\theta_\eta^2) - \cos\theta_\eta \sin\theta_\eta}{\sqrt{5}}$	0

Fits

The matrix element $\mathcal{M}$

$$d\Gamma = \frac{1}{32\pi^2}|\mathcal{M}|^2\frac{q}{m^2}d\Omega$$

contains a coupling constant, $\mathbf{C_{T\to PS+PS}}$ or $\mathbf{C_{T\to V+PS}}$ (which is calculable in dynamical models), the SU(3) amplitudes $\mathbf{c_{isoscalar}}$ and a dynamical function F(q) with q being the breakup momentum.

$$B_2(qR) = \sqrt{\frac{13(qR)^2}{9+3(qR)+9(qR)^2}}$$

$$BW(m) = \frac{m_0\Gamma_0}{m^2-m_0^2-im_0\Gamma_0}$$

Decay	Data		Fit	χ^2
	Γ	σ_Γ	Γ	
$a_2 \to \pi\eta$	15.95	±1.32	24.8	2.99
$a_2 \to \pi\eta'$	0.63	±0.12	1.2	4.39
$a_2 \to K\bar{K}$	5.39	±0.88	5.2	0.01
$f_2 \to \pi\pi$	157.0	±5.0	117.1	2.77
$f_2 \to K\bar{K}$	8.5	±1.0	8.0	0.08
$f_2 \to \eta\eta$	0.8	±1.0	1.5	0.44
$f_2' \to \pi\pi$	4.2	±1.9	3.7	0.07
$f_2' \to K\bar{K}$	55.7	±5.0	48.6	0.43
$f_2' \to \eta\eta$	6.1	±1.9	5.3	0.12
$f_2' \to \eta\eta'$	0.0	±0.8	0.7	0.77
$K_2 \to K\pi$	48.9	±1.7	61.1	0.99
$K_2 \to K\eta$	0.14	±0.28	0.2	0.02

Decay	Data		Fit	χ^2
	Γ	σ_Γ	Γ	
$a_2 \to \pi\rho$	77.1	± 3.5	66.0	0.67
$f_2 \to K^*\bar{K}$	0.0	± 1.8	0.2	0.01
$f_2' \to K^*\bar{K}$	10.0	±10.0	11.8	0.03
$K_2 \to K\rho$	8.7	± 0.8	11.5	1.29
$K_2 \to K\omega$	2.7	± 0.8	1.0	0.00
$K_2 \to K^*\pi$	24.8	± 1.7	24.1	0.02
$K_2 \to K^*\eta$	0.0	± 1.0	0.9	0.81

Results of the final fit. The χ^2 values include 20% SU(3) symmetry breaking.

What have we learned ?

- **Tensor meson decays are compatble with SU(3) assuming 20% symmetry breaking**

$$
\begin{aligned}
\Theta_{ps} &= -(14.4 \pm\ 2.9)^\circ \\
\Theta_{vec} &= -(37.5 \pm\ 8.0)^\circ \\
\Theta_{ten} &= (28.3 \pm\ 1.6)^\circ \\
\lambda &= 0.77 \pm\ 0.1 \\
R &= 0.2 \pm\ 0.04\, fm \\
C_{T\to PS+PS} &= 1.11 \pm 0.05 \\
C_{T\to PS+V} &= 2.07 \pm 0.13
\end{aligned}
$$

Why is λ not 0.225 ?

Diagrams of $q\bar{q}$ decays into two strange mesons (a) and into two (b), three (c) and more (d) nonstrange mesons.

Diagrams of the type (e), (f) and (g) are suppressed due to the OZI rule.

SU(3) compares only a) and b)

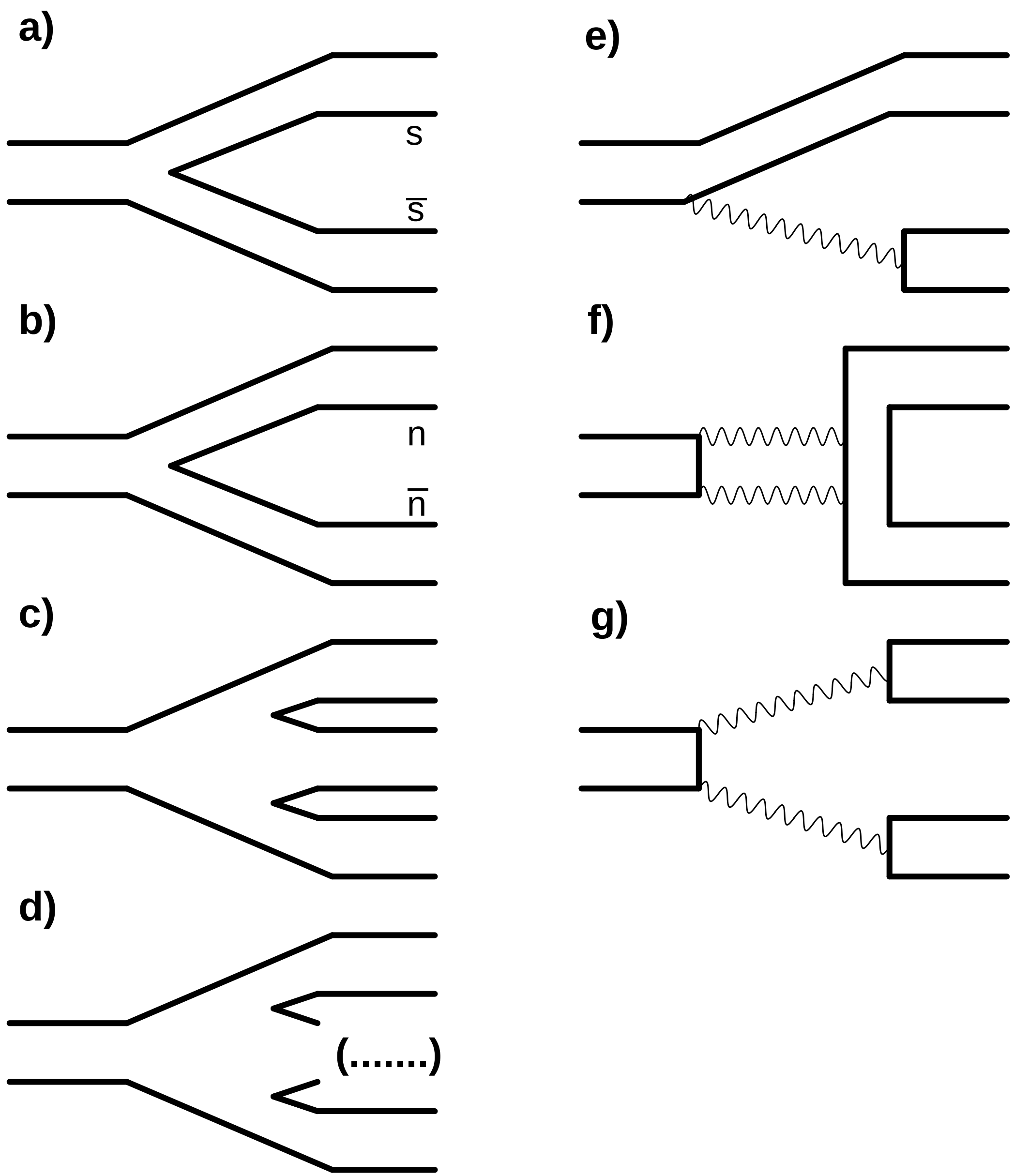

Summary

- **QCD inspired models are well suited to describe meson mass spectrum.**
- **Pseudoscalar and scalar meson sector tricky.**
- **QCD predicts other forms of hadonic matter:**
  Glueballs, hybrids, and multiquark states.
- **Present interest focusses on mesons beyond the quark model.**

The E/ι saga and the first glueball

- Short history of the $\eta(1440)$
- The $\eta(1440)$in $p\bar{p}$ annihilation
- The $\eta(1440)$ in $\gamma\gamma$ at LEP
- E/ι decays in the $^3P_0$ model
- What do we conclude ?

4 E/ι saga

4.1 Short history of the $\eta(1440)$

- **Discovered 1967 in $\mathbf{p\bar{p}}$ annihilation at rest into $(\mathbf{K\bar{K}}\pi)\pi^+\pi^-$ and called E-meson**

  $\mathbf{M = 1425 \pm 7, \Gamma = 80 \pm 10\ \ MeV;}$ $J^{PC} = 0^{-+}$

- **Also seen, 1967, in $\pi^-\mathbf{p} \to \mathbf{n}\mathrm{K\bar{K}}\pi$; $\mathbf{p}_{\pi^-} \sim \mathbf{3\,GeV/c}$, still called E-meson**

  $\mathbf{M = 1420 \pm 20, \Gamma = 60 \pm 20\,MeV;}$ $\mathbf{J^{PC} = 1^{++}}$

- **1979 claim for $\eta(1295)$; confirmed in several experiments**

- **E 'rediscovered' 1980 in radiative $\mathbf{J}/\psi$ decays into $(\mathbf{K\bar{K}}\pi)$ and called $\iota(1440)$**

  $\mathbf{M = 1440 \pm 20, \Gamma = 50 \pm 30\,MeV;}$ $\mathbf{J^{PC} = 0^{-+}}$

- **Seen to be split into two components:**

  $\eta_{\mathbf{L}} \to \eta\pi\pi$ $\qquad$ $\mathbf{M = 1405 \pm 5, \Gamma = 56 \pm 6\,MeV}$

  $\eta_{\mathbf{H}} \to \mathrm{K\bar{K}}\pi$ $\qquad$ $\mathbf{M = 1475 \pm 5, \Gamma = 81 \pm 11\,MeV}$

- **3 η states in mass range from 1280 to 1480 MeV**

- **The $\eta(\mathbf{1295})$ is likely the radial excitation of the η**
  It is mass degenerate with the $\pi(1300)$, hence there is ideal mixing !

- **The $\eta_{\mathbf{s\bar{s}}}$ is expected 240 MeV higher:**
  $\eta_{\mathbf{H}}$ could be its partner.

- **The $\eta_{\mathbf{H}}$ cannot be a glueball due to its $\mathrm{K^*K}$ decay mode**

The $\eta_{\mathbf{L}}$ is the first glueball !

A few basics:

- **A pure flavor octet η(xxxx) state decays into $\mathbf{K^*K}$ but not into $a_0(980)\pi$**
- **A pure flavor singlet η(xxxx) state decays into $a_0(980)\pi$ but not into $\mathbf{K^*K}$**
- **$(\mathrm{u\bar{u}} + \mathrm{d\bar{d}})$ and $\mathrm{s\bar{s}}$ states decay into both $\mathbf{K^*K}$ and $a_0(980)\pi$**
- **There are no flavor restrictions for $\sigma\eta$**
- **Secondary decay modes are**
  $\mathbf{K^*K}$ and $a_0(980)\pi$ decay to $\mathbf{K\overline{K}}\pi$ (and may interfer)
  $a_0(980)\pi$ and $\sigma\eta$ decay to $\pi\pi\eta$ (and may interfer)

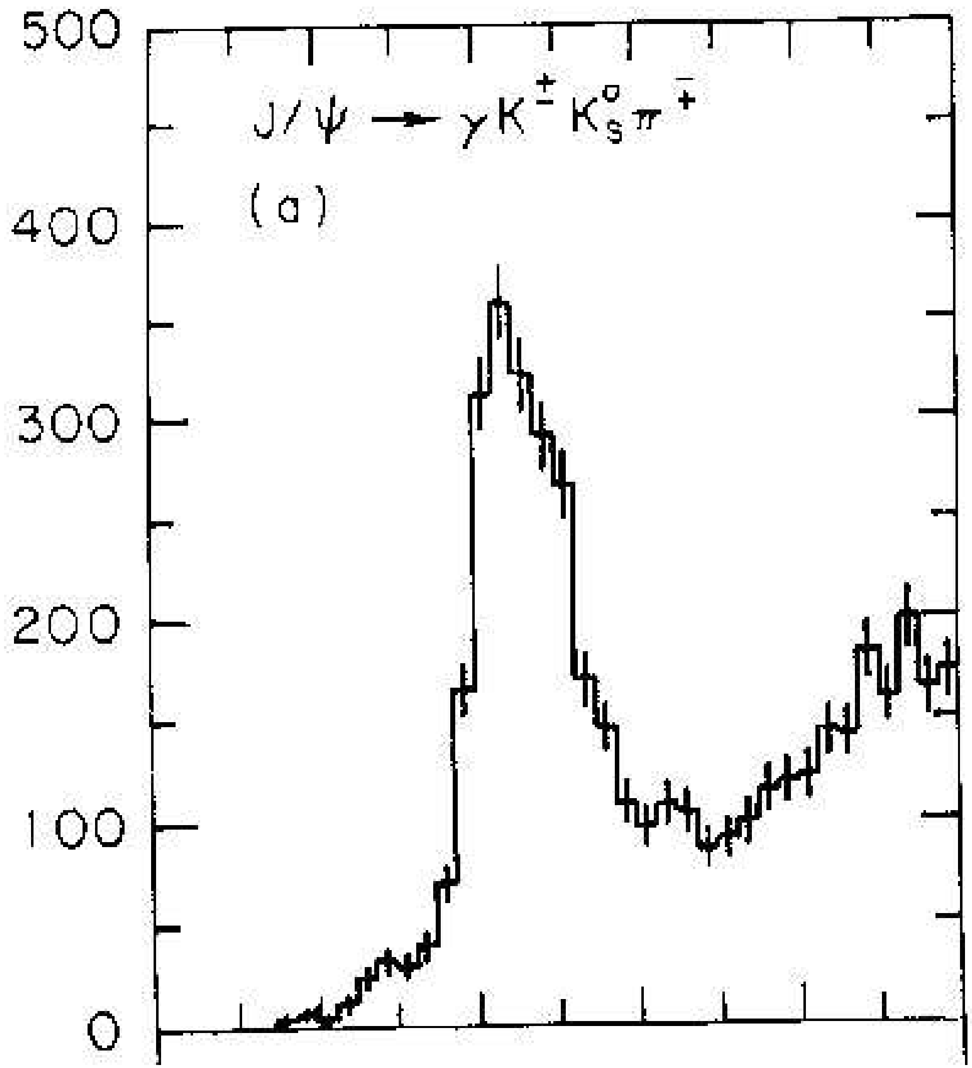

$\Uparrow$ **1295 MeV**

The $\iota(1440)$ is a strong signal in radiative J/ψ decay. The $\iota(1440)$ cannot be described by one Breit-Wigner resonance.

There is no evidence for the $\eta(1295)$ from radiative J/ψ decay.

Caution:

As s$\bar{\text{s}}$ state the η_H should be produced in
$K^- \, p \rightarrow \Lambda \; \eta_H$.

As s$\bar{\text{s}}$ state the η_H should not be produced in
$\pi^- \, \mathbf{p} \rightarrow \mathbf{n} \; \eta_H$.

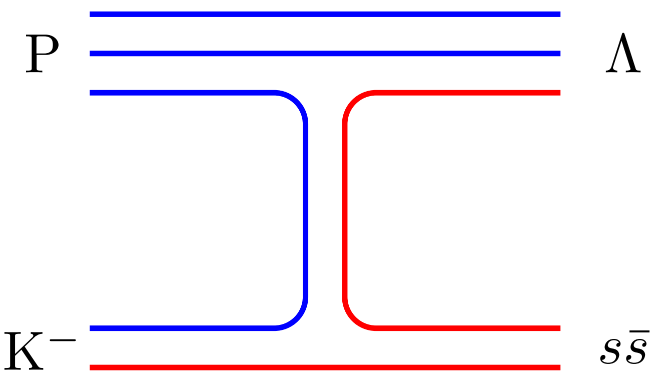

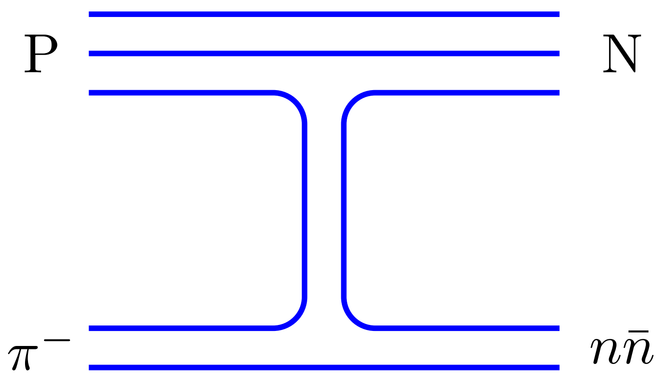

It is not !

But it is !

The $\eta(1440)$ region does not contain a large s$\bar{\text{s}}$ component

J/ψ decays into
γX, ωX, ΦX.

$X = \mathrm{K}\bar{\mathrm{K}}\pi$

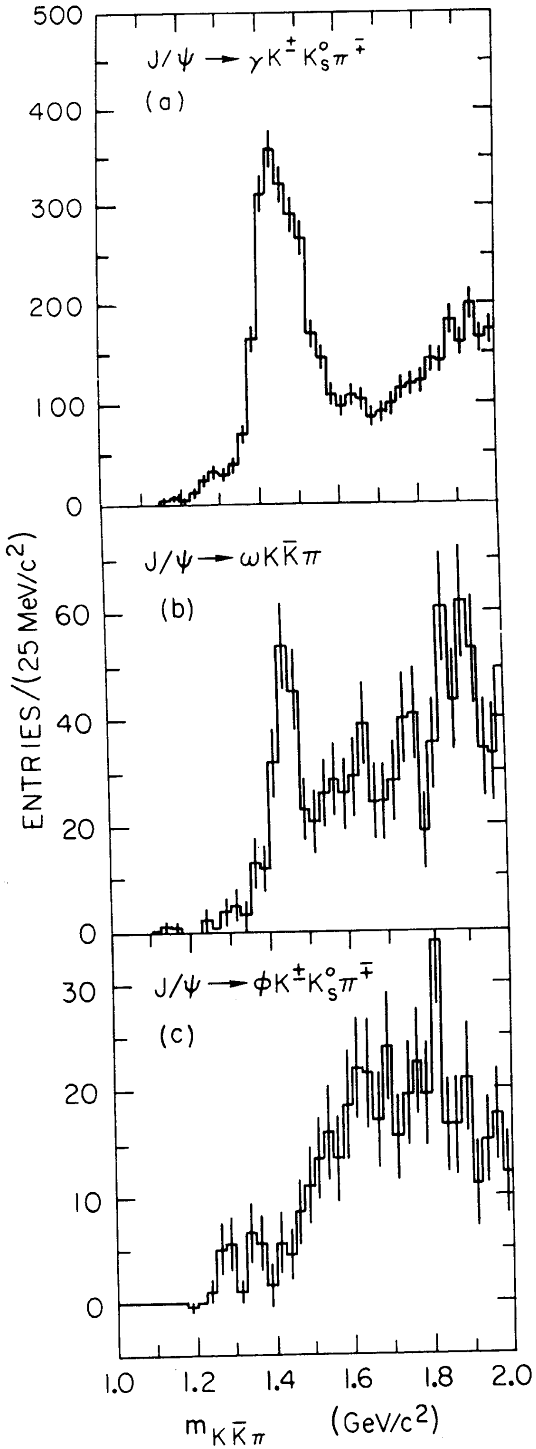

- dominant 'iota' structure

- $f_1(1420)$ signal
- too narrow for 'iota'

- no 'iota' signal
- no $f_1(1420)$
- events in $f_1(1285)$ region

4.2 The $\eta(1440)$ in $p\bar{p}$ annihilation

Study of the reaction $p\bar{p} \to \pi^+\pi^-\eta(1440), \eta(1440), \to \eta\pi^+\pi^-$:

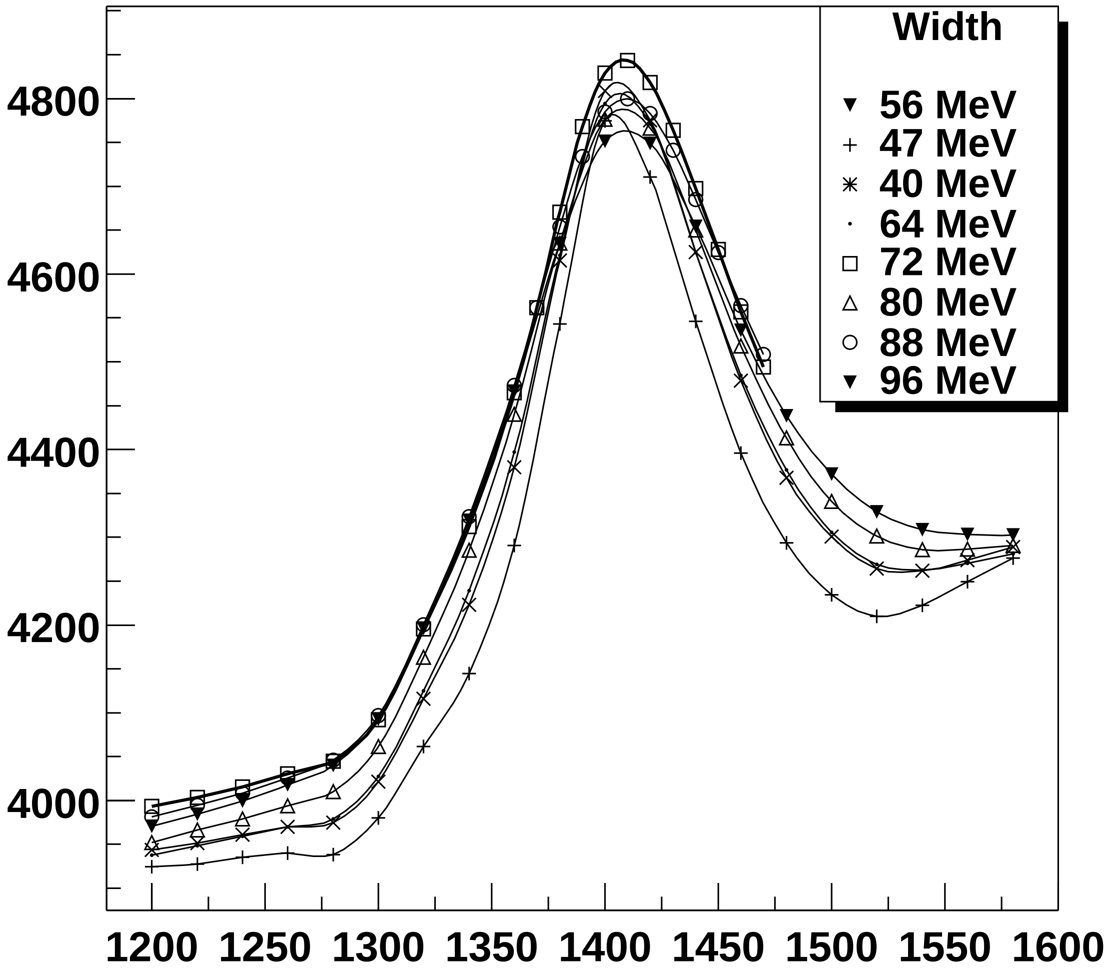

Scan for a 0^+0^{-+} resonance with different widths

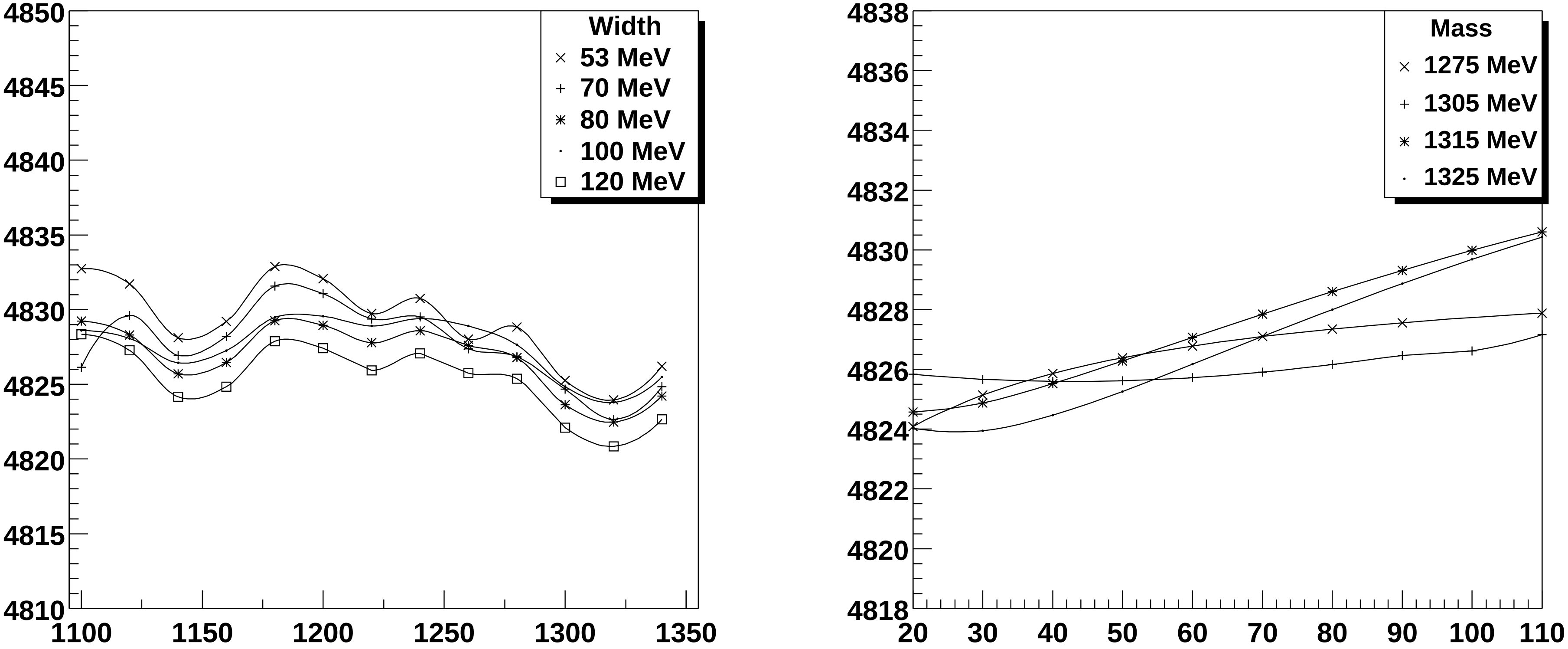

Scan for an additional $0^{+}0^{-+}$ resonance with fixed widths (a) and with fixed masses (b)

There is no evidence for the $\eta(1295)$ from $\mathrm{p\bar{p}}$ annihilation

4.3 The $\eta(1440)$ in $\gamma\gamma$ at LEP

No evidence for the $\eta(1295)$ from $\gamma\gamma$ fusion

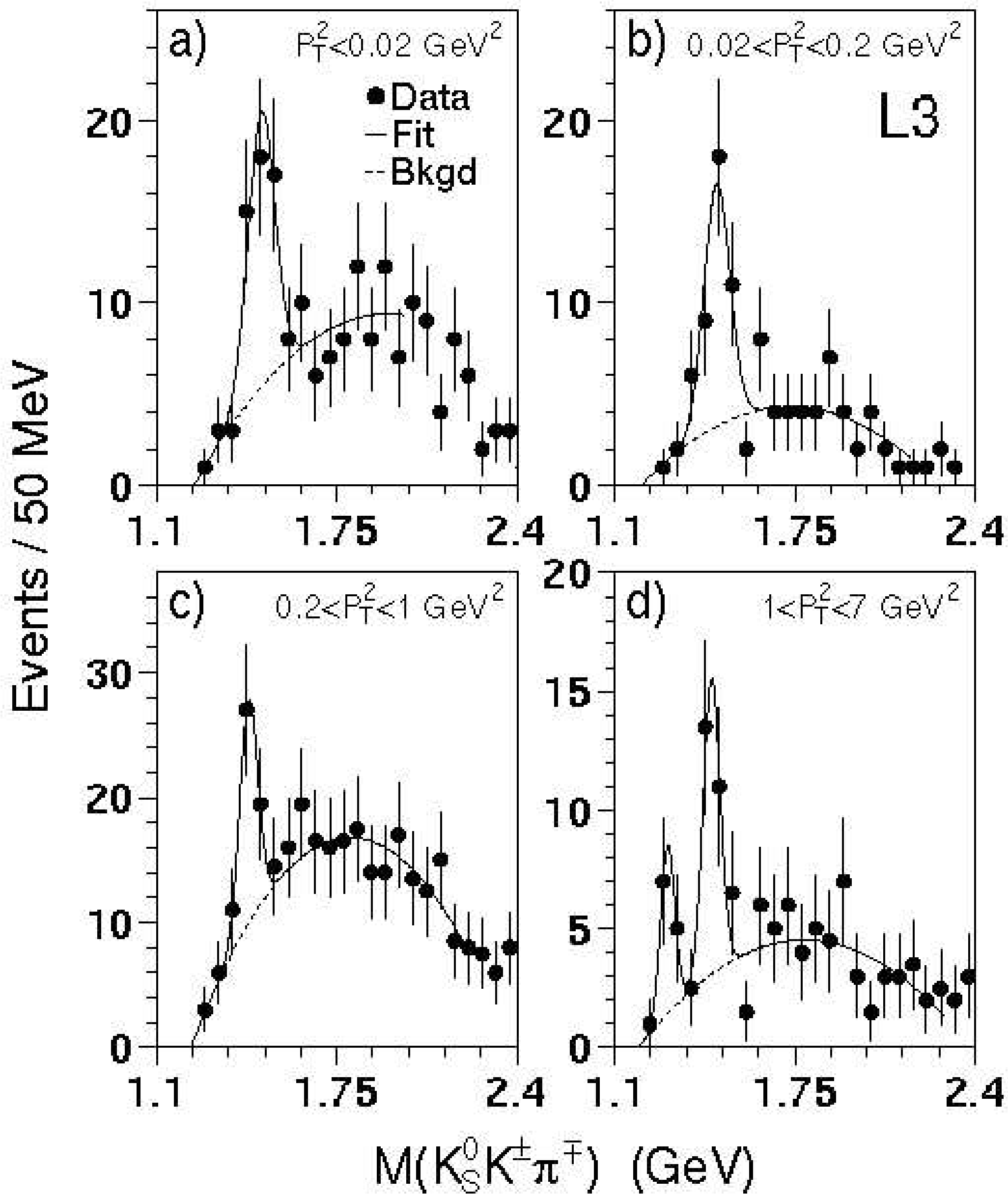

$\gamma\gamma \to \eta(1295)$:

$\mathbf{CG}_{(1,0)+(1,0)\to(0,0)} \neq 0$

$\gamma\gamma \not\to f_1(1285)$:

$\mathbf{CG}_{(1,0)+(1,0)\to(1,0)} = 0$

$\gamma^*\gamma \to f_1(1285)$:

$\mathbf{CG}_{(1,M)+(1,0)\to(1,M)} \neq 0$

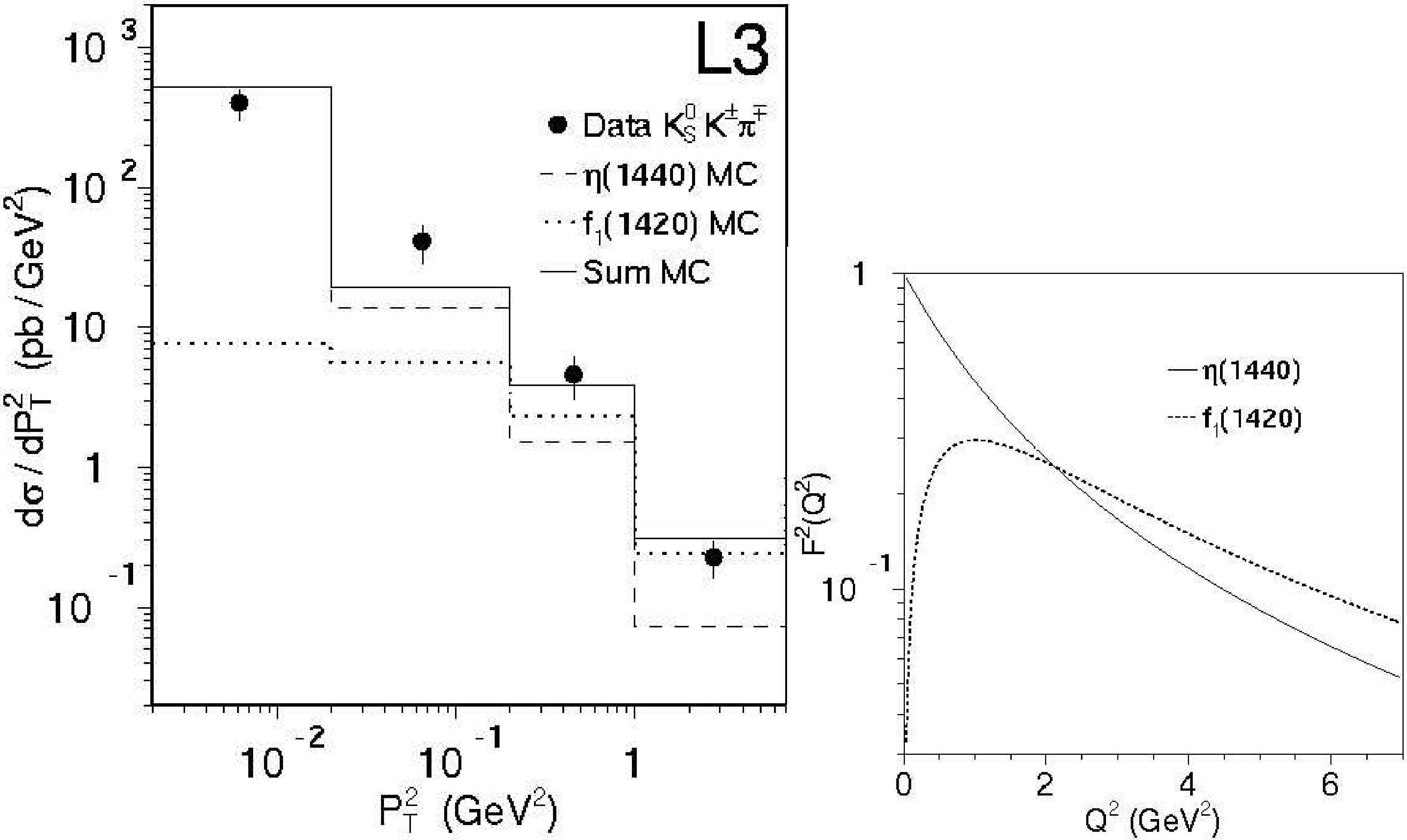

The $\mathbf{Q^2}$ or $\mathbf{P_T^2}$ dependence allows a separation of $\mathbf{f_1}$ and η contributions: $\eta(\mathbf{1440})$ is produced in $\gamma\gamma$ collisions

One word of warning ?

ΔP_T^2 (GeV^2)	Events	M (MeV)	σ (MeV)	CL (%)	ϵ (%)	$\Delta\sigma$ (pb)
$0 - 0.02$	37 ± 9	1481 ± 12	48 ± 9	89	1.03 ± 0.04	8.0 ± 2.0
$0.02 - 0.2$	28 ± 7	1473 ± 11	37 ± 8	77	0.85 ± 0.09	7.4 ± 2.3
$0.2 - 1.$	29 ± 9	1435 ± 10	32 ± 10	99	1.74 ± 0.14	3.7 ± 1.2
$1 - 7$	21 ± 6	1452 ± 11	35 ± 10	55	3.49 ± 0.24	1.4 ± 0.4
$1 - 7$	10 ± 4	1290 ± 12	29 ± 10		—	—

Table 2: Results of the Gaussian plus polynomial background fits performed on the mass spectra of Figure 3. The number of the events in the Gaussian, the mass M and the width σ are listed with the error given by the fit. All fits reproduce the data well, as proven by the confidence level (CL) value. The partial efficiency ϵ and the partial cross-section $\Delta\sigma$ (errors include systematic uncertainties) are also given for each P_T^2 interval.

Detection efficiency decreases with Q^2 and is large for $Q^2 \sim 0$.

Why ?

The contribution from $\gamma\gamma$ is mainly to $\eta_H \rightarrow K^*K$

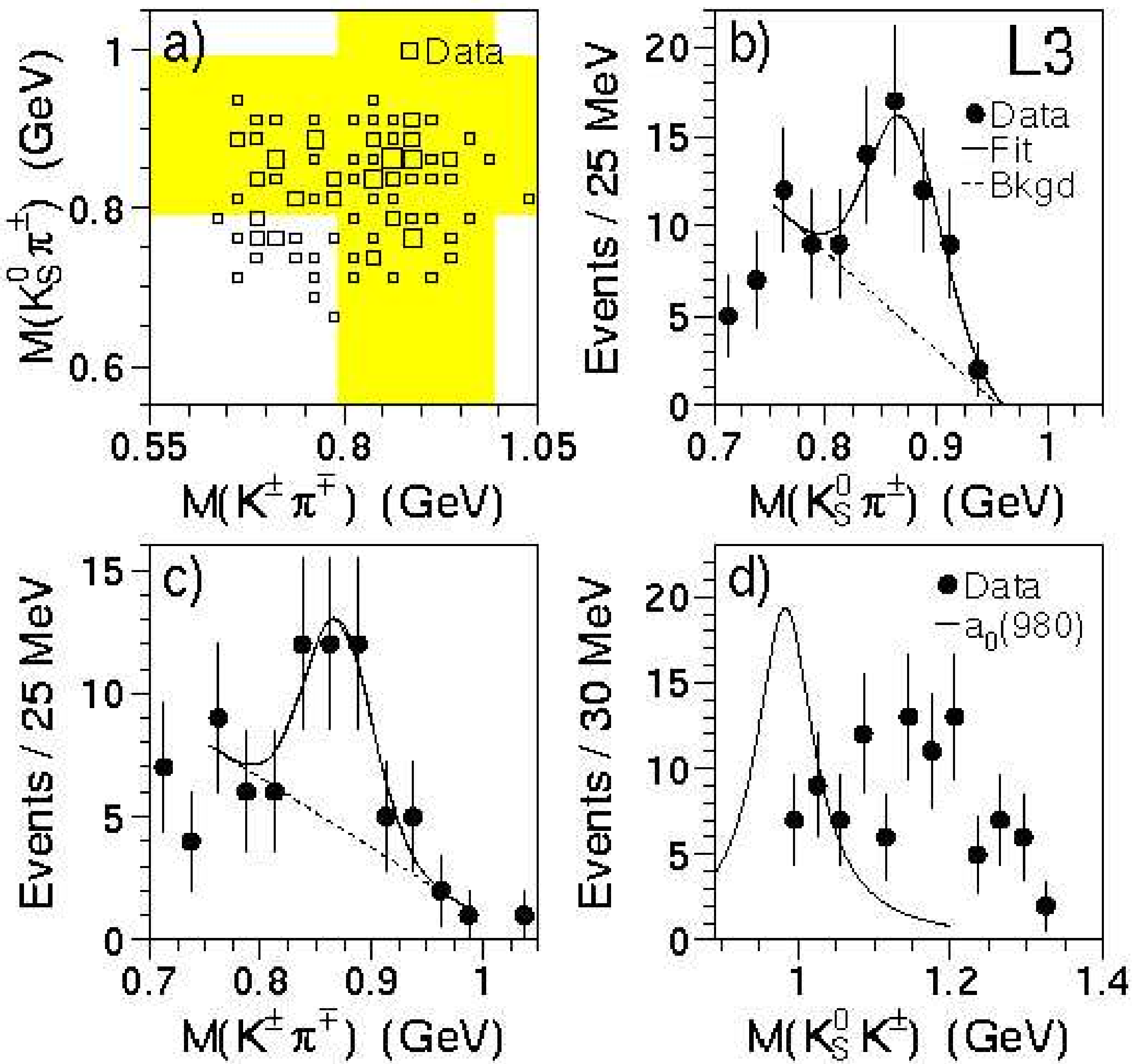

4.4 E/ι decays in the $^3P_0$ model

- **The $\eta(1295)$ is only seen in $\pi^- p \to n(\eta\pi\pi)$ Not in $p\bar{p}$ annihilation, nor in radiative J/ψ decay,nor in $\gamma\gamma$ fusion**
- **The $\eta(1440)$ is not produced as $s\bar{s}$ state but decays into $K\bar{K}\pi$**
- **The $\eta(1440)$ is too narrow !**
  The width of the $\pi(1300)$ is 400 ± 200 MeV
  The squared isoscalar coefficient for $\pi(1300) \to \rho\pi$ is 1/2; for $\eta(1440) \to K^*K + cc$ is 3/2
  The width of the $\eta(1440)$ should be $\sim$ 600MeV.

We suggest that the origin of all these anomalies are due to a node in the wave function of the $\eta(1440)$!

Matrix elements calculated within $^3P_0$ model.

T. Barnes, F. E. Close, P. R. Page and E. S. Swanson, "Higher quarkonia," Phys. Rev. D 55, 4157 (1997)

$\boxed{2S \rightarrow 1S + 1S}$

(See 1S → 1S + 1S for channel coefficients.)

$$f_P = -\frac{2^{9/2}5}{3^{9/2}}\, x \left(1 - \frac{2}{15}x^2\right)$$

$\boxed{2S \rightarrow 1P + 1S}$

$$f_S = \frac{2^4}{3^4}\left(1 - \frac{7}{9}x^2 + \frac{2}{27}x^4\right)$$

$$f_D = \frac{2^{9/2}(13)}{3^6}\, x^2\left(1 - \frac{2}{39}x^2\right)$$

Matrix elements for decays of the η radial excitation: ($=\eta_R$)

- η_R **decay to** K*K
  Matrix element vanishes for $\mathbf{x^2 = 15/2}$**,** $\mathbf{x = p/[0.4\,GeV] = 1\,GeV/c}$**.**
- η_R **decay to** $\mathbf{a_0(980)\pi}$
  Matrix element vanishes for $\mathbf{p = 0.45\,GeV/c}$**.**
- **If** $\eta_R = \eta(1440)$**, the decay to** $\mathbf{a_0(980)\pi}$ **vanishes at the mass 1470 MeV.**

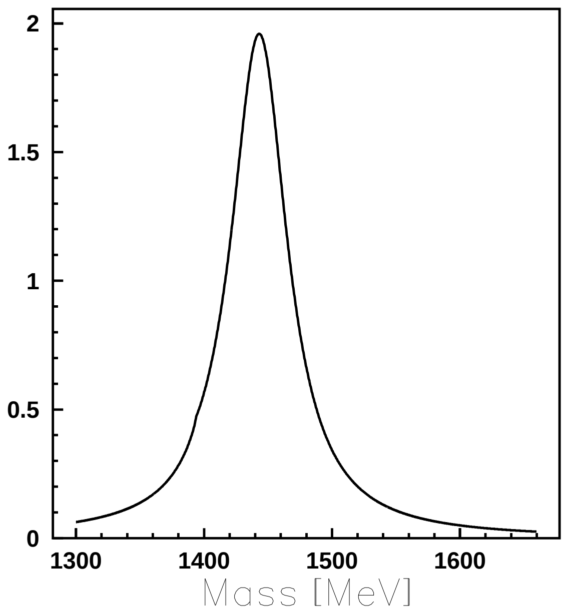

Undistorted BW

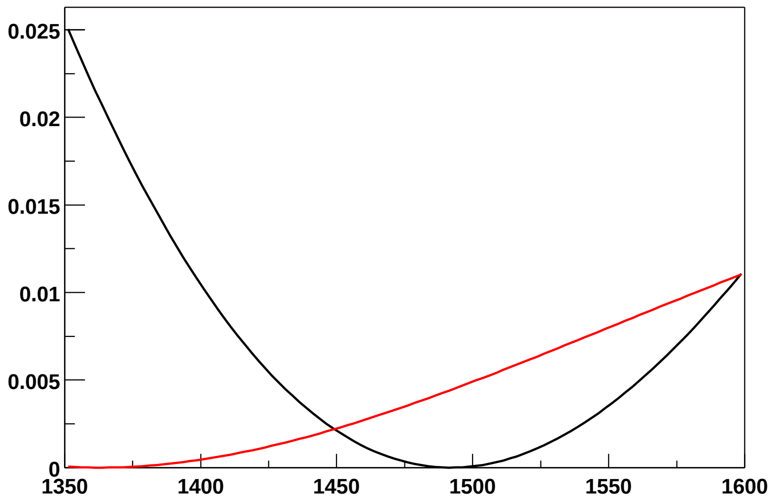

matrix element

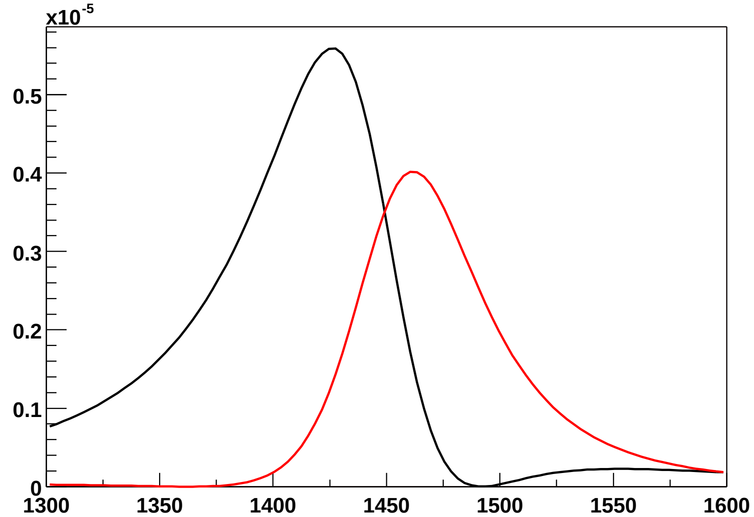

distorted BW

The $\eta(1440)$ $\rightarrow \mathbf{a_0(980)}\pi$, $\rightarrow \mathbf{a_0(980)}\pi$ and $\rightarrow K^*K$ have different peak positions; η_L and η_H could be one state.

4.5 What do we conclude

- **The $\eta(1440)$ is split into two components, η_L and η_H The splitting reflects the node of the 2S wave function.**
- **The node suppresses OZI allowed decays into $a_0(980)\pi$ and allows K^*K decays.**
- **The $\eta(1295)$ is not a $q\bar{q}$ meson.**
- **There is only one η state, the $\eta(1440)$ in the mass range from 1200 to 1500 MeV and not 3 !**
- **The $\eta(1440)$ wave function has a node;**
  the $\eta(1440)$ is the radial excitation of the η.
- **The $\eta(1440)$ is not a glueball.**

Warning lesson from $\iota(1440)$: you can build up a case, convince the community and still be wrong !

And what is the radial excitation of the η' ?

The $\eta(1760)$, perhaps.

The quest for the scalar glueball

- **Where do we expect glueballs ?**
- **Glueballs in "gluon-rich" processes**
- **Scalar mesons: data**
- **Scalar mesons: interpretation 1**
- **Scalar mesons: interpretation 1**
- **Conclusion**

5 The quest for the scalar glueball

5.1 Where do we expect glueballs ?

The glueball spectrum from an anisotropic lattice study (Morningstar)

Pseudoscalar glueball should have a mass of about 2.5 GeV !

The $\eta(1440)$ is not a glueball.

Scalar glueball expected at 1.7 GeV

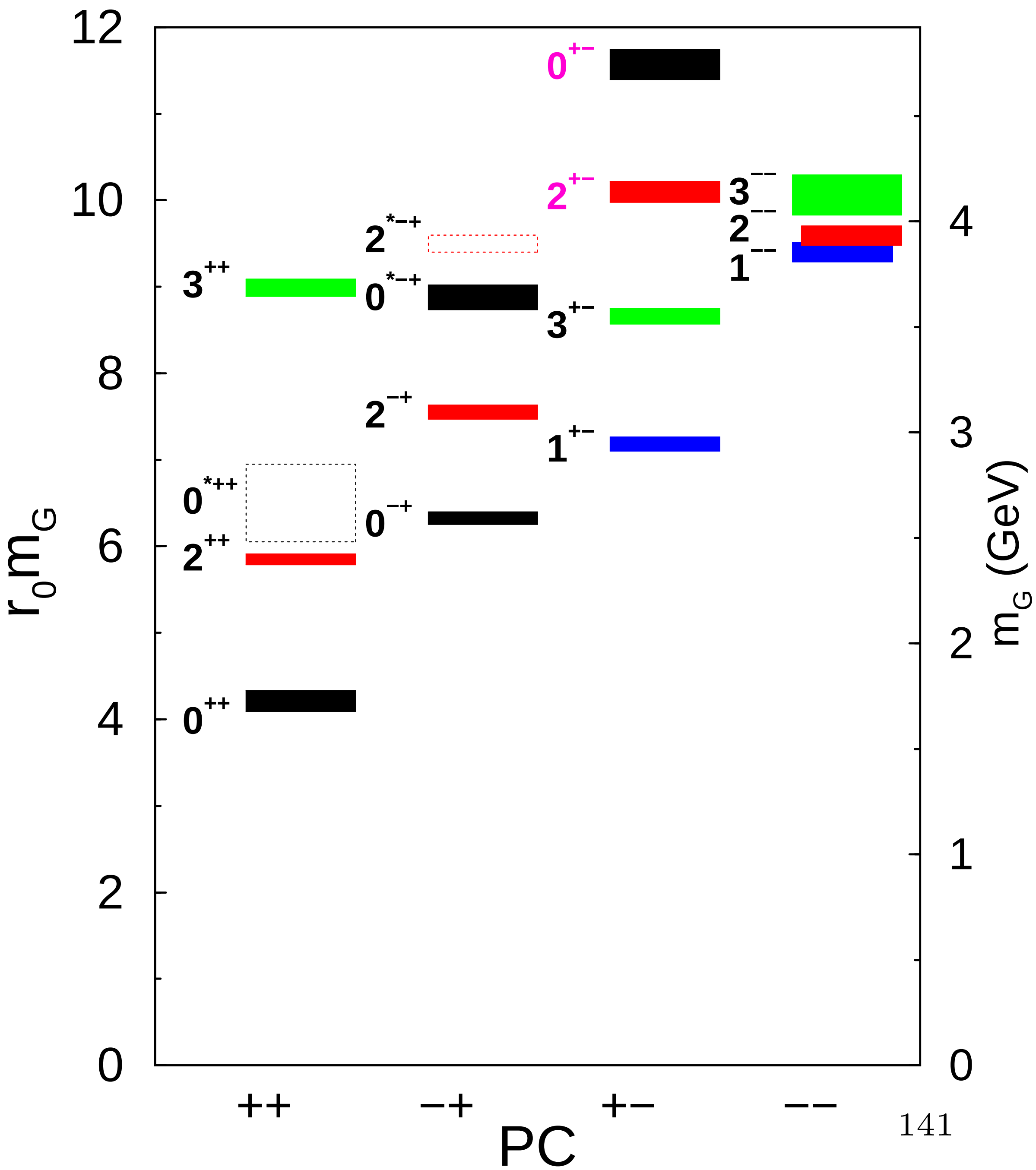

5.2 Glueballs in "gluon-rich" processes

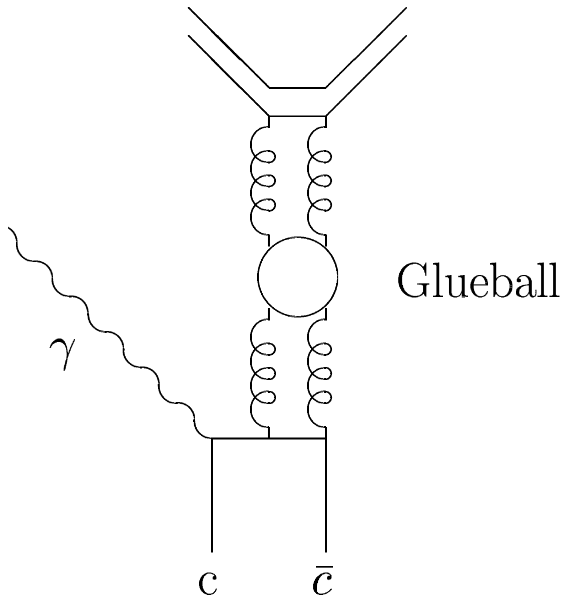

J/Ψ may convert into 2 gluons and a photon. The 2 gluons interact and form glueballs.

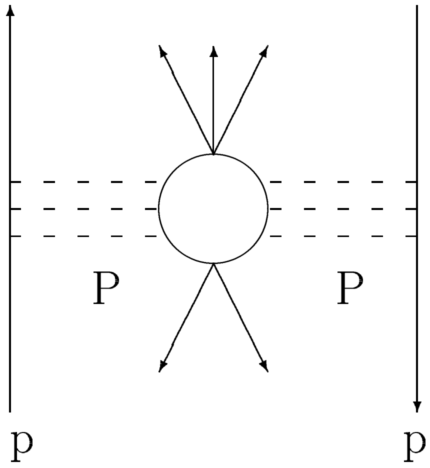

In central production two hadrons scatter diffractively, no valence quarks are exchanged.

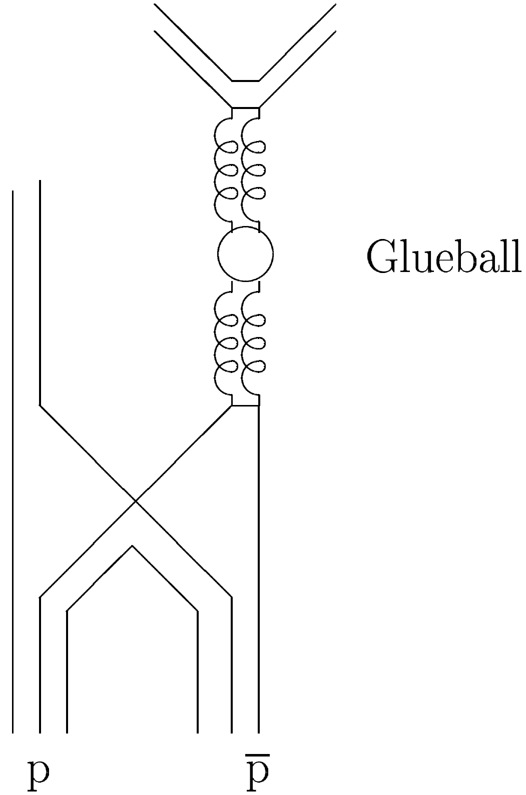

In p$\bar{\mathrm{p}}$ annihilation quark-antiquark pairs annihilate into gluons forming glueballs.

Radiative J/ψ decay

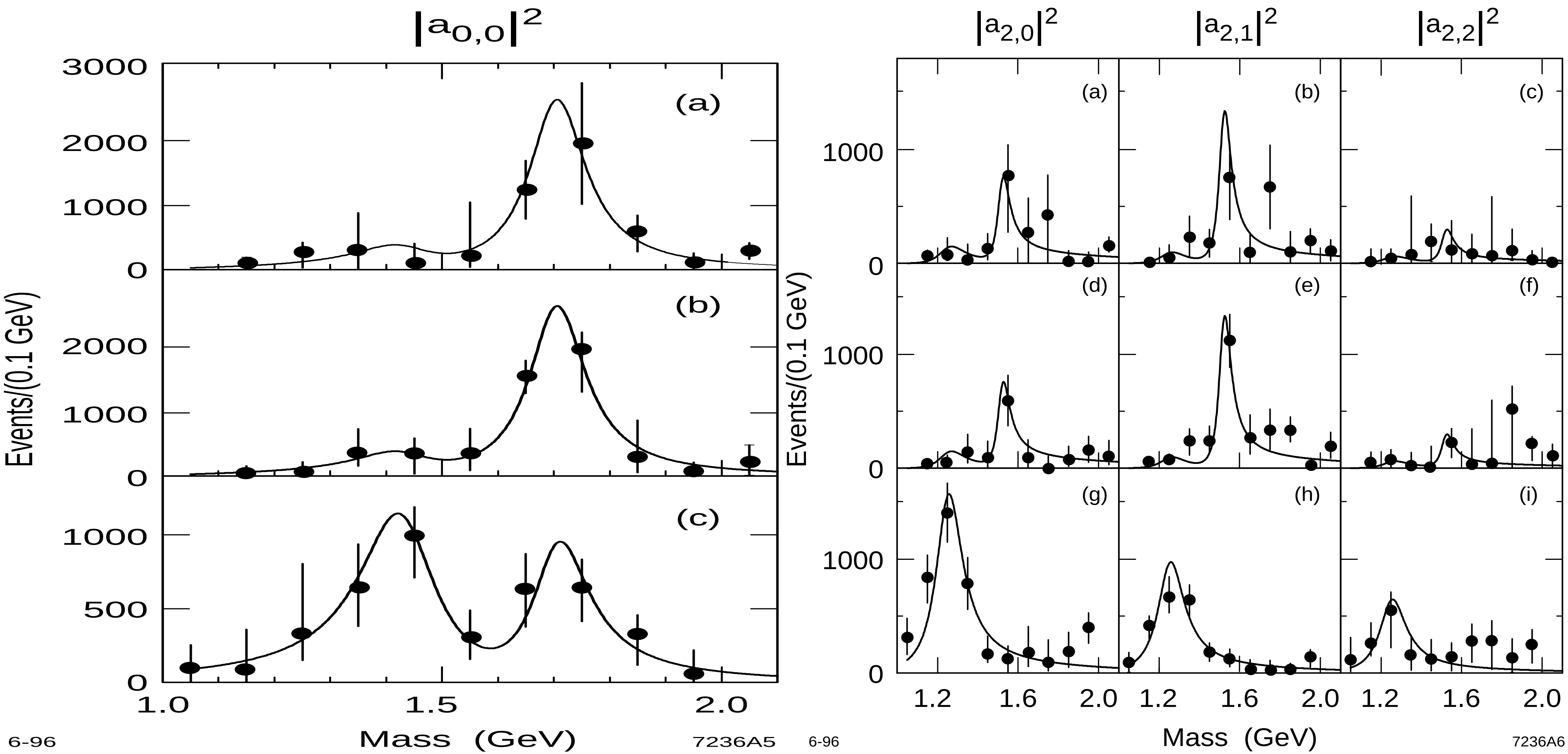

J/ψ radiative decay to two pseudoscalar mesons, (Mark III).
Top: $J/\psi \rightarrow \gamma K_S K_S$, middle: $J/\psi \rightarrow \gamma K^+ K^-$, bottom: $J/\psi \rightarrow \gamma\pi\pi$.

$f_0(1450)$ $f_0(1700)$

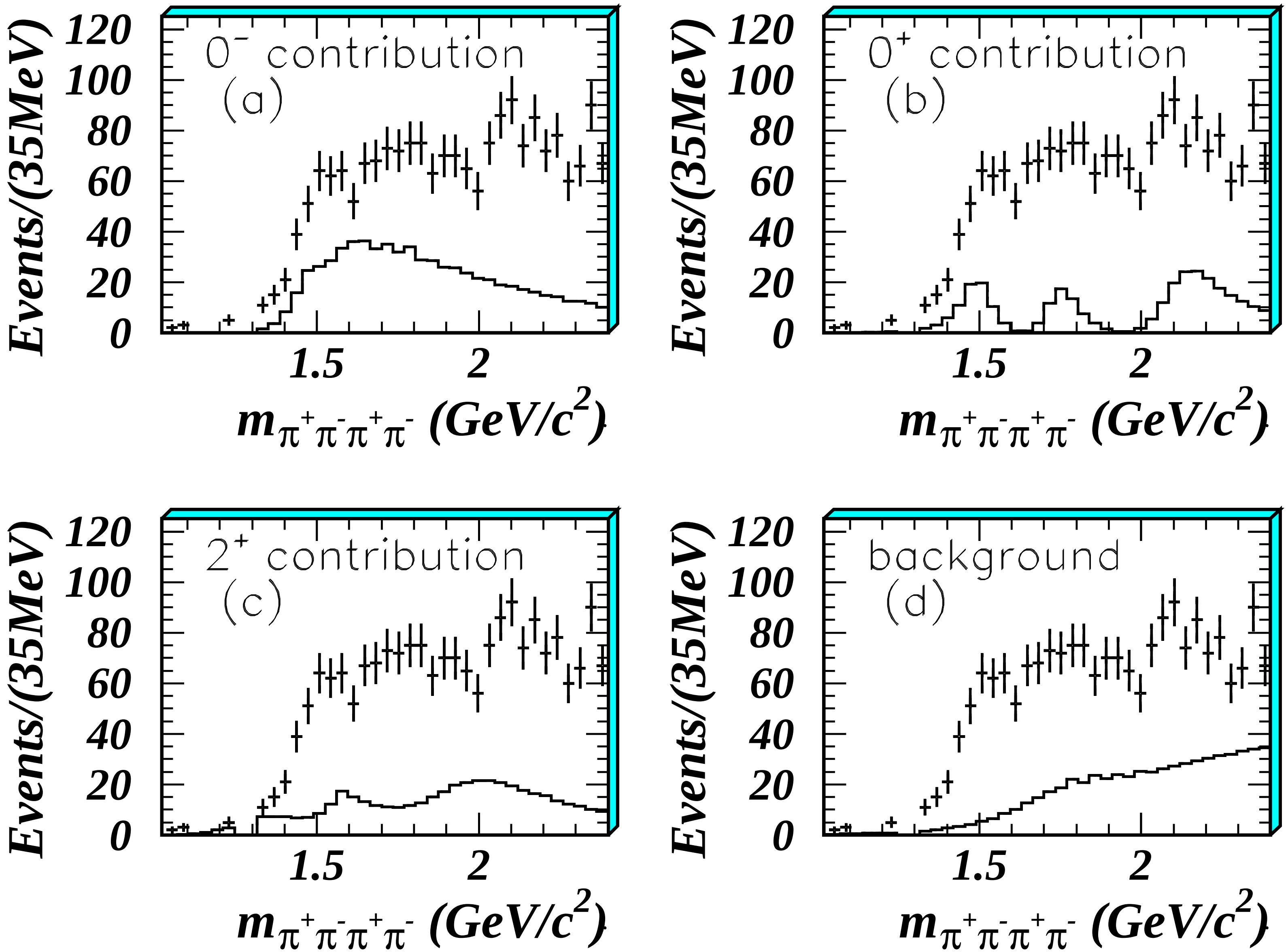

Partial wave decomposition of radiative J/ψ decays into $2\pi^+\pi^-$ shows 3 distinct peaks at $f_0(1500)$, $f_0(1750)$, $f_0(2100)$, no $f_0(1370)$.

Central production

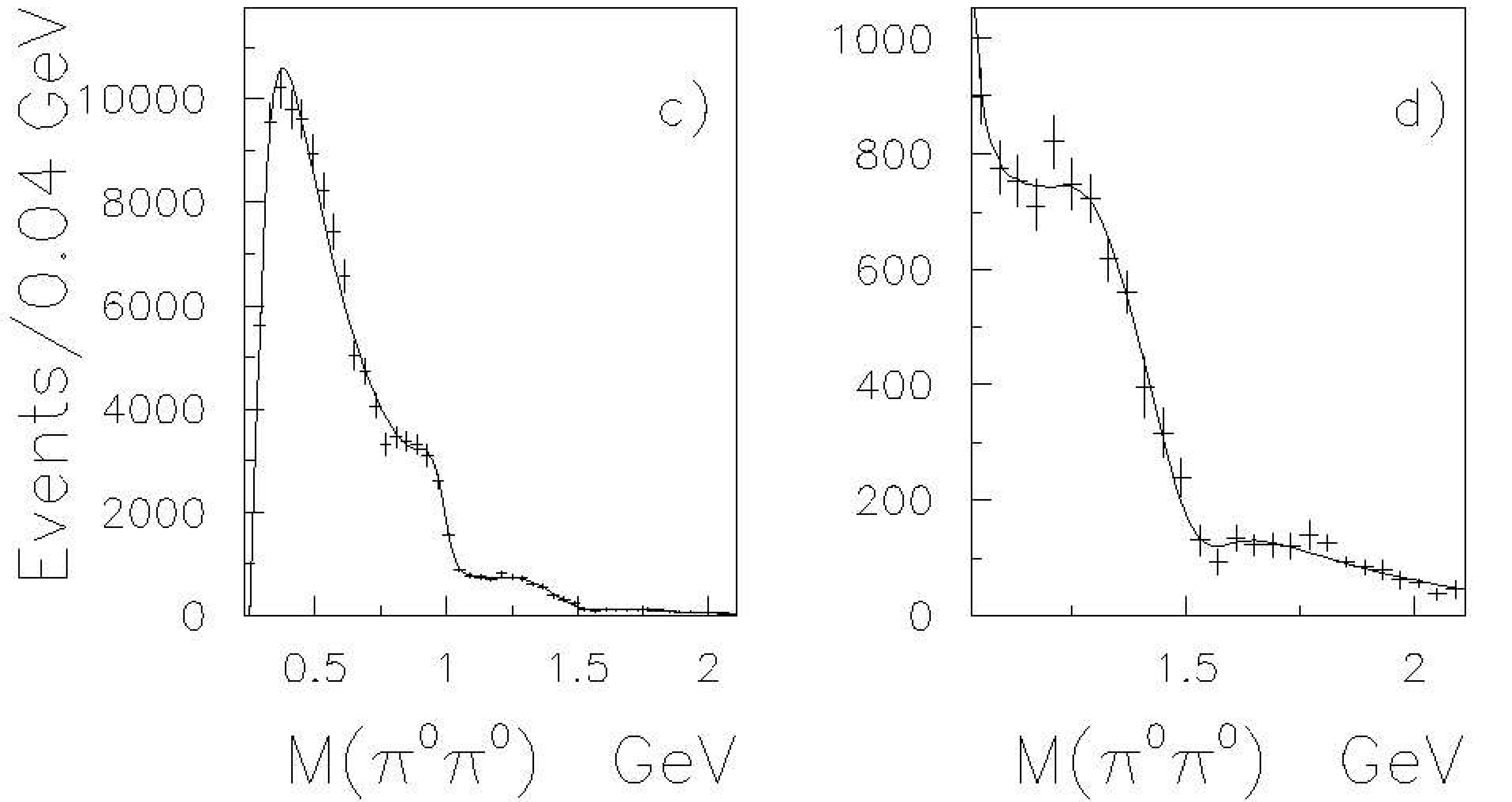

Dips at $f_0(980)$ **and** $f_0(1500)$

Central production of

$\pi^+\pi^-\pi^+\pi^-$

$\pi^+\pi^-\pi^0\pi^0$

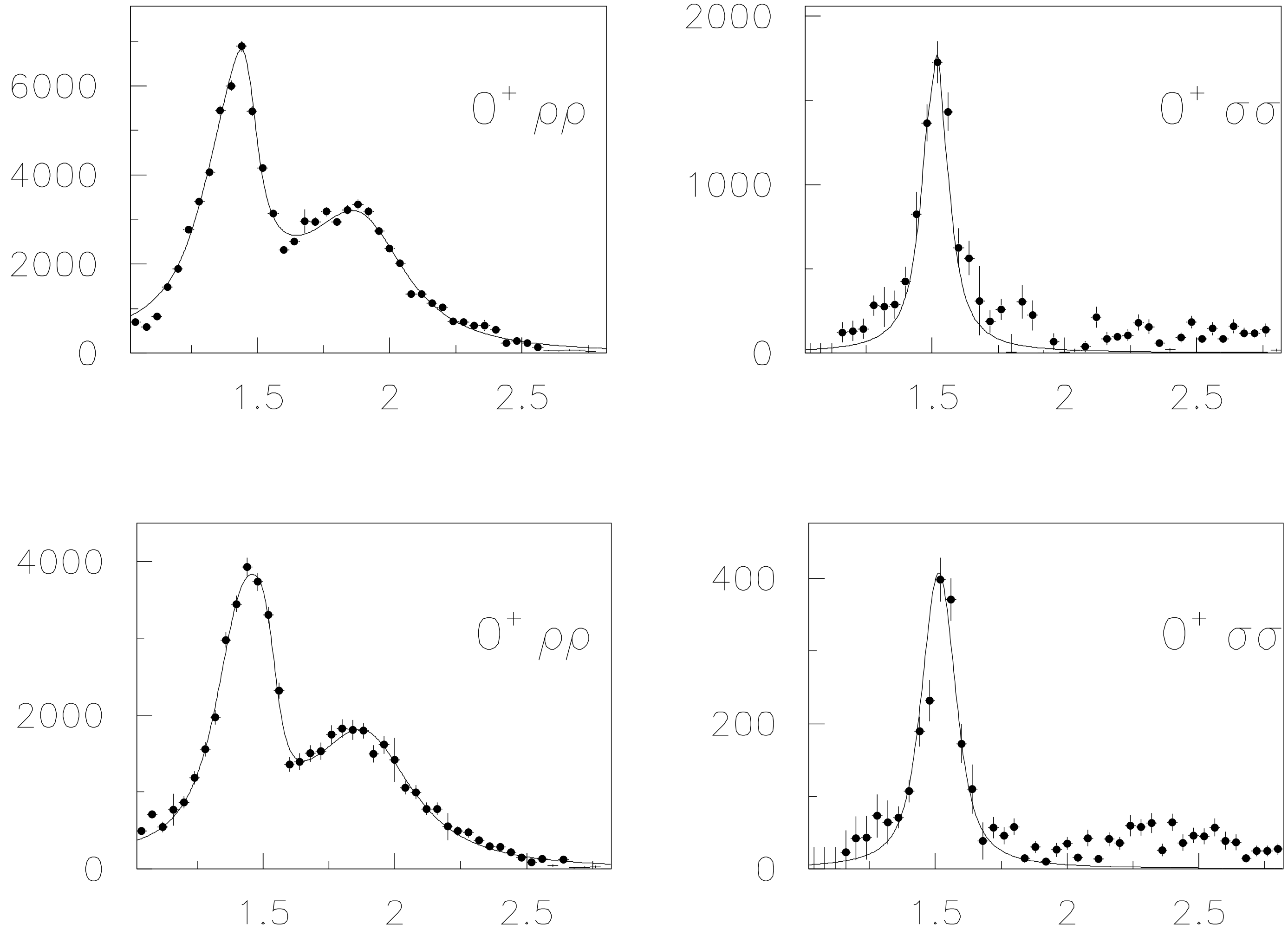

Peak-dip structure at 1400-1500 MeV in $\rho\rho$;

peak at 11500 MeV in $\sigma\sigma$

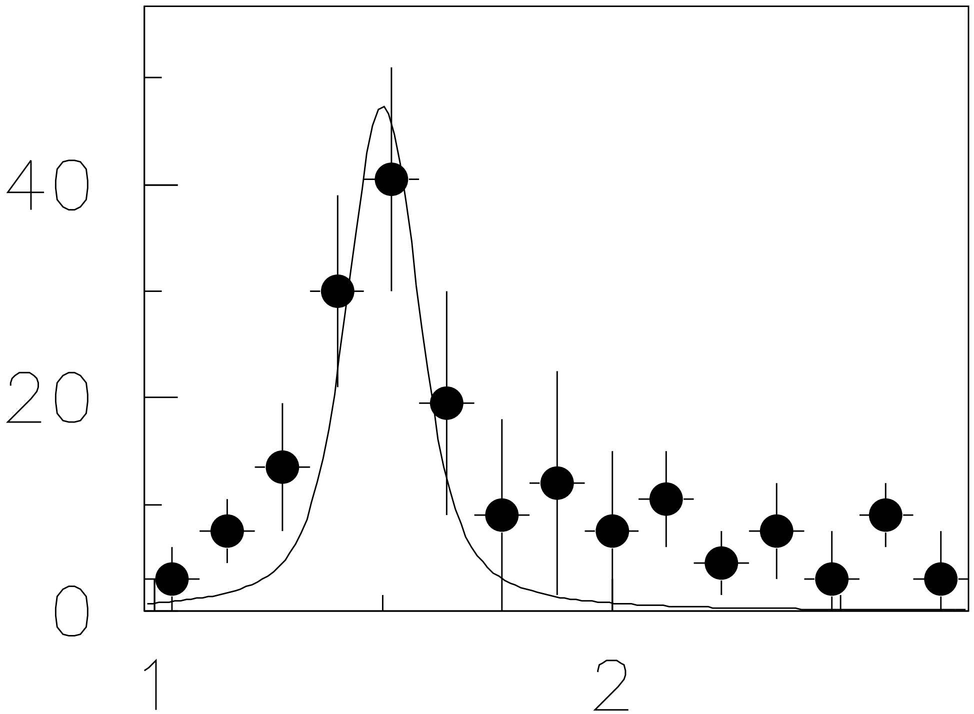

$4\pi^0$ **invariant mass from WA102**

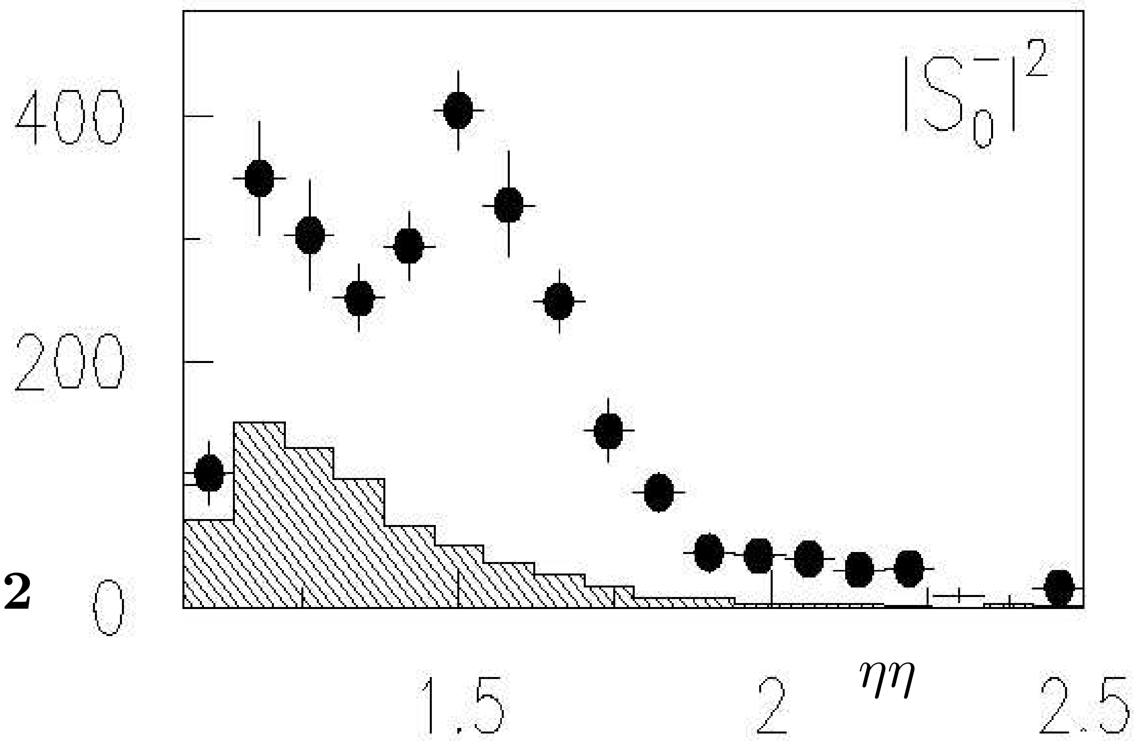

Peaks at 1500 MeV

$\mathbf{p\bar{p}}$ annihilation

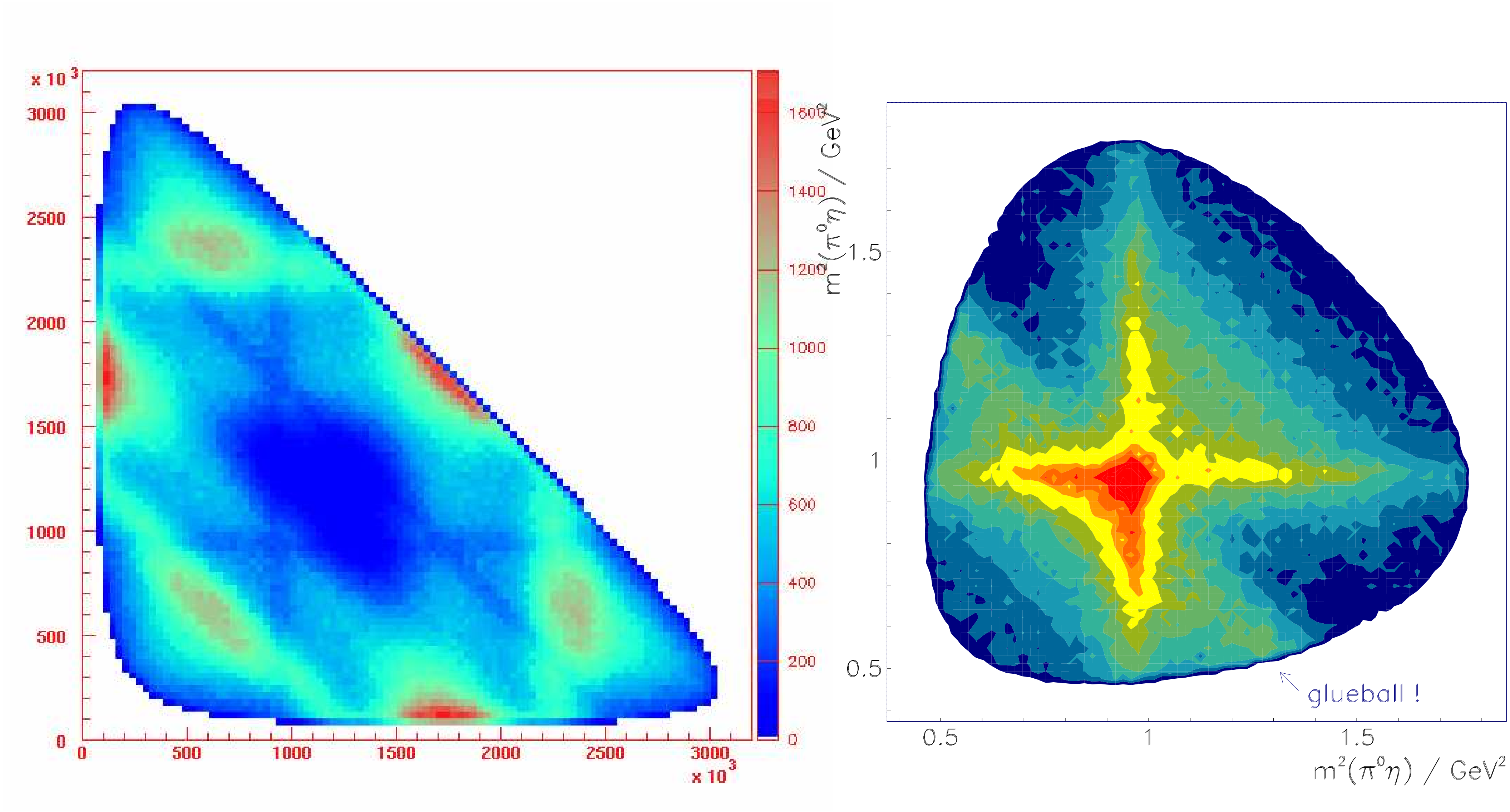

Dalitz plots for $\mathbf{p\bar{p}}$ annihilation at rest into $\mathbf{3|\pi^0>}$ (left), $\mathbf{|\pi^0>2|\eta>}$ (right).

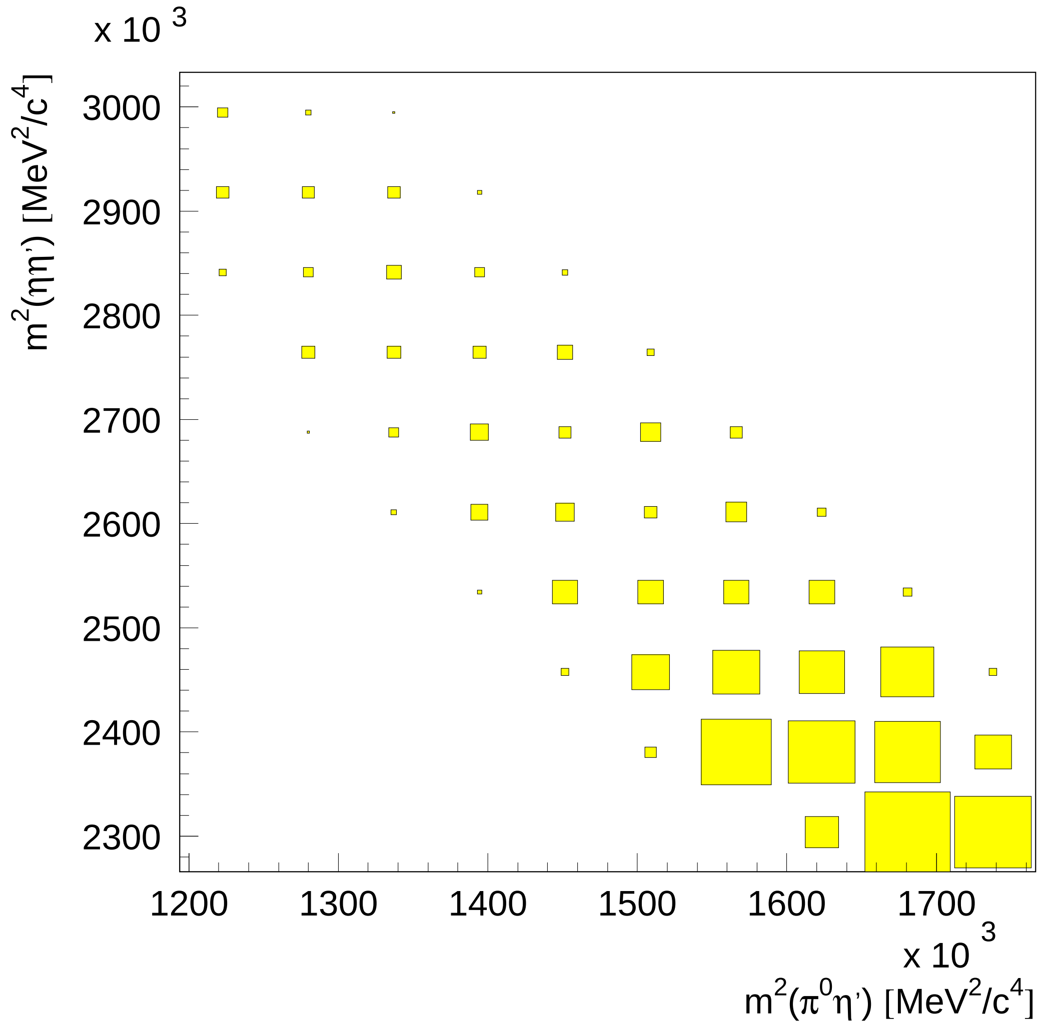

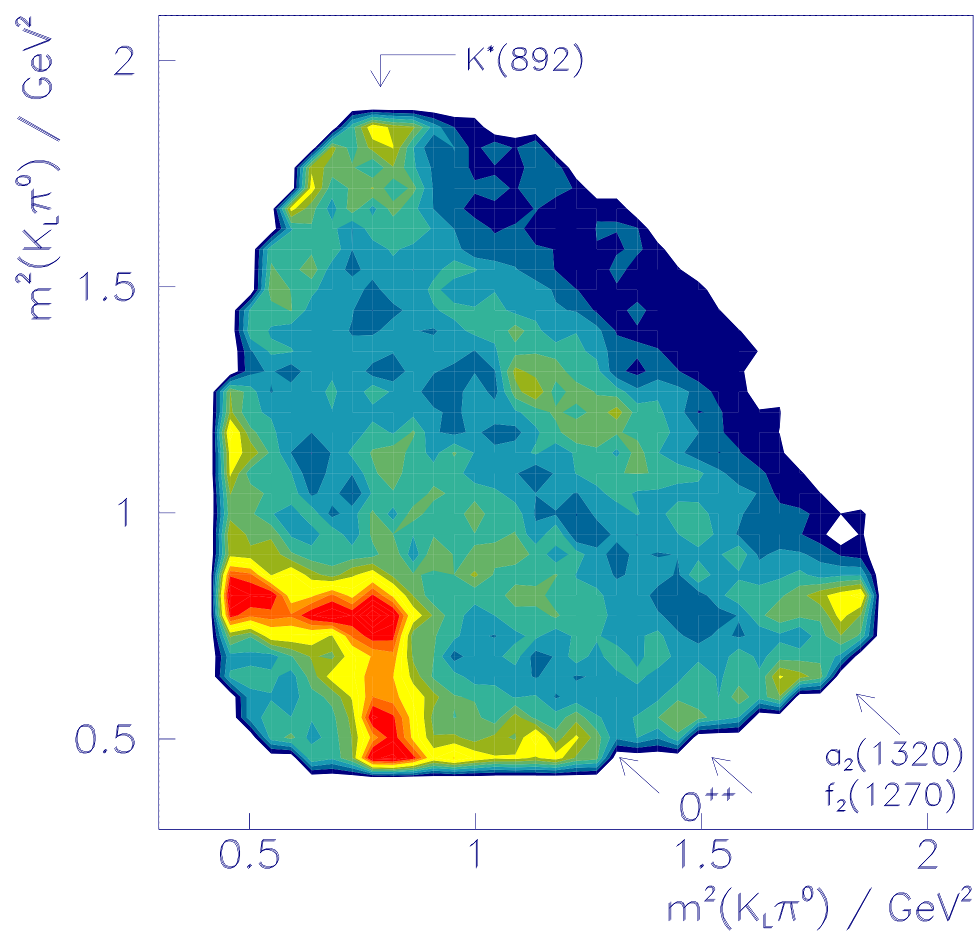

Dalitz plots for $\mathbf{p\bar{p}}$ annihilation at rest into $|\pi^0>|\eta>|\eta'>$ (left), $\mathbf{K}_l\mathbf{K}_l|\pi^0>$ (right).

$f_0(1370)$ **and** $f_0(1500)$

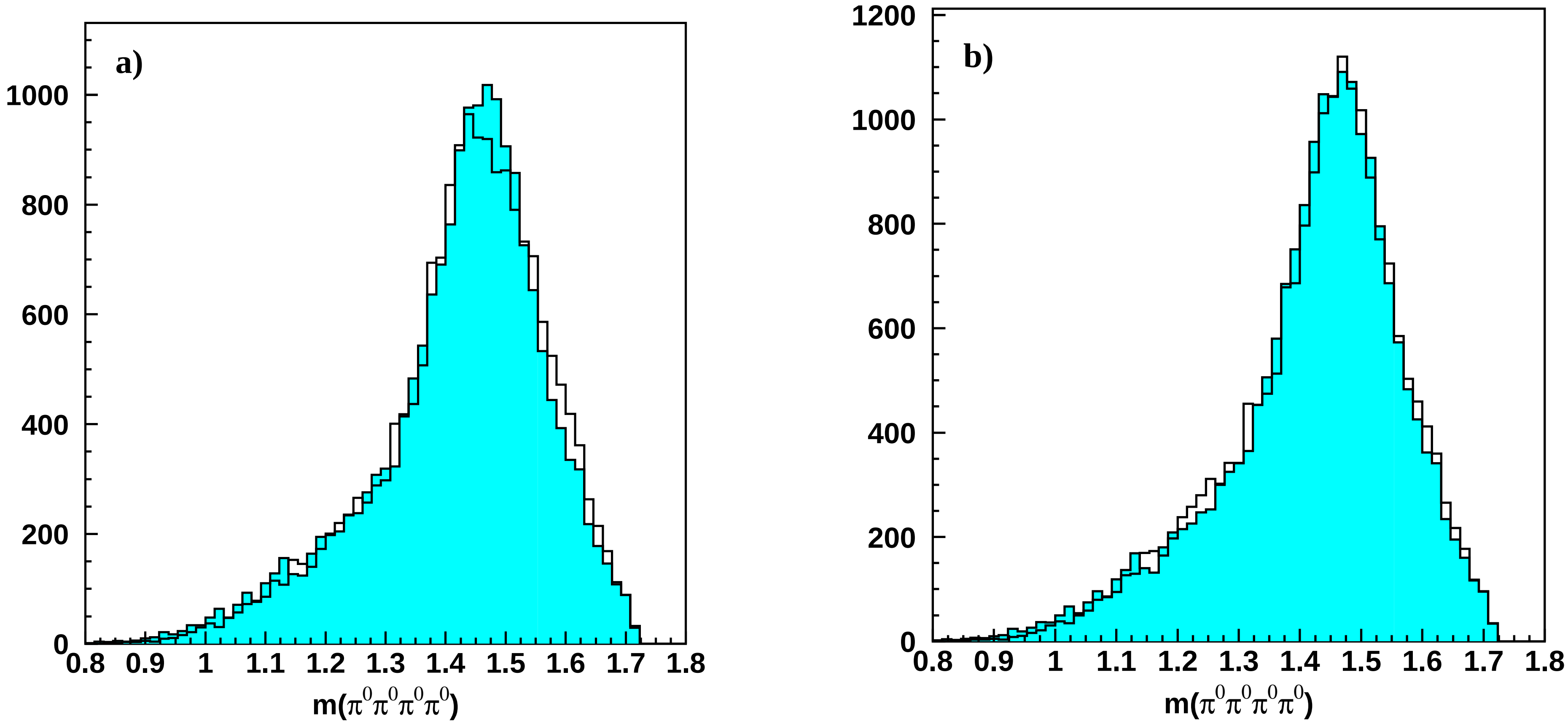

The $4|\pi^0>$ invariant mass in the reaction $\bar{\mathrm{p}}\mathrm{n} \to |\pi^- >4|\pi^0>$. A fit (including other amplitudes) with one scalar state fails; two scalar resonances at 1370 and 1500 MeV give a good fit. Note that the full 8-dimensional phase space is fitted and not just the mass projection shown here.

	$\mathbf{f_0(1370)}$	$\mathbf{f_0(1500)}$
$\mathbf{\Gamma_{tot}}$	$\mathbf{275 \pm 55}$	$\mathbf{130 \pm 30}$
$\mathbf{\Gamma_{\sigma\sigma}}$	$\mathbf{120.5 \pm 45.2}$	$\mathbf{18.6 \pm 12.5}$
$\mathbf{\Gamma_{\rho\rho}}$	$\mathbf{62.2 \pm 28.8}$	$\mathbf{8.9 \pm 8.2}$
$\mathbf{\Gamma_{\pi^*\pi}}$	$\mathbf{41.6 \pm 22.0}$	$\mathbf{35.5 \pm 29.2}$
$\mathbf{\Gamma_{a_1\pi}}$	$\mathbf{14.10 \pm 7.2}$	$\mathbf{8.6 \pm 6.6}$
$\mathbf{\Gamma_{\pi\pi}}$	$\mathbf{21.7 \pm 9.9}$	$\mathbf{44.1 \pm 15.4}$
$\mathbf{\Gamma_{\eta\eta}}$	$\mathbf{0.41 \pm 0.27}$	$\mathbf{3.4 \pm 1.2}$
$\mathbf{\Gamma_{\eta\eta'}}$		$\mathbf{2.9 \pm 1.0}$
$\mathbf{\Gamma_{\bar{K}K}}$	$\mathbf{(7.9 \pm 2.7)}$ **to** $\mathbf{(21.2 \pm 7.2)}$	$\mathbf{8.1 \pm 2.8}$

Partial decay widths of the $f_0(1370)$ and $f_0(1500)$ from Crystal Barrel data

5.3 Scalar mesons: data

The Particle Data Group lists 12 scalar mesons. Within the quark model we expect 4 ground state mesons and 4 radial excitations.

$\mathbf{I = 1/2}$	$\mathbf{I = 1}$	$\mathbf{I = 0}$
		$\mathbf{f_0(600)}$
	$\mathbf{a_0(980)}$	$\mathbf{f_0(980)}$
		$\mathbf{f_0(1370)}$
$\mathbf{K_0^*(1430)}$	$\mathbf{a_0(1490)}$	$\mathbf{f_0(1500)}$
		$\mathbf{f_0(1710)}$
$\mathbf{K_0^*(1950)}$		
		$\mathbf{f_0(2100)}$
		$\mathbf{f_0(2200, 2330)}$

5.4 Scalar mesons: interpretation 1

$\mathbf{I = 1/2}$	$\mathbf{I = 1}$	$\mathbf{I = 0}$	
		$\mathbf{f_0(600)}$	σ **meson**
			chiral partner of the π
	$\mathbf{a_0(980)}$	$\mathbf{f_0(980)}$	$\mathbf{K\bar{K}}$ **molecules**
		$\mathbf{f_0(1370)}$	$\mathbf{q\bar{q}}$ **states**
$\mathbf{K_0^*(1430)}$	$\mathbf{a_0(1490)}$	$\mathbf{f_0(1500)}$	**Glueball**
		$\mathbf{f_0(1710)}$	
$K_0^*(1950)$			
		$\mathbf{f_0(2100)}$	
		$\mathbf{f_0(2200, 2330)}$	

K-matrix poles			Bonn model, B		
	$\mathbf{a_0(989)}$	$\mathbf{f_0(654)}$		$\mathbf{a_0(1057)}$	$\mathbf{f_0(665)}$
$\mathbf{K_0^*(1168)}$	$\mathbf{a_0(1555)}$	$\mathbf{f_0(1203)}$	$\mathbf{K_0^*(1187)}$	$\mathbf{a_0(1665)}$	$\mathbf{f_0(1262)}$
		$\mathbf{f_0(1560)}$			$\mathbf{f_0(1554)}$
$\mathbf{K_0^*(1850)}$			$\mathbf{K_0^*(1788)}$		
		$\mathbf{f_0(1822)}$			$\mathbf{f_0(1870)}$

5.5 Interpretation 2

There is a remarkable agreement between the K-matrix poles from the analysis of Anisovich et al. and model B from Metsch et al.

- **What are K-matrix and what are T-matrix poles ?**

  The T-matrix poles define the position of a peak in the cross section; they are the quantities which go into the PDG

  The K-matrix is used to parameterise the scattering amplitude in a probability conserving way (adding two Breit Wigner resonance amplitudes may exceed the modulus one; one $\pi\pi$ in, two $\pi\pi$ out, that must be wrong !).

- **In the limit of vanishing decay couplings of a resonance, its Breit-Wigner pole approaches the K-matrix pole:**
  the K-matrix pole could be the resonance position of a 'naked' resonance with all decay modes switch off !

5.6 Conclusion:

Do glueballs exist ?

still an unresolved issue !

We do find natural explanations for the spectrum without request for the presence of a glueball.

There is also no compelling evidence for the existence of hybrids

BARYONS

- **The particles: quarks and leptons**
- **The interactions**
- **Quark models for mesons**

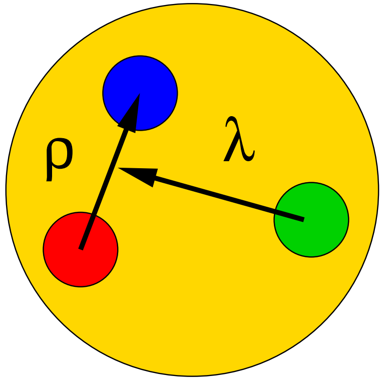

6 Baryons

Experimental Status

The Particle Data Group lists:

Octet	N		Σ	Λ	Ξ	
Decuplet		Δ	Σ		Ξ	Ω
Singlet				Λ		
****	11	7	6	9	2	1
***	3	3	4	5	4	1
**	6	6	8	1	2	2
*	2	6	8	3	3	0
No J	-	-	5	-	8	4
Total	22	22	26	18	11	4

- $\sim$ 100 resonances
- $\sim$ 85 known spin and parity
- $\sim$ 50 established baryons of known spin parity
- K. Hagiwara *et al.*, Phys. Rev. D 66, 010001 (2002).

Theoretical models and results

- **Assume quarks move in an effective confinement potential generated by a very fast color exchange between quarks (antisymmetrising the total wave function)**
- **Assume the light quarks acquire effective mass by spontanous symmetry breaking**
- **Assume residual interactions**
  - **One gluon exchange**

    relativized **quark model,**

    S. Capstick and N. Isgur, Phys. Rev. D 34 (1986) 2809.

    OGE fixed to HFS (N-Δ)

    $\mathbf{L} \cdot \mathbf{S}$ large, in contrast to data

    Set to zero, (comp. by $\mathbf{L} \cdot \mathbf{S}$ from Thomas prec. ?)

- **Goldstone (pion) exchange**
  Take spin-spin, neglect tensor interactions,
  L. Y. Glozman, W. Plessas, K. Varga and
  R. F. Wagenbrunn,
  Phys. Rev. D 58 (1998) 094030.
- **Instanton interactions**
  Relativistic quark model with instanton-induced forces
  U. Löring, B. C. Metsch and H. R. Petry,
  Eur. Phys. J. A 10 (2001) 395-446, 447-486.

- **Solve equation of motion**
  (using wave functions of the harmonic oscillator)

Δ^* resonances with one – gluon exchange

OGE model

Godfrey, Isgur and others

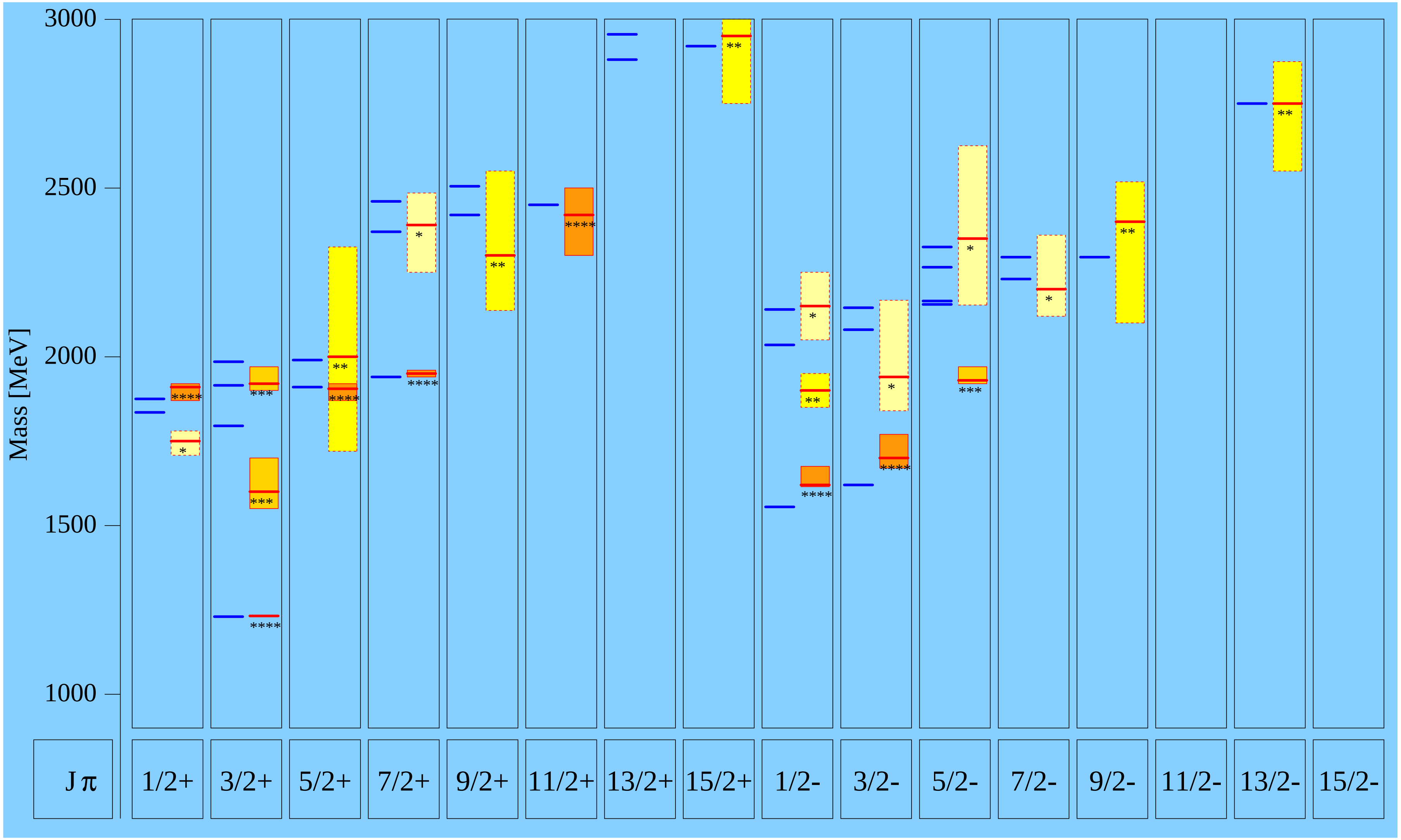

Δ^* resonances with instanton induced forces — Bonn model

U. Löring, B. Metsch, H. Petry and others

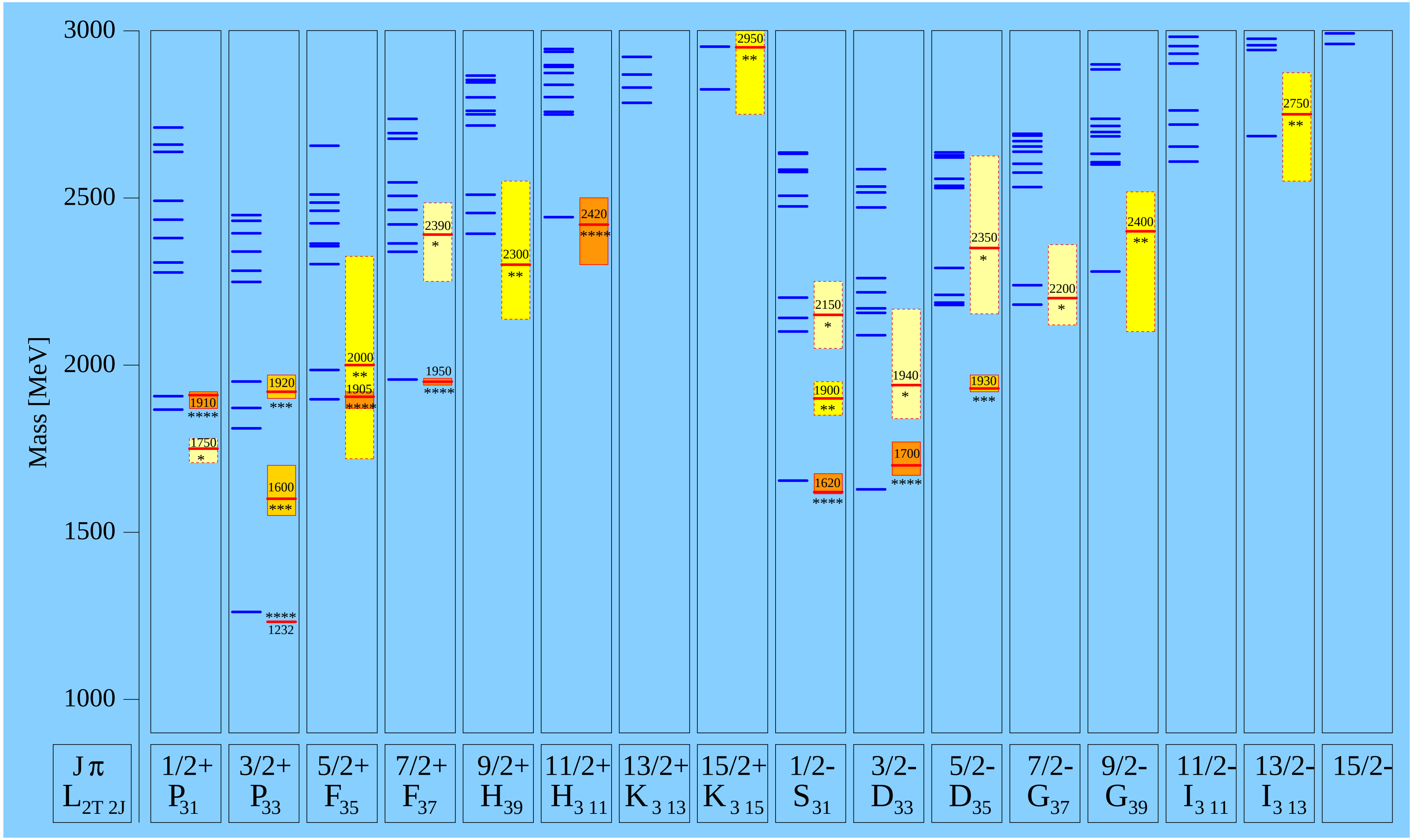

N* resonances with one – gluon exchange

OGE model

Godfrey, Isgur and others

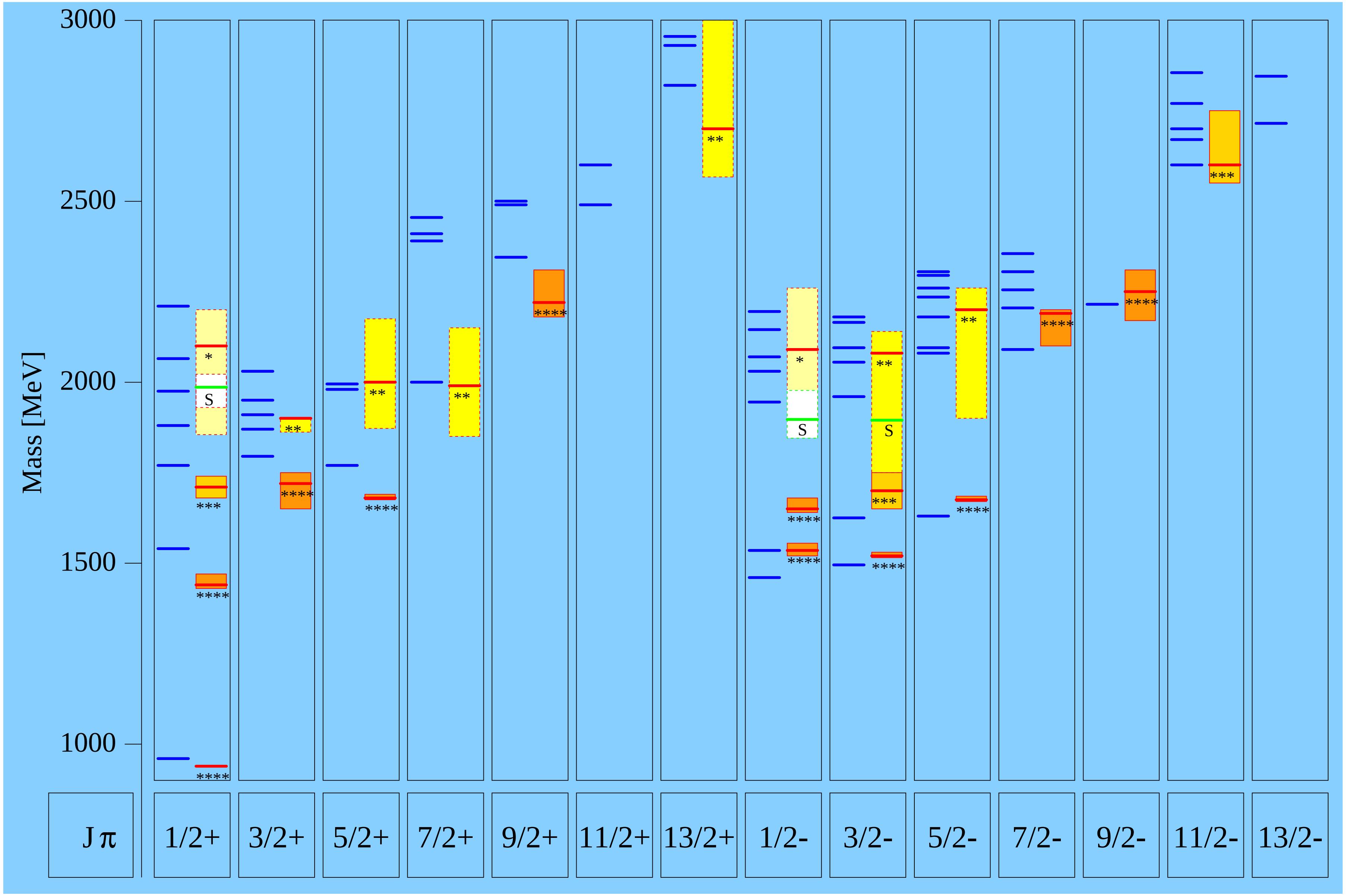

N* resonances with instanton induced forces — Bonn model

U. Löring, B. Metsch, H. Petry and others

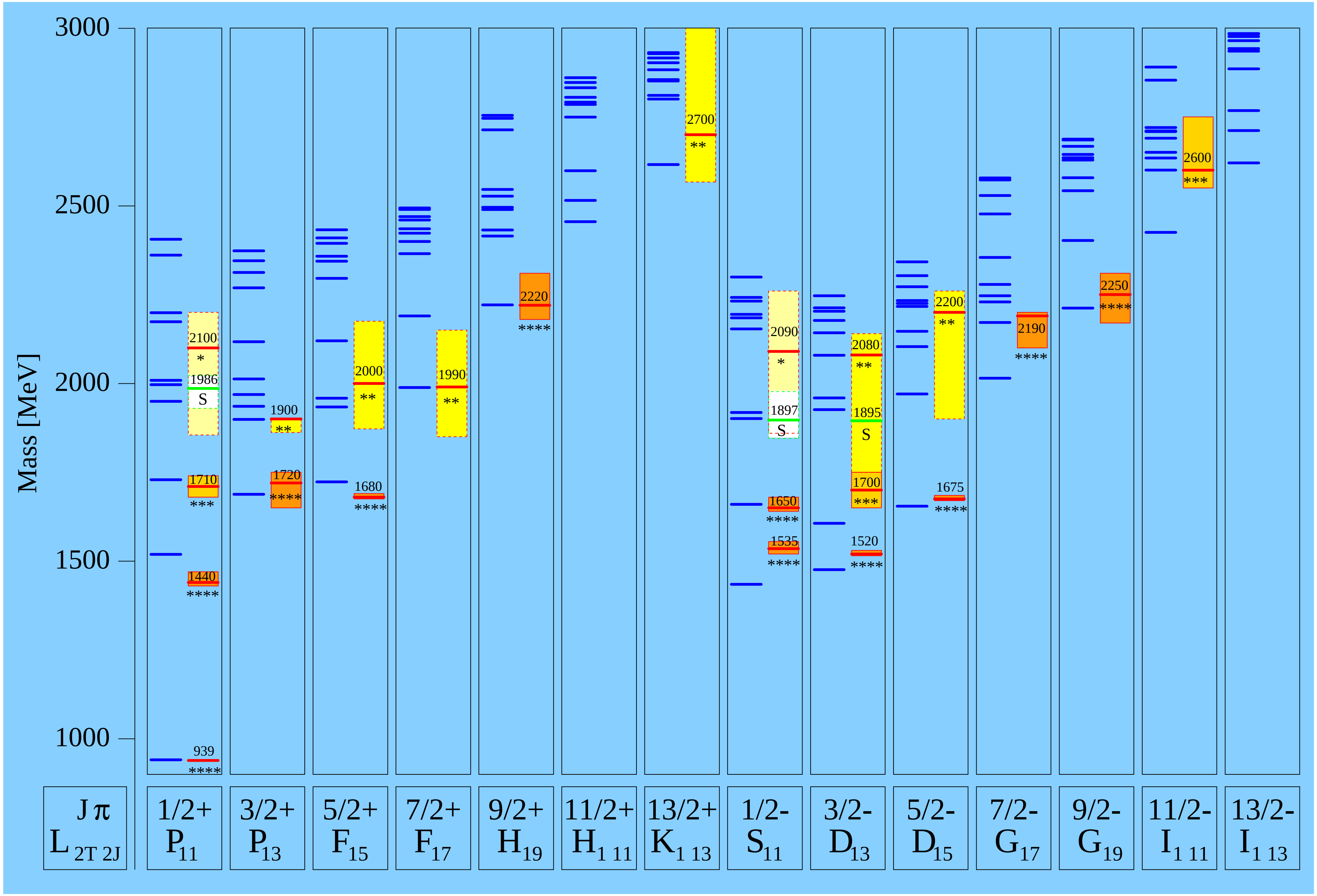

Many problems still unsolved:

→ What is the relation between quark models
and structure functions?

→ Which model is right?

→ Is it true that one interaction dominates?

→ Decay properties of resonances

→ Missing resonances

→ Low mass of Roper, $\Delta_{3/2^+}(1600)$ ...

→ Low mass of negative-parity Δ^*'s at 1950 MeV

Here:

Try to get at physics from phenomenolgy

The Baryon Wave Function

$$|\mathbf{qqq}>= |\mathbf{color}>_{\mathbf{A}} \cdot \quad |\mathbf{space, spin, flavor}>_{\mathbf{S}}$$

$$\mathbf{O(6)} \qquad \mathbf{SU(6)}$$

The total wave function must be antisymmetric w.r.t. the exchange of any two quarks. The wave function is antisymmetric, hence the space-spin-flavor wave function must be symmetric. We now construct wave functions.

SU(6)

Baryons (with 3 quarks): 3 flavors x 2 spins.

$$\mathbf{6} \otimes \mathbf{6} \otimes \mathbf{6} = \mathbf{56} \oplus \mathbf{70_M} \oplus \mathbf{70_M} \oplus \mathbf{20}$$

$$\mathbf{56} = {}^{4}\mathbf{10} \oplus {}^{2}\mathbf{8}$$

$$\mathbf{70} = {}^{2}\mathbf{10} \oplus {}^{4}\mathbf{8} \oplus {}^{2}\mathbf{8} \oplus {}^{2}\mathbf{1}$$

$$\mathbf{20} = {}^{2}\mathbf{8} \oplus {}^{4}\mathbf{1}$$

The 56-plet contains

N^*'s with spin 1/2

Δ^*'s with spin 3/2

The 70-plet contains

N^*'s with spin 1/2 and with spin 3/2

Δ^*'s with spin 1/2

The singlet contains

N^*'s with spin 1/2

(8_M) have a mixed flavor symmetry,
the 10 multiplet is symmetric,
the 1 antisymmetric in flavor space.

Phenomenological approach to the baryon mass spectrum using Regge trajectories

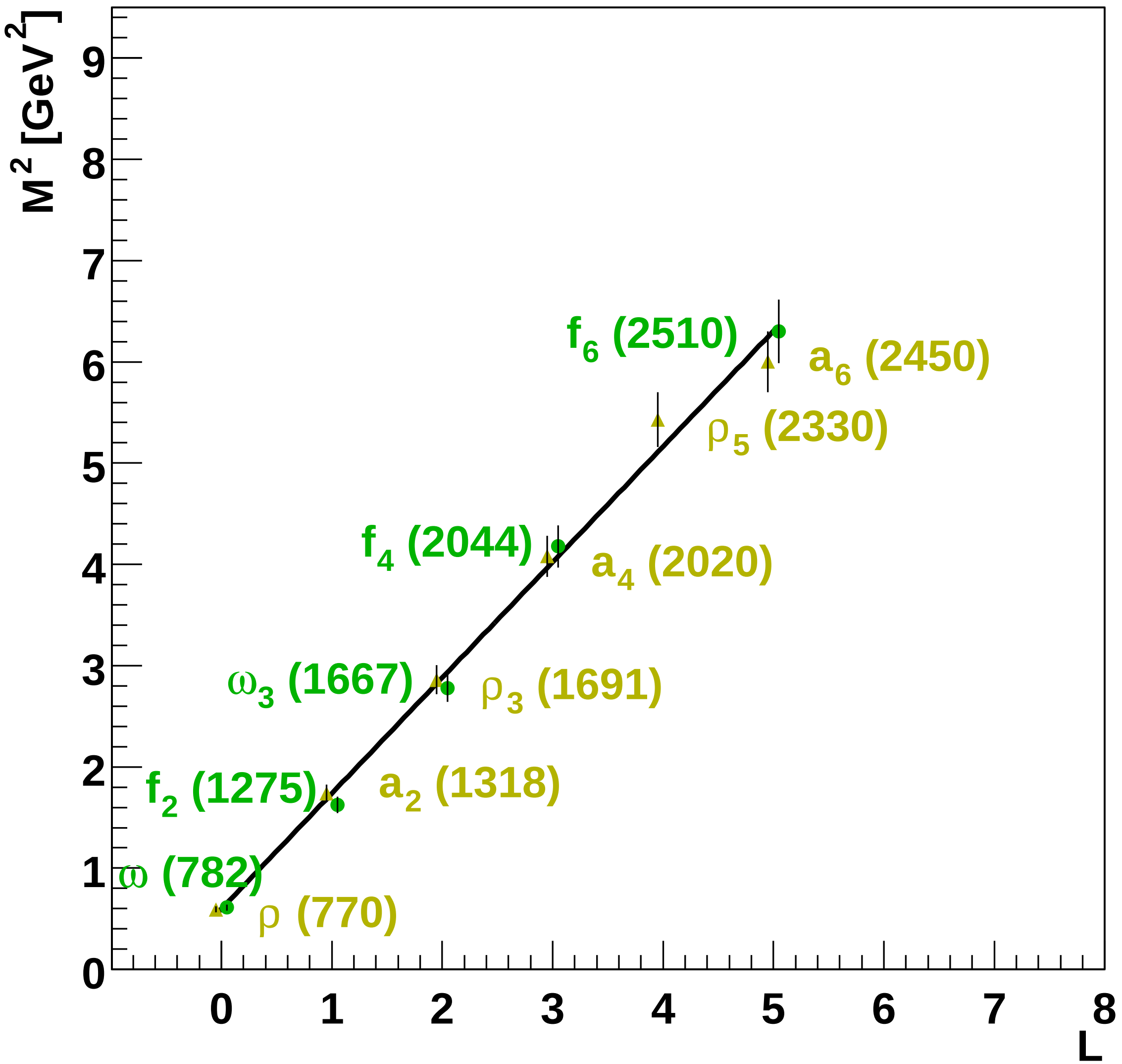

Mesons with $\mathbf{J = L + S}$ lie on a Regge trajectory with a slope of 1.142 GeV^2.

Meson and baryon trajectories

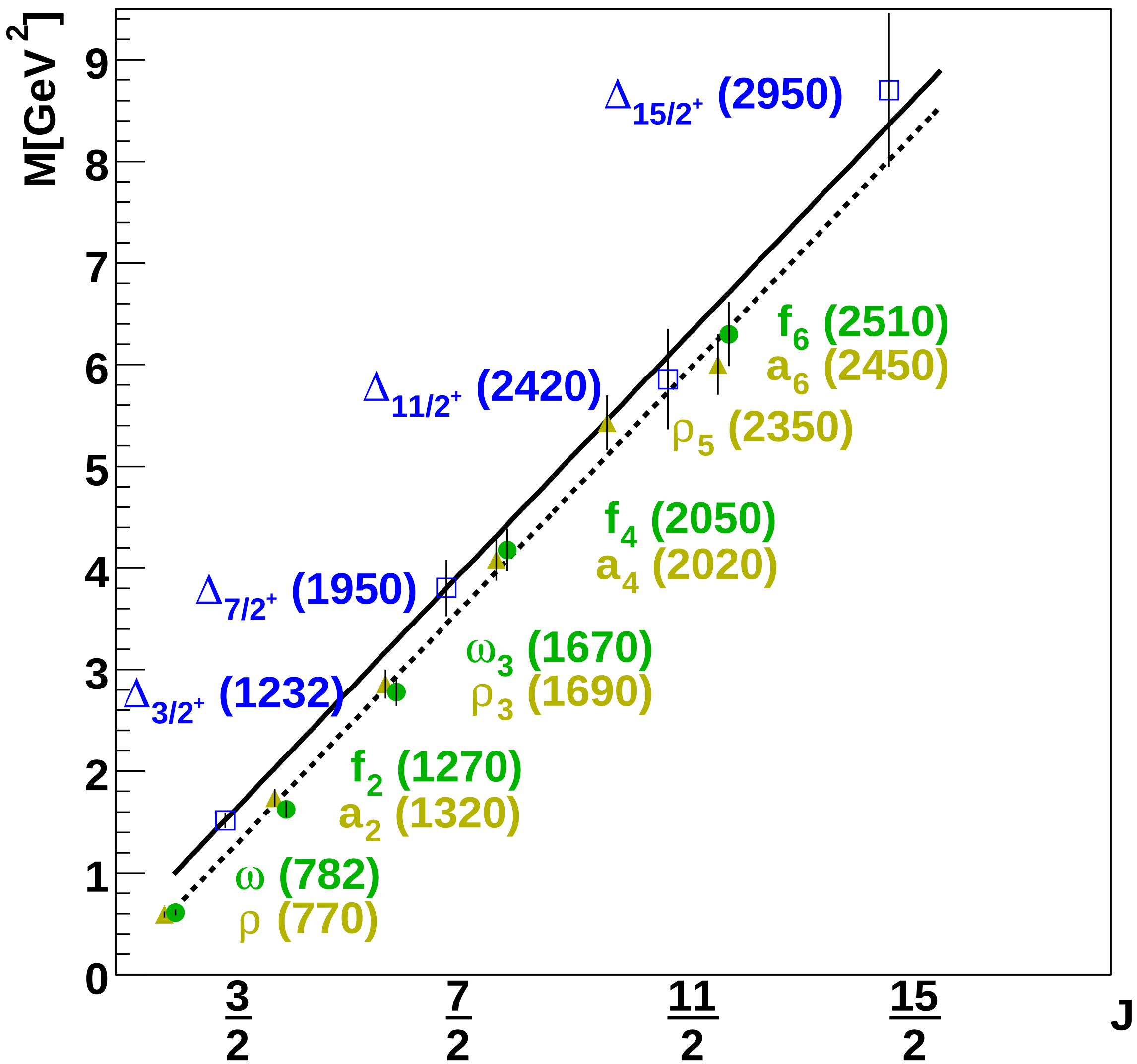

Δ^*'s with L even and $J = L + 3/2$ have the same slope as mesons.

Spin-orbit couplings

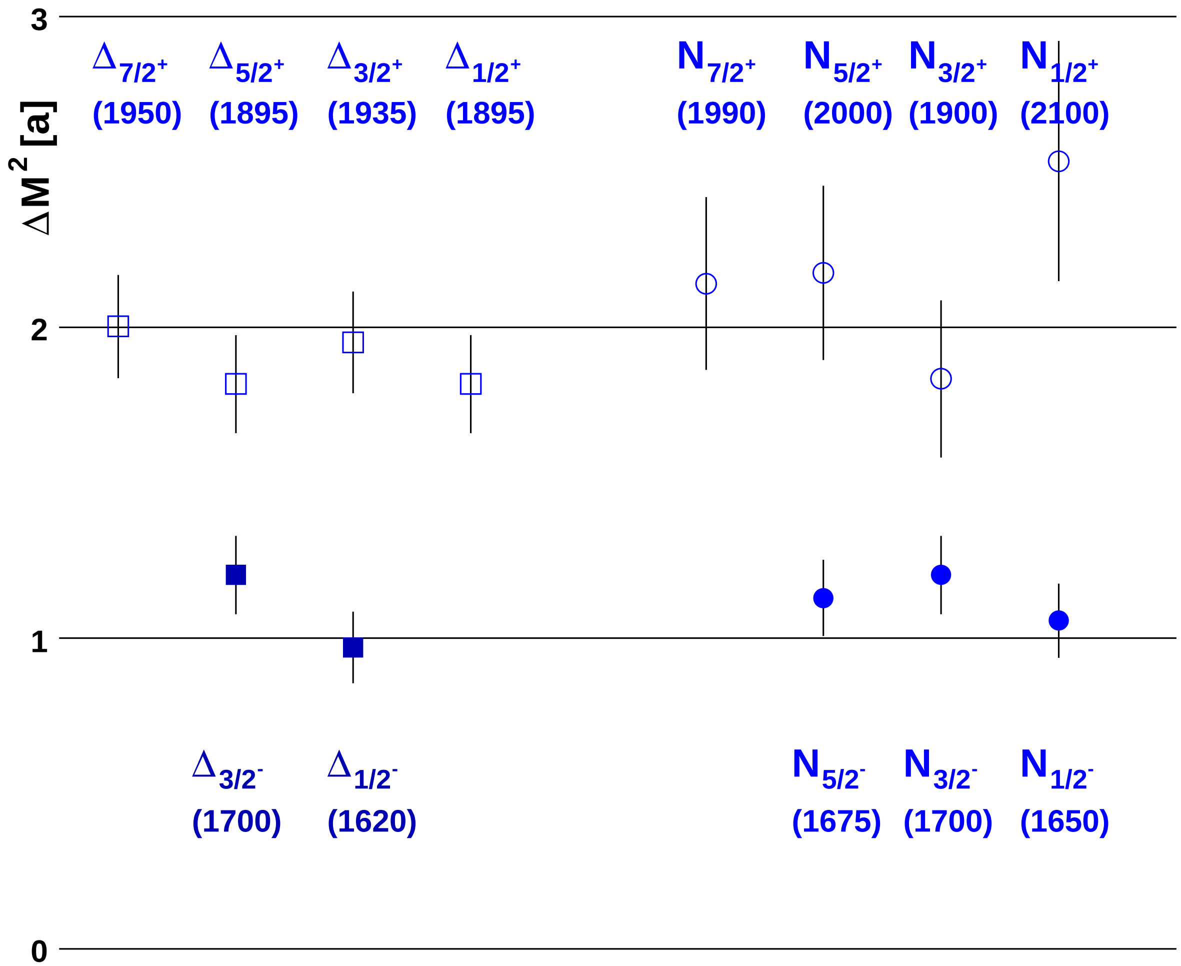

$$\mathbf{L}(1) + \mathbf{S}(1/2) = \mathbf{J}(3/2^+, 1/2^+)$$

Δ^*'s and N^*'s assigned to super-multiplets with defined orbital angular momentum.

$$\mathbf{L}(2) + \mathbf{S}(3/2) = \mathbf{J}(7/2^+, 5/2^+, 3/2^+, 1/2^+).$$

$$\mathbf{L}(1) + \mathbf{S}(3/2) = \mathbf{J}(5/2^+, 3/2^+, 1/2^+)$$

D	S	L	N	Multiplet structure of N* and Δ*				Mass (5)
56	**1/2**	**0**	**0-3**	$\mathbf{N}_{1/2+}$ **(939)**	$\mathbf{N}_{1/2+}$ **(1440)**	$\mathbf{N}_{1/2+}$ **(1710)**	$^{1}\mathbf{N}_{1/2+}$ **(2100)**	**939 MeV**
	3/2	**0**	**0-3**	$\Delta_{3/2+}$ **(1232)**	$\Delta_{3/2+}$ **(1600)**	$\Delta_{3/2+}$ **(1920)**		**1232 MeV**
70	1/2	1	0		$\mathbf{N}_{1/2-}$ **(1535)**	$\mathbf{N}_{3/2-}$ **(1520)**		**1530 MeV**
	3/2	1	0		$\mathbf{N}_{1/2-}$ **(1650)**	$\mathbf{N}_{3/2-}$ **(1700)**	$\mathbf{N}_{5/2-}$ **(1675)**	**1631 MeV**
	1/2	1	0		$\Delta_{1/2-}$ **(1620)**	$\Delta_{3/2-}$ **(1700)**		**1631 MeV**
56	1/2	1	1		$\mathbf{N}_{1/2-}$	$\mathbf{N}_{3/2-}$		**1779 MeV**
	3/2	1	1		$^{a}\Delta_{1/2-}$ **(1900)**	$^{b}\Delta_{3/2-}$ **(1940)**	$^{c}\Delta_{5/2-}$ **(1930)**	**1950 MeV**
70	1/2	1	2		$^{1}\mathbf{N}_{1/2-}$ **(2090)**	$^{2}\mathbf{N}_{3/2-}$ **(2080)**		**2151 MeV**
	3/2	1	2		$\mathbf{N}_{1/2-}$	$\mathbf{N}_{3/2-}$	$\mathbf{N}_{5/2-}$	**2223 MeV**
	1/2	1	2		$\Delta_{1/2-}$ **(2150)**	$\Delta_{3/2-}$		**2223 MeV**
56	1/2	2	0		$\mathbf{N}_{3/2+}$ **(1720)**	$\mathbf{N}_{5/2+}$ **(1680)**		**1779 MeV**
	3/2	2	0	$^{a}\Delta_{1/2+}$ **(1910)**	$^{b}\Delta_{3/2+}$ **(1920)**	$^{c}\Delta_{5/2+}$ (1905)	$^{d}\Delta_{7/2+}$ **(1950)**	**1950 MeV**
70	1/2	2	0		$\mathbf{N}_{3/2+}$	$\mathbf{N}_{5/2+}$		**1866 MeV**
	3/2	2	0	$\mathbf{N}_{1/2+}$	$^{2}\mathbf{N}_{3/2+}$ **(1900)**	$^{3}\mathbf{N}_{5/2+}$ **(2000)**	$^{4}\mathbf{N}_{7/2+}$ **(1990)**	**1950 MeV**
	1/2	2	0		$\Delta_{3/2+}$	$\Delta_{5/2+}$		**1950 MeV**

Negative-parity Δ's

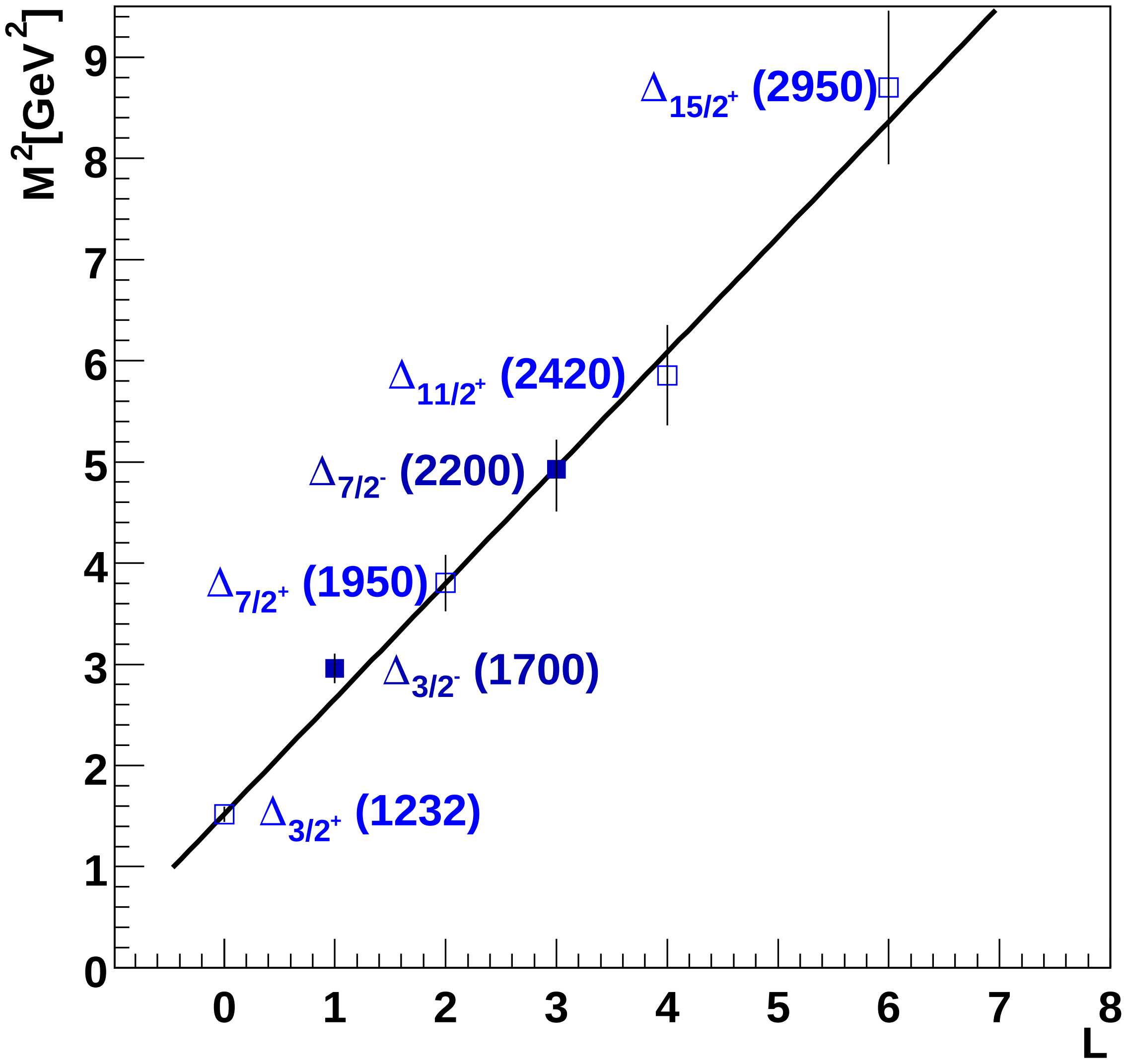

Δ^*'s with odd L and J = L+1/2 fall on the same trajectory.

N*'s and Δ's with $S = 3/2$

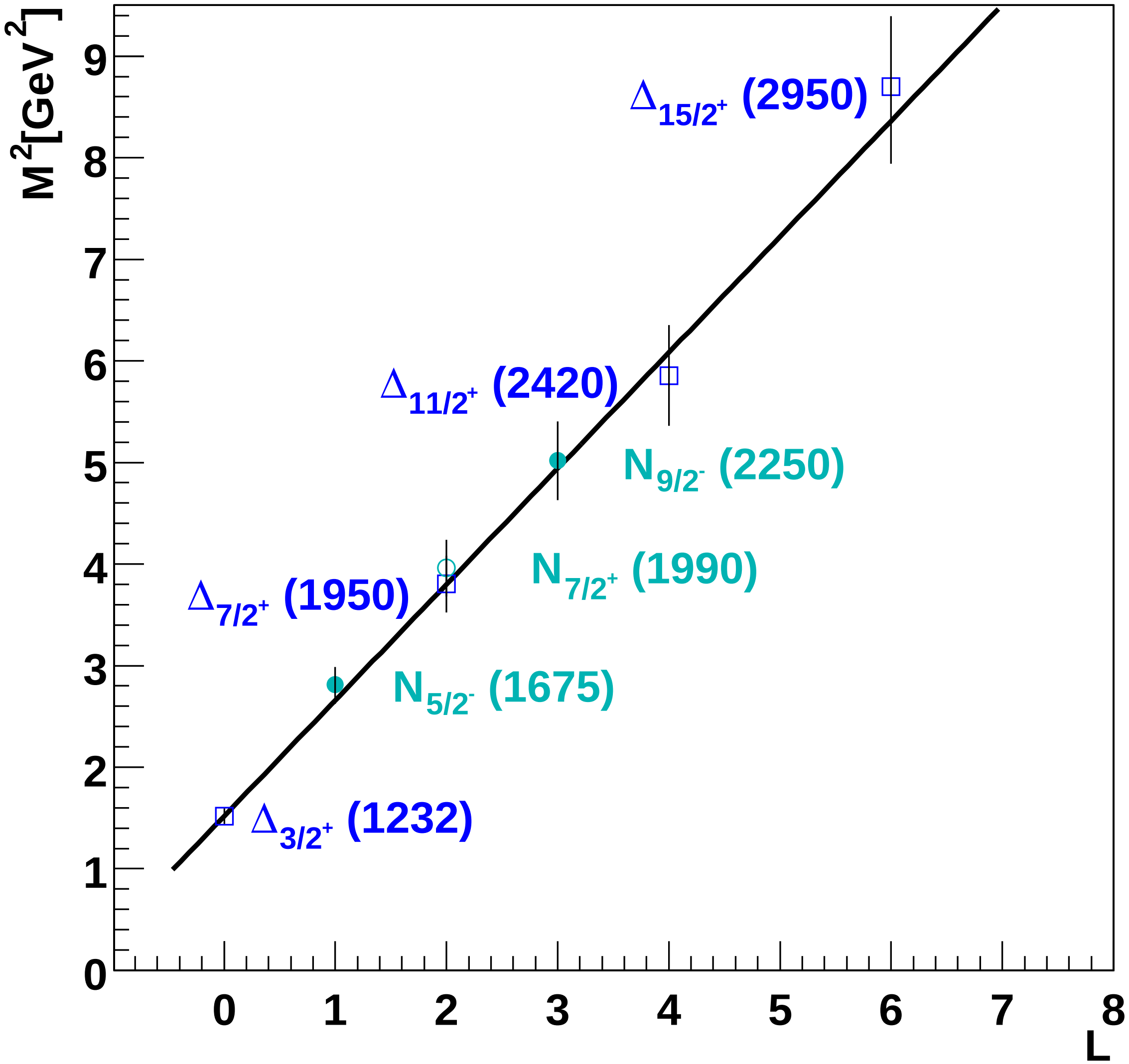

N*'s with intrinsic spin 3/2 fall on the same trajectory.

N*'s ($S = 3/2$) and Δ's ($S = 1/2, 3/2$)

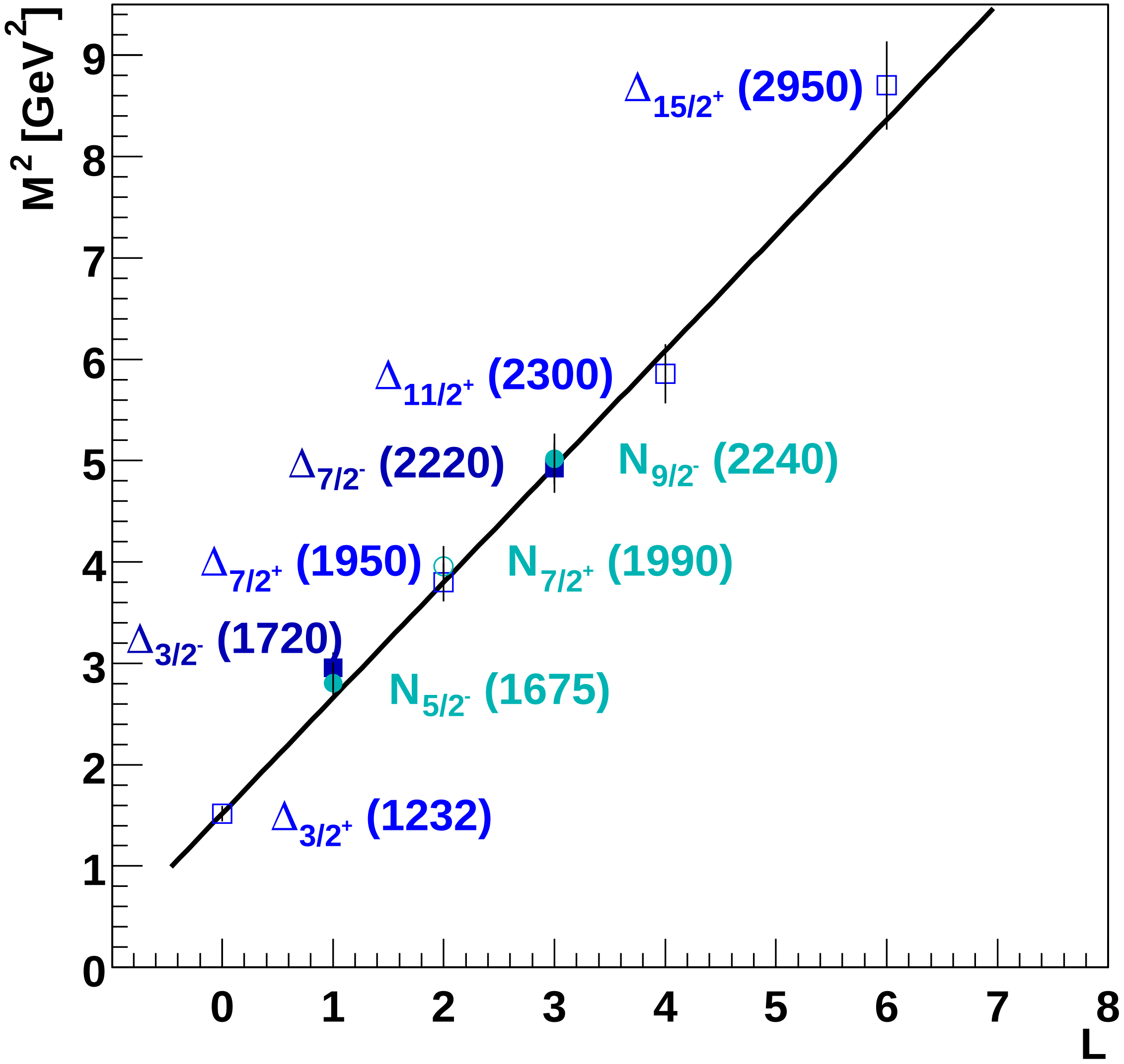

The lowest Δ^* (with spin 1/2 and 3/2) and the N*'s with intrinsic spin 3/2 and J = L + 3/2 fall on the same Regge trajectory.

What is about N^* with intrinsic spin $S = 1/2$?

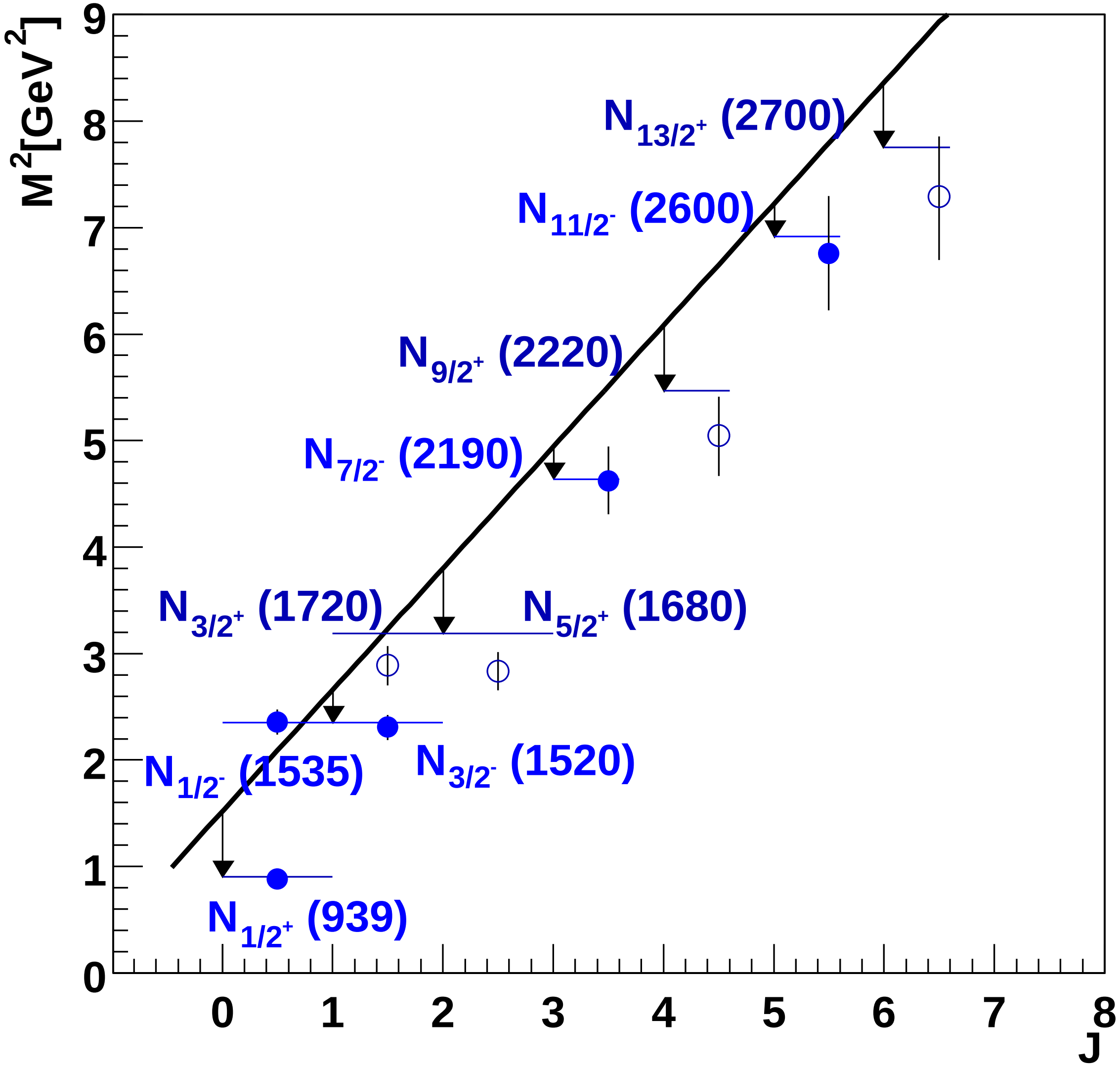

The N^* masses (with intrinsic spin $S = 1/2$) lie below the standard Regge trajectory. They are smaller by about 0.6 GeV^2 for N^* in the 56-plet, and by 0.3 GeV^2 for N^* in the 70-plet.

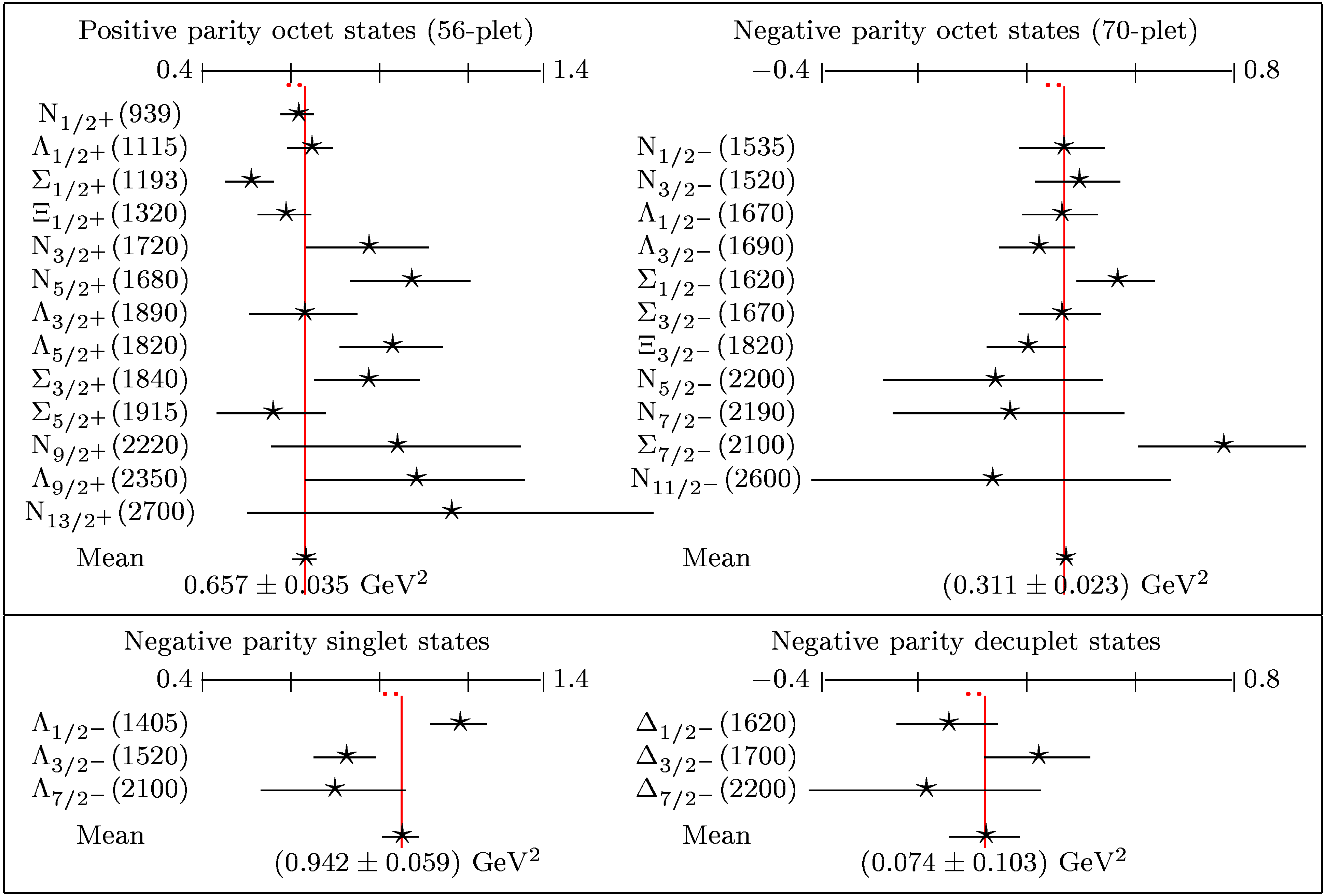
Positive parity octet states (56-plet)
0.4
1.4
N$_{1/2+}$(939)
Λ$_{1/2+}$(1115)
Σ$_{1/2+}$(1193)
Ξ$_{1/2+}$(1320)
N$_{3/2+}$(1720)
N$_{5/2+}$(1680)
Λ$_{3/2+}$(1890)
Λ$_{5/2+}$(1820)
Σ$_{3/2+}$(1840)
Σ$_{5/2+}$(1915)
N$_{9/2+}$(2220)
Λ$_{9/2+}$(2350)
N$_{13/2+}$(2700)
Mean
0.657 ± 0.035 GeV^2
Negative parity octet states (70-plet)
−0.4
0.8
N$_{1/2-}$(1535)
N$_{3/2-}$(1520)
Λ$_{1/2-}$(1670)
Λ$_{3/2-}$(1690)
Σ$_{1/2-}$(1620)
Σ$_{3/2-}$(1670)
Ξ$_{3/2-}$(1820)
N$_{5/2-}$(2200)
N$_{7/2-}$(2190)
Σ$_{7/2-}$(2100)
N$_{11/2-}$(2600)
Mean
(0.311 ± 0.023) GeV^2
Negative parity singlet states
0.4
1.4
Λ$_{1/2-}$(1405)
Λ$_{3/2-}$(1520)
Λ$_{7/2-}$(2100)
Mean
(0.942 ± 0.059) GeV^2
Negative parity decuplet states
−0.4
0.8
Δ$_{1/2-}$(1620)
Δ$_{3/2-}$(1700)
Δ$_{7/2-}$(2200)
Mean
(0.074 ± 0.103) GeV^2

Radial excitations

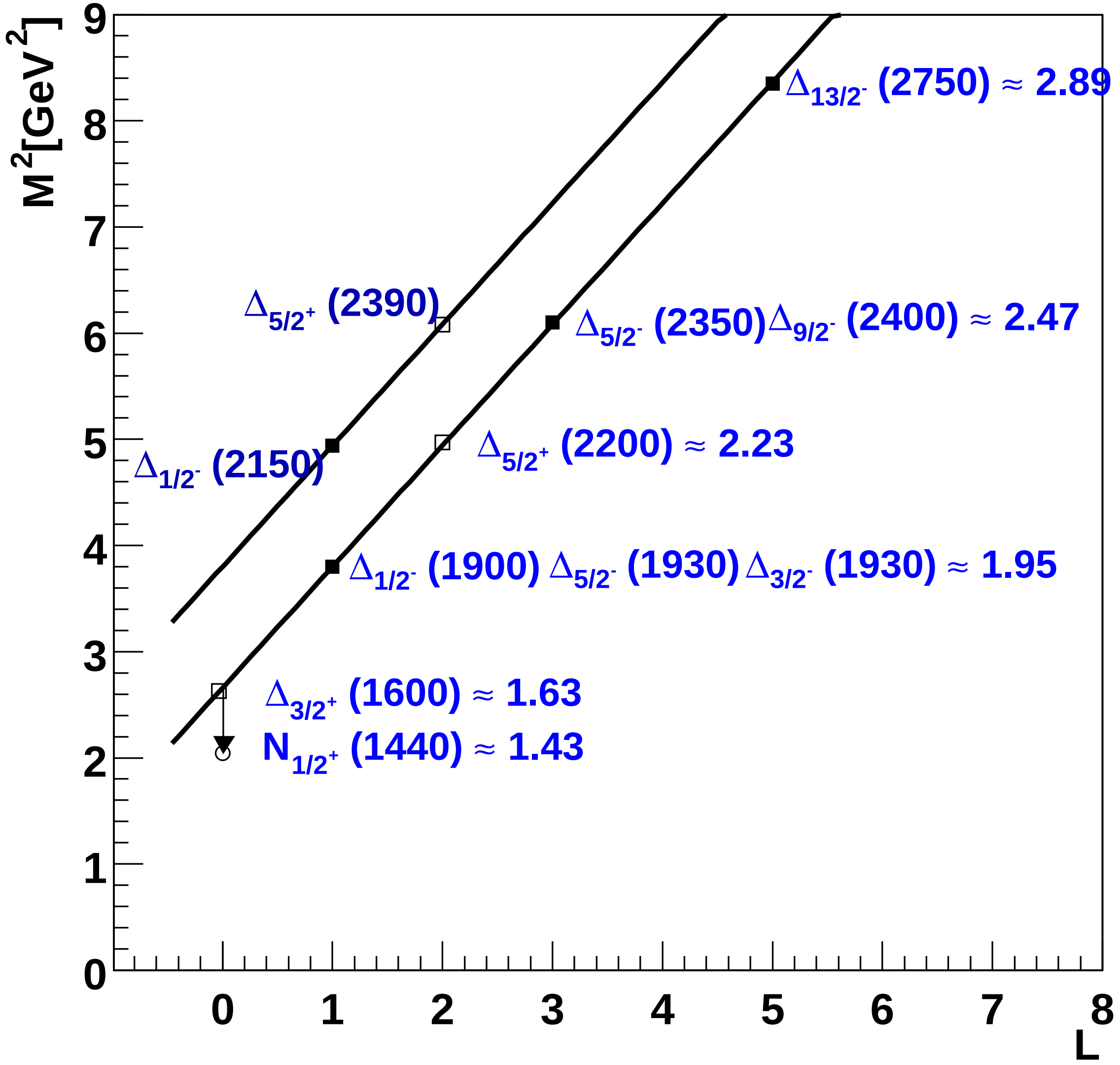

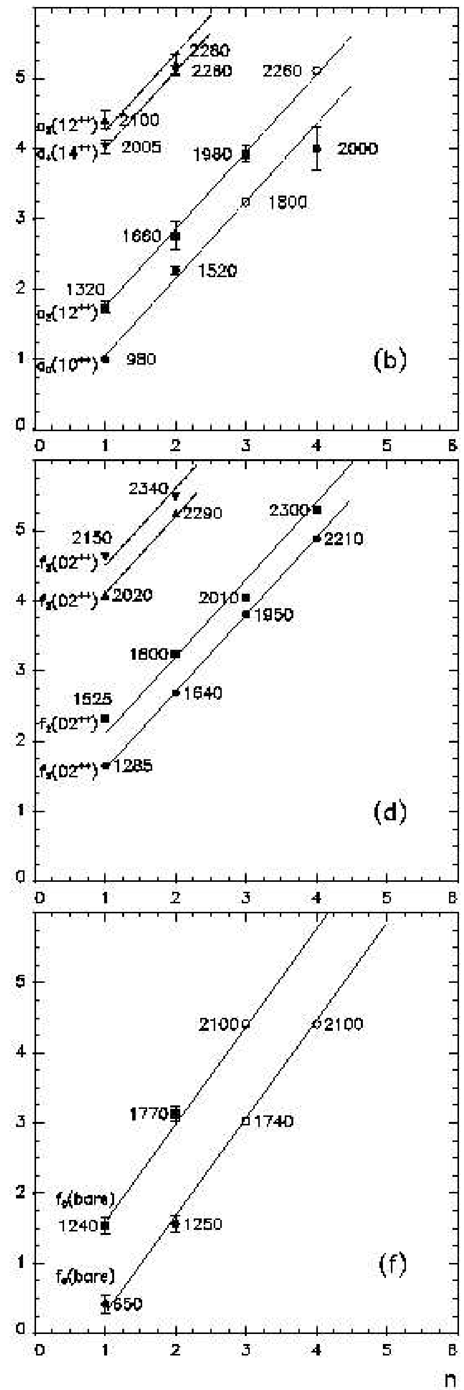

Radial excitations have masses larger by one $\hbar\omega$, like mesons

Baryon	δM^2 (GeV^2)	Baryon	δM^2 (GeV^2)
$\mathbf{N}_{1/2^+}(939)$		$\Delta_{3/2^+}(1232)$	
$\mathbf{N}_{1/2^+}(1440)$	$1 \cdot 1.18$	$\Delta_{3/2^+}(1600)$	$1 \cdot 1.04$
$\mathbf{N}_{1/2^+}(1710)$	$2 \cdot 1.02$	$\Delta_{3/2^+}(1920)$	$2 \cdot 1.08$
$\mathbf{N}_{1/2^+}(2100)$	$3 \cdot 1.18$		
$\Delta_{1/2^-}(1620)$		$\Delta_{3/2^-}(1700)$	
$\Delta_{1/2^-}(1900)$	$1 \cdot 0.99$	$\Delta_{3/2^-}(1940)$	$1 \cdot 0.87$
$\Delta_{1/2^-}(2150)$	$2 \cdot 1.00$		
$\mathbf{N}_{1/2^-}(1530)$		$\mathbf{N}_{3/2^-}(1520)$	
$\mathbf{N}_{1/2^-}\mathbf{(1897)}$	$1 \cdot 1.26$	$\mathbf{N}_{3/2^-}\mathbf{(1895)}$	$1 \cdot 1.28$
$\mathbf{N}_{1/2^-}(2090)$	$2 \cdot 1.01$	$\mathbf{N}_{3/2^-}(2080)$	$2 \cdot 1.01$
$\Lambda_{1/2^+}(1115)$		$\Sigma_{1/2^+}(1193)$	
$\Lambda_{1/2^+}(1600)$	$1 \cdot 1.24$	$\Sigma_{1/2^+}(1560)$	$1 \cdot 1.04$
$\Lambda_{1/2^+}(1810)$	$2 \cdot 0.98$	$\Sigma_{1/2^+}(1880)$	$2 \cdot 1.06$

Radial excitations of baryons; in red: two Saphir resonances.

Observations and conclusions

1. **The slope of the Regge trajectory for mesons is the same as for Δ^*, $a = 1.142\,\mathrm{GeV}^2$ $\Rightarrow$ Effective quark - diquark interaction !**

2. **N and Δ resonances with spin $S = 3/2$ lie on a common Regge trajectory.**

   $\Rightarrow$ No significant genuine octet-decuplet splitting.

3. **Δ^* resonances with S=1/2 and S=3/2 are on the same Regge trajectory.**

   $\Rightarrow$ No significant genuine spin-spin interaction.

4. **N^*'s and Δ^*'s can be grouped into supermultiplets with defined L and S but different J. $\Rightarrow$ No significant $L \cdot S$ splitting.**

5. **There is a mass shift $\propto$ to $(q_1q_2 - q_2q_1)(\uparrow\downarrow - \downarrow\uparrow)$ in baryonic wave functions. $\Rightarrow$ Instanton interactions are important.**

6. **Daughter trajectories have the same slope and an intercept which is higher by $\mathbf{a = 1.142\,GeV^2}$ per n, both for mesons and baryons.**

$\Rightarrow$ Effective quark - diquark interaction !

7. **For L larger than 3,**

$$\mathbf{N^*\text{'s have } J = L + 1/2\,;}$$

$$\mathbf{\Delta^*\text{'s have } J = L + 3/2} \qquad \Rightarrow \textbf{Spin and flavor are locked !}$$

These observations can be condensed into a baryon mass formula

A mass formula for baryon resonances

E. Klempt, Phys. Rev. C 66 (2002) 058201

$$\mathbf{M^2 = M_\Delta^2 + \frac{n_s}{3} \cdot M_s^2 + a \cdot (L + N) - s_i \cdot I_{sym}}$$

where

$$\mathbf{M_s^2} = \left(\mathbf{M_\Omega^2 - M_\Delta^2}\right), \qquad s_i = \left(M_\Delta^2 - M_N^2\right),$$

M_N, M_Δ, M_Ω **are input parameters (PDG),** $\mathbf{n_s}$ **number of strange quarks in a baryon.** $\mathbf{a = 1.142/GeV^2}$ **Regge slope (from meson spectrum).** $\mathbf{L = l_\rho + l_\lambda}$**,** $\mathbf{N = n_\rho + n_\lambda}$**, L+2N harmonic-oscillator band** ***N*****.**

I_{sym} **is the fraction of the wave function (normalized to the nucleon wave function) which is antisymmetric in spin and flavor:**

$\mathbf{I_{sym} =}$	**1**	**for S=1/2 and**	**octet in 56-plet;**
$\mathbf{I_{sym} =}$	**1/2**	**for S=1/2 and**	**octet in 70-plet;**
$\mathbf{I_{sym} =}$	**3/2**	**for S=1/2 and**	**singlet;**
$\mathbf{I_{sym} =}$	**0**	**otherwise.**	

- $\chi^2 = 105$ **for 97 data points.**
- **All but 4 observed states are predicted:**

$\Rightarrow$ **No evidence for (baryonic) hybrids !**
$\Rightarrow$ **No evidence for pentaquarks !**

However, a new resonance is reported in several experiments, the $\mathbf{Z^+}$ which decays to $\mathbf{nK^+}$.

Quark content:

$$(\mathbf{u}, \mathbf{d}, \mathbf{d}) + (\mathbf{u}, \bar{\mathbf{s}}) = (\mathbf{u}, \mathbf{u}, \mathbf{d}, \mathbf{d}, \bar{\mathbf{s}}) \text{ pentaquark !}$$

Is there evidence for chiral symmetry restoration in the high-mass nucleon spectrum ?

L. Y. Glozman, Phys. Lett. B 541, 115 (2002)

Quarks are (nearly) massless; there is chiral symmetry. At low energies, chiral symmetry is broken, e.g. by instanton-induced interactions:

- **Quarks acquire mass**
- **The masses of pion and of $f_0(600)$ are different**
- **The mass of the $\mathrm{N}_{1/2^+}$(938) and of the $\mathrm{N}_{1/2^-}$(1535) are different.**

Chiral symmetry might be restored

- **at large temperatures**
- **and high densities**
- **at high excitation energies ???**

$J=\frac{1}{2}$	1	$N_{1/2^+}(2100)$	$N_{1/2^-}(2090)$	a	$\Delta_{1/2^+}(1910)$	$\Delta_{1/2^-}(1900)$
$J=\frac{3}{2}$	2	$N_{3/2^+}(1900)$	$N_{3/2^-}(2080)$	b	$\Delta_{3/2^+}(1920)$	$\Delta_{3/2^-}(1940)$
$J=\frac{5}{2}$	3	$N_{5/2^+}(2000)$	$N_{5/2^-}(2200)$	c	$\Delta_{5/2^+}(1905)$	$\Delta_{5/2^-}(1930)$
$J=\frac{7}{2}$	4	$N_{7/2^+}(1990)$	$N_{7/2^-}(2190)$	d	$\Delta_{7/2^+}(1950)$	$\Delta_{7/2^-}(2200)$
$J=\frac{9}{2}$	5	$N_{9/2^+}(2220)$	$N_{9/2^-}(2250)$	e	$\Delta_{9/2^+}(2300)$	$\Delta_{9/2^-}(2400)$
$J=\frac{11}{2}$	6	$N_{11/2^+}$	$N_{11/2^-}(2600)$	f	$\Delta_{11/2^+}(2420)$	$\Delta_{11/2^-}$
$J=\frac{13}{2}$	7	$N_{13/2^+}(2700)$	$N_{13/2^-}$	g	$\Delta_{13/2^+}$	$\Delta_{13/2^-}(2750)$
$J=\frac{15}{2}$	8	$N_{15/2^+}$	$N_{15/2^-}$	h	$\Delta_{15/2^+}(2950)$	$\Delta_{15/2^-}$

Parity doublets of N^* and Δ^* resonances of high mass, after Glozman. The states in color are predicted to have the same mass as their chiral partner when chiral symmetry is restored in the high-mass excitation spectrum of baryon resonances. We suggest that the states marked with in red should have considerably higher masses than their chiral partners while those in blue should be degenerate in mass with corresponding states of opposite parity.

High Δ states with negative parity

There are three high-mass Δ states with negative parity:

$$\Delta_{5/2^-}\mathbf{(1930)} \qquad \Delta_{9/2^-}\mathbf{(2400)} \qquad \Delta_{13/2^-}\mathbf{(2750)}$$

Possible L,S configurations are:

	Unlikely	
$\Delta_{5/2^-}$**(1930)**	$\Delta_{9/2^-}$**(2400)**	$\Delta_{13/2^-}$**(2750)**
L=3, S=1/2	**L=5, S=1/2**	**L=7, S=1/2**
	Likely	
$\Delta_{5/2^-}$**(1930)**	$\Delta_{9/2^-}$**(2400)**	$\Delta_{13/2^-}$**(2750)**
L=1, S=3/2	**L=3, S=3/2**	**L=5, S=3/2**

Flavor wave function: symmetric; spin wave function: symmetric.

$\rightarrow$ spacial wave function must be symmetric !

One unit of radial excitation !

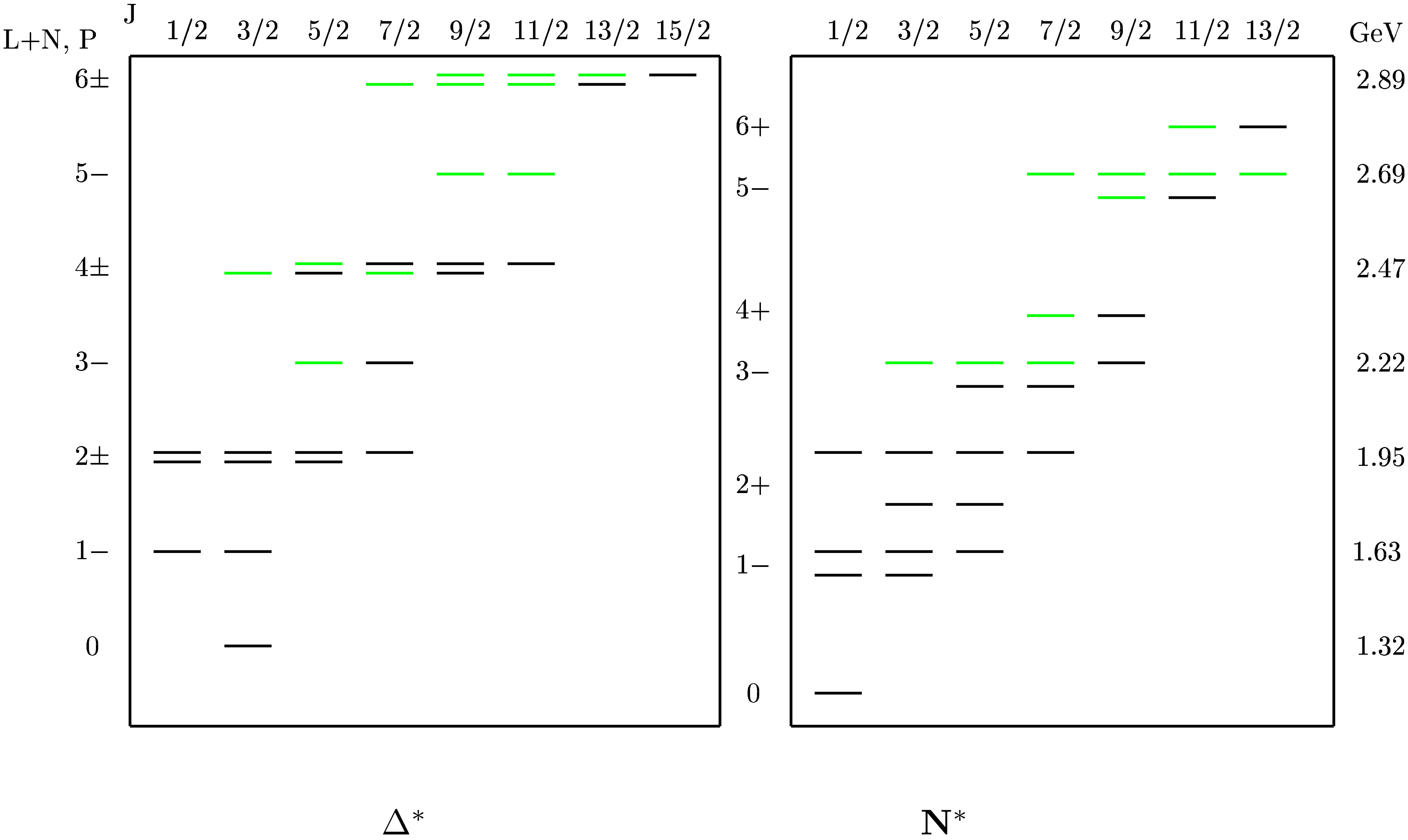

E. Klempt, Phys Lett. B 559 (2003) 114

7 Summary and Conclusions

- Quantum Chromodynamics is (likely) the correct theory of strong interactions.
- However, it is untested at low energies.
- Spectroscopy is a powerful tool to scrutinize ideas what the effective particles are that govern he dynamics and how they interact.

- **QCD oriented model have seen great successes:**
- **Quark models describe rather successfully the spectrum of mesons and baryons, and their decays, form factors, transition form factors, magnetic moments, ...**
- **QCD-oriented models predict new classes of hadrons: glueballs and mesonic and baryonic hybrids. These predictions have provided an important stimulus to the field.**

- **QCD oriented model have important failures:**
- **Different (conflicting) models provide a description of similar quality (even though instanton induced models are better).**
- **Quark models provide no link between the partonic degrees of freedom seen in deep inelastic scattering and the constituent quark.**
- **Quark models are in conflict with the flux tube picture.**
- **Inspite of 20 years of intensive searches, there is no compelling evidence for the existence of glueballs and hybrids.**

A sketch of quark dynamics

There is a contradiction:

1. **Baryon resonances are quark-diquark excitations**
2. **Baryon resonances need the full multiplet structure**

Solution:

1. **refers to the color interaction**
2. **refers to the flavor decomposition**

Example:

$$\mathbf{N_{3/2^-}(1520)} \qquad\qquad \mathbf{L = 1 \quad S = 1/2 \rightarrow\ J = 3/2}$$

Both harmonic oscillators are coherently excited (in flavour space).
Dynamics is given by color !

$$\boxed{\textbf{Flavour diquark}} \neq \boxed{\textbf{Colour diquark}}$$

1. **Confinement**

Colour-neutral (Pomeron-like)
Quarks polarise vacuum
Vacuum transmits interaction

When two quarks are separated, the space between them is filled with polarised vacuum. The net color charge remains unchanged, the energy density is constant. This gives a linear confinement potential.

2. **Flavor exchange**

   $\boldsymbol{\Lambda = 1\,\mathrm{GeV} = \Lambda_\chi}$

Meson exchange (long range)
and/or instanton interactions

3. **Color exchange**

   $\boldsymbol{\Lambda = 200\,\mathrm{MeV} = \Lambda_{\mathrm{QCD}}}$

Gluon exchange (short range)
Screened by polarised vacuum

FAQ

- **What are the effective degrees of freedom ?**

  Quarks polarise the quark and gluon condensates; quark plus polarisation cloud form a constituent quark which carries defined color. Color exchange is screened by the polarisation cloud. Flavor exchange is fast: flavor is not a property of constituent quarks.

- **Why are quarks confined ?**

  The net color-charge of a quark plus polarisation cloud is the color of the current quark before 'dressing'. When quarks are separated, constituent-quark masses increase with distance. The color 'source' needs a 'color' sink. The energy density along the string due to the polarised condensates is constant.

- **What are the effective forces ?**

  Confinement originates from Pomeron-exchange-like forces transmitted by the polarisation of the vacuum condensates. Flavor-exchange between constituent quarks is important and occurs with a frequency of $1/\tau \sim \Lambda_\chi$. It could be realised by meson exchange or by instantons at the surface between two constituent quarks. Instanton interactions play an important role.

Related topics:

- **Spin crisis**

  Quark spin induces polarisation into condensates;

  the polarised gluon-condensate provides the gluonic contribution to the proton spin

  quark condensate provides the quark and orbital ($^3P_0$) contributions

- **$^3P_0$ model for decays**

  A $\bar{q}q$ pair from condensate shifted to mass shell

- **New interpretation of glueballs and hybrids**

  Do hybrids exist ? Does the flux tube filled with polarised condensates support transverse oscillations/rotations ? Or only longitudinal 'acustical' shock waves ?

  Can a state of localised polarised-condensate propagate in space (in a soliton-like solution) ?

You have been an extremely nice class!

I hope you enjoy the coming lectures and will return to work with new ideas and enthusiasm !

Thank you !

Good bye !